Maastricht University

Lipids and lipid transporters

Citation for published version (APA):

Giovagnoni, C. (2022). Lipids and lipid transporters: key role in membrane dynamics, inflammation and Alzheimer's disease. [Doctoral Thesis, Maastricht University]. Maastricht University.
https://doi.org/10.26481/dis.20220628cv

Document status and date:
Published: 01/01/2022

DOI:
10.26481/dis.20220628cv

Document Version:
Publisher's PDF, also known as Version of record

Please check the document version of this publication:

• A submitted manuscript is the version of the article upon submission and before peer-review. There can be important differences between the submitted version and the official published version of record. People interested in the research are advised to contact the author for the final version of the publication, or visit the DOI to the publisher's website.
• The final author version and the galley proof are versions of the publication after peer review.
• The final published version features the final layout of the paper including the volume, issue and page numbers.

Link to publication

Lipids and lipid transporters: key role in membrane dynamics, inflammation and Alzheimer's disease

Caterina Giovagnoni

Lipids and lipid transporters: key role in membrane dynamics, inflammation and Alzheimer's disease

DISSERTATION

to obtain the degree of Doctor at the Maastricht University,

on the authority of the Rector Magnificus, Prof. dr. Pamela Habibović

in accordance with the decision of the Board of Deans,

to be defended in public

on Tuesday 28 June 2022 at 10:00 hours

by

Caterina Giovagnoni

Supervisors:

Prof. Dr. Pilar Martinez-Martinez

Prof. Dr. Bart Rutten

Co-supervisor:

Dr. Mario Losen

Assessment Committee:

Prof. Dr. Marc de Baets (Chair)

Prof. Dr. M. Honing

Dr. L. Ledesma, Centro de Biología Severo Ochoa, Madrid, Spain; Senior Scientist
CSIC at CBMSO

Prof. Dr. L. Moroni

Prof. Dr. F. Rustichelli, Senior Scientist Istituto Nazionale Biostrutture Biosistemi,
Roma, Italy; Guest Professor at AGH University of Krakow, Poland

Table of contents

Chapter 1

General Introduction

The role of sphingolipid and sphingolipid transporters in membrane dynamics, inflammation and Alzheimer disease is the central topic of this thesis.

This chapter serves as introduction on the relevant background concerning sphingolipids and their transporters in the context of pathophysiological events during inflammation and neurodegeneration.

Sphingolipid metabolism

Sphingolipids (SLs) belong to a class of lipids composed of a backbone of a long-chain sphingoid, identified in the brain as first described by prof. Thudichum in the late 19th century.

Initially, SLs were categorized as molecules with a structural function, responsible for the physical properties of different cellular compartments, but the technological advancement of the 20th century in the study of lipids revealed specific biochemical properties of this class of lipids. Besides their function in structure, their metabolism and metabolic products have been linked to numerous cellular processes regulating cellular growth, differentiation, and cell apoptosis [1]. Nowadays, SLs such as ceramide, sphingomyelin (SM) and sphingosine 1-phosphate are thought to play an essential role as second messengers [2].

Ceramides are the central core of complex SLs. They are synthetized via three pathways through which the level of ceramide and other complex SLs produced in the cell can be controlled. The *de novo* pathway, a series of highly regulated reactions, takes place in the endoplasmic reticulum (ER) and the Golgi apparatus. Ceramide is synthesized from serine and then converted in the Golgi apparatus into complex SLs, such as sphingomyelin, Cer1-p or glycosphingolipids. Ceramides are also synthesized by the cells through two catabolic pathways: the hydrolytic and the salvage pathway. Both have the sphingomyelin as starting molecule, which can be hydrolysed in the cell membrane or in the endosomes respectively.

Ceramide can also be hydrolysed to sphingosine, then phosphorylated to generate sphingosine 1 phosphate (S1P), another central molecule in the physiology of SLs [3]. The metabolism of SLs is highly regulated by a tight, controlled network of proteins and enzymes permitting the formation of complex, physiologically important SLs. In this context, the ceramide transfer proteins (CERTs) are important as they are now being recognized as regulators of cellular Ceramide and SM balance.
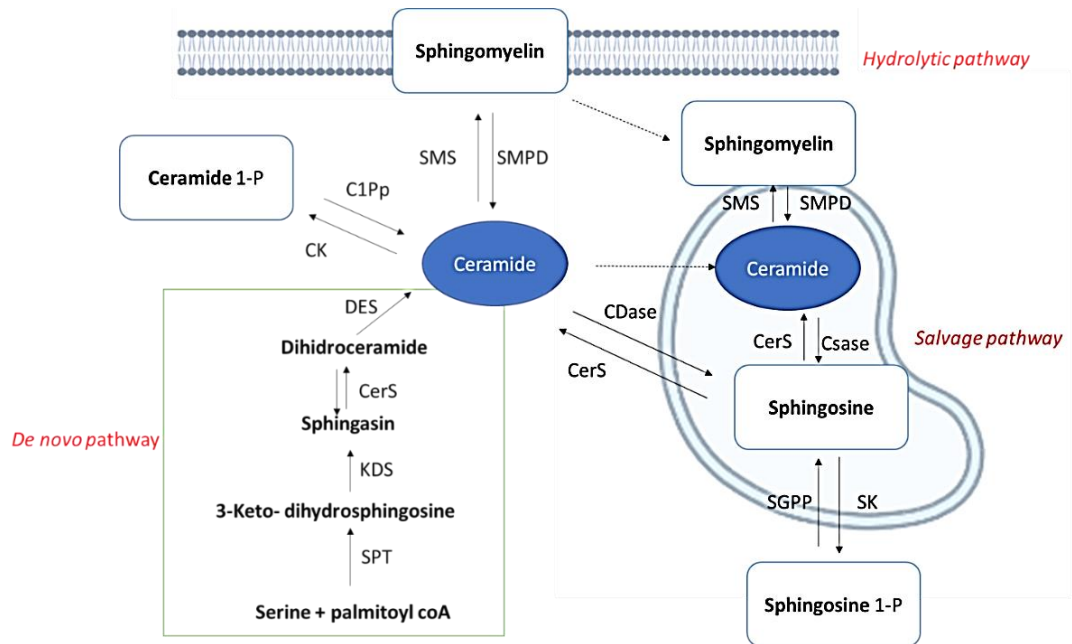
Figure 1: Simplified schematic representation of the three pathways leading to the synthesis of ceramide. In the *de novo* synthesis pathway, serine palmitoyltransferase (SPT) generates 3-keto dihydrosphinganine by condensation of the precursor's serine and palmitoyl-CoA. SPT product 3-keto dihydrosphinganine is subsequently converted into dihydrosphingosine by 3-keto dihydrosphinganine reductase (KDS). Dihydrosphingosine is the substrate of a family of acyl-CoA transferases, called ceramide synthases (CS) that metabolize dihydrosphingosine into dihydroceramide, which is subsequently converted to ceramide (Cer) by dihydroceramide desaturase (DES). Ceamider can be further degraded to sphingosine by ceramidases (CDases) or phosphorylated by ceramide kinase (CK) to produce ceramide-1-phospathe (C1P). Sphingosine can originate sphingosine-1-phosphate (S1P) through the activity of sphingosine kinases (SKs). The reverse reaction catalyzed by Sphingosine N-acyltransferase (CerS)is called salvage pathway. Cer may also derive from the hydrolysis of sphingomyelin (SM) by sphingomyelinases (SMPDs), the opposite reaction is catalyzed by sphingomyelin synthases (SMSs). S1P and C1P can be dephosphorylated and re-converted to sphingosine and Cer by S1P phosphatases (SPPs) and C1P phosphatases (C1Pp) respectively.

CERT Proteins

While more details of SLs and their metabolites are clearer than before, the precise physiological function of SL-related proteins such as enzymes and transporters remain elusive. Of particular interest are the ceramide transfer proteins (CERTs), lipid-binding proteins influencing cellular lipid balance and homeostasis.

CERTs are non-conventional serine threonine kinases able to bind and transfer ceramide from the ER to the Golgi apparatus in an ATP dependent manner. They participate in the *de novo* synthesis pathway and, therefore, contribute to the formation of complex SLs [4]. CERTs are encoded by the COL4A3BP gene and have at least 3 different isoforms due to differences in the translation initiation site. The second longest isoform was first discovered as a kinase specifically phosphorylating the N-

terminal region of the non-collagenous domain of the alpha 3 chain of type IV collagen, known as the Goodpasture antigen, which is the target of autoantibodies in the Goodpasture syndrome [5]. Hanada and colleagues subsequently uncovered another role of CERTs, namely the ability to bind ceramide and to carry it elsewhere [4]. This discovery has impulse the research on the metabolism of SLs since it elucidates not only its compartmentalization but also explains that a possible disturbance leads to detrimental effects. CERT proteins, in fact, are gaining interest in the field for their essential role in mediating diverse pathways in which it influences SLs metabolism and also interacts with immune reactions.

CERTs are widely expressed in the CNS and they have been implicated in different neural pathways including processes underlying neurogenesis and neuronal death. [6] [7] [8]. In particular, point mutations of CERTs are associated with neurodevelopmental disorders and intellectual disability [9]. CERT-KO mice show physiological dysfunction [10] that is lethal at embryonic stage by decreasing SM level in the plasma membrane and increasing ceramide in the ER and mitochondria [11]. Moreover, CERTL (the long isoform of CERTs) is present in lipid rafts and can be secreted extracellularly [12] suggesting a potential role in controlling the membrane stiffness or participating in membrane signalling cascades. In addition, CERTL was found to partially co-localize with serum amyloid P component (SAP) and with amyloid plaques in Alzheimer's disease (AD) brain. Moreover, it has been demonstrated that CERTs bind C1q, a mediator of the complement system and activate the complement cascade in apoptotic cells [13, 14]. All these findings strengthened the initial hypothesis that CERT is involved in immune response. Along these lines, overexpression of CERTs in the brain reduces the excess of inflammatory ceramide C16, shifting microglia phenotype into an anti-inflammatory state [8].

All in all, it would be of great interest to know which pathways are modulated or triggered by the presence or lack of CERTs. Also, it would be important to know in which way CERTs, e.g. as transporters of lipids, or as immune modulator, are involved in the pathophysiology of AD.

Sphingolipids and sphingolipid transporters in neuroinflammation and neurodegeneration
The brain is highly enriched in SLs. As aforementioned, SLs are crucial for homeostasis and development of the central nervous system. Since the early phases of neurodevelopment, SLs influence the cell cycle, blocking nuclear division, and apoptosis. Moreover, it has been shown that they influence the formation of synapses, the cell-to-cell communication and cellular mobility,

remodelling the membrane fluidity [15]. Those functions are maintained also in later stages of development (and during ageing) allowing the modulation of several cellular processes maintaining the physiological homeostasis [16].

Recent evidence has shown a correlation between the disbalance of SLs and related proteins with neurodegeneration. Many neurodegenerative disorders such as AD, Parkinson's disease (PD), Huntington's disease (HD), and amyotrophic lateral sclerosis (ALS) appear to have as common hallmark a disbalance in the content of SLs [17].

Of particular interest, as revealed in many studies, is that changes in SLs appear early in AD suggesting a role in the onset and the progression of the disease. AD is a multifactorial, age-related disorder characterised by gradual cognitive decline which is thought to be underpinned by several molecular events leading to severe neurodegeneration. Aberrant accumulation of misfolded proteins, neuronal loss and neuroinflammation are only a few of the many molecular events that can be observed in AD [18]. Accumulating evidence points to the involvement of SLs in prodromal stages of AD. In fact, it has been shown that there is a correlation between the concentration of ceramide and amyloid β(Aβ) in the cerebrospinal fluid (CSF) and plasma of AD patients [19] [20]. Lipidomic, proteomic and genomic data are in support of the hypothesis of a cause-and-effect relation between neurodegeneration and disbalance of SLs and their related molecules in AD diseased brains.

In general, in AD brain, there is an excess of ceramide compared to SM and S1P that are usually downregulated [21]. In addition, it has been shown that protein-encoding genes and proteins/enzymes involved in the SL pathway are also altered in AD, suggesting that dysfunctional regulation of SLs metabolism and disbalance in the concentration of certain lipids can be the trigger of physiologically deleterious events leading to neurodegeneration [22].

Moreover, recent research has suggested a connection between the concentration of SLs in cells and tissues and the activation of pathways leading to inflammation, such as those involve in microglia activation, and in cytokine release [23] .

Creating a comprehensive picture of all the processes involved is quite a challenge due to the complexity of the lipid molecules, the complex pathophysiology and the multifactorial nature of AD. Therefore, despite the ground-breaking work in the last years, the correlation between disbalance of SLs and AD and neuroinflammation remains insufficiently characterised. Therefore, due to these

unsolved research gaps, it is of fundamental importance to perform research on lipids and lipid transporters, also because they are actionable targets for potential new pharmaceutical strategies to prevent, attenuate or possibly reverse the pathophysiology of the neurodegenerative process. SL research is an attractive and active field of research, as its significant and undisputed implication in neurodegenerative diseases has been the focus of increasing interest. Understanding the crosstalk between neuroinflammation and SLs disbalance is likely to be of great importance for neurodegenerative diseases with implications for translational and clinical studies.

Therefore, new research initiatives are needed to unravel the interconnection between these processes and to understand not only how the SL and SL-related proteins disbalance could possibly influence the neurodegeneration, but also how SLs and SLs transporters could be modulated and re-stabilized in the attempt of trying to stop the disease. The study of new SL drug targets is the key focus of investigations leading to possible translational and clinical research applications aiming to slow or reverse the disease progression.

General objective

SLs are building blocks of cells membranes influencing the composition of lipid rafts micro-domains, vesicle fusion, and secretion [24]. Furthermore, it has been shown that their metabolism produces bioactive second messengers regulating multiple cellular functions including signalling, apoptosis, immune function, and metabolism [2].

SLs are highly abundant in the brain while variations in their levels or in their metabolic products have been clearly linked to several brain disorders such as schizophrenia, and neuro-inflammatory and neurodegenerative diseases (Parkinson, Niemann-Pick disease, and amyotrophic lateral sclerosis) [17]. A highly regulated metabolism of SLs is essential to maintain the cellular homeostasis and preserve the intactness of the systems [25]. Importantly, CERTs, with their unique property to transfer ceramide between cellular membranes, influence the SL balance and regulate not only SL composition but also the cellular cascades they are involved in, both in physiological and patho-physiological conditions [5, 8]. In AD, there is an increase in ceramide levels early during the disease process [26]. This increase of ceramide, results in a decreased concentration of SM, leading to a disbalance in SL metabolic products and in the enzymes/transporters regulating the formation of complex SLs [27, 28]. In fact, genomic and proteomic studies showed that the SL disbalance in AD is also associated with upregulated expression levels of genes involved in the formation of ceramide via de *de novo* pathway and SM cascades [29] [30]. In line with that, our group showed that CERTs, were downregulated in AD brain, implying that also their role in transferring ceramide from the ER to the Golgi to form SM might be disrupted during the disease. Consistently, this results in a disbalance of the SL pathway. Importantly, it is essential to assess the impact/contribution of this phenomenon on AD pathophysiology. For this reason, understanding to what extent CERTs can affect SL concentration and function in physiological conditions can help to understand its effect during the disease process. Moreover, in view of the abundance and importance of lipids in the homeostasis of the brain, and that prior focus in the study of DNA and protein alterations have not resulted in treatments for most neurodegenerative brain disorders, targeting lipids and specifically SLs to resolve neuroinflammation and neurodegeneration may be an original approach to be used for further studies of clinical relevance in a similar approach as the fingolimod, a modulator of SLs, is used to treat multiple sclerosis (MS) [31]. The know how that this thesis will generate will, therefore, create an important impact not only for AD but also for other neurodegenerative and neuroinflammatory diseases such as PD and MS, which are characterized by a dysfunction of SLs [32].

I hypothesized that understanding the biological function of SLs in the brain can help to design new treatment strategies to target them when they are dysregulated during brain disease.

The overall aim of my thesis was to deepen the knowledge on SLs and SL transporters in physiological processes and pathophysiological cascades during neurodegeneration and neuroinflammation in order to open new venues for both fundamental research and the development of clinical trials in this area.

For this reason, we analysed the role that CERTs have in regulating ceramide concentration and vesicle formation. C**hapter 2** reports my studies on CERT as a possible mediator of the direct transport of ceramide to endosomes at ER-endosomes contact sites. The process is regulated by the PH domain of CERT and PI4P generated by PI4KIIα in the endosomes. Considering the capacity of CERTs in binding ceramide, one of the main components of lipid rafts, **Chapter 3** describes a newly developed method to visualize and monitor lipid rafts dynamics using antibodies targeting different isoforms of CERTs, strengthening the hypothesis that CERTs are ubiquitous proteins involved in diverse biological pathways. This chapter was conceived as a methodological chapter in order to facilitate the visualisation of lipid rafts with the use of antibodies. Taking into account, that CERTs are becoming significant proteins influencing several molecular processes in the brain, the work described in **Chapter 4** focus on screening potential interactors of the different domains of CERTs in order to identify binding partners of CERTs, to understand better in which processes CERTs is involved. This chapter was designed to elucidate the role of CERTs not only as a mediator of SLs metabolism but also its role in neuro-inflammatory and neurodegenerative processes others than those mediated by SLs. We were able to detect several CERTs binding proteins involved in AD pathophysiology, inflammation and cellular homeostasis. **Chapter 5** reports our review of the current state of knowledge regarding the role of SLs and their metabolites in neuroinflammatory processes with a focus on immune reactions and inflammation during AD. In particular, we highlight how SLs influence microglia and astroglia activation and oxidative stress modulation analysing the state of the art, gaps and limitation of the crosstalk between SLs and inflammation. **Chapter 6** reviews the current literature about the role of SLs and SL metabolites, as second messengers, in AD pathophysiology. Moreover, we assessed available molecules targeting SL metabolites as potential new drugs resolving AD pathology. Lately, as reported above, not only disbalance on SL concentration but also changes on expression level of SL related genes have been linked to AD

exacerbation. However, there is not an integrative approach yet to understand in which extend SL related genes are altered during AD. Therefore, **Chapter 7** describes an integrative approach to better understand the relationship between epigenetic and transcriptomic processes in regulating SL function in the middle temporal gyrus of AD patients. The epigenomic and transcriptomic approach used in this chapter highlights the importance of SL-related genes in AD, and may provide novel biomarkers and therapeutic alternatives to traditionally investigated biological pathways in AD. **Chapter 8** encompasses a general discussion and conclusion of the thesis, with a focus on the limitations of the studies and further perspectives. **Chapter 9** emphasizes the scientific impact and the importance of the studies developed in this thesis.

References

1. *Pralhada Rao, R., et al., Sphingolipid Metabolic Pathway: An Overview of Major Roles Played in Human Diseases. Journal of Lipids, 2013.* **2013**: *p. 178910.*

2. *Hannun, Y.A. and L.M. Obeid, Sphingolipids and their metabolism in physiology and disease. Nature Reviews Molecular Cell Biology, 2018.* **19***(3): p. 175-191.*

3. *Gault, C.R., L.M. Obeid, and Y.A. Hannun, An overview of sphingolipid metabolism: from synthesis to breakdown. Adv Exp Med Biol, 2010.* **688**: *p. 1-23.*

4. *Hanada, K., et al., Molecular machinery for non-vesicular trafficking of ceramide. Nature, 2003.* **426***(6968): p. 803-9.*

5. *Mencarelli, C., et al., The ceramide transporter and the Goodpasture antigen binding protein: one protein--one function? J Neurochem, 2010.* **113***(6): p. 1369-86.*

6. *Large-scale discovery of novel genetic causes of developmental disorders. Nature, 2015.* **519***(7542): p. 223-8.*

7. *Rao, R.P., et al., Ceramide transfer protein deficiency compromises organelle function and leads to senescence in primary cells. PLoS One, 2014.* **9***(3): p. e92142.*

8. *Crivelli, S.M., et al., CERT(L) reduces C16 ceramide, amyloid-β levels, and inflammation in a model of Alzheimer's disease. Alzheimers Res Ther, 2021.* **13***(1): p. 45.*

9. *Murakami, H., et al., Intellectual disability-associated gain-of-function mutations in CERT1 that encodes the ceramide transport protein CERT. PLoS One, 2020.* **15***(12): p. e0243980.*

10. *Wang, X., et al., Mitochondrial degeneration and not apoptosis is the primary cause of embryonic lethality in ceramide transfer protein mutant mice. The Journal of cell biology, 2009.* **184***(1): p. 143-158.*

11. *Wang, X., et al., Mitochondrial degeneration and not apoptosis is the primary cause of embryonic lethality in ceramide transfer protein mutant mice. Journal of Cell Biology, 2009.* **184***(1): p. 143-158.*

12. *Giovagnoni, C., et al., Immunofluorescence Labeling of Lipid-Binding Proteins CERTs to Monitor Lipid Raft Dynamics. Methods Mol Biol, 2021.* **2187**: *p. 327-335.*

13. *Mencarelli, C., et al., Goodpasture antigen-binding protein/ceramide transporter binds to human serum amyloid P-component and is present in brain amyloid plaques. J Biol Chem, 2012.* **287***(18): p. 14897-911.*

14. *Bode, G.H., et al., Complement activation by ceramide transporter proteins. J Immunol, 2014.* **192***(3): p. 1154-61.*

15.   Olsen, A.S.B. and N.J. Færgeman, *Sphingolipids: membrane microdomains in brain development, function and neurological diseases.* Open Biol, 2017. **7**(5).

16.   Hussain, G., et al., *Role of cholesterol and sphingolipids in brain development and neurological diseases.* Lipids Health Dis, 2019. **18**(1): p. 26.

17.   Alessenko, A.V. and E. Albi, *Exploring Sphingolipid Implications in Neurodegeneration.* Front Neurol, 2020. **11**: p. 437.

18.   Fan, L., et al., *New Insights Into the Pathogenesis of Alzheimer's Disease.* Frontiers in Neurology, 2020. **10**(1312).

19.   Mielke, M.M., et al., *Cerebrospinal fluid sphingolipids, β-amyloid, and tau in adults at risk for Alzheimer's disease.* Neurobiol Aging, 2014. **35**(11): p. 2486-2494.

20.   Satoi, H., et al., *Astroglial expression of ceramide in Alzheimer's disease brains: a role during neuronal apoptosis.* Neuroscience, 2005. **130**(3): p. 657-66.

21.   Mielke, M.M. and C.G. Lyketsos, *Alterations of the Sphingolipid Pathway in Alzheimer's Disease: New Biomarkers and Treatment Targets?* NeuroMolecular Medicine, 2010. **12**(4): p. 331-340.

22.   Giovagnoni, C., et al., *Altered sphingolipid function in Alzheimer's disease; a gene regulatory network approach.* Neurobiol Aging, 2021. **102**: p. 178-187.

23.   Nikolova-Karakashian, M.N. and M.B. Reid, *Sphingolipid metabolism, oxidant signaling, and contractile function of skeletal muscle.* Antioxid Redox Signal, 2011. **15**(9): p. 2501-17.

24.   Mencarelli, C. and P. Martinez-Martinez, *Ceramide function in the brain: when a slight tilt is enough.* Cell Mol Life Sci, 2013. **70**(2): p. 181-203.

25.   Bruce, K.D., A. Zsombok, and R.H. Eckel, *Lipid Processing in the Brain: A Key Regulator of Systemic Metabolism.* Frontiers in Endocrinology, 2017. **8**.

26.   Filippov, V., et al., *Increased ceramide in brains with Alzheimer's and other neurodegenerative diseases.* J Alzheimers Dis, 2012. **29**(3): p. 537-47.

27.   He, X., et al., *Deregulation of sphingolipid metabolism in Alzheimer's disease.* Neurobiol Aging, 2010. **31**(3): p. 398-408.

28.   Yin, F., *Lipid metabolism and Alzheimer's disease: clinical evidence, mechanistic link and therapeutic promise.* The FEBS Journal. **n/a**(n/a).

29.   Katsel, P., C. Li, and V. Haroutunian, *Gene expression alterations in the sphingolipid metabolism pathways during progression of dementia and Alzheimer's disease: a shift toward ceramide accumulation at the earliest recognizable stages of Alzheimer's disease?* Neurochem Res, 2007. **32**(4-5): p. 845-56.

30. Jęśko, H., et al., *Fingolimod Affects Transcription of Genes Encoding Enzymes of Ceramide Metabolism in Animal Model of Alzheimer's Disease.* Mol Neurobiol, 2020. **57**(6): p. 2799-2811.

31. Willis, M.A. and J.A. Cohen, *Fingolimod therapy for multiple sclerosis.* Semin Neurol, 2013. **33**(1): p. 37-44.

32. Galvagnion, C., et al., *Sphingolipid changes in Parkinson L444P GBA mutation fibroblasts promote α-synuclein aggregation.* Brain, 2022.

Chapter 2

Function of ceramide transfer protein for biogenesis and sphingolipid composition of extracellular vesicles

Simone M. Crivelli[1,2], Caterina Giovagnoni[3], Zhihui Zhu[1], Priyanka Tripathi[1,2], Ahmed Elsherbini[1], Zainuddin Quadri[1], Liping Zhang[1,2], Branislav Ferko[4], Dusan Berkes[4], Stefka D. Spassieva[1], Pilar Martinez-Martinez[3#], Erhard Bieberich[1,2#]

[1]Department of Physiology, University of Kentucky, Lexington, KY
[2]Veterans Affairs Medical Center, Lexington, KY 40502, United States
[3]Maastricht University, Department of Psychiatry and Neuropsychology, School for Mental Health and Neuroscience, Maastricht, the Netherlands
[4]Department of Organic Chemistry, Slovak University of Technology, Radlinského 9, 81237, Bratislava, Slovak Republic
#Shared senior authorship

Abstract

The formation of extracellular vesicles (EVs) is induced by the sphingolipid ceramide. How this pathway is regulated is not entirely understood. Here, we report that the ceramide transport protein (CERT) mediates a non-vesicular transport of ceramide between the endoplasmic reticulum and the multivesicular endosome at contact sites. The process depends on the interaction of CERT's PH domain with PI4P generated by PI4KIIα at endosomes. Furthermore, a complex is formed between the START domain of CERT, which carries ceramide, and the Tsg101 protein, which is part of the endosomal sorting complex required for transport (ESCRT-I). Inhibition of ceramide biosynthesis reduces CERT-Tsg101 complex formation. Overexpression of CERT increases EV secretion while their inhibition reduces EV formation and the concentration of ceramides and sphingomyelins in EVs. In conclusion, we discovered a function of CERT in regulating the sphingolipid composition and biogenesis of EVs, which links ceramide to the ESCRT-dependent pathway.

2.1 Introduction

The sphingolipid ceramide is important for extracellular vesicle (EV) formation in vitro and in vivo [1-4]. Generation of ceramide at the plasma membrane and/or at the endosomal system by the enzyme neutral sphingomyelinase 2 (N-SMase 2) regulates EV biogenesis [3, 4]. By breaking down sphingomyelin (SM), N-SMase 2 increases the membrane levels of ceramide, which favors membrane budding because of its peculiar cone-shaped structure [3]. This process is thought to be independent of the endosomal sorting complex required for transport (ESCRT), which consist of approximately twenty proteins assembling into four complexes (ESCRT-0, -I, -II and -III) that regulates cargo selection and biogenesis of EVs [5].. However, other enzymes in sphingolipid metabolism have been shown to regulate EV formation, such as sphingomyelin synthase 1 (SMS1) and sphingomyelin synthase 2 (SMS2) which convert ceramide into SM in the trans-Golgi and plasma membrane, respectively. When SMS1 transcription is silenced, cells increase the number of EVs by about twofold [6]. Similarly, inhibition of SMS2 stimulates a remarkable fourfold increase of EV secretion [6]. Therefore, the accumulation of ceramide in the trans-Golgi and plasma membrane seems to regulate EV formation without necessarily invoking the activation of N-SMase-2. How these ceramide-dependent pathways are controlled remains poorly understood. Furthermore, it is still not clear how the lipid profile of EVs is regulated. In fact, the lipid composition of EVs is not identical to the lipid profile of the donor cells [7]. Interestingly, the EV membrane is particularly enriched in sphingolipids compared to the membrane of the donor cells [7]. How the sphingolipid composition is regulated in the endosome pathway and in EVs is yet to be investigated.

The ceramide transfer protein (CERT) is an essential protein of the sphingolipid metabolism [8-11]. After ceramide is synthetized in the endoplasmic reticulum (ER), CERT extracts and relocates ceramide to the trans-Golgi where SM is synthesized [12, 13]. There are three functional domains of CERT involved in this process. The steroidogenic acute regulatory protein (StAR)-related lipid transfer START domain binds to ceramide and very poorly to other lipids such as diacylglycerols, which structurally resemble ceramide [11]. The pleckstrin homology domain (PH) targets phosphatidylinositol 4-monophosphate (PI4P), which is particularly enriched in the *trans*-Golgi [14, 15]. Finally, the two phenylalanines in an acidic tract (FFAT) motif interact with the ER-resident protein VAMP-associated protein (VAP) [16]. Pharmacological displacement of ceramide from the START domain pocket with ceramide analogs such as HPA-12, or genetic mutation and inactivation of the of PH domain, rapidly reduces SM synthesis [17, 18]. HPA-12 displaces endogenous ceramide and occupies the amphiphilic cavity of the START domain of CERT preventing ceramide to be

shuttled to the *trans*-Golgi [18, 19]. Interestingly, Fukushima et al., proposed a model in which CERT mediates the release of EVs enriched in ceramide, under lipotoxic conditions [20]. Furthermore, Barman et al. just recently highlighted the role of CERT in the biogenesis of a unique subset of RNA-containing EVs [21]. However, it remains unknown whether CERT plays a role in the EV machinery under physiological conditions and how CERT mechanistically participates in EV biogenesis.

In this study, we show that CERT enters the endocytic pathway and is released in EVs. Translocation of CERT to the multivesicular endosome (MVE) is dependent on the interaction of CERT's PH domain with PI4P at the MVE. We also discovered that a CERT-mediated transport of ceramide from the ER to late endosomes is regulated by PI4P generated by PI4KIIα. A complex is formed between CERT and tumor susceptibility gene 101 protein (Tsg101), which is part of the ESCRT-I complex. Inhibition of ceramide synthesis in the ER by Fumonisin B1 (FB1) reduces CERT-Tsg101 complex formation. Overexpression of CERT in neuronal cells increases EV secretion while functional inhibition of CERT with the drug HPA-12 reduces EV formation and the concentration of ceramide and SM in EVs. Our data indicate a crucial role of CERT in the biogenesis and regulation of ceramide and SM levels in EVs. We also provide for the first time evidence that CERT links ceramide to the ESCRT-dependent pathway for EV biogenesis.

2.2   Materials and Methods

Cloning, constructs and antibodies

The human CERT (isoform 2, 1800bp, NCBI Reference Sequence: NM_NM_031361.3) and CERTL (isoform 1, 1875bp, NCBI Reference Sequence: NM_005713.3) were constructed in the pcDNA3.1 plasmid, obtaining plasmids pcDNA3.1-CERT and pcDNA3.1-CERTL respectively. CERTL was also subcloned in the pEGFP-N1 plasmid to generate full length GFP tagged CERTL plasmid (FL-CERTL-GFP) with the following primers: forward CAG ATC TCG AGA TGT CGG ATA ATC AGA GCT GGA ACT CGT CG and reverse CAT GGT ACC GCG AAC AAA ATA GGC TTT CCT GCA GT. The PH deficient CERT was cloned in the pEGFP-N1 plasmid (PH-deficient CERTL-GFP) with the following primers: forward CAG ATC TCG AGA TGA ATC AGC TT GCG TCG ACA TGG CTC AAT GG and reverse CAT GGT ACC GCG AAC AAA ATA GGC TTT CCT GCA GT. For transfection, the pEGFP-N1 plasmid was used as a control vector. pcDNA3.1-CERT, pcDNA3.1-CERTL, FL-CERTL-GFP or PH-deficient CERTL-GFP were used for overexpression of CERT. The two isoforms, CERT and CERTL, had a similar effect on EVs biogenesis, which enabled us to use the two CERT isoforms interchangeably depending on the assay performed. A plasmid containing tdTomato-CD9 (AddGene, plasmid #58076) was used for colocalization studies at the MVE. Transfection was performed using Lipofectamine 3000 (ThermoFisher), Effectene Transfection reagent (Qiagen) or Polyethyleneimine.

The labelling primary antibodies were used: anti-Alix mouse IgG (1:1000, Santa Cruz, 1A12), anti-βactin mouse (1:1000, Santa Cruz, AC-15), anti-Calnexin goat IgG (1:100 for immunofluorescence (IF) Santa Cruz, C-20), anti-CD81 mouse IgG (1:100 for IF, and 1:500 for Western blotting, Santa Cruz, B-11), anti-CD81 rabbit IgG (1:100 for IF, Santa Cruz, H-121), anti-CERT rabbit IgG (1:500 for IF and 1:2500 for Western blotting, Bethyl Laboratories, A300-669A), mouse monoclonal anti-CERTL antibody (clone 3A1H9) [22], anti-EEA1 mouse IgG (1:100 IF Santa Cruz, E-8), anti-Flotillin-2 mouse IgG (1:1000 for Western blotting, BD Biosciences, 610383), anti-Flotillin-1 mouse IgG (1:1000 for Western blotting, BD Transduction Laboratories, 610820), anti-GFP mouse IgG (1:1000 for Western blotting, Santa Cruz, B-2), anti-GM130 mouse IgG (1:100, BD Biosciences), anti-LAMP1 mouse IgG (1:100 IF Santa Cruz, H4A3), anti-LBPA mouse IgG (1:300 IF, Echelon Bioscience), anti-N-Smase-2 mouse (1:1000, Santa Cruz, G-6) and anti-Tsg101 mouse IgG (1:100 for IF and 1:1000 for Western blotting, Santa Cruz, C-2). The rabbit γ-immunoglobin (Jackson ImmunoResearch) was used as technical control in the PLA assay with anti-Tsg101 at a final concentration of 4 ng / μL. Secondary

antibodies were Cy2-conjugated or Alexa-647 donkey anti-mouse IgG, or Cy3-conjugated donkey anti-rabbit IgG, (1:500 Jackson ImmunoResearch).

Yeast Two-Hybrid Analysis (Y2Hs)

Yeast two-hybrid screening was performed by Hybrigenics Services, S.A.S., Evry, France (http://www.hybrigenics-services.com).The coding sequence of the N-terminus (aa 1-116) of human CERT (NM_005713.3) was PCR-amplified and cloned into pB29 as an N-terminal fusion to LexA (CERT-Nter-LexA) and pB66 as a C-terminal fusion to the Gal4 DNA-binding domain (Gal4-CERT-Nter). The coding sequence of the C-terminus (aa 397-624) of CERT was PCR-amplified and cloned into pB27 and pB66 as a C-terminal fusion to LexA (LexA-CERT-Cter) and the Gal4 DNA-binding domain (Gal4-CERT-Cter), respectively. The constructs were checked by sequencing and used as baits to screen a random-primed human adult brain cDNA library constructed into pP6 as described previously [23] [24], [25] [26]. The clones and colonies were screened and selected as previously described [30].The prey fragments of the positive clones were amplified by PCR and sequenced at their 5' and 3' junctions. The resulting sequences were used to identify the corresponding interacting proteins in the GenBank database (NCBI) using a fully automated procedure. A confidence score (PBS, for Predicted Biological Score) was attributed to each interaction as previously described [27].

Immunoassay for detection of the CERT-Tsg101 complex and complex modelling with AlphaFold2 in ColabFold

ELISA. Maxisorp plates (Nunc, 423501, Biolegend) were coated with 2 µg / mL of recombinant human CERTL (rCERTL), produced as previously described [28], overnight at room temperature in 0.1 M carbonate buffer (pH 9.6), 100 µL / well. The next day plates were washed with 0.005% Tween 20 in PBS (washing buffer 200 µL / well) and blocked for 1 h at 37°C with 3% BSA in PBS 200 µL / well. Recombinant full length human Tsg101 (Origene, TP710086) was incubated for 1 h at 37°C in serial dilutions 1, 0.5, 0.25, 0.125, 0.0625 and 0.03125 µg / mL in incubation buffer composed by 0.1% BSA in washing buffer 100 µL / well. After washing, 1 µg / mL of anti-Tsg101 mouse IgG (Santa Cruz, C-2) was incubated for 1 h followed by washing and anti-mouse-HRP donkey IgG (Jackson ImmunoResearch) diluted in incubation buffer to 0.1 µg / mL. After developing with 3,3',5,5'-Tetramethylbenzidine (TMB) the absorption was measured at 450 nm within 15 min of stopping the reaction with 2M H_2SO_4 using Synergy H1 (BioTek) multi-mode microplate reader. Wells coated

with 2 μg / mL Ovalbumin were used as technical control. When coating with rTsg101 (1 μg / mL, 100 μL / well) detection of rCERTL (serial dilutions 2, 1, 0.5, 0.25, 0.125, 0.062, 0.031.μg / mL) was performed with anti-CERTs rabbit IgG (Bethyl Laboratories, A300-668A, epitope 1-50) or anti-CERTs rabbit IgG (Bethyl Laboratories, A300-669A, epitope 300-350) followed by anti-rabbit-HRP donkey IgG (Jackson ImmunoResearch).

AlphaFold 2 in CoLabFold. In the open source Google CoLabFold platform the human FASTA sequence of the START domain (Uniprot ID: |Q9Y5P4|389-618) and UEV domain of human Tsg101 (Uniprot ID: |Q99816| 2-145) were pasted in the query sequence box and the complex prediction was run with the following advance settings: msa mode: Mmseqs, model type AlphaFold2-multimer, pair mode unpaired+paired and number of recycles were set to 12 as suggested [29]. Here we report only the output of the best ranked model. The output consists of: 1) the schematic structure colored by polymers chain, 2) schematic structure colored by predicted Local Distance Difference Test (pLDDT) and the predicted aligned error (PAE) [29]. pLDDT value close to 100 (darker blue areas in pLDDT schematic structure) represent alignments with high confident prediction. Nevertheless, the PAE (or the predicted Tmscore, which is derived from PAE) are better to assess the confidence of the predicted complex structure. Very low PAE score are associated with high confidence predictions [29]. The 3D structure and the color surface electrostatic potential of the complex were created with UCSF ChimeraX version: 1.3 [30].

Animals

C57BL/6 wild type (WT) mice were bred in-house. Animals were socially housed under a 12 h light/dark cycle in individually ventilated cages. Food and water were provided ad libitum throughout the study. Neonates P0 were used to generate primary neurons as explained in the section below. HPA-12 was dissolved in ethanol and further diluted in Dulbecco's Phosphate-Buffered Saline (DPBS) without calcium and magnesium (Corning, MA, USA) to reduce ethanol concentration to 5%, which is well tolerated by mice [31]. HPA-12 was administered intraperitoneally (IP) at the dose 2 μg / g animals given every 48 h. The vehicle (5% ethanol in DPBS) was used as a control. The volume injected per animal was adjusted to 0.2 mL and administered with insulin syringes. Two-month-old mice, 10 females and 10 males, were equally divided in vehicle control or HPA-12-treated group. All experiments using mice to generate primary cell cultures or drug testing were carried out according to an Animal Use Protocol approved by the Institutional Animal Care and Use Committee at the University of Kentucky.

<u>Cell culture</u>

Neuro-2a (N2a) were obtained from ATCC (CCL-131™) and maintained at 37°C and 5% CO2 atmosphere in Dulbecco's modified Eagle's medium (DMEM) (Gibco, Invitrogen, CA, USA) supplemented with 10% fetal bovine serum (FBS) (Corning, MA, USA) and 100U / mL penicillin-streptomycin (hyClone, GE Healthcare, UT, USA). For immunocytochemistry, N2a cells were seeded on poly-L-lysine (Milipore-Sigma, MT, USA) coated coverslips at 50,000 cells/coverslip. Cells were gradually deprived of serum for 2 to 3 days to allow for differentiation into a neuronal phenotype before immunostaining.

HeLa wild type (WT) and HeLa CERT-deficient (TAL-CE#14)[17] were a kind gift from Prof. Kentaro Hanada, Department of Biochemistry and Cell Biology, National Institute of Infectious Diseases, Tokyo, Japan. Cells were maintained in DMEM supplemented with 10% FBA and penicillin-streptomycin.

Primary neurons were cultured from wild type neonates (P0) as previously described [28]. In brief, the cortical area was digested with 0.25% Trypsin in HBSS (Corning, MA, USA) for 15 min at 37º C and the reaction stopped with pre-warmed plating medium, DMEM (Gibco, Invitrogen, CA, USA) containing 10% FBS and N2 supplement. Then, the cell suspension was passed through a 40 µm cell strainer, spun down, and cells seeded in plating medium for 4 h. The plating medium was replaced with Neurobasal medium supplemented with B27 supplement, Penicillin/Streptomycin, L-glutamine, and cells cultivated for 10-14 days. Every other day, half of the Neurobasal medium with supplements was replaced.

<u>Incubation of cells with Fumonisin B1, PI4KIIIβ-IN-10, NC03, anti-HPA-12, syn-HPA-12 and Cer 18:1/16:0</u>

Fumonisin B1 (FB1) was purchased from Enzo Lifesciences and a stock solution (10 mM) prepared in water. FB1 was used in cells at a final concentration of 10 µM for 24 h. The compound PI4KIIIβ-IN-10 was purchased from MedChemExpress and a stock solution of 50 µM was prepared in water and stored at -20°C. PI4KIIIβ-IN-10 was used in cells at a final concentration of 25 nM for 24 h. The PI4KIIα inhibitor NC03 was purchased from Aobious and dissolved in DMSO. NC03 was used at a final concentration of 10 or 5 µM. Both HPA-12 stereoisomers were synthesized as previously reported [32] and dissolved in ethanol. anti-HPA-12 and syn-HPA-12 were added to the cells at a concentration of 4 or 8 µM for 24h. Before incubating of cells, FB1, PI4KIIIβ-IN-10, NC03 anti-HPA-

12, syn-HPA-12 were diluted in DMEM phenol red-free medium (Gibco, Invitrogen, CA, USA) without serum and supplemented with L-glutamine and 100U / mL penicillin-streptomycin (hyClone, GE Healthcare, UT, USA). The solution of Cer d18:1/16:0 2% dodecane in ethanol was dissolved in DMEM phenol red-free medium with supplements as listed above and 0.34 mg / mL of defatted bovine serum albumin (Sigma). Cells were incubated for 24 h with 5 µM of Cer d18:1/16:0 alone or with 8 µM of syn-HPA-12.

Immunofluorescence Labelling

N2a or neuronal cells, prepared as described above, were fixed with ice-cold 4% PFA in PBS for 10 min, permeabilized with 0.25% Triton-X in PBS for 5 min and blocked with 3% BSA in PBS for 1 h. Primary antibodies were diluted in incubation buffer 0.3% BSA in PBS at 4 °C overnight. The next day, cells were washed 3-times with PBS and incubated with secondary antibodies for 1 h at 37 °C. Coverslips were mounted using Fluoroshield supplemented with DAPI (Sigma-Aldrich) to visualize the nuclei. Fluorescence microscopy was performed using an Eclipse Ti2-E inverted microscope system or Nikon A1R Confocal Microscope (Nikon, New York, USA). Images were processed and analyzed using Nikon NIS-Elements software equipped with a 3D deconvolution program and particle analyzer.

Proximity ligation assay

N2a or neuronal cells were cultivated on coverslips and transfected with Lipofectamine P3000 (ThermoFisher) and tdTomato-CD9, pcDNA3.1-CERTL or FL-CERTL-GFP plasmid or treated with the drugs FB1 and HPA-12. After 24 h, cells were fixed and permeabilized as described above. The primary antibodies, anti-CD81 rabbit and anti-CERTL mouse IgG or anti-Tsg101 mouse and anti-CERT rabbit IgG, were incubated overnight. Rabbit γ-immunoglobin was used as technical control. The next day, cells were washed with PLA labelling buffer prior to the PLA reaction following the manufacturer's manual (Duolink). Images obtained with only one primary antibody or using rabbit IgG and both secondary antibodies for PLA were used as negative controls to correct for background fluorescence signals. Photomicrographs were acquired in multiple planes at different depths and a maximum intensity projection was created for counting of PLA signals and DAPI staining (for cell counts) with particle analyzer of Nikon software.

Analysis of Phdeficient-CERT$_L$-GFP and FL-CERT$_L$-GFP cell distribution

N2a cells on coverslips were transfected with Phdeficient or FL-CERTL-GFP for 24-48 hours with Effectene Transfection reagent (Qiagen). Then, cells were fixed and permeabilized as described above. The primary antibodies to detect Golgi, early and late endosome were incubated overnight. The subcellular distribution was analyzed in multiplane z-stack images acquired on confocal microscope Nikon A1R Confocal Microscope (Nikon, New York, USA). Before determining the quantity of colocalization of the green channel (CERTL-GFP) with the magenta channel (GM130, EEA1 or LPBA) by Pearson's correlation coefficient, the images were deconvolved with Nikon NIS-Elements software.

Analysis of BODIPY FL C5-Cer redistribution to Golgi and MVE/LE

For BODIPY FL C5-Cer (BODIPY™ FL C5-Ceramide complexed to BSA, ThermoFisher) transport to the Golgi and MVE/LE, HeLa WT or CERT-deficient cells were plated onto bottom glass 6 wells plates with 14 mm micro wells (Cellvis P06-12-0-N). For the Golgi transport, on the day of the experiment cells, were pre-treated with PI4KIIIβ-IN-10 (25 nM and 50 nM) and NC03 (5 and 10 µM) for 15 min. Next, cells were incubated on ice for 20 min with 0. 5 µM BODIPY FL C5-Cer in phenol red and serum-free DMEM, and the excess fluorescent dye was removed by washing with serum-free DMEM. Next, BODIPY FL C5-Cer was allowed to be distributed in cells for 10-15 min at 37°C before cells were fixed in 2.5% PFA and 2.5% glutaraldehyde. For the MVE/LE transport, HeLa WT or CERT-deficient cells were transfected with a fusion construct of Rab7a and TagRFP (CellLight™ Late Endosomes-RFP, BacMam 2.0, ThermoFisher) 24 hours before incubation with BODIPY FL C5-Cer. The distribution of BODIPY FL C5-Cer was analyzed with the Eclipse Ti2-E inverted confocal microscope using a 100x objective. A minimum of 4 images with 9-13 planes in Z-direction were acquired for each condition and deconvolved before quantifying Golgi mean fluorescent intensities (MFI) or BODIPY FL C5-Cer correlation to late endosomes-RFP. MFI and correlation were assessed with the Nikon analyzer software.

Incubation of cells with fluorescent HPA-12-NBD and bifunctional pacHPA-12

Fluorescent HPA-12 (HPA-12-NBD) was synthesized as previously described [33]. The synthesis of bifunctional HPA-12 (pacHPA-12) is described in Supporting Information. HPA-12-NBD and pacHPA-12 were dissolved in ethanol at 1.77 and 5.5 mM, respectively, and stored at -80 °C.

N2a cells were seeded on coverslips or 6 well glass bottom plates (Cellvis, Mountain View, CA). The following day, cells were transfected with tdTomato-CD9 plasmid for 24-48 hours. Then, the medium was changed to a medium containing 1 μM HPA-12-NBD and immediately live-imaged by fluorescent microscopy using a 60x objective.

The bifunctional HPA-12 analog (pacHPA-12) was used following the protocol previously published for the bifunctional Cer analog (pacFACer) [34]. In brief, cells were incubated with 1 μM pacHPA-12 for 15- or 30-min. Cells were washed with medium and then irradiated with UV light (366 nm) for 15 min to cross-link the analog to CERT. Then, cells were washed with culture medium to remove unbound analog and 3-times with cold DPBS, fixed, and permeabilized as described above. The fluorophore, Alexa Fluor 647 azide was covalently linked to the alkyl group of pacHPA-12 using the Click-iT™ Cell Reaction Buffer Kit (Thermo Fisher, MA, USA). Next, cells were co-labelled for MVE markers, e.g., CD81. Coverslips were mounted and imaged by fluorescence microscopy.

<u>EV isolation</u>

Cell culture supernatants. Evs were isolated from cell culture supernatants by differential ultracentrifugation. N2a cells were grown to 80-90% confluency and medium replaced with phenol red- and serum-free DMEM medium (Gibco, Invitrogen, CA, USA) and cultivated for 48 h. The media were transferred to a 15 ml Falcon conical tube and centrifuged at 300 x g for 5 min to remove floating cells. Supernatants were collected and centrifuged for 20 min at 4,000 x g to remove dead cells and at 10,000 x g for 40 min to collect larger Evs. Lastly, samples were transferred into polypropylene centrifuge tubes (Beckman Coulter, CA, USA), balanced and ultra-centrifuged at 100,000 x g for 2 h. Pelleted Evs were resuspended in 0.1 mL DPBS (Corning, MA, USA). Alternatively, two additional approaches were performed: i) after the 4,000 x g centrifugation step, Evs were isolated with ExoEasy Maxi kit (Qiagen, MD, USA) following the manufacturer's instruction; ii) or after the 100,000 x g centrifugation step, a discontinuous sucrose gradient was used. The gradient formed by 10, 30, 40 and 60% sucrose was spun for 16 h at 100,000 x g. The four fractions corresponding to each interface were collected. All fractions were diluted 1:5 in DPBS and centrifuged again for 2 h at 100,000 x g. Pellets were dissolved in 0.1 mL of DPBS. The interfaces at 10-30% and 30-40% sucrose were positive for the EV marker Alix1.

Serum. Blood was collected as previously described [35]. In brief, blood was drawn from the heart and was allowed to clot at room temperature for 30 min. Next, samples were centrifuged at 1,800

x g for 10 min at 4 °C. to prepare the serum fraction. The clear upper layer (serum) was transferred to a fresh tube and centrifuged at 10,000 x g for 15 min to pellet residual blood cells. Then Evs were isolated from 150 μL of serum using ExoQuick solution (EXOQ; System Biosciences, Inc., Mountain View, CA, USA). The ExoQuick preparation was used for NTA measurement and lipid analysis or further purified with sucrose gradient and NTA measurements repeated.

Brain tissue. Brains were collected soon after the blood was drawn from the heart. Then, the forebrain was dissected in ice cold PBS and snap-frozen in liquid nitrogen inside an Eppendorf previously weighed. Evs were isolated as previously described with modifications [36]. In brief, frozen forebrain was digested with papain for 20 min at 37°C and passed through a 10 mL serological pipette before the reaction was stopped on ice with proteinase inhibitors. Then, the solution was sequentially centrifuged as follows: 300 x g for 5 min, 4,000 × g for 20 min, and 10,000 x g for 40 min. Before precipitating the Evs at 100,000 x g, the solution was filtered using a 0.45 μm membrane filter. The precipitate was dissolved in 5% sucrose in DPBS and loaded onto a discontinuous gradient formed by 10, 30, 40 and 60% sucrose in DPBS. The gradient was spun for 16 h with at 100,000 x g. Four fractions were collected corresponding to each interface. All fractions were diluted 5-fold in DPBS and centrifuged again for 2 h at 100,000 x g. Pellets were dissolved in 0.3 mL DPBS.

Alternatively, after the 10,000 x g centrifugation and 0.45 μm filtration, Evs were collected using the ExoEasy Maxi kit (Qiagen) following the manufacturer's instructions.

Nanoparticle Tracking Analysis (ZetaView) and ExoView

ZetaView. Nanoparticle Tracking Analysis was performed using a Zetaview instrument. All samples were diluted in DPBS (Corning, MA, USA) before injection into the instrument. Measurement concentrations were determined by pre-testing the ideal particle per frame value (100–200 particles/frame). Optimal camera settings were initially established and kept constant throughout the analyses (Sensitivity: 150-250; Shutter: 74-76; cell temperature: 25°C). After capture, the videos were analyzed by the built-in ZetaView Software. The Evconcentration was normalized to the number of cells measured by an automated cell counter (TC20 Biorad), volume of serum, or by tissue weight.

ExoView. Brain Evs were diluted in Solution A (NanoView bioscience, EV-SOLA10-30) while serum Evs were loaded without purification or dilutions steps. 40 μL of sample were incubated O.N. at RT on pre-scanned ExoView Tetraspanin chips, placed in a sealed 24-well plate. The chips contained

spots printed with anti-CD81, or anti-CD9 antibodies or mouse IgG1κ matching isotype antibody, used as a control for non-specific EV binding (NanoView bioscience, EV-TETRA-MI). Chips were then moved to an automated ExoView® CW100 Chip Washer and the tetraspanin program was selected. The following antibody mixture was used to label Evs: anti-Ceramide labelled with anti-rabbit IgG conjugated to Alexa 647 using the Zenon™ Rabbit IgG Labeling Kit (ThermoFisher), anti-CD81 conjugated 555 (NanoView bioscience, EV-mCD81-A-555) and anti-CD9 conjugated 488 (NanoView bioscience, EV-mCD9-A-488), all of them diluted in blocking solution. Chips were then imaged with the ExoView R100 reader using the ExoScan 3.0 acquisition software. Images acquired were analyzed using ExoViewer 3.0 software.

Electron microscopy

HeLa WT cell were grown on Costar® 6-well Clear (3506) to 100% confluency, fixed in 4% PFA in PBS for 45 min and permeabilized for 10 min with 50% Ethanol. After washing with PBS, cells were blocked with 3% BSA for 1 h and the anti-CERT antibody (Bethyl Laboratories, A300-669A) was incubated O.N. at 4°C. Next day anti-rabbit IgG Alexa Fluor® 647 Fluoro (1.4nm)Nanogold (Nanoprobes) was incubated for 2 hours. Then samples were washed 3x in PBS, post-fixed with 1% glutaraldehyde in PBS (10 min) rinsed with deionized water 2x and HG Silver enhancement kit (Nanoprobes, 2012-45ML) was performed following manufacturer instruction. Samples were rinsed in deionized water and lastly with PBS. Next, samples were incubated with 0.2% osmium tetroxide in PBS (30 min on ice), rinsed with deionized water and exposed to 0.25% Uranyl acetate for 1 h on ice to better preserve immunogold labelling [37]. Finally, samples were dehydrated at room temperature in a graded series of ethanol (4 min interval) at 50%, 70%, 90%, and 3 changes of 100%, and were embedded after 2 changes of 100% resin for 45–60 min in 60 °C oven. Polymerization was allowed to proceed for 2 days. Embedded cells were separated from the plastic culture ware, trimmed and ~70 nm sections were cut with microtome and mounted on FCF-200-Cu grids. Brain-derived EV were fixed in 2% PF and 5-7 μL were loaded on FCF-200-Cu grids for 1 min and stained with 1% uranyl acetate for 10 seconds. After excess of uranyl acetate was removed samples were dried before imaging. Images were acquired using a Thermo Scientific™ Talos™ F200X TEM operating at 200 kV accelerating voltage in STEM mode. Low beam current and long dwell times (50 μs) were used to maximize contrast while minimizing beam damage.

Cytosolic and membrane-bound protein extraction

Cells were washed with ice-cold DPBS, trypsinized and centrifuged at 300 x g for 5 min at 4°C. The cell pellet was resuspended in 0.5 mL ice-cold homogenization buffer containing 250 mM sucrose, 1 mM EDTA, 10 mM Tris-HCl buffer at pH to 7.2, and Halt™ Protease Inhibitor Cocktail (Thermo Fisher, MA, USA) and sonicated using a probe sonicator. The homogenate was centrifuged at 700 x g for 10 min at 4°C to remove intact cells, nuclei and cell debris. The supernatant was further centrifuged at 100,000 x g for 1 h at 4°C. The supernatant was considered the cytosolic fraction and the pellet was resuspend in 0.5 mL RIPA buffer (250 mM Tris-HCl (pH 7.4), 750 mM NaCl, 5% NP-40, 2.5% sodium deoxycholate, 0.5% SDS) and incubated for 15 min at 4°C with occasional vortexing. Lastly, the sample was centrifuged at 100,000 × g for 30 min at 4°C and the supernatant was transferred to a fresh tube and considered the membrane fraction.

Immunoblot analysis

Evs derived from equal amounts of cells, serum or brain were solubilized with 5X Laemmli sample buffer (10% SDS, 250 mM Tris pH 6.8, 1 mg / mL bromophenol blue, 0.5 M DTT, 50% glycerol, 5% β-mercaptoethanol) and heated to 95°C for 5 min. When protein extraction from cells or brain was not prepared by fractionation as explained above protein were extracted in RIPA buffer. Proteins were separated using SDS-PAGE gels (8 or 10%) or pre-cast gels 4-20% (mini-PROTEAN TGX, Biorad) and transferred to nitrocellulose membranes. After blocking with 5% NFDM (Blotting-grade blocker, Biorad) for 1 h, blots were probed with primary antibodies overnight at 4°C and incubated with an HRP-conjugated secondary antibody. The membranes were developed with Clarity Western ECL Substrate (Biorad) or SuperSignal™ West Femto Substrate (ThermoFisher) and images were acquired on a ChemiDoc imaging system (Biorad).

Sphingolipid analysis

The sphingolipid analyses on cells and cell-derived Evs were performed by the VCU Lipidomics/Metabolomics Core (VLMC). Cell pellets and 100k fractions were analyzed for the following sphingolipids: sphingosine, sphinganine, sphingosine-1-phosphate, sphinganine-1-phosphate, ceramide (N-acyl chain lengths = C14:0, C16:0, C18:1, C18:0, C20:0, C22:0, C24:1, C24:0, C26:1, C26:0), monohexosylceramide (N-acyl chain lengths = C14:0, C16:0, C18:1, C18:0, C20:0,

C22:0, C24:1, C24:0, C26:1, C26:0) and SM (N-acyl chain lengths = C14:0, C16:0, C18:1, C18:0, C20:0, C22:0, C24:1, C24:0, C26:1, C26:0).

The sphingolipids of serum and brain-derived Evs were measured by to the lipidomics core facility at the Medical University of South Carolina, Charlston, SC (Dr. Besim Ogretmen, director) (https://hollingscancercenter.musc.edu/) as previously described [38, 39].

<u>Statistical analysis</u>

The statistical analyses were performed using GraphPad Prism version 8.4.3 (686). Unpaired t-test was used for comparing of two means or Whitney Mann test when normality distribution was not met. One-way ANOVA followed by Sidak's or Dunnett's multiple comparisons test was used for comparing more than 2 conditions or for investigating HPA-12 effect across ceramide or SM species. A p-value of <0.05 was considered significant.

2.3   Results

<u>CERT is associated with MVE and interacts with Tsg101 via the START domain.</u>

It has been reported that CERT is important for EV secretion under palmitic acid overload state in hepatocytes [20]. However, it remains unknown whether CERT plays a role in EV formation under physiological conditions and how mechanistically CERT participates in EV biogenesis.

Immunofluorescence labeling in N2a cells showed partial colocalization of CERT with Early Endosome Antigen 1 (EEA1) and lysobisphosphatidic acid (LBPA), which are markers for early and late endosomes/MVE (Figure 1A). A similar pattern was found with primary cultured mouse neurons (Supplementary Figure 1A). CERT also colocalized with other MVE markers such as the cluster of differentiation 9 (CD9) (Supplementary Figure 1B). To analyze whether CERT is released in association with small EVs, we isolated EVs from the culture medium of N2a cells at 90-100% confluency by using ultracentrifugation on a discontinuous sucrose gradient. The majority of CERT was enriched in the same fraction as the exosomal marker protein Alix (Figure 1B).

Since we found CERT to be part of the MVE and EVs, we tested if CERT interacted with the proteins of the ESCRT complex. Therefore, we screened for possible interactors by using a two-hybrid system with the PH domain, the middle region (comprising the SR and FFAT motifs) and the START domain of CERT, as separate baits. We found that CERT interacted with two proteins (Tsg101 and UBAP1) via the START domain (Table 1). The PH domain interacted with VAMP1, a protein which has been implicated with EV formation (Table 1). Both Tsg101 and UBAP1 are part of the ESCRT-I complex [40, 41]. To confirm Tsg101-CERT interaction to be physiologically relevant, we performed a proximity ligation assay (PLA), which yields an in situ fluorescence signal for proteins that are closer than 30-40 nm, suggesting that they form a complex [34]. N2a cells were transfected with a tdTomato-CD9 plasmid and then subjected to PLA following incubation with anti-Tsg101 (mouse) and anti-CERT (rabbit) antibodies. Figure 1C shows perinuclear PLA signals, indicating that TSG101 and CERT form a protein complex in tdTomato-CD9 positive intracellular vesicles. These results were corroborated in mouse primary neurons and astrocytes (Supplementary Figure 1C-D). No positive signals were found when performing PLA only with anti-Tsg101 antibody and rabbit IgG as controls. The kinetic of CERT and Tgs101 interaction was established by ELISA using full length human rCERTL and rTgs101. The rTsg101 concentration at which the reaction rate achieved half of its maximal value (Km) was 3.59 nM (Figure 1D). Also, the reverse set-up with rTsg101 immobilized to ELISA plate and

detection with rCERTL gave positive signal confirming complex formation between Tsg101 and CERT. Of notice, the polyclonal antibody anti-CERT against the first 50 amino acids gave slower kinetics compared to antibody anti-CERT against epitope 300-350 (Supplementary Figure 1E). Since the interaction between Tsg101 and CERT involved the START domain, which binds to ceramide, we determined whether the complex formation was regulated by ceramide. Interestingly, the PLA signals for the Tsg101-CERT complex, were reduced when cells were treated with Fumonisin B1 (FB1), which inhibits ceramide biosynthesis in the ER (Figure 1E-F). Lastly, we modeled the complex using AphaFold2 in CoLabFold which predicted, with high confidence, the structure of the complex between the human START domain of CERT, and the human UEV domain of Tsg101 (Figure 1G).

Of note, even though it was not detected by the two-hybrid system as interaction partner of CERT, immunocytochemistry showed that the tetraspanin like cluster of differentiation 81 (CD81) can be found in close proximity to CERT as indicated by PLA signals. CD81 is a transmembrane protein which takes part in forming the tetraspanin-enriched microdomains (TEM) [42]. TEM have been proposed to play a role on EV biogenesis and sorting of EV cargo [42, 43]. As for Tsg101 and CERT, the PLA positive signals, between CERT and CD81, were reduced when cells were treated with FB1 (Supplementary Figure 1F-G).

These data indicate that CERT enters the endosomal pathway and is released in EVs. Furthermore, CERT physically interacts with Tsg101 via the START domain and this interaction requires ceramide biosynthesis in the ER.

Overexpression of CERT induces EV formation and secretion.

The discovery that CERT is found in EVs and forms a protein complex with Tsg101 prompted us to investigate whether CERT is actively taking part in EV biogenesis. To answer this question, N2a were transfected with a control vector expressing GFP or pcDNA 3.1-hCERT expressing human CERT. Overexpression of CERT increased the cytosolic and membrane-bound CERT levels (Supplementary Figure 2A). Consistent with our hypothesis that CERT participates in EV formation, overexpression of CERT increased EV numbers released by N2a cells. NTA measurements showed that both, the 10K and 100k EV fraction isolated by ultracentrifugation were increased significantly by CERT expression after 48 h transfection (Figure 2A). The particle size distribution profile appeared to be different only in the 10K EV fraction, which displayed more than one peak in the particle size distribution upon transfection with the pcDNA3.1-hCERT (Supplementary Figure 2B).

To confirm the NTA results, 100k EVs were subjected to Western blot for quantitation of the EV markers Tsg101, Alix and Flotillin-2, the levels of which were significantly increased after overexpression of CERT (Figure 2B). Furthermore, the concentration of CERT in EVs precipitated at 100k was 3.7x higher with CERT-transfected cells after normalization to Flotillin-2 compared to control vector condition, suggesting that the increment of EV secretion was associated with increase of CERT levels per EV (Figure 2C). In the cytosolic and membrane fractions of cells, no difference was found between the control vector and pcDNA3.1-hCERT in Tsg101, CD81 and N-SMase-2 levels (Supplementary Figure 2C-D).

To explore if the increase of EVs mediated by CERT expression was caused exclusively by increase of SM levels entering the trans-Golgi network to the plasma membrane, we inhibited N-SMase-2 with the drug GW4869 after transfection with pcDNA3.1-hCERT. We found that GW4869 did not completely reverse the increase of EV secretion mediated by CERT expression (Figure 2D). Additionally, when inhibiting SMS1/2 with D609, the number of EVs increased of about 4-fold and CERT was down-regulated in EVs and cells (Figure 2E-F). This suggests that EVs produced by ceramide generated by N-SMase-2 and SMS1/2 are an alternative pathway to CERT-mediated EVs formation.

To determine whether overexpression of CERT was associated with increased complex formation between Tsg101 and CERT, we quantified PLA signals after transfecting N2a cells with control vector or FL-CERTL-GFP. We found that FL-CERTL-GFP transfected cells showed an increased number of positive PLA signals compared to control vector-transfected cells (Figure 2G).

These data indicate that CERT is participating in EV biogenesis by interaction with the ESCRT-dependent pathway machinery and not only by providing the substrate SM to N-SMase-2 and/or ceramide to SMS2.

<u>The PH domain is necessary for CERT to enter the endocytic pathway and for redistribution of ceramide to MVE.</u>

The trans-Golgi network and the early endosome create a hub where protein cargo and sphingolipid profile of EVs are likely determined. Therefore, we tested if sorting of CERT to the MVE requires the protein to anchor the trans-Golgi via the PH domain, a protein domain binding to PI4P [44]. We generated a plasmid containing cDNA encoding PH-deficient CERTL tagged to GFP as described in Material and Methods. After transfecting N2a cells with PH-deficient-CERTL-GFP or full length (FL)-

CERTL-GFP, the distribution of the GFP-tagged protein was tracked by confocal microscopy. Cells grown on coverslips were immunolabeled to quantify the levels of CERTL specifically in the Golgi region (anti-GM130), early endosome (EEA-1) and late endosomes (anti-LBPA). As expected, the FL-CERTL-GFP protein strongly colocalized with the Golgi, while the PH-deficient-CERTL-GFP protein was more diffused in the cytosol (Figure 3A). Quantification of the green fluorescent intensity emitted by CERTL-GFP in the Golgi co-immunolabeled with GM130 was significantly higher compared to PH-deficient-CERTL-GFP (Figure 3B). The removal of the PH domain also significantly reduced the association of early and late endosome immunolabeling with CERTL-GFP fluorescence (Figure 3C-F). Furthermore, the CERT-deficient HeLa cell line which expresses a truncated form of CERT, missing the PH domain, dysplayed a reduced number of small EVs compared to the HeLa WT cell line (Supplementary Figure 3A-C), absent BODIPY FL C5-Cer distribution to the Golgi region and diminished redistribution of BODIPY FL C5-Cer to the MVE labelled by Rab7a and TagRFP (Figure 3G-H).

This data indicates that the PH domain is critical for CERT to enter the endocytic pathway and for ceramide to be translocated to the MVE.

PI4P produced by PI4KIIα controls CERT-mediated ceramide transport from the ER to the MVE and CERT-mediated EV formation.

It has been reported that the ER forms contact sites with the MVE [45]. Furthermore, a direct lipid transport between the ER and MVE has been described at membrane contact sites [46]. Since we found that CERT-deficiency reduces ceramide translocation to the MVE we explored if this was a consequence of a reduction of ceramide transfer to the Golgi apparatus or by a reduction of ceramide transfer (CERT-mediated) between ER and endosomes.

The ceramide transport to the Golgi apparatus is regulated by the interaction of the PH domain of CERT with PI4P generated by PI4IIIβ kinases [44, 47]. Pharmacological inhibition of PI4 kinases reduces SM generation, which is dependent on CERT function [44, 48]. This reduction is most likely due to the depletion of PI4P, which decreases CERT engagement to the trans-Golgi and limits SM production. Firstly, with HeLa WT cells we tested if the highly specific PI4KIIIβ inhibitor, PI4KIIIβ-IN-10[49], reduced CERT-dependent ceramide transport from the ER to Golgi by tracking BODIPY FL C5-Cer. HeLa cells were used for better visibility of BODIPY FL C5-Cer transport and for comparison to CERT-deficient cells which completely lack this transport. As expected, the PI4KIIIβ inhibitor reduced BODIPY FL C5-Cer redistribution to the Golgi (Supplementary Figure 3D-E). Meanwhile, we

hypothesized that CERT-mediated transport of ceramide between the ER and MVE, was controlled by the interaction between the PH domain of CERT and PI4P generated by PI4KIIα at endosomes. In HeLa WT cells we found CERT to be located in the proximity of the ER-MVE contact sites by confocal microscopy and TEM (Figure 4A-C). Additional TEM images localizing CERT at the limiting membrane of MVE are reported in Supplementary Figure 3F. Next, to test that CERT transports ceramide from the ER and to the MVE, we specifically inhibited PI4KIIα with the drug NC03 [50]. To employ a dose of NC03 that was not affecting the PI4P levels in the Golgi, we traced BODIPY FL C5-Cer redistribution and tested different concentrations of NC03 in HeLa WT cells. We found that 5 μM (or lower concentration) of NC03 did not affect BODIPY FL C5-Cer redistribution to the Golgi (Figure 4D and E).

Next, in N2a cells, we investigated the effect of the PI4KIIIβ and PI4KIIα inhibitors on EV biogenesis. The number of EVs was reduced in cells treated with PI4KIIIβ and PI4KIIα inhibitors (Figure 4F-G), while the levels of the EV marker Flotillin-1 remained unchanged in cell lysate (Supplementary Figure 3G). It is important to highlight that PI4KIIIβ-IN-10 and NC03 had no effect on the EV number in CERT-deficient HeLa cells, confirming that PI4KIIIβ and PI4KIIα inhibitors mode of action are dependent on CERT function (Supplementary Figure 3H). Furthermore, by mass spectrometry we found that only the PI4KIIα inhibitor reduced the C16:0 ceramide content in EVs (Figure 4H).

This data indicates that there are two pathways for CERT mediated EV biogenesis: one which is determined by CERT engaging the Golgi apparatus which is regulated by PI4KIIIβ and a second which is controlled by the interaction of the PH domain of CERT with PI4P produced by PI4KIIα in endosomes. Furthermore, the PI4KIIα dependent pathway determines the ceramide content in EVs.

CERT inhibitor HPA-12 reduces formation and sphingolipid content of EVs.

We used HPA-12, a CERT inhibitor first described by Hanada [18], to further study the effect of CERT on EV biogenesis. HPA-12 has to be in (1R,3S) configuration to successfully dock ceramide from the START domain of CERT [51]. Racemic preparation or other configurations like (1R,3R)-diastereoisomer are 4-20 times less potent in cell-free competition assays for the START domain [32].

Firstly, to study cell uptake and distribution of HPA-12, we designed and synthesized the fluorescent and photoactivatable analogs of HPA-12, NBD-HPA-12 and pacHPA-12. Incubation of N2a cells with fluorescent HPA-12 (NDB-HPA-12) showed instantaneous cell uptake and colocalization with

transiently expressed tdTomato-CD9 (Figure 5A). A fluorescent signal was detected in the 10K and 100k EV fractions after 24 h incubation with NDB-HPA-12 (Supplementary figure 4A). When using the bio-orthogonal form of HPA-12 (pacHPA-12), we detected intracellular colocalization between pacHPA-12 conjugated to Alexa Fluor 647 azide by click chemistry and immunolabeled CD81 (Supplementary figure 4B). Taken together this data implies that is HPA-12 is found in proximity of the MVE and is released in association with EVs.

The IC50 of HPA-12 was previously established in a cell-free assay to be 4 µM [32]. Incubation for 48 h with HPA-12 reduced 100k EVs release dose-dependently, and only in the most active stereochemical configuration, syn-HPA-12 (Figure 5B). To confirm a reduction of EV secretion, we performed Western blots for CD81 and Tsg101 in the 100k EV fractions (Figure 5C). No differences in Tsg101 was found in the cell lysate (Supplementary figure 4C).

It has been reported that HPA-12 reduces SM synthesis by interfering with the CERT-mediated ceramide transfer from the ER to the trans-Golgi [18]. However, the effects on ER-to-MVE transfer and ceramide and SM content in EVs are not known. Cell pellets and the 100k EV fractions were analyzed for sphingolipids. In the 100k EV fraction, the content of ceramide, SM, sphingosine and sphinganine were significantly reduced (Supplementary Figure 4D). In particular, ceramide d18:0/16:0 and SM d18:0/16:0 levels were reduced by incubation with syn-HPA-12 (Figure 5D). Our data indicated that HPA-12 had no significant impact on monohexosylceramides, ceramide and SM determined in the cell pellet (Supplementary Figure 4E). In addition, sphingosine and sphinganine, as well as their phosphorylated forms were unchanged (Supplementary Figure 4E). When N2a cells were co-incubated with exogenous ceramide d18:0/16:0 and HPA-12, EV numbers were restored (Figure 5E). This was confirmed by Western blot for CD81, Tsg101 and Alix (Figure 5F).

We also tested if HPA-12 interfered with the interaction between CERT and Tsg101 by treating cells with or without HPA-12 for 24 h. The number of positive PLA signals per cell was significantly reduced in the HPA-12 treated cells (Figure 5G-H).

This data suggests that HPA-12 interference with ceramide transport reduces the formation and sphingolipid content of EVs. Furthermore, HPA-12 interferes with CERT-Tsg101 complex formation probably by displacing ceramide from the START domain.

HPA-12 decreases total ceramides levels in blood circulating EVs and total SM levels in brain-derived EVs

Previously, we have determined that HPA-12 crosses the blood brain barrier and reaches the brain parenchyma intact, suggesting that it is bioavailable for CERT in the brain [52]. To investigate if HPA-12 could reduce numbers and ceramide content in brain EVs, we administered the drug for 1 week every other day at a dose of 2 µg / g body weight (Figure 6A).

The drug had no effect on the body weight (Supplementary Figure 5A). After 7 days of treatment with vehicle or HPA-12, NTA analysis of EVs isolated from serum, using the ExoQuick precipitation method, showed no difference in EV numbers between groups (Figure 6B). When further purifying the ExoQuick samples through a sucrose gradient the number of EVs were similar in vehicle and HPA-12 groups (Supplementary figure 5B). However, the ceramide content, as measured in the ExoQuick preparation, was reduced in the HPA-12-treated group (Figure 6C). These findings were confirmed by ExoView where serum-derived CD81+ and CD9+ EVs were counted (Figure 6D). In addition, the levels of ceramide positive EVs in CD81+ particles were significantly reduced (Figure 6E).

The EVs were isolated from the brain by discontinuous sucrose gradient or the ExoEasy kit as explained in the Method section. The number of EVs was determined in the fractions enriched with CD81 (interface 10% - 30% and 30% – 40%). The homogeneity/purity of the EV preparation was confirmed by Western blot and TEM (Supplementary Figure 5C and D). The numbers of EVs, normalized by tissue weight, were similar in the HPA-12 treated group compared to the vehicle group (Figure 6D). A similar result was obtained with the ExoEasy purification method after enumeration by NTA and ExoView (Supplementary Figure 5E and 5F). While the content of SMs was reduced in the HPA-12 treated group, the ceramide levels were similar (Figure 6G-H). This data suggests that in vivo, CERT inhibition with HPA-12 may not affect the total number of EVs, but it changes the EV sphingolipid composition by reducing ceramide and SM.

2.4 Discussion

In this study, we provide several lines of evidence that CERT plays a role in the biogenesis and regulation of the sphingolipid composition of EVs. CERT enters the endocytic pathway and is released in association with EVs. Furthermore, CERT transfers ceramide from the ER to the endosome at contact sites. This ceramide transport is regulated by the interaction of the PH domain of CERT with PI4P produced by PI4KIIα in endosomes. Furthermore, a complex is formed between the START domain of CERT, which binds to ceramide, and Tsg101, which is part of the ESCRT-I complex. Inhibition of ceramide biosynthesis in the ER reduces the number of CERT-Tsg101 complexes per cell, while overexpression of CERT increases the number of CERT-Tsg101 complexes and number of EVs. Consistently, functional inhibition of CERT with HPA-12 reduces CERT-Tsg101 complexes, EV numbers and sphingolipid content of EVs. All together our data suggest two routes by which CERT regulates EVs: the indirect pathway via the trans-Golgi network and the direct pathway via ER-endosomes contact sites.

The trans-Golgi network and the early endosome create a hub where the protein cargo and sphingolipid profile of EVs are likely determined [53]. We show that CERT partially colocalized with the early and late endosomes. This finding agrees with the observation made by Fukushima et al., on hepatocytes showing that CERT was distributed to the MVE [20]. Our data show that the recruitment of CERT to the endosomal pathway and MVE is dependent on PI4P production. The PH domain of CERT has a high affinity for PI4P-embedded in phospholipid membranes, which are typical domains of the Golgi membranes [44, 54]. The pool of PI4P required for CERT to anchor to the trans-Golgi region is primarily generated by PI4KIIIβ [48]. Removal of the PH domain of CERT reduced the distribution of CERT to the Golgi apparatus, and early and late endosomes. Additionally, inhibition of PI4KIIIβ reduced EV release. This suggests that the generation of PI4P and its interaction with the CERT PH domain is necessary for CERT association and biogenesis of EVs. Figure 7 shows that this indirect pathway of CERT for EV formation is probably associated with SM production at the trans-Golgi and the activity of other enzymes such as N-SMase-2, SMS1 and SMS2, which are known to regulate EV biogenesis [3]. In fact, inhibition of the PI4P pool in the Golgi also reduces transfer of ceramide to the Golgi and SM production.

In contrast to the indirect pathway, the direct pathway of CERT for EV formation does not require SM production or other enzymes of the sphingolipid pathway (Figure 7). In fact, we discovered a direct ceramide transport mediated by CERT at ER-endosomes contact sites. The regulation of this

transport is likely dependent on the interaction of the PH domain of CERT with PI4P produced by PI4KIIα in endosomes. During remodeling of early endosomes to late endosomes, PI4P levels increase significantly in late endosomes [55], providing CERT an anchor to transport ceramide from the ER to late endosomes. The PI4P formed in endosomes is generated mainly by PI4KIIα and not PI4KIIIβ [56]. In fact, specific inhibition of PI4P generation in endosomes reduced redistribution of ceramide in EVs and the number of EVs released. However, we cannot completely exclude that there might be other binding partners through which CERT engages the endosomes and that there might be other regulators in addittion to PI4KIIα which controls CERT recruitment to the endosomes. Our data suggest a new role of ceramide in EV biogenesis. We show that ceramide biosynthesis regulates the formation of the complex between Tsg101 and the START domain of CERT. Thus, the inhibition of ceramide biosynthesis reduced CERT-Tsg101 complexes. This was further confirmed using HPA-12 which interfered with CERT-Tsg101 complex formation by probably displacing endogenous ceramide from the START domain. Upon CERT overexpression, the number of EVs and CERT-Tsg101 complexes increased. This ceramide-dependent pathway did not seem to be dependent on N-SMase-2 or SMS2. Therefore, the increase of EV production, upon CERT overexpression, may be triggered by enrichment of ceramide in EVs or by ceramide acting as a "switch-on" inducing complex formation between CERT and Tsg101.

How sphingolipids are enriched in EVs is not completely understood. However, ceramide levels in EVs are highly important in disease condition [57]. Recently, Dichlberger et al., found that the ceramide interacting protein, lysosome associated protein transmembrane 4B (LAPTM4B), regulates the glycosphingolipid composition of small EVs [58]. Interestingly, LAPTM4B deficiency increased glycosphingolipids in the EVs, leaving ceramide unaffected even though LAPTM4B regulates the subcellular distribution of ceramide [58]. In our study, when the ceramide transporter function of CERT was inhibited with HPA-12, not only EVs were decreased in numbers, but also in their content of ceramide, SM, sphingosine and sphinganine, while glycosphingolipids were poorly affected. In particular, Cer d18:0/16:0 and SM d18:0/16:0 levels were reduced by HPA-12 treatment: This result agrees with the observation of Fukushima et al, showing that CERT mediated enrichment of EVs with Cer d18:1/16:0 under lipotoxic stress in hepatocytes. Consistently, downregulation of CERT reduced the Cer d18:1/16:0 content in EVs [20]. In other studies, Cer d18:1/16:0 overload in neurons or in muscle, under disease conditions, such as diabetes and Alzheimer's disease (AD), was rescued by overexpression of CERT, suggesting that CERT may control cellular ceramide levels through EV release [28, 59]. Notably, Barman et al. discovered that downregulating VAP, which anchors CERT

to the ER, not only reduces EV secretion but also a unique subset of RNA-containing EVs [21]. This finding suggests a role of CERT in packaging of RNA in EVs as well.

These findings open-up new intervention strategies to control the number and ceramide content of EVs in disease condition. EVs have been proposed as the "Trojan horses of neurodegeneration" [60]. For instance, in AD, the release of amyloid-β (Aβ) peptides by EVs may be involved in the slow progression of the disease, similarly to prion proteins that mediate their intercellular transfer via EVs [61]. While great attention has been given to the protein and RNA cargo of EVs, the lipid composition of the EVs is poorly studied [57]. Our group showed that EVs enriched in ceramide contribute to Aβ aggregation and neurotoxicity in vitro and in the brain of AD mice models [62, 63]. Furthermore, reduction of ceramide generation by inhibition or genetic deficiency of N-SMase2 reduced EV formation and plaque numbers, and improved cognition in vivo in a transgenic model of AD [1, 2]. Therefore, investigation of drugs with the dual action of reducing EV numbers and reducing ceramide content in EVs could potentially give rise to new treatments for neurodegenerative diseases where ceramide-enriched EVs play a role. When administering HPA-12 intraperitoneally to mice for a week every other day, the number of EVs in brain and blood were not significantly affected. However, ceramide and SM were reduced in blood- and brain-derived EVs, respectively. Therefore, our study unravels a novel mechanism underlying the function of ceramide and CERT in EV biogenesis. This mechanism of N-SMase-2-independent, but Cer/CERT-dependent EV formation will also offer a novel pharmacological target to manipulate EV biogenesis and lipid composition, which is important for our understanding of the physiological and pathophysiological function of EVs and development of disease therapies.

2.5   Conclusion

In conclusion, we report that CERT enters the endocytic pathway and is sorted to the MVE where a complex is formed between CERT and Tsg101, which is promoted by ceramide biosynthesis. CERT mediates a direct transport of ceramide between the ER and late endosomes/MVE at contact sites which determines the ceramide content of EVs. Translocation of ceramide-associated CERT to the MVE and biogenesis of EVs is potentially regulated by the interaction between the PH domain of CERT and PI4P generated by PI4KIIIβ in the Golgi apparatus or PI4KIIα in endosomes. Overexpression of CERT in neuronal cells increases EV secretion while inhibition of CERT with the drug HPA-12 reduces EV formation and the concentration of ceramide and SM in EVs. Our data support a novel function of CERT in regulating the biogenesis and sphingolipid composition of EVs, which links ceramide to the ESCRT-dependent pathway.

2.6   Declarations

Author contribution

EB, SMC and PMM conceived the project and designed the experiments. SMC with EB performed the microscope experiments. SMC, AE and ZQ performed EV isolation and characterization. ZZ cloned the GFP-tagged plasmids. SMC and PT performed Western blotting. SMC and LZ contributed to the production of primary neurons and the in vivo experiments. DB and BF synthetized HPA-12, NDB-HPA-12 and pacHPA-12. SDS, SMC and EB contributed to the analysis and interpretation of lipid measurements. PMM and CG contributed with two hybrid system data. JP contributed with sample preparation for TEM. SMC and EB wrote the manuscript. All authors contributed by critically revising the manuscript.

Disclosure statement

The authors declare that they have no competing interests.

2.7   References

1. *Dinkins, M.B., et al., Exosome reduction in vivo is associated with lower amyloid plaque load in the 5XFAD mouse model of Alzheimer's disease. Neurobiol Aging, 2014. **35**(8): p. 1792-800.*

2. *Dinkins, M.B., et al., Neutral Sphingomyelinase-2 Deficiency Ameliorates Alzheimer's Disease Pathology and Improves Cognition in the 5XFAD Mouse. J Neurosci, 2016. **36**(33): p. 8653-67.*

3. *Trajkovic, K., et al., Ceramide triggers budding of exosome vesicles into multivesicular endosomes. Science, 2008. **319**(5867): p. 1244-7.*

4. *Menck, K., et al., Neutral sphingomyelinases control extracellular vesicles budding from the plasma membrane. J Extracell Vesicles, 2017. **6**(1): p. 1378056.*

5. *Kenific, C.M., H. Zhang, and D. Lyden, An exosome pathway without an ESCRT. Cell Res, 2021. **31**(2): p. 105-106.*

6. *Yuyama, K., et al., Sphingolipid-modulated exosome secretion promotes clearance of amyloid-beta by microglia. J Biol Chem, 2012. **287**(14): p. 10977-89.*

7. *Skotland, T., et al., Exosomal lipid composition and the role of ether lipids and phosphoinositides in exosome biology. J Lipid Res, 2019. **60**(1): p. 9-18.*

8. *Rao, R.P., et al., Ceramide transfer protein function is essential for normal oxidative stress response and lifespan. Proc Natl Acad Sci U S A, 2007. **104**(27): p. 11364-9.*

9. *Rao, R.P., et al., Ceramide transfer protein deficiency compromises organelle function and leads to senescence in primary cells. PLoS One, 2014. **9**(3): p. e92142.*

10. *Hanada, K., et al., Molecular machinery for non-vesicular trafficking of ceramide. Nature, 2003. **426**(6968): p. 803-9.*

11. *Kumagai, K., et al., CERT mediates intermembrane transfer of various molecular species of ceramides. J Biol Chem, 2005. **280**(8): p. 6488-95.*

12. *Gault, C.R., L.M. Obeid, and Y.A. Hannun, An overview of sphingolipid metabolism: from synthesis to breakdown. Adv Exp Med Biol, 2010. **688**: p. 1-23.*

13. *Mencarelli, C., et al., The ceramide transporter and the Goodpasture antigen binding protein: one protein--one function? J Neurochem, 2010. **113**(6): p. 1369-86.*

14. *Hanada, K., et al., Molecular machinery for non-vesicular trafficking of ceramide. Nature, 2003. **426**: p. 803.*

15. *Prashek, J., T. Truong, and X. Yao, Crystal Structure of the Pleckstrin Homology Domain from the Ceramide Transfer Protein: Implications for Conformational Change upon Ligand Binding. PLoS One, 2013. **8**(11).*

16. Kawano, M., et al., *Efficient trafficking of ceramide from the endoplasmic reticulum to the Golgi apparatus requires a VAMP-associated protein-interacting FFAT motif of CERT. J Biol Chem*, 2006. **281**(40): p. 30279-88.

17. Yamaji, T. and K. Hanada, *Establishment of HeLa cell mutants deficient in sphingolipid-related genes using TALENs. PLoS One*, 2014. **9**(2): p. e88124.

18. Yasuda, S., et al., *A novel inhibitor of ceramide trafficking from the endoplasmic reticulum to the site of sphingomyelin synthesis. J Biol Chem*, 2001. **276**(47): p. 43994-4002.

19. Santos, C., et al., *Identification of novel CERT ligands as potential ceramide trafficking inhibitors. Chembiochem*, 2014. **15**(17): p. 2522-8.

20. Fukushima, M., et al., *StAR-related lipid transfer domain 11 (STARD11)-mediated ceramide transport mediates extracellular vesicle biogenesis. J Biol Chem*, 2018. **293**(39): p. 15277-15289.

21. Barman, B., et al., *VAP-A and its binding partner CERT drive biogenesis of RNA-containing extracellular vesicles at ER membrane contact sites. Dev Cell*, 2022. **57**(8): p. 974-994 e8.

22. Mencarelli, C., et al., *Goodpasture antigen-binding protein/ceramide transporter binds to human serum amyloid P-component and is present in brain amyloid plaques. J Biol Chem*, 2012. **287**(18): p. 14897-911.

23. Vojtek, A.B. and S.M. Hollenberg, *Ras-Raf interaction: two-hybrid analysis. Methods Enzymol*, 1995. **255**: p. 331-42.

24. Béranger, F., et al., *Getting more from the two-hybrid system: N-terminal fusions to LexA are efficient and sensitive baits for two-hybrid studies. Nucleic Acids Res*, 1997. **25**(10): p. 2035-6.

25. Kabani, M., et al., *A highly representative two-hybrid genomic library for the yeast Yarrowia lipolytica. Gene*, 2000. **241**(2): p. 309-15.

26. Bartel, P., et al., *Elimination of false positives that arise in using the two-hybrid system. Biotechniques*, 1993. **14**(6): p. 920-4.

27. Formstecher, E., et al., *Protein interaction mapping: a Drosophila case study. Genome Res*, 2005. **15**(3): p. 376-84.

28. Crivelli, S.M., et al., *CERTL reduces C16 ceramide, amyloid-beta levels, and inflammation in a model of Alzheimer's disease. Alzheimers Res Ther*, 2021. **13**(1): p. 45.

29. Mirdita, M., S. Ovchinnikov, and M. Steinegger, *ColabFold - Making protein folding accessible to all.* 2021: p. 2021.08.15.456425.

30. Pettersen, E.F., et al., *UCSF ChimeraX: Structure visualization for researchers, educators, and developers. Protein Sci*, 2021. **30**(1): p. 70-82.

31.   Gad, S.C., et al., Nonclinical vehicle use in studies by multiple routes in multiple species. Int J Toxicol, 2006. **25**(6): p. 499-521.

32.   Santos, C., et al., The CERT antagonist HPA-12: first practical synthesis and individual binding evaluation of the four stereoisomers. Bioorg Med Chem, 2015. **23**(9): p. 2004-9.

33.   Crivelli, S.M., et al., Ceramide analog [18F]F-HPA-12 detects sphingolipid disbalance in the brain of Alzheimer's disease transgenic mice by functioning as a metabolic probe. Scientific Reports, 2020. **10**(1): p. 19354.

34.   Jiang, X., et al., Visualization of Ceramide-Associated Proteins in Ceramide-Rich Platforms Using a Cross-Linkable Ceramide Analog and Proximity Ligation Assays With Anti-ceramide Antibody. Front Cell Dev Biol, 2019. **7**: p. 166.

35.   Elsherbini, A., et al., Association of Abeta with ceramide-enriched astrosomes mediates Abeta neurotoxicity. Acta Neuropathol Commun, 2020. **8**(1): p. 60.

36.   Perez-Gonzalez, R., et al., A Method for Isolation of Extracellular Vesicles and Characterization of Exosomes from Brain Extracellular Space. Methods Mol Biol, 2017. **1545**: p. 139-151.

37.   Tao-Cheng, J.H., et al., Optimization of protocols for pre-embedding immunogold electron microscopy of neurons in cell cultures and brains. Mol Brain, 2021. **14**(1): p. 86.

38.   Bielawski, J., et al., Sphingolipid analysis by high performance liquid chromatography-tandem mass spectrometry (HPLC-MS/MS). Adv Exp Med Biol, 2010. **688**: p. 46-59.

39.   Bielawski, J., et al., Comprehensive quantitative analysis of bioactive sphingolipids by high-performance liquid chromatography-tandem mass spectrometry. Methods Mol Biol, 2009. **579**: p. 443-67.

40.   Minciacchi, V.R., M.R. Freeman, and D. Di Vizio, Extracellular vesicles in cancer: exosomes, microvesicles and the emerging role of large oncosomes. Semin Cell Dev Biol, 2015. **40**: p. 41-51.

41.   Soares Martins, T., et al., Diagnostic and therapeutic potential of exosomes in Alzheimer's disease. J Neurochem, 2021. **156**(2): p. 162-181.

42.   Andreu, Z. and M. Yanez-Mo, Tetraspanins in extracellular vesicle formation and function. Front Immunol, 2014. **5**: p. 442.

43.   Perez-Hernandez, D., et al., The intracellular interactome of tetraspanin-enriched microdomains reveals their function as sorting machineries toward exosomes. J Biol Chem, 2013. **288**(17): p. 11649-61.

44.   Sugiki, T., et al., Structural basis for the Golgi association by the pleckstrin homology domain of the ceramide trafficking protein (CERT). J Biol Chem, 2012. **287**(40): p. 33706-18.

45.   Raiborg, C., E.M. Wenzel, and H. Stenmark, ER-endosome contact sites: molecular compositions and functions. EMBO J, 2015. **34**(14): p. 1848-58.

46. Wilhelm, L.P., et al., *STARD3 mediates endoplasmic reticulum-to-endosome cholesterol transport at membrane contact sites.* EMBO J, 2017. **36**(10): p. 1412-1433.

47. De Matteis, M.A., C. Wilson, and G. D'Angelo, *Phosphatidylinositol-4-phosphate: the Golgi and beyond.* Bioessays, 2013. **35**(7): p. 612-22.

48. Kumagai, K. and K. Hanada, *Structure, functions and regulation of CERT, a lipid-transfer protein for the delivery of ceramide at the ER-Golgi membrane contact sites.* FEBS Lett, 2019. **593**(17): p. 2366-2377.

49. Rutaganira, F.U., et al., *Design and Structural Characterization of Potent and Selective Inhibitors of Phosphatidylinositol 4 Kinase IIIbeta.* J Med Chem, 2016. **59**(5): p. 1830-9.

50. Sengupta, N., et al., *A large scale high-throughput screen identifies chemical inhibitors of phosphatidylinositol 4-kinase type II alpha.* J Lipid Res, 2019. **60**(3): p. 683-693.

51. Berkes, D., et al., *Chemistry and Biology of HPAs: A Family of Ceramide Trafficking Inhibitors.* Chemistry, 2016. **22**(49): p. 17514-17525.

52. Crivelli, S.M., et al., *Synthesis, Radiosynthesis, and Preliminary in vitro and in vivo Evaluation of the Fluorinated Ceramide Trafficking Inhibitor (HPA-12) for Brain Applications.* J Alzheimers Dis, 2017. **60**(3): p. 783-794.

53. Nagano, M., et al., *Rab5-mediated endosome formation is regulated at the trans-Golgi network.* Commun Biol, 2019. **2**: p. 419.

54. De Matteis, M.A. and G. D'Angelo, *The role of the phosphoinositides at the Golgi complex.* Biochem Soc Symp, 2007(74): p. 107-16.

55. Yoshida, A., et al., *Segregation of phosphatidylinositol 4-phosphate and phosphatidylinositol 4,5-bisphosphate into distinct microdomains on the endosome membrane.* Biochim Biophys Acta Biomembr, 2017. **1859**(10): p. 1880-1890.

56. Henmi, Y., et al., *PtdIns4KIIalpha generates endosomal PtdIns(4)P and is required for receptor sorting at early endosomes.* Mol Biol Cell, 2016. **27**(6): p. 990-1001.

57. Elsherbini, A. and E. Bieberich, *Ceramide and Exosomes: A Novel Target in Cancer Biology and Therapy.* Adv Cancer Res, 2018. **140**: p. 121-154.

58. Dichlberger, A., et al., *LAPTM4B controls the sphingolipid and ether lipid signature of small extracellular vesicles.* Biochim Biophys Acta Mol Cell Biol Lipids, 2021. **1866**(2): p. 158855.

59. Bandet, C.L., et al., *Ceramide Transporter CERT Is Involved in Muscle Insulin Signaling Defects Under Lipotoxic Conditions.* Diabetes, 2018. **67**(7): p. 1258-1271.

60. Ghidoni, R., L. Benussi, and G. Binetti, *Exosomes: the Trojan horses of neurodegeneration.* Med Hypotheses, 2008. **70**(6): p. 1226-7.

61.   *Sardar Sinha, M., et al., Alzheimer's disease pathology propagation by exosomes containing toxic amyloid-beta oligomers. Acta Neuropathol, 2018. **136**(1): p. 41-56.*

62.   *Wang, G., et al., Astrocytes secrete exosomes enriched with proapoptotic ceramide and prostate apoptosis response 4 (PAR-4): potential mechanism of apoptosis induction in Alzheimer disease (AD). J Biol Chem, 2012. **287**(25): p. 21384-95.*

63.   *Dinkins, M.B., et al., Exosome reduction in vivo is associated with lower amyloid plaque load in the 5XFAD mouse model of Alzheimer's disease. Neurobiol Aging, 2014.*

64.   *Willms, E., et al., Cells release subpopulations of exosomes with distinct molecular and biological properties. Scientific Reports, 2016. **6**(1): p. 22519.*
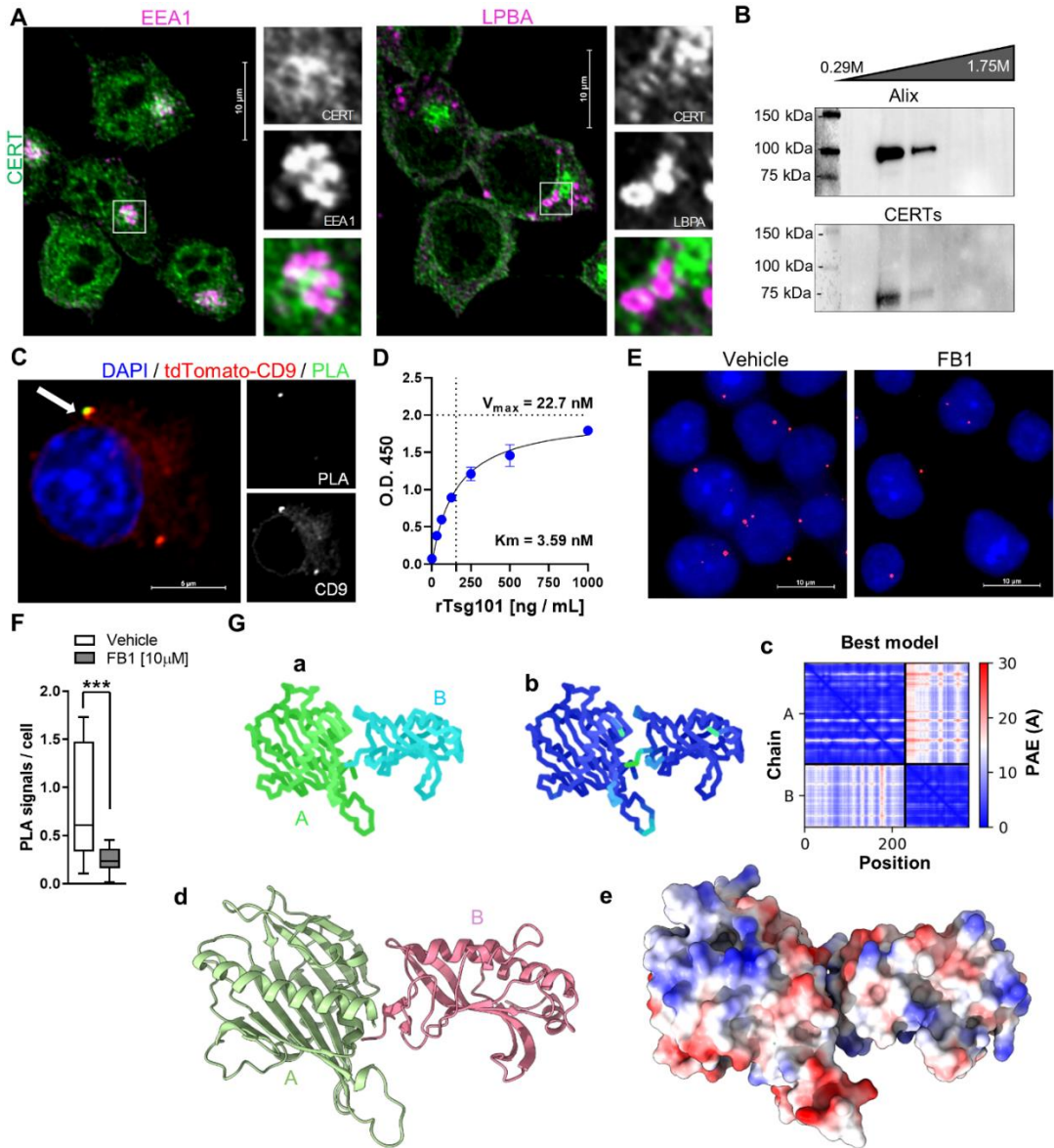
2.8   Figures and tables

Figure 1. CERT is associated with the MVE and interacts with Tsg101. A) Confocal photomicrograph of fluorescent labelling of CERT (green) showing partial colocalization/juxtaposition (white) with EEA1 or LPBA (magenta) in N2a cells. Scale bar 5 µm. B) CERT detected by immunoblot in the same fractions of Alix after EV purification by sucrose gradient ultracentrifugation 0.29-1.75M. C) Confocal photomicrograph of PLA assay (green) in tdTomato-CD9 (red) transfected N2a cells indicating complex formation between Tsg101 and CERT (arrow). DAPI (blue) was used to stain the nuclei. Scale bar 5 µm. D) Binding kinetics of rTsg101 to immobilized rCERT$_L$ measured by ELISA. The Michaelis-Menten constant (Km) equaled 5.59nM with Vmax equal to 22.7nM. E) Representative photomicrographs of Tsg101 and CERT PLA signals (red), after treatment with vehicle and 10 µM FB1. Scale bar 5 µm. F) Box and Whiskers plots of 14-23 pictures per condition, of n = 3 independent experiments, showing PLA signals normalized to the number of nuclei (blue). Unpaired t-test (*p<0.05). G)

AlphaFold2 highest ranked structure prediction of the complex between (a) the human START domain of CERT (green A) and the human UEV domain of Tsg101 (chain colored in light blue B). In (b) the colored polymers based on pLDDT (score = 93.3) and in (c) PAE plot (pTMscore = 0.742). In (d) the 3D structure of the complex (START domain in green A and UEV domain in magenta B) and in (e) the color surface electrostatic potential of the complex.
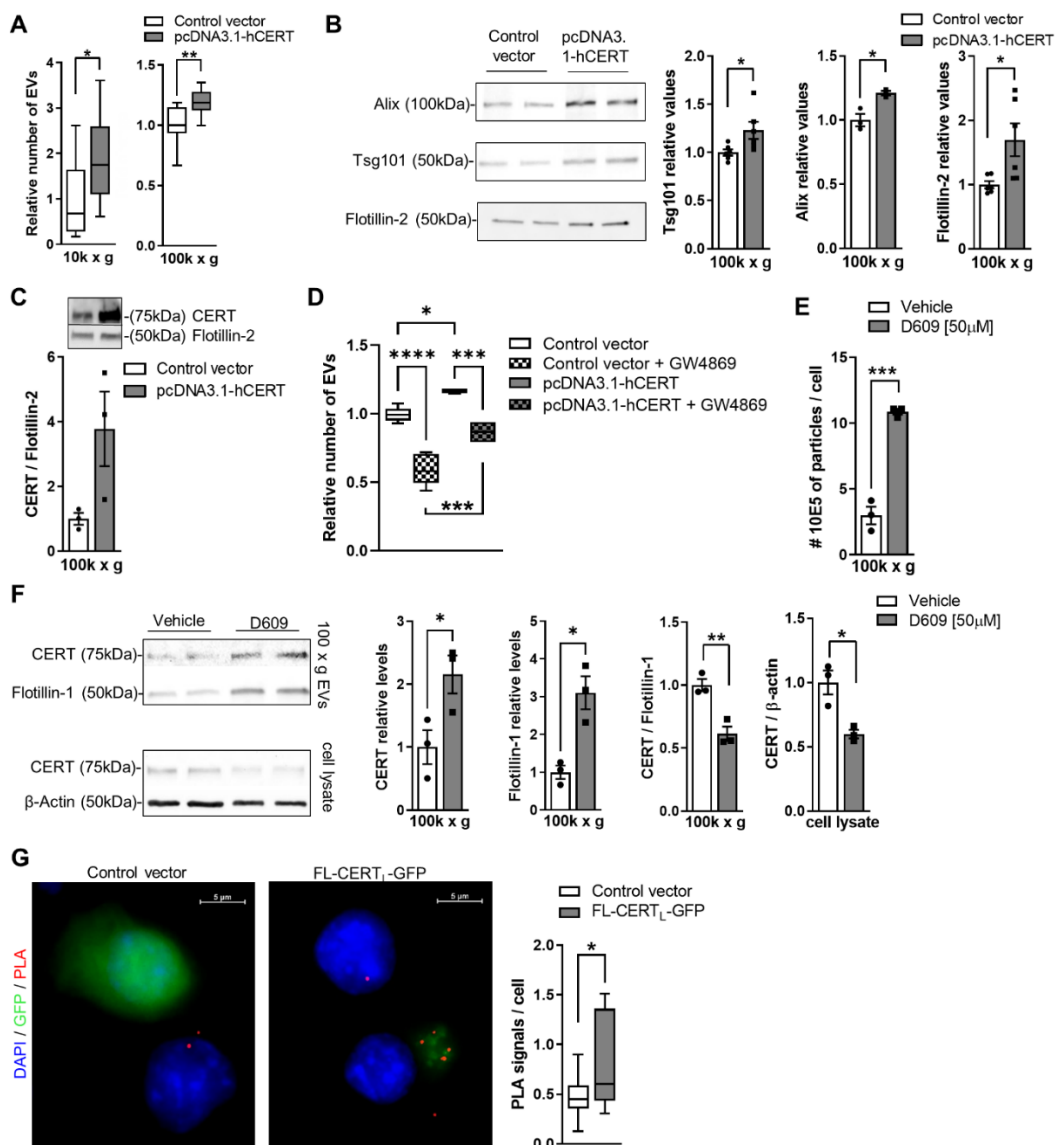
Figure 2. Overexpression of CERT induces EV formation and secretion. A) Numbers of EVs in the 10K and 100k EV fractions measured by NTA after pcDNA-hCERT transfection. Box and Whiskers plot represent N=6 / group. B) Quantification of Tsg101, Alix and Flotillin-2 by Western blots. Bar graphs represent average +/-SEM of N=6 / group. C) Enrichment of CERT in 100k EV fraction after transfection with pcDNA-hCERT. Intensities of bands corresponding to CERT were normalized to Flotilin-2. Bar graph represents average +/-SEM with N= 3 / group. D) The 100k EVs numbers measured by NTA after pcDNA-hCERT transfection and co-treatment of N-SMase2 inhibitor GW4869 (15 µM). Box and Whiskers plot represent N=4-9/ group. One-way ANOVA, Sidak's posthoc

testing (*p<0.05; ***p<0.001; ****p<0.0001). E) The 100k EV numbers measured by NTA after treatment with D609 (50 µM). Bar graph represents average +/-SEM with each N=3 / group. F) Quantification of CERT by immunoblots after treatment with D609 (50 µM) in EVs and cell lysate. Bar graph represents average +/-SEM with each N=3 / group. G) Representative photomicrographs of Tsg101 and CERT PLA signals (red), after transfection with control vector (green) or FL-CERT$_L$-GFP (green). Scale bar 5 µm. Box and Whiskers plot of three independent experiments including a total of 16 pictures / condition showing PLA signals normalized to the number of nuclei (blue). Unpaired t-test (*p<0.05).

A PHdeficient-CERT_L-GFP FL-CERT_L-GFP

C PHdeficient-CERT_L-GFP FL-CERT_L-GFP

E PHdeficient-CERT_L-GFP FL-CERT_L-GFP
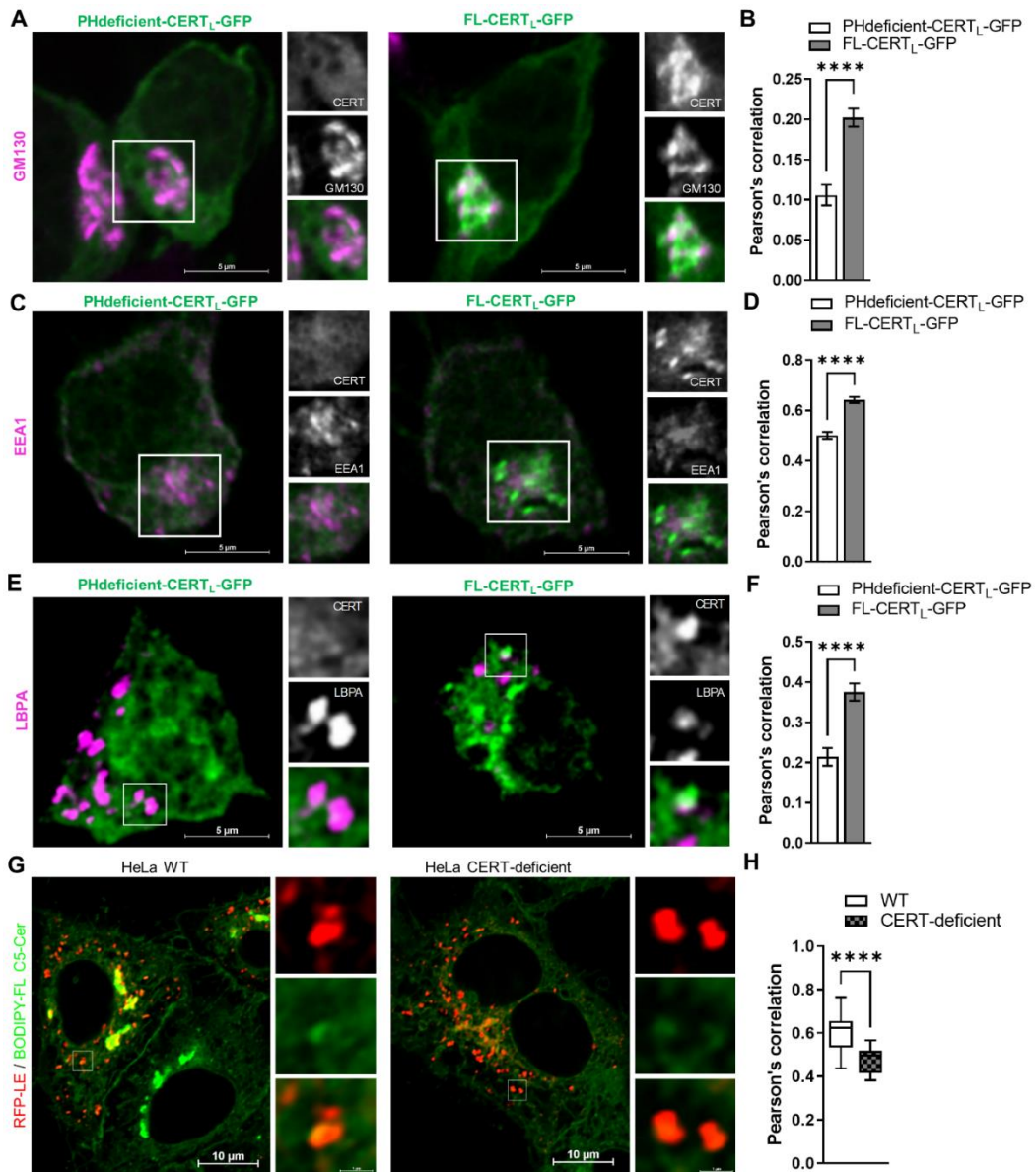
G HeLa WT HeLa CERT-deficient

Figure 3. The Interaction of PI4P with the PH domain is necessary for CERT to enter the endocytic pathway and for redistribution of ceramide to the MVE. A) Confocal photomicrographs displaying partial colocalization between PHdeficient-CERTL-GFP or FL-CERTL-GFP and the Golgi, immunolabeled with anti-GM130. Scale bar 5 µm. B) Correlation coefficient of fluorescence intensities of PHdeficient-CERTL-GFP or CERTL-GFP and GM130 (Golgi apparatus) immunolabeling. Bar graph represents +/- SEM of 9 photomicrographs per condition. Unpaired t-test was applied, ***p<0.001. C) Confocal photomicrographs displaying colocalization between PHdeficient-CERTL-GFP or CERTL-GFP and early endosome, immunolabeled with anti-EEA1 antibody. Scale bar 5 µm. D) Correlation coefficient of fluorescence intensities of PHdeficient-CERTL-GFP or CERTL-GFP and EEA1 immunolabeling. Bar graph represents average +/- SEM of 9 photomicrographs per condition. Unpaired t-test was applied, **p<0.01. E) Confocal photomicrographs displaying colocalization between PHdeficient-CERTL-GFP or CERTL-GFP and late endosomes, immunolabeled with anti-LBPA antibody. Scale bar 5 µm. F) Correlation coefficient of fluorescence intensities of PHdeficient-CERTL-GFP or CERTL-GFP and LPBA immunolabeling. Bar graph represents mean +/- SEM of 9 photomicrographs per condition. Unpaired t-test was applied, ***p<0.001. G) Confocal photomicrographs showing BODIPY FL C5-Cer redistribution to the LE/MVE In HeLa-WT and HeLa CERT deficient cell line. H) Pearson's correlation of fluorescence intensities of BODIPY FL C5-Cer and RFP-LE Whiskers plot represent average +/-SEM of N= photomicrographs / group. Unpaired t-test was applied, ****p<0.001. I)
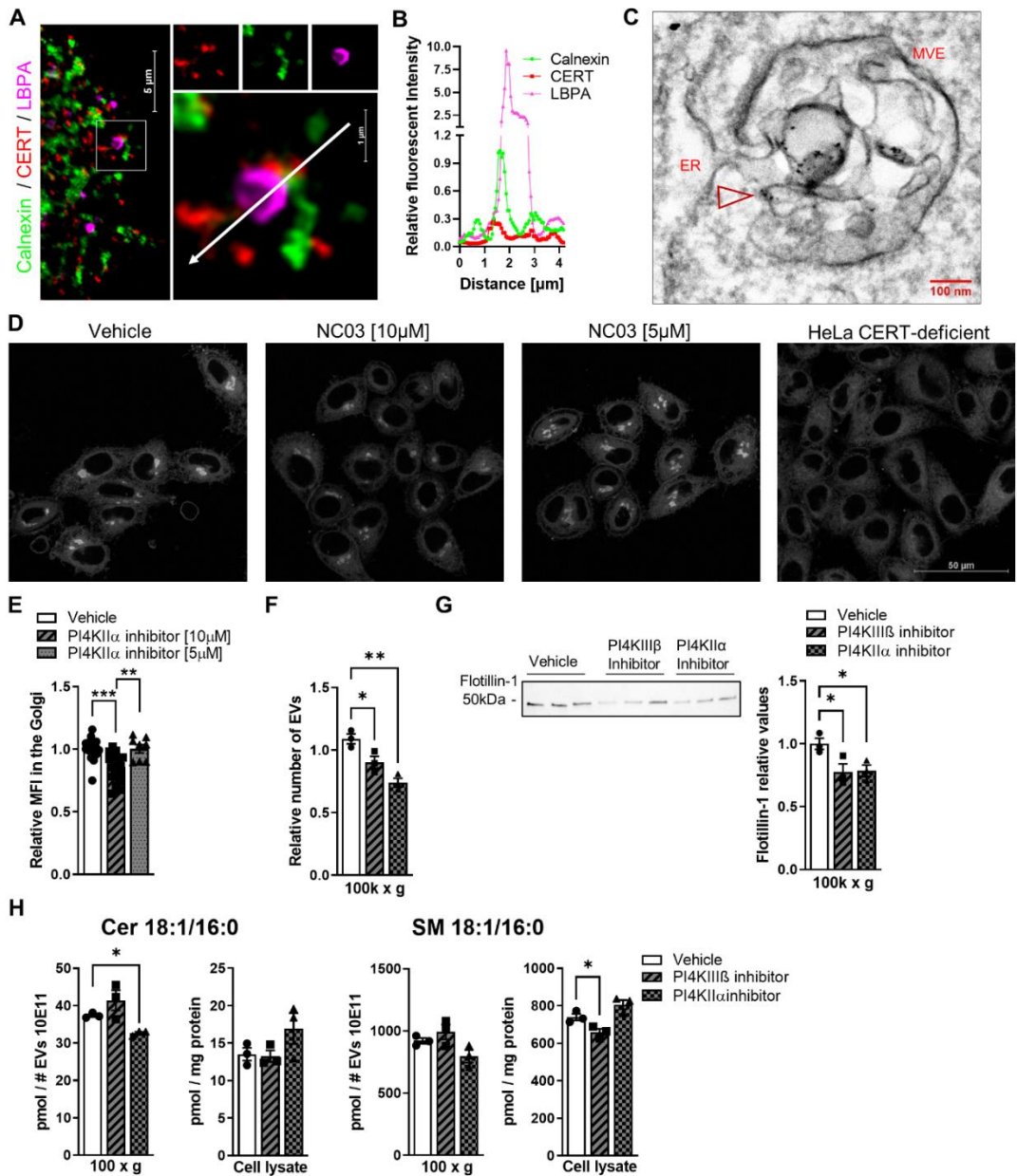
Figure 4. PI4P produced by PI4KIIα controls a direct ceramide transport from the ER to the MVE and CERT-mediated EV generation. A) Confocal photomicrographs displaying immunolabeled CERT (red) partially colocalizing with the ER immunolabeled with Calnexin (green) and MVE immunolabeled with LBPA (magenta) at contact sites. B) Linescan analyses with fluorescence intensities of the ER (Calnexin), MVE (LPBA) and CERT along the arrow shown in A. C) TEM image of Immunogold labeling of CERT in the limiting membrane of MVE and in proximity to ER. Arrow shows labeling on limiting membrane of MVE. D) Confocal photomicrographs showing BODIPY FL C5-Cer redistribution to the Golgi region without or with PI4KIIα inhibitor (NC03) 10 µM or 5 µM. HeLa CERT-deficient cell line was used as negative control. E) Quantification of the relative MFI measured at the Golgi region after BODIPY FL C5-Cer incubation in absence or presence of 10 µM or 5 µM of PI4KIIα inhibitor. Bar graphs represent average +/-SEM of N= 8-18 / group. One-way ANOVA, Tukey's posthoc testing

(*p<0.05; **p<0.01) F) Number of EVs in the 100k fraction measured by NTA after 24 h incubation with vehicle, 50 nM of PI4KIIIβ inhibitor or with 5 μM of PI4KIIα inhibitor (NC03) . Bar graph represent average +/-SEM of N=3 / group. One-way ANOVA, Sidak's posthoc testing (*p<0.05; **p<0.01). G) Quantification of Flotillin-1 by Western blots. Bar graphs represent average +/-SEM of N=3 / group. H) Cer d18:1/16:0 and SM d18:1/16:0 levels measured in the 100k x g EV fraction or cell lysate after after 24 h incubation with vehicle, 50 nM of PI4KIIIβ inhibitor or with 5 μM of PI4KIIα inhibitor (NC03). Bar graph shows average +/-SEM with N=3/ group. One-way ANOVA, Sidak's posthoc testing (*p<0.05).
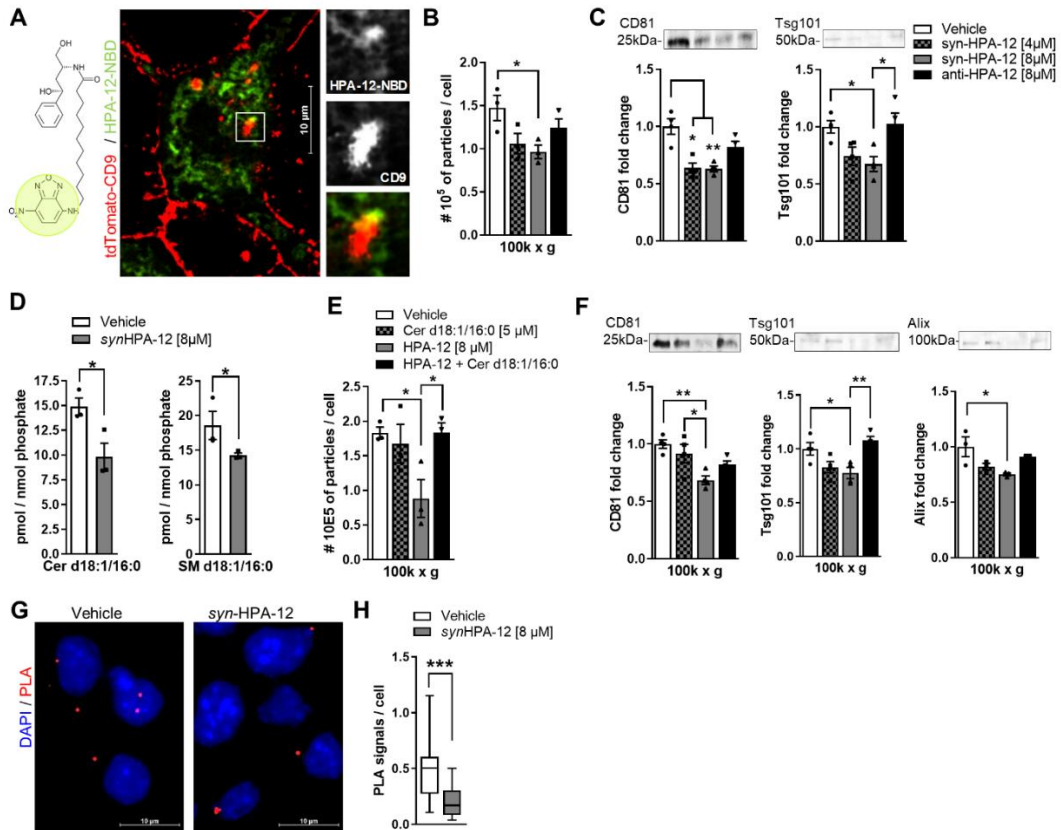
Figure 5. CERT inhibitor HPA-12 reduces production and sphingolipid content of EVs. A) Fluorescent HPA-12 (HPA-12-NBD) chemical structure. Single plane photomicrograph of fluorescence live microscopy of HPA-12-NBD-treated (green) and tdTomato-CD9 (red) transfected cells showing partial colocalization. Scale bar 10 μm. B) 100k EV numbers measured by NTA and normalized to cells after 24 h treatment with *syn*-HPA-12 or the less potent stereoisomer *anti*-HPA-12. Bar graph shows average +/-SEM of N=3/group. One-way ANOVA, Tukey posthoc testing (*p<0.05). C) Quantification of CD81 and Tsg101 by Western blots. Bar graph show average +/-SEM of N=4/ group. One-way ANOVA, Tukey posthoc testing *p<0.05. D) Cer d18:1/16:0 and SM d18:1/16:0 levels measured in the 100k EVs fraction. Bar graph shows average +/-SEM with N=3/ group. Unpaired t-test (*p<0.05). E) 100k EVs numbers measured by NTA and normalized to cells after 24 h treatment with *syn*-HPA-12 and/or Cer d18:1/16:0. Bar graph shows average +/-SEM with N=3/ group. One-way ANOVA, Tukey's posthoc testing (*p<0.05). F) Quantification of CD81, Tsg101 and Alix by Western blots. Bar graph shows average +/-SEM of two independent experiments with each N=4/ group. One-way ANOVA, Tukey's posthoc testing *p<0.05. G) Representative photomicrographs of Tsg101 and CERT PLA signals after treatment with vehicle or synHPA-12 (8 μM). Scale bar 10 μm. H). Box and Whiskers plot of PLA signals normalized to the number of nuclei of three independent experiments including a total of 12-20 pictures / condition. Unpaired t-test (***p<0.001).
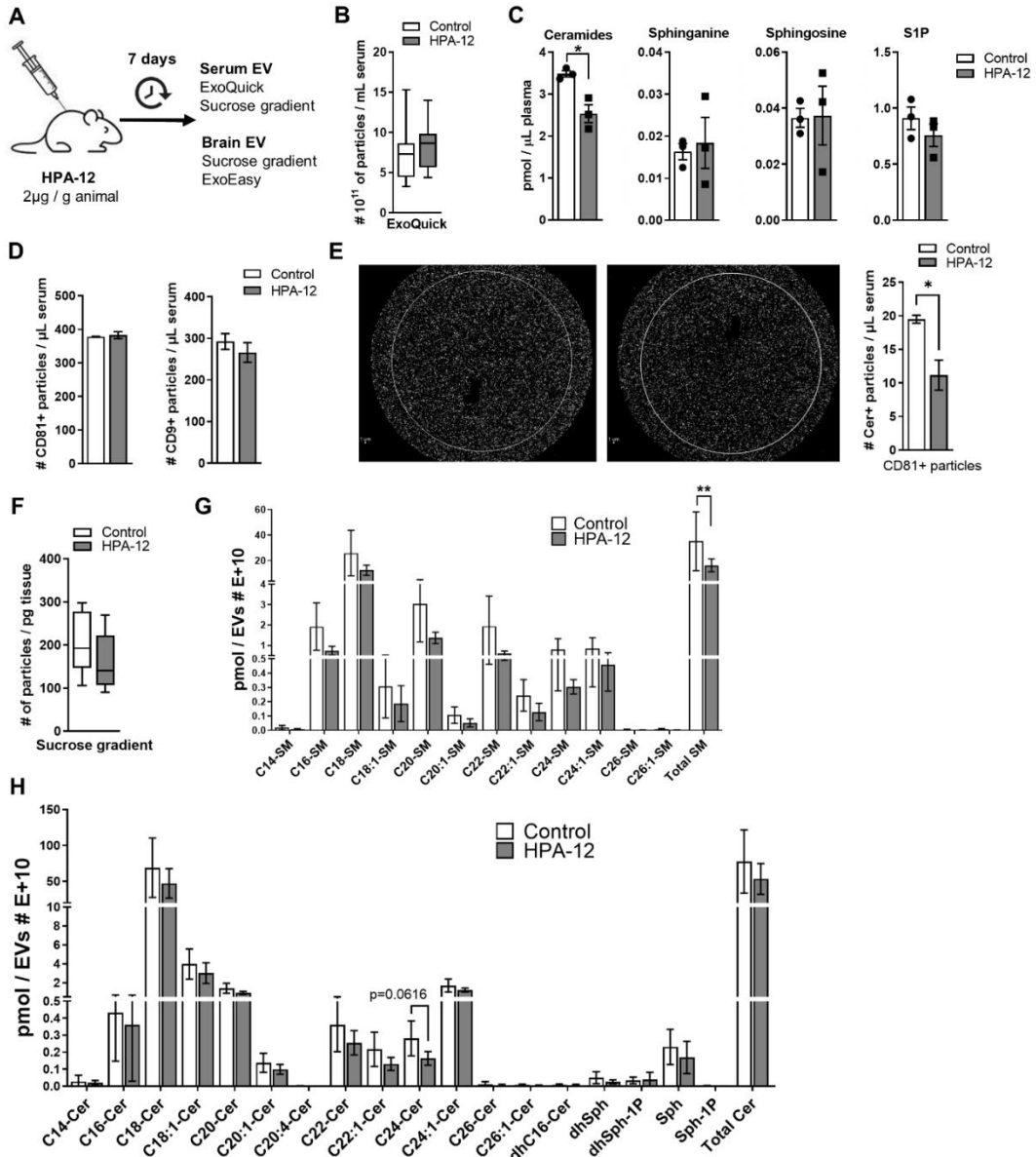
Figure 6. HPA-12 decreases ceramide levels in blood circulating EVs and total SM in brain EVs. A) Animals were treated with HPA-12 for 7 days. Dose was given intraperitoneally every other day. EVs were isolated from serum and brain. B) NTA measurement of EVs isolated from serum with ExoQuick. Box and Whiskers plot represents the distribution of 10 animals per condition. C) Quantification of ceramide, S1P, sphingosine and sphinganine by mass spectrometry in EVs isolated from serum with ExoQuick. Bar graph represents average +/-SEM with each N=3/ group. Unpaired t-test (*p<0.05). D) Representative particle counts on different CD81 and CD9 capture spots. Bar graph represents average +/-SEM. for three capture spots of N = 4 (pooled) / group of two chips. E) Representative images for ceramide detection in CD81+ EVs. Representative particle counts on different of ceramide + EVs. Bar graph represents average +/-SEM. for three capture spots of N = 4 (pooled) / group of two chips.F) NTA measurement of EVs isolated from brain with sucrose gradient in fractions enriched with Alix1. Box and Whiskers plot represents the distribution of 10 animals per condition. E) Quantification of SMs C14:0, C16:0, C18:0, C18:1, C20, C20:1, C22:0, C24:0, C24:1, C26:0, and C26:1 by mass spectrometry of brain EVs. Bar graph represents average +/-SEM with each N=3-5/ group. One-way ANOVA followed by Sidak's multiple comparison (**p<0.01).

F) Quantification of ceramide, S1P, sphingosine and sphinganine by mass spectrometry of brain EVs. Bar graphs represent average +/-SEM with each N=4-5/ group. Unpaired t-test (p=0.061).
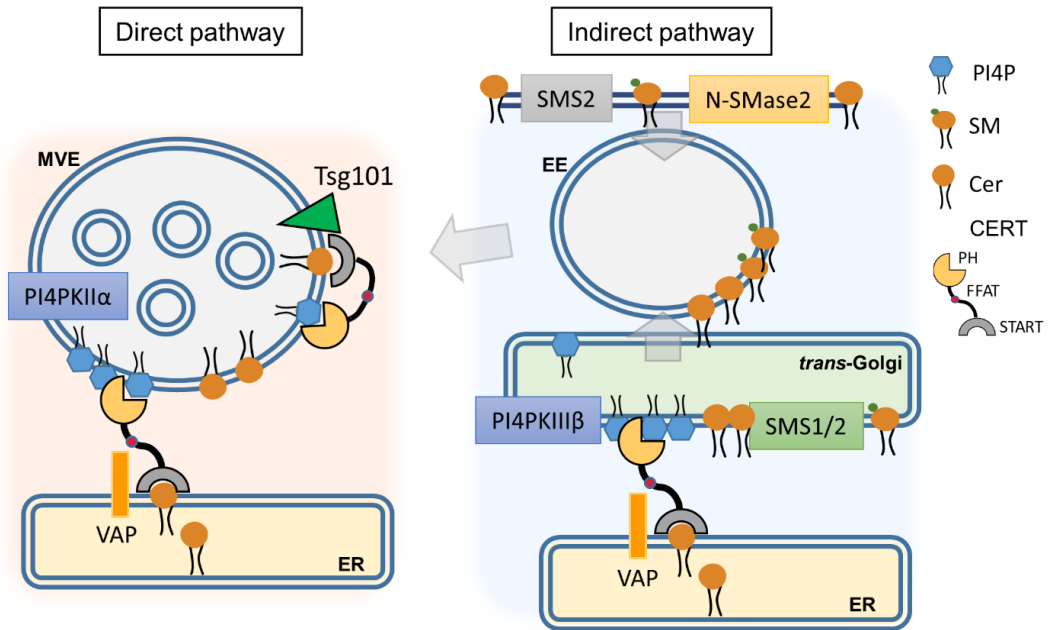
Figure 7. Schematic representation of CERT function for EV biogenesis. There are two routes for CERT-mediated EV biogenesis. The indirect pathway via the *trans*-Golgi network which is regulated by PI4P generated by PI4PIIIβ and involves SM production. This pathway is related to SMS1, SMS2 and N-Smase-2 dependent EV formation. The direct pathway is located in ER-endosomes/MVE contact sites. The enzyme PI4PIIα regulates CERT transfer of ceramide to the MVE. At the MVE, a complex is formed by Tsg101 and CERT, which requires ceramide.

Table 1. List of interactors of CERTL domains associated to EVs biogenesis.

CERT$_L$ domain	Screening	Interactor_Protein name	Gene ID	# Clones	PBS score	Reference
PH domain (N-terminal)	Gal 4	VAMP1	6843	1	D	[40]
START domain (C-terminal)	Gal 4	UBAP1	51271	2	C	[41]
	LexA	Tsg101	7251	2	D	[64]

The number of clones (# clones) represents the number of times the protein emerged during Y2HS screening. For each interaction, a PBS was computed to assess the interaction reliability. This score represents the probability of an interaction to be non-specific, primarily based on the comparison between the number of independent prey fragments found for an interaction and the chance of finding them at random.

Supplementary figures
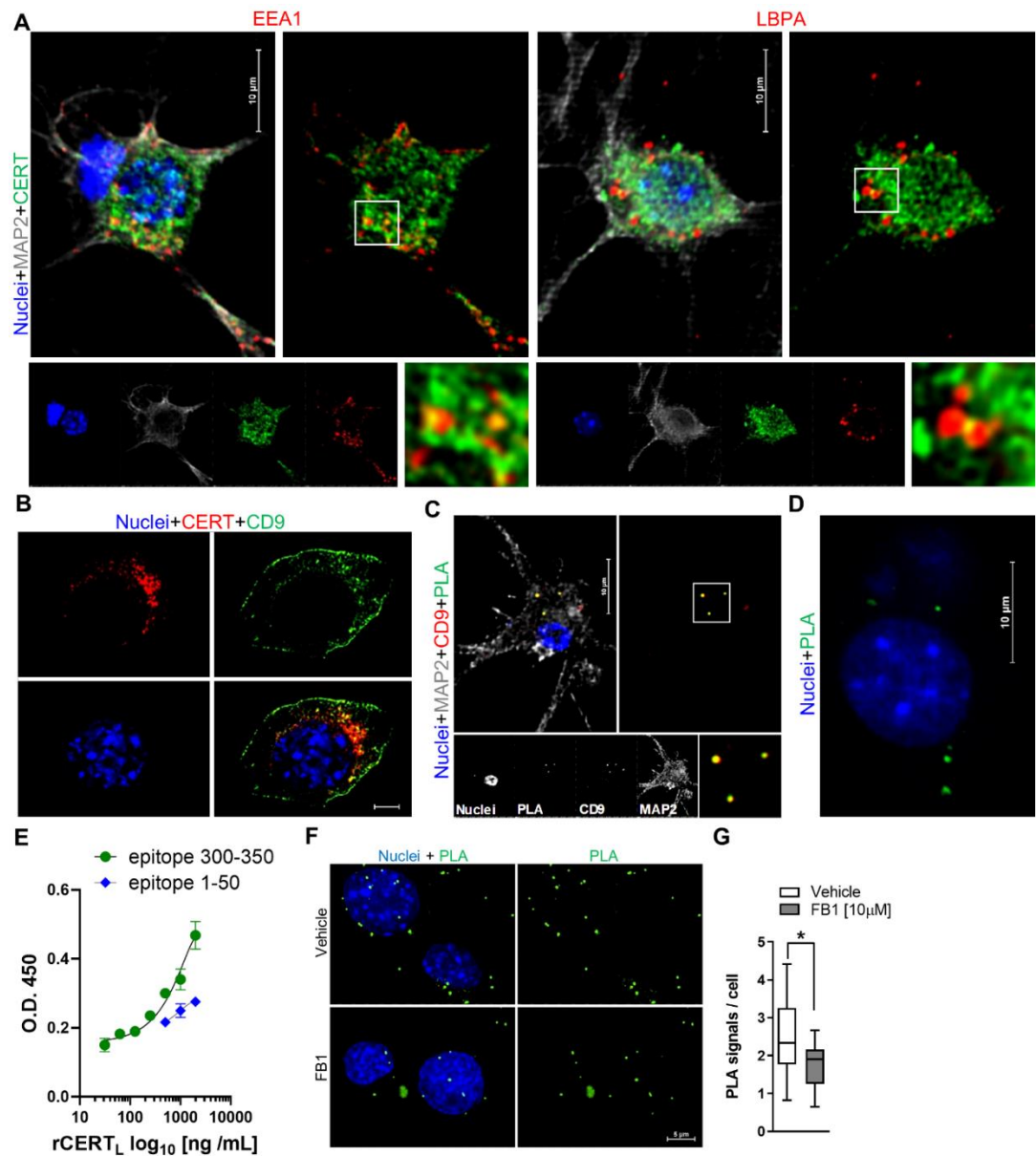
Supplementary Figure 1. The complex formation between CD81 and CERT requires ceramide biosynthesis. A) Confocal photomicrograph of fluorescence labeling of CERT (green) showing partial colocalization with EEA1 or LBPA (red) in neuronal cells. Neurons are identified by MAP-2 staining (grey). Scale bar 10 μm. B) Photomicrograph of fluorescence labeling of CERT (green) showing partial colocalization with immunolabeled CD9 (red). Nuclei were stained with DAPI (blue). Scale bar 5 μm. C) Photomicrograph of PLA (green) assay in primary neurons transfected with tdTomato-CD9 (red) showing proximity between Tsg101 and CERT. Neurons are identified by MAP-2 staining (grey). Scale bar 10 μm. D) Photomicrograph of PLA (green) assay in primary astrocytes showing proximity between Tsg101 and CERT. Scale bar 10 μm. E) Binding kinetics of

rCERT$_L$ to immobilized rTsg101 measured by ELISA. The complex was detected with anti-CERT antibody against epitope 300-350 (CERT$_L$ serial dilutions 2, 1, 0.5, 0.25, 0.125, 0.062, 0.031.µg / mL) and 1-50 (CERT$_L$ serial dilution: 2, 1, and 0.5). G) Representative photomicrographs of CD81 and CERT PLA signals after treatment with vehicle or FB1. PLA signals were detected by fluorescence microscopy with a 60x objective. Scale bar 5 µm. G) Box and Whiskers plot of two independent experiments including a total of 14-18 pictures / condition of 3 independent experiments reporting PLA signals normalized to the number of nuclei in the field of view, stained with DAPI. Whitney Mann U test (*p<0.05).
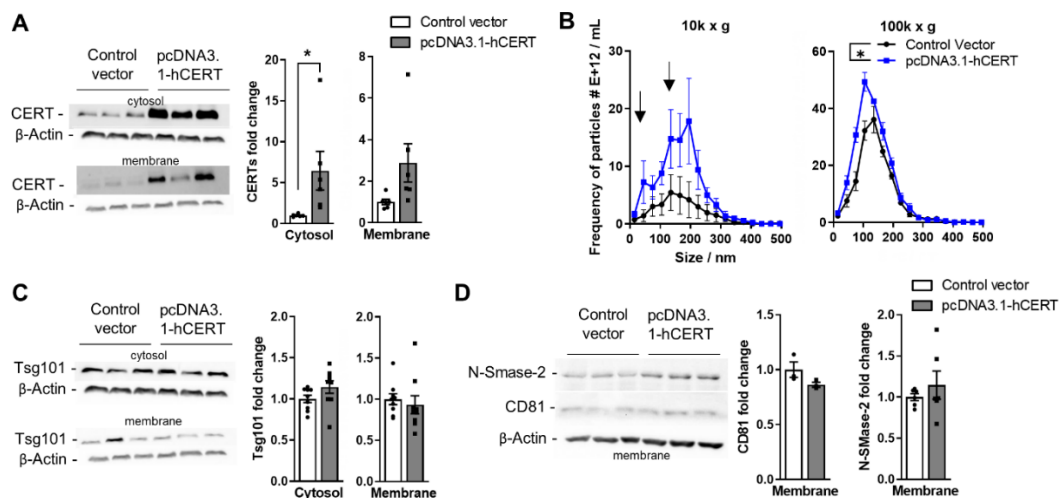
Supplementary Figure 2. Overexpression of CERT increases cytosolic and membrane levels of CERT without altering Tsg101, CD81 or N-SMase2 protein levels. A) Quantification of CERT in the cytosol and membrane fraction by immunoblotting after transfection with control vector and pcDNA-hCERT transfection. The β-actin bands were used for normalization. Bar graph represents average +/-SEM of N=3 / group. Unpaired t-test was applied, *p<0.05, and **p<0.01. B) 10K and 100k EVs size frequency distribution calculated by NTA after control vector and pcDNA-hCERT transfection (representative experiment with N = 3 / group). The areas under the curves were compared by Unpaired t-test *p<0.05. C-D) Quantification of Tsg101, CD81 and N-SMase in the cytosol and/or membrane fractions by immunoblotting after transfection with control vector and pcDNA-hCERT transfection. The β-actin bands were used for normalization. Bar graph represents average +/-SEM of N=3 / group. E) NTA measurement of EVs isolated from supernatant of N2a cells treated with vehicle, PI4KIIIβ, or PI4KIIα inhibitor. Bar graphs represent the mean +/-SEM of N=4 / condition.
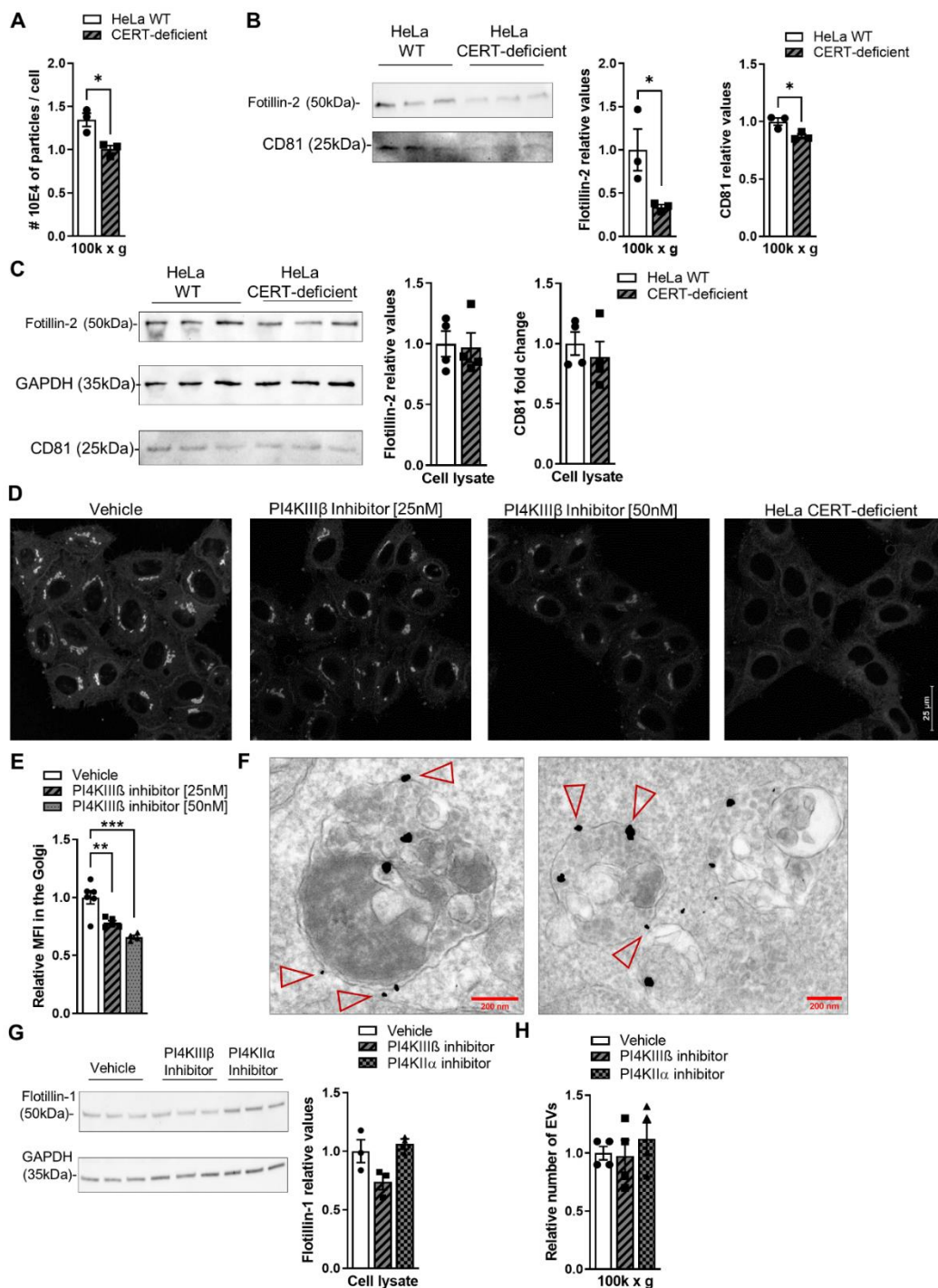
Supplementary Figure 3. CERT-deficient cell line secretes lower numbers of small EVs which are unaffected by PI4KIIIβ or PI4KIIα inhibitors. A) Numbers of EVs in the 100k EV fractions measured by NTA in HeLa WT and CERT-deficient cell lines. Bar graph represent +/-SEM of N=3 / group. B) Quantification of Flotillin-2 and CD81 of 100k EVs by Western blots. Bar graphs represent average +/-SEM of N=3 / group. C) Quantification of Flotillin-2 and CD81 Western blots

in cell lysate. Bar graphs represent average +/-SEM of N=4 / group. D) Confocal photomicrographs showing BODIPY FL C5-Cer redistribution to the Golgi region without or with PI4KIIIβ inhibitor (PI4KIIIβ-IN-10) 25nM and 50nM. HeLa CERT-deficient cell line was used negative control. E) Quantification of the relative MFI measured at the Golgi region after BODIPY FL C5-Cer incubation in absence or presence of 25nM or 50nM of PI4KIIIβ inhibitor. Bar graphs represent average +/-SEM of N= 4-6 / group. One-way ANOVA, Sidak's posthoc testing (**p<0.01; ***p<0.001). F) TEM image of Immunogold labeling of CERT in the limiting membrane of MVE. Arrow shows labeling on limiting membrane of MVE. H) Quantification of Flotillin-1 by Western blots in cell lysate. Bar graphs represent average +/-SEM of N=3 / group. H) Numbers of EVs in the 100k EV fractions measured by NTA in CERT-deficient cell lines after 24 h treatment with PI4KIIIβ or PI4KIIα inhibitors. Bar graph represent +/-SEM of N=4 / group.
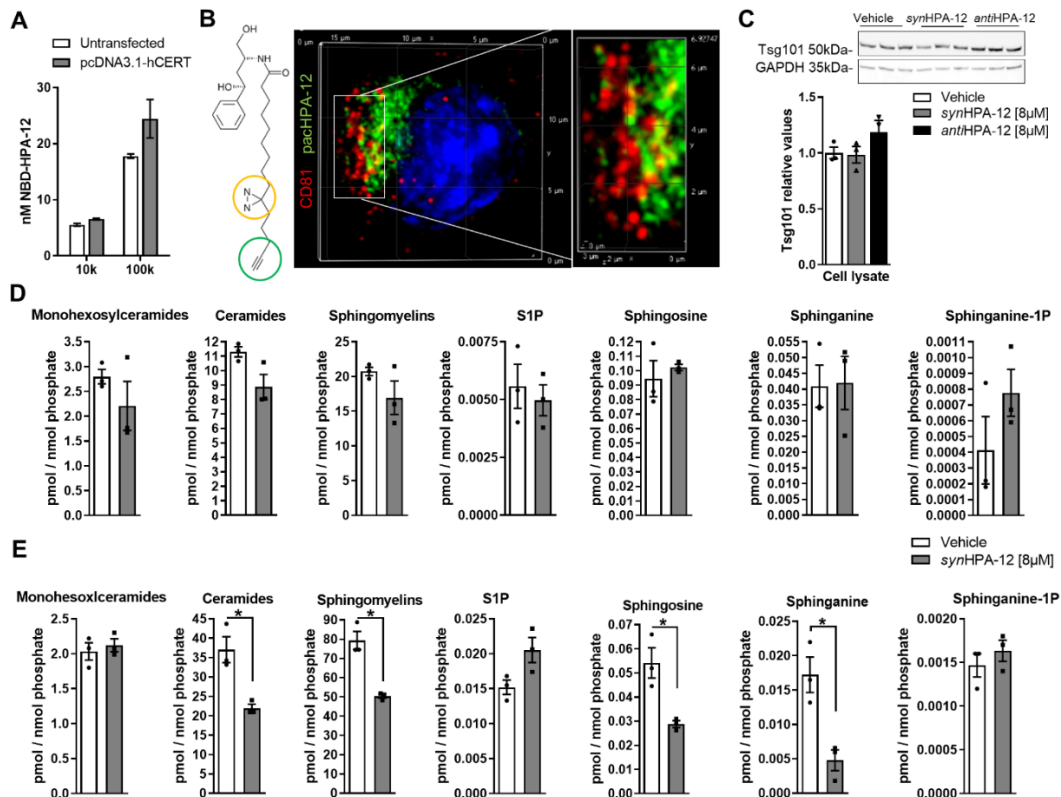
Supplementary Figure 4. HPA-12 partially colocalizes with CD81 and reduces ceramide, SMs, sphingosine and sphinganine in 100k EVs but not in cells. A) Extrapolation of HPA-12-NBD concentration in 10k and 100k EVs after transfection with pcDNA-hCERT and incubation for 24 h of HPA-12-NBD. Bar graph represents average +/-SEM of N=2 / group. B) Multi-plane deconvolved photomicrograph of fluorescent staining of pacHPA-12 (green), DAPI (blue) and CD81 (red) showing partial colocalization in N2a cells. Scales for each plane are noted in picture. C) Quantification of Tsg101 Western blots in cell lysate. Bar graphs represent average +/-SEM of N=3 / group. D, E) Quantification of monohexosylceramides, ceramide, SMs, S1P, sphingosine, sphinganine and sphinganine-1-P by mass spectrometry in cell pellet (D) and 100k EV (E) preparation. Bar graph represents average +/-SEM with each N=3/ group. Unpaired t-test (*p<0.05).
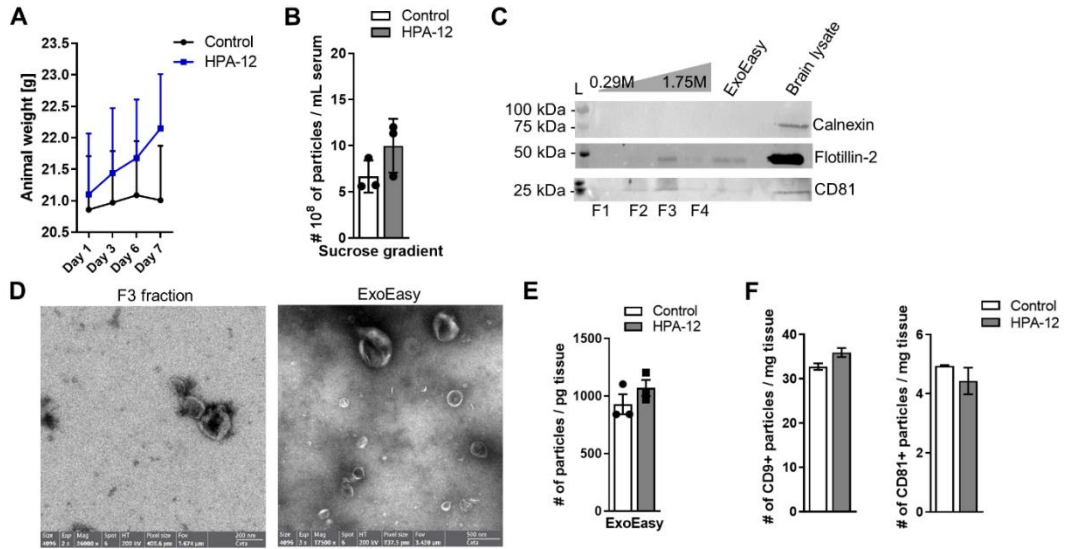
Supplementary Figure 5. Characterization of EVs from serum and brain extracellular space. A) Animal weights expressed in grams measured during HPA-12 administration. Bar graph represents average +/-SEM with each N=10/ group. B) NTA measurement of EVs isolated from serum with sucrose gradient. Bar graphs represents the mean +/-SEM of 3 animals per condition. C) Western blot images show protein expression from each fraction (F1-F4) or Exoeasy preparation (equal volume were loaded onto the gel) for the presence of the EV-associated proteins Flotillin-2 and CD81 and non-EVs marker calnexin. 10 μg of brain lysate was loaded as positive control. D) TEM images of F3 fraction and Exoeasy preparation. E) NTA measurement of EVs isolated from mouse brain with ExoEasy kit. Bar graph represents the mean +/-SEM of 3 animals per condition. F) Representative particle counts on different CD81 and CD9 capture spots. Bar graph represents average +/-SEM. for three capture spots of N = 4 (pooled) / group of two chips.

Supplementary Materials and Methods

Determination of HPA-12-NBD

After 48 h transfection with pcDNA3.1-CERT, N2a cells were incubated for 24 hours with 1 µM HPA-12-NBD. Next, EVs were isolated from the supernatant by centrifugation method as explained above. The fluorescence intensity was measured by a Synergy H1 (BioTek) multi-mode microplate reader.

Chromatography and mass spectrometry

^{1}H NMR and ^{13}C NMR spectra were recorded using a Varian 600 MHz spectrometer (600 MHz for ^{1}H and 150.9 MHz for ^{13}C). Chemical shifts (δ) were reported in parts per million (ppm) relative to tetramethylsilane (TMS, δ = 0.00 ppm) and referenced to deuterated solvent signals (CDCl$_3$, δ = 7.26 ppm (^{1}H) and δ = 77.16 ppm (^{13}C)). Analytical thin-layer chromatography (TLC) was carried out on silica gel glass plates (60 F254) using UV light (λ = 254 nm and λ = 366 nm) to visualize the compounds. Purifications using flash chromatography were performed on silica gel (40–73 µm). Reagents and solvents were purchased at reagent grade from Acros Organics and Sigma Aldrich and used without further purification unless stated. Solvents for column chromatography were of technical quality. Anhydrous dichloromethane (DCM) was used as supplied (Acros Organics). 2-(1H-Benzotriazole-1-yl)-1,1,3,3-tetramethylaminium tetrafluoroborate (TBTU) was purchased from Sigma Aldrich. 9-(3-(pent-4-yn-1-yl)-3H-diazirin-3-yl)nonanoic acid (pacFA, **1**) was prepared by literature procedure.[1] 1-Phenyl-3-amino-butane-1,4-diol (**2**) was prepared by our method.[2]

Supplementary experimental procedure

Synthesis of HPA-12-pacFA **3**
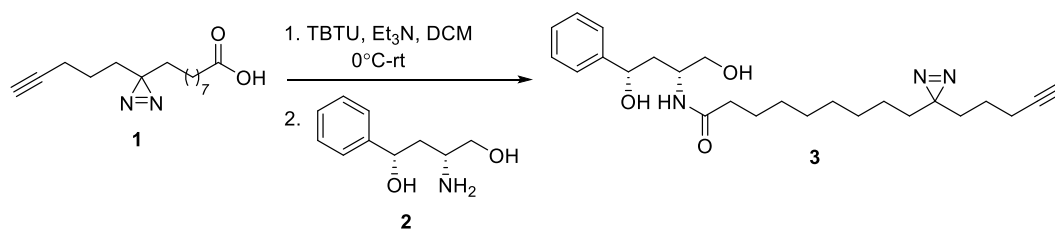
pacFa **1** (136 mg; 0.514 mmol) was suspended in dry DCM (3.5 ml) under argon atmosphere, and the flask was wrapped with aluminum foil to prevent the presence of light. The resulting solution was cooled to 0°C, and TBTU (1.1 equiv; 182 mg; 0.565 mmol) was added, followed by the addition of Et$_3$N (1.5 equiv; 78 mg; 108 µl; 0.771 mmol). After 10 min, aminodiol **2** (1 equiv; 93.2 mg; 0.514 mmol) was added in one portion, and the reaction mixture was stirred at rt for 12 h. After consuming starting material, the reaction mixture was concentrated under vacuum and purified by column chromatography (gradient: ethyl acetate/MeOH) to afford HPA-12-pacFA **3** as a yellowish solid (143 mg; 65%).

^{1}H NMR (600 MHz, CDCl$_3$) δ 7.34 – 7.27 (m, 5H) 6.41 (d, *J* = 6.4 Hz, 1H), 4.82 (dd, *J* = 9.1, 3.3 Hz, 1H), 4.10 – 4.01 (m, 1H), 3.72 – 3.63 (m, 2H), 2.19 – 2.12 (m, 4H), 2.04 – 1.93 (m, 3H), 1.63 – 1.45 (m, 4H), 1.38 – 1.23 (m, 13H), 1.11 – 1.03 (m, 1H).

¹³C NMR (151 MHz, CDCl₃) δ 174.5, 144.3, 128.8, 128.0, 125.7, 83.6, 72.3, 69.0, 66.0, 50.8, 40.8, 36.9, 32.9, 32.0, 29.3(x3), 29.2, 28.6, 25.8, 23.9, 22.9, 18.1.

Supplementary references

[1]	Haberkant, P.; Raijmakers, R.; Wildwater, M.; Sachsenheimer, T.; Brügger, B.; Maeda, K.; Houweling, M.; Gavin, A.-C.; Schultz, C.; van Meer, G.; Heck, A. J. R.; Holthuis, J. C. M. *Angew. Chem. Int. Ed.* **2013**, *52*, 4033.

[2]	Santos, C.; Fleury, L.; Rodriguez, F.; Markus, J.; Berkeš, D.; Daïch, A.; Ausseil, F.; Baudoin-Dehoux, C.; Ballereau, S.; Génisson, Y. *Bioorg. Med. Chem.* **2015**, *23*, 2004.

¹H and ¹³C NMR spectra

HPA-12-pacFA **3**

^{13}C-NMR (151 MHz, CDCl$_3$)

70
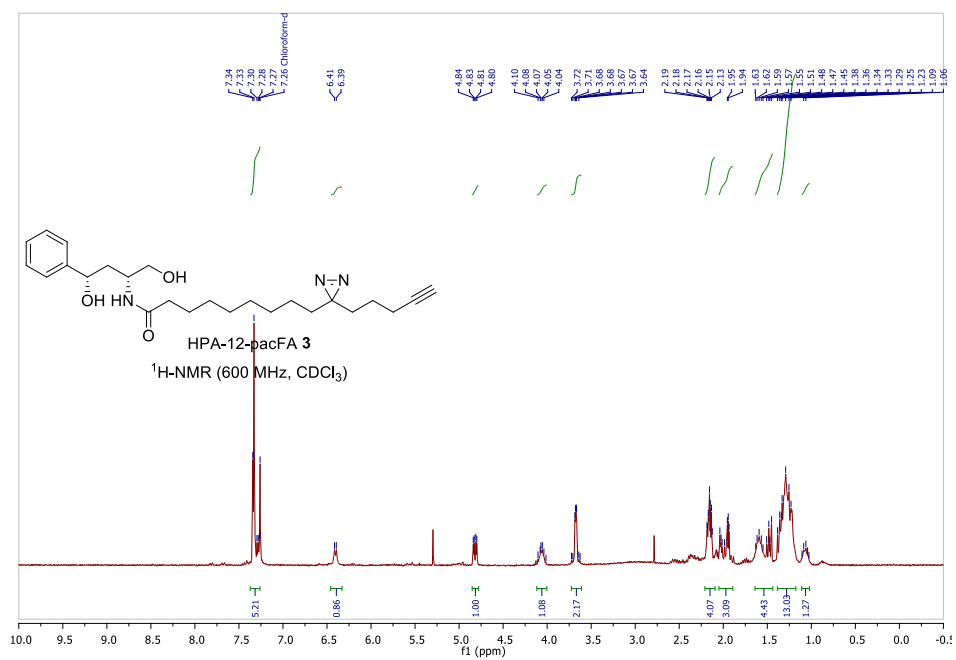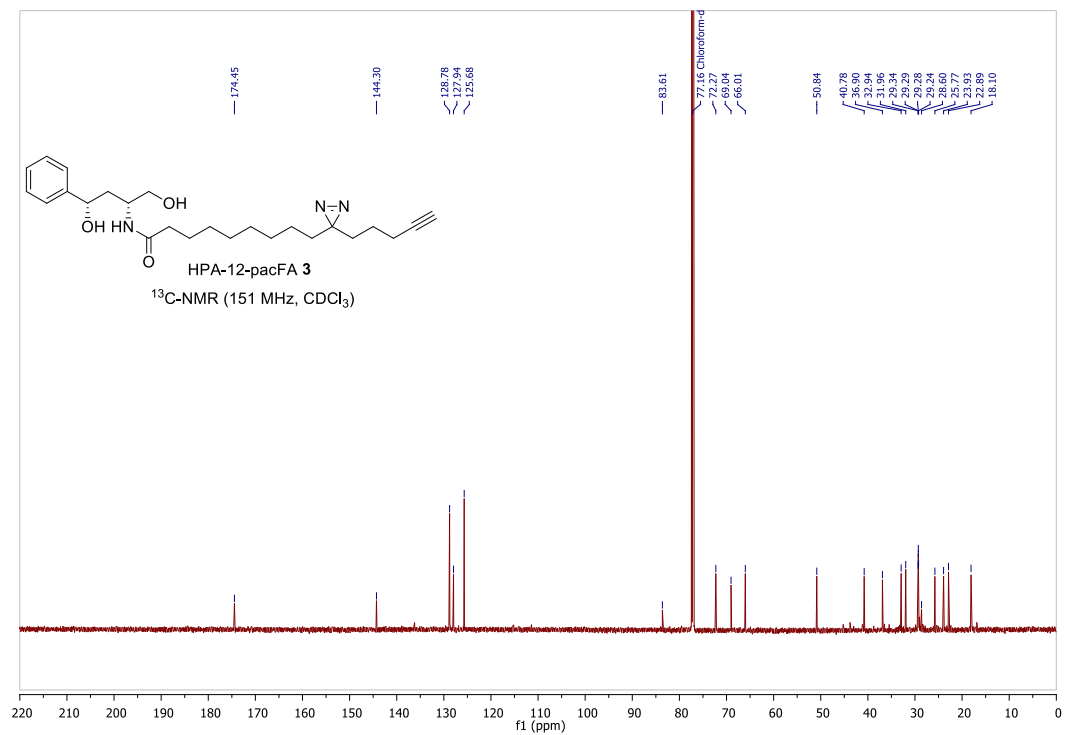
Chapter 3

Immunofluorescence labeling of lipid-binding proteins CERTs to monitor lipid rafts dynamics

Caterina Giovagnoni [1], Simone Crivelli [1,2], Mario Losen [1], Pilar Martinez-Martinez[1]

[1] Division of Neuroscience, School for Mental Health and Neuroscience, Maastricht University, Maastricht, the Netherlands
[2] Department of Physiology, University of Kentucky College of Medicine, Lexington, KY, USA

Abstract

Fluorescence microscopy is a powerful and widely used tool in molecular biology. Over the years, the discovery and development of lipid-binding fluorescent probes has established new research possibilities to investigate lipid composition and dynamics in the cell. For instance, fluorescence microscopy has allowed the investigation of lipid localization and density in specific cell compartments such as membranes or organelles. Often, the characteristics and the composition of lipid-enriched structures are determined by analyzing the distribution of a fluorescently labeled lipid probe, which intercalates in lipid-enriched platforms, or specifically binds to parts of the lipid molecule. However, in many cases antibodies targeting proteins have higher specificity and are easier to generate. Therefore, we propose to use both antibodies targeting lipid transporters and lipid binding probes to better monitor lipid membrane changes. As an example, we visualize lipid rafts using the fluorescently labeled-B-subunit of the cholera toxin in combination with antibodies targeting ceramide-binding proteins CERTs, central molecules in the metabolism of sphingolipids.

Key words

Fluoresce microscopy, fluoresce lipid probes, lipid rafts, β-subunit cholera toxin, CERTs.

3.1   Introduction

Fluorescence microscopy (FM) is an imaging technique that due also to the development of innovative imaging systems has become a robust method to investigate proteins, glycans, small biological and nonbiological molecules in different cell types and tissues [1]. The basic concept of FM is the detection of a target molecule by specific probes, directly or indirectly labeled, that are then visualized by fluorescence microscopes. One of the main advantages of FM is the possibility to combine two or more probes, to investigate simultaneously the presence and the localization of different molecules and structures. For many years, FM was used only to target proteins, but lately, new fluorescence probes have been developed to detect lipids localized in intracellular compartments and in cell membranes [2]. These probes can be analogs of natural lipids, lipophilic organic dyes but most commonly, they are lipid-binding toxins [3]. Relevant to these methods are the fluorescent probes used to label lipid rafts and how they can be easily combined with antibodies to visualize and characterize lipid associated proteins in lipid-enriched domain in cell membranes and organelles. Many probes have been developed to detect these membrane structures in living and fixed cells, but one in particular, the membrane-binding B domain of cholera toxin (CTxB) is the most commonly used [4]. The idea that CTxB associates with lipid rafts was demonstrated in 2000 when it was found in detergent-resistant membranes [5], later on this was corroborated by additional methods [6]. CtxB binds to monosialotetrahexosylganglioside, the prototype ganglioside (GM1) that is highly expressed in lipid rafts [7]. As a result, fluorescently labeled CTxB added to cells can be directly visualized by fluorescence microscopy, with the aim to investigate lipid rafts intracellularly and in the plasma membrane [4]. Fluorescence-labeled CTxB can be used in combination with immunofluorescence, where antibodies, which bind to lipid interacting proteins such as lipid transporters, help to monitor membrane composition and dynamics. Combining immunofluorescence and fluorescence probes enables the possibility to obtain high specificity and sensitivity of detection with rapid and reproducible outcomes. For this reason, to better understand the composition of rafts in cell membranes we combined CTxB staining with immunostaining of ceramide binding proteins CERTs, well-characterized ceramide transporters. CERT was described for the first time in 2003 as a transporter of ceramide from the endoplasmic reticulum to the Golgi apparatus [8]. There are at least three isoforms of CERTs, one long variant composed of 770 amino acids (named CERTLΣ128), a 642 amino-acid isoprotein (here named $CERT_L$), and a short form that lacks 26 amino acids in the middle domain (here named CERT) [9]. Presumably, the shorter isoform is more active in the intracellular compartments and mediates the lipid transfer, whereas the long

ones are mainly insoluble membrane bound polypeptides also involved in the extracellular pathways [10]. CERTs interaction with ceramide, an important modulator of rafts, and regulator of sphingomyelin production might influence lipid composition and polarity of intra- and extracellular membranes ultimately determining lipid raft conformation and physiology [11–13]. Lipid rafts have a central role in homeostasis and maintenance of cells and often proapoptotic pathways are linked to changes in raft composition and lipid–protein interactions. Ceramide levels are elevated in apoptotic cells and this is believed to be one of the main causes of rafts changes during cell death [14, 15]. interestingly, $CERT_L$ are highly expressed in apoptotic cells meaning that there is a correlation between ceramide levels and the expression of its binding protein. The activity of CERTs during apoptosis can be seen as an indirect but outstanding cause-consequence event on ceramide dysregulation and the subsequent physiological changes at lipid and protein level [16]. Here, therefore, we make use of CTxB staining to detect lipid rafts in HEK293 cells in combination with CERTs antibodies in order to better monitor cell membrane dynamics (Fig. 1)
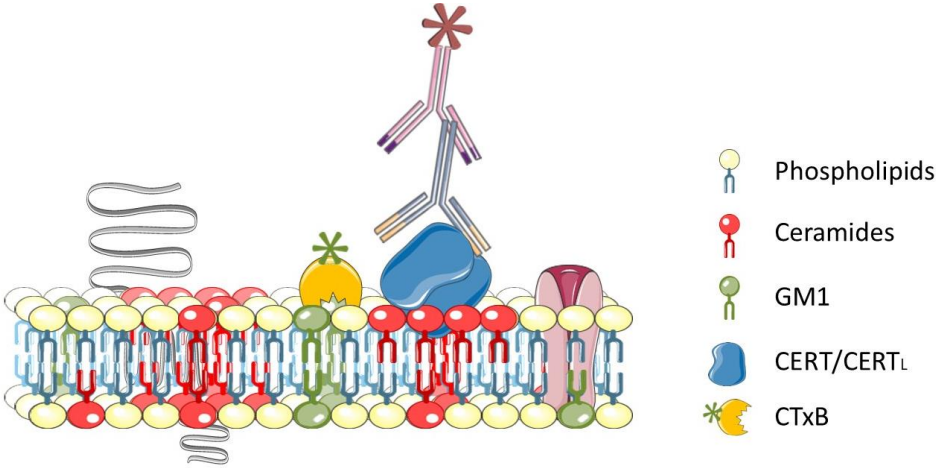
Figure 1: Representation of the method used to stain lipid rafts with Alexa 488 Cholera Toxin Subunit B (CTxB), anti CERT/CERTL antibodies and Alexa 594/ 647 labelled secondary antibodies

3.2   Materials

All the reagents are prepared with 1 x Phosphate-Buffered Saline (PBS) pH 7.4, unless otherwise indicated and are prepared fresh before the experiments.

Cell culture

1. Cell line- Human embryonic kidney cells (HEK 293)

2. Maintenance medium - Dulbecco's Modified Eagle Medium (DMEM) is supplemented with 10% inactivated fetal calf serum (FCS - 5% Penicillin-Streptomycin and 5%,L-glutamine.

3. 1x Trypsin

4. 1x PBS

Transfection

1. 12 mm x 12 mm coverslips

2. 1x Poly- D- lysine (PDL) in 1xPBS

3. Transfection reagent: Lipofectamine 2000

4. Transfection medium - Dulbecco's Modified Eagle Medium (DMEM-) supplement free

5. DNAs: Flag - PcDNA 3.1 CERT (NCBI – 10087- NM_031361.3) / CERTL (NCBI- 10087- NM_005713.3) and PcDNA3.1

Labeling

1. Cholera Toxin Subunit B (Recombinant), Alexa Fluor™ 488 Conjugate

2.Polyclonal rabbit anti CERT/ CERT$_L$

3. Monoclonal mouse anti CERT$_L$ mAb1 [17]

4. Donkey-anti rabbit Alexa Fluor 647

5. Donkey- anti mouse Alexa Fluor 594

6. Hoechst dissolved in 1x PBS

7. 80% glycerol in 1x PBS

8. 4% formaldehyde dissolved in 1x PBS

9. 1% Bovine Serum Albumin (BSA, dissolved in 1x PBS (BSA-PBS)

Microscopy

1. Microscopy slides

2. Olympus BX51WI spinning-disk confocal fluorescence microscope with a Hamamatsu EM-CCD C9100 digital camera

3. Software μManager and Image J [18]

3.3   Methods

Cell culture

1. Maintain the HEK 293 in complete DMEM in an incubator with 5% CO_2 and 21% of oxygen at 37 C (see Note 1).

2. 24 h prior to the experiment, place 10 coverslips in a 60 mm plate, add 5 ml of poly-D-lysine diluted in 1 PBS to the plate and incubate for 1 h at 37 C. Before plating the cells wash the plate with 1X PBS.

3. Wash the cells with 1 PBS, trypsinize for 5 min in the incubator, and resuspend them in 10 ml of prewarmed (37 C) complete DMEM.

4. Centrifuge the cells for 5 min at 1000 g and resuspend the pellet in prewarmed complete DMEM (see Note 2).

5. Plate 1.5x 10^5 cells in 5 ml of complete DMEM (see Note 3)76

Transfection

1. After 24 h, dissolve 2500 ng of total DNA in 250 μl of medium and 5 μl of lipofectamine 2000 in 250 μl of medium. After 5 min mix them together, vortex, spin down and incubate for 20 min.

2. In the meanwhile, change the complete medium with 5 ml no-supplemented DMEM

Add the DNA- lipofectamine 2000 mix to the cells; gently shake the plate to let the complex diffuse over the whole plate. (See note 4)

3. Maintain the cells for 72 h in the incubator

Fixation and blocking

1. Wash the cells 3 times with 300 μL chilled 1x PBS

2. Add 5 ml of 4% PFA to the plate

3. Incubate for 15 min at 4 °C

4. Wash three times with PBS

5. Block the cells for at least 30 min in pre-chilled blocking solution (BSA-PBS)

Labeling with Cholera Toxin Subunit B (See note 5 and 6)

1. Prepare the working solution diluting mixing1 µl of the CTxB stock solution (1mg/ml) in 500 µl of medium (see Note 7)

2. Add 300 µl of the CTxB to the cells directly in the coverslips

3. Incubate for 10 min at 4 °C in the dark

4. Wash three times the cells with 300 µl 1xPBS

Labeling with CERTL mAb1 antibody (See note 8)

1. Prepare the working solution of the antibody diluting 1 µl of stock solution (3mg/ml) in 500 µl of blocking solution

2. Incubate the cells with 40 µl of antibody for 1 h at room temperature

Labeling with CERTs HPA608 antibody

1. Prepare the working solution of the secondary diluting 1 µl of the stock solution in 500 µl of blocking solution.

2. Incubate the cells with 40 µl of antibody for 1 h at room temperature

Labeling with secondary antibodies – donkey anti mouse 594 and donkey anti rabbit 647

1. Wash the cells three times in 300 µL 1x PBS

2. Prepare the working solution of the secondary antibodies diluting 1 µl of the stock solution in 1000 µl of blocking solution

3. Incubate the cells with 40 µl of antibody for 1 hour at room temperature (see note 9)

Mounting and imaging

1. Wash the cells three times with 1x PBS

2. Incubate for 5 min the cells with Hoechst diluted (1:1000) in 1x PBS

3. Wash the cells three times with MilliQ water

4. In the meanwhile, drop 3 µl of 80% glycerol onto the microcopy slides

5. Mount the coverslip on the microscopy slides with small forceps

6. Let dry the coverslip in glycerol overnight at 4 °C in the dark (see note 10)

7. Image with Olympus BX51WI spinning-disk confocal fluorescence microscope with a Hamamatsu EM-CCD C9100 digital camera. Use the software µManager for the acquisition (see note 11)

8. Analyze the images with ImageJ

Image analysis

1. Save the images as stacks with µManager Open Source Microscopy Software

2. Analyze the images with ImageJ adjust the contrast minimum and maximum values for each fluorescence channel

3. Add the scale bar

4. Make a stack and create a montage of the images

5. Save the montages as TIFF files (Figure 2-3)
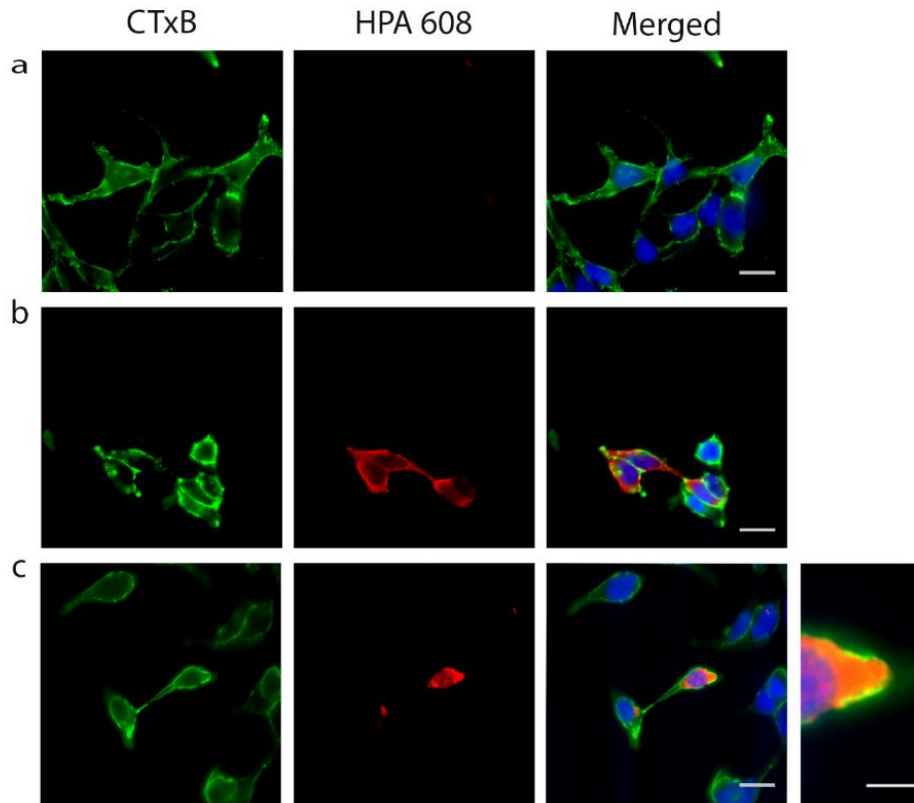
Figure 2: Co-staining with HPA 608 rabbit anti-CERT and CERTL (red) , Alexa 488 CTxB (green) and nuclei (blue) a .Cholera toxin B subunit staining and CERT/CERTL immunostaining in PcDNA3.1 transfected cells b. Cholera toxin B subunit stai ning and CERT/CERTL immunostaining in CERT transfected cells c. Cholera toxin B subunit staining and CERT/CERTL immunostaining in CERTL transfected cells. Scale bar 20μm (zoom region scale bar 5 μm)
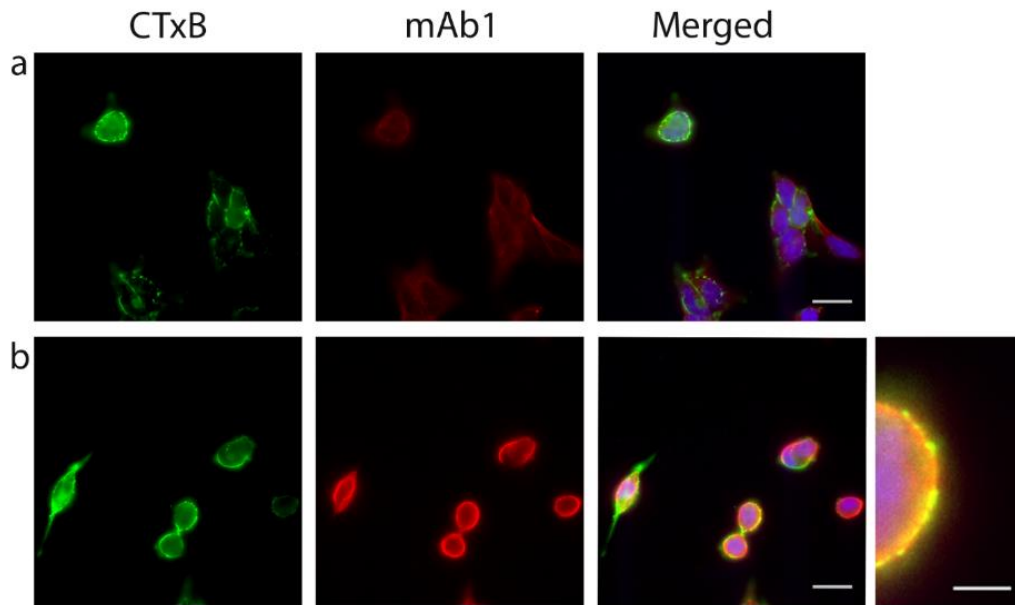
Figure 3: Co-staining with mAb1 Mouse anti-CERTL (in red) , Alexa 488 CTxB (in green) and nuclei (in blue).
a. Cholera toxin B subunit staining and CERTL immunostaining in PcDNA3.1 transfected cells. b. Cholera toxin B subunit staining and CERTL immunostaining in CERTL transfected cells. Scale bar 20µm (zoomed region scale bar 5 µm)

3.4   Notes

1. Cells after thawing have to be sub-cultured at least for 3 passages before the experiments allowing the re-establishment of normal cell cycle [19].

2. Before plating the cells, wash and centrifuge them for 5 min at 1000 rpm. After the centrifugation, it is crucial to resuspend them carefully in order to break cell clumps and allowing a homogenous distribution of single cells into the plate.

3. For a high transfection efficiency in 72 h, HEK293 must be 60-70% confluent and prior to the transfection they have to be attached to the plate. If they show round shape or they are floating, is not recommended to perform the transfection.

4. During the transfection is crucial to incubate the cells and the DNA: lipofectamine 2000 in supplement free DMEM, since FCS can influence drastically the transfection efficacy.

5. Vortex the CTxB stock solution before diluting it in the medium in order to resuspend the aggregates.

6. Labelling with the CTxB can be performed in living cells and in fixed cells. Cells can also be first labelled with the CtxB and afterwards fixed with 4% PFA. All methods show good results and comparable labelling.

7. Before labelling, place the coverslips in a 24 well plate for the washing. Perform the staining with the CTxB adding 300 ul of diluted working solution in the wells. The staining must be performed at 4 °C in the dark in a shaker[20].

8.Wash the cells at least three times in the 24 well plate with 1 x PBS. Bad washing leads to high background during the imaging.

9. For the antibodies staining, drop 40 μl of antibody in a tight parafilm piece and place the coverslip upside down facing the antibodies. Follow the same procedure for the secondary antibodies, but the incubation has to be performed in the dark [21].

10. To avoid artefacts, 80 % glycerol must be prepared fresh, and the microscopy slides need to be cleaned with ethanol [21].

11. It is optimal to image all the samples the same day [21].

3.5   References

1.   *Donaldson, J.G., Immunofluorescence staining. Curr Protoc Cell Biol, 2001. Chapter 4: p. Unit 4.3.*

2.   *Maekawa, M. and G.D. Fairn, Molecular probes to visualize the location, organization and dynamics of lipids. J Cell Sci, 2014. 127(Pt 22): p. 4801-12.*

3.   *Laguerre, A. and C. Schultz, Novel lipid tools and probes for biological investigations. Curr Opin Cell Biol, 2018. 53: p. 97-104.*

4.   *Day, C.A. and A.K. Kenworthy, Functions of cholera toxin B-subunit as a raft cross-linker. Essays Biochem, 2015. 57: p. 135-45.*

5.   *Badizadegan, K., et al., Heterogeneity of detergent-insoluble membranes from human intestine containing caveolin-1 and ganglioside G(M1). American journal of physiology. Gastrointestinal and liver physiology, 2000. 278(6): p. G895-G904.*

6.   *Yuan, C., et al., The size of lipid rafts: an atomic force microscopy study of ganglioside GM1 domains in sphingomyelin/DOPC/cholesterol membranes. Biophysical journal, 2002. 82(5): p. 2526-2535.*

7.   *Moreno-Altamirano, M.M.B., I. Aguilar-Carmona, and F.J. Sánchez-García, Expression of GM1, a marker of lipid rafts, defines two subsets of human monocytes with differential endocytic capacity and lipopolysaccharide responsiveness. Immunology, 2007. 120(4): p. 536-543.*

8.   *Hanada, K., et al., Molecular machinery for non-vesicular trafficking of ceramide. Nature, 2003. 426(6968): p. 803-9.*

9.   *Mencarelli, C., et al., The ceramide transporter and the Goodpasture antigen binding protein: one protein--one function? J Neurochem, 2010. 113(6): p. 1369-86.*

10.   *Revert, F., et al., Goodpasture antigen-binding protein is a soluble exportable protein that interacts with type IV collagen. Identification of novel membrane-bound isoforms. J Biol Chem, 2008. 283(44): p. 30246-55.*

11.	Crivelli, S.M., et al., CERTL reduces C16 ceramide, amyloid-β levels, and inflammation in a model of Alzheimer's disease. Alzheimer's Research & Therapy, 2021. **13**(1): p. 45.

12.	Gupta, N. and A.L. DeFranco, Visualizing lipid raft dynamics and early signaling events during antigen receptor-mediated B-lymphocyte activation. Mol Biol Cell, 2003. 14(2): p. 432-44.

13.	Bieberich, E., Sphingolipids and lipid rafts: Novel concepts and methods of analysis. Chemistry and Physics of Lipids, 2018. 216: p. 114-131.

14.	George, K.S. and S. Wu, Lipid raft: A floating island of death or survival. Toxicology and applied pharmacology, 2012. 259(3): p. 311-319.

15.	Haimovitz-Friedman, A., R.N. Kolesnick, and Z. Fuks, Ceramide signaling in apoptosis. Br Med Bull, 1997. 53(3): p. 539-53.

16.	Bode, G.H., et al., Complement activation by ceramide transporter proteins. J Immunol, 2014. 192(3): p. 1154-61.

17.	Mencarelli, C., et al., Goodpasture antigen-binding protein/ceramide transporter binds to human serum amyloid P-component and is present in brain amyloid plaques. The Journal of biological chemistry, 2012. 287(18): p. 14897-14911.

18.	Edelstein, A.D., et al., Advanced methods of microscope control using µManager software. 2014, 2014.

19.	Molinas M et al (2014) Optimizing the transient transfection process of HEK-293 suspension cells for protein production by nucleotide ratio monitoring. Cytotechnology 66(3):493–514

20.	Kenworthy A et al, (2000) High-Resolution FRET Microscopy of Cholera Toxin B-Subunit and GPI-anchored Proteins in Cell Plasma Membranes. Molecular Biology of the Cell 11 (5):1645–1655

21.	Hoffmann C, Stevens J, Zong S, et al. (2018) Alpha7 acetylcholine receptor autoantibodies are rare in sera of patients diagnosed with schizophrenia or bipolar disorder. PLoS One 13(12):e0208412

Chapter 4

Identification of the binding partners of ceramide transfer proteins in the brain

Caterina Giovagnoni[1], Mario Losen[1], Sandra Claessens[1], Gerard Bode[1], Pilar Martinez-Martinez[1]

[1.] School for Mental Health and Neuroscience (MHeNs), Department of Psychiatry and Neuropsychology, Maastricht University, Maastricht, the Netherlands.

Chapter 5

Sphingolipids and immunity: insights on neuroinflammation and neurodegeneration

Caterina Giovagnoni[1], Philip Sänger[1], Mario Losen[1], Bart Rutten[1], Pilar Martinez-Martinez[1]

[1.] School for Mental Health and Neuroscience (MHeNs), Department of Psychiatry and Neuropsychology, Maastricht University, Maastricht, the Netherlands.

Invitation to Ageing Research Reviews

Chapter 6

Sphingolipids in Alzheimer's disease, how can we target them?

Simone M. Crivelli[1,2], Caterina Giovagnoni[1], Lars Visseren[1], Anna-Lena Scheithauer[3], Nienke de Wit[4], Sandra den Hoedt[5], Mario Losen[1], Monique T Mulder[5], Jochen Walter[3], Helga E. de Vries[4], Erhard Bieberich[2], Pilar Martinez-Martinez[1#]

[1] Division of Neuroscience, School for Mental Health and Neuroscience, Maastricht University, Maastricht, the Netherlands
[2] Department of Physiology, University of Kentucky College of Medicine, Lexington, KY, USA
[3] Department of Neurology, University of Bonn, Bonn, Germany
[4] Department of Molecular Cell Biology and Immunology, Amsterdam Neuroscience, Amsterdam UMC, Vrije Universiteit Amsterdam, VU University Medical Center, Amsterdam, the Netherlands.
[5] Department of Internal Medicine, Division of Pharmacology, Vascular and Metabolic Diseases, Erasmus MC University Medical Center, Rotterdam, the Netherlands

Abstract

Altered levels of sphingolipids and their metabolites in the brain, and the related downstream effects on the immune system, provide a framework for understanding mechanisms in neurodegenerative disorders and for developing new intervention strategies. In this review we will discuss: the metabolites of sphingolipids that function as second messengers; and functional aberrations of the pathway resulting in Alzheimer's disease pathophysiology. Furthermore, we discuss the evidence of the sphingolipid pathway druggability. We argue on how the sphingolipid pathway may represent a new framework for developing novel intervention strategies in AD. We will highlight the possible use of clinical and non-clinical drugs to modulate sphingolipid pathways and sphingolipid-related biological cascades.

6.1 Sphingolipid metabolism in the nervous system

Sphingolipids (SLs) were discovered in the brain as structural components of cell membranes by J.L.W. Thudichum in 1874. SL composition and metabolism are intimately connected to brain development and synaptic plasticity [1]. Altered sphingolipid metabolism due to genetic mutations can lead to their abnormal deposition in neuronal tissue, causing severe cognitive retardation [2]. SL disbalance has been implicated in neurological disorders such as depression, Parkinson's disease (PD) and Alzheimer's disease (AD) [3, 4]. Therefore, the biochemistry of SLs under normal and pathological conditions has generated new interest recently. SL metabolism is a highly compartmentalized pathway and mislocation of key intermediate products, like ceramide, from one cellular compartment to another might condemn cells to death [5-7]. Ceramide is considered the central product of SL metabolism and it is formed via two main pathways: the anabolic pathway known as the SL de novo synthesis and the catabolic pathway referred to as the salvage pathway.

De novo sphingolipid synthesis

The first step of SL synthesis is the production of 3-keto-dihydrosphinganine in the cytosolic face of the endoplasmic reticulum (ER) by condensation of the precursors serine and palmitoyl-CoA [8]. This reaction is mediated by the enzyme serine palmitoyl transferase (SPT). This enzyme is strongly expressed in pyramidal neurons in the brain [9] and generates 3-keto-dihydrosphinganine, which is subsequently converted into sphinganine by the enzyme 3-keto-dihydrosphingosine reductase [10].

Sphinganine or sphingosine is the substrate of a family of acyl-CoA transferases, called ceramide synthases (CerSs) [11]. Six established CerSs are present in eukaryotic cells, which perform the same chemical reaction (i.e., N-acylation of the sphingoid long chain base) however, each CerS has a high specificity toward the acyl CoA chain length used for N-acylation as reported in detail by Mullen et al., [12]. Thus, the CerSs are responsible for the fatty acid composition of ceramides [12-14]. In neuronal cells, C18 acyl chains are coupled to sphinganine at the highest rate and in glial cells, C18 and C24 acyl chains [15].

The central product of the de novo biosynthetic pathway are ceramides. Ceramides are formed by the enzyme dihydroceramide desaturase which removes two hydrogen atoms creating the 4,5-trans double bond in the sphinganine base of dihydroceramide [16]. Once formed, ceramide is delivered to the Golgi complex to produce more complex SLs. Major modifications can be introduced at the C-1 hydroxyl group. This hydroxyl group serves as an acceptor group for monosaccharide to produce

glycosphingolipids, or as phosphoryl choline acceptor to yield sphingomyelin [17, 18]. Majority of ceramides are transported from the ER to the Golgi apparatus, either through vesicular transport to act as a precursor for glucosyl-ceramide, or via an ATP-dependent process mediated by the ceramide transfer protein (CERT) to act as a precursor for sphingomyelin [19]. Transport of ceramides via CERT is highly specific and dependent on the acyl chain length [20]. In the trans-Golgi, the ceramide transferred by CERT is almost exclusively converted into sphingomyelin by sphingomyelin synthase 1 (SMS1). Glucosylsphingolipids are synthesized by glucosylceramide synthases (GCS) and are mainly formed by ceramide that is transferred through a non-ATP dependent vesicular process. Glycosphingolipids can be classified based on the number of sugar residues: glycosphingolipids containing monosaccharides are termed cerebrosides while if they contain oligosaccharides are referred to as globosides or gangliosides (with one or more sialic acids linked on the sugar chain). This review primarily focuses on ceramide and sphingosine. Readers interested in the function of glycolipids, particularly globosides and gangliosides in neural differentiation are kindly referred to the following excellent reviews on this topic: [21-28].

The ceramide salvage pathway

Activation of several catabolic enzymes yields ceramide and phosphatidylcholine or monosaccharide units from complex SLs which are recycled to produce other lipid metabolites [29]. This catabolic cascade is also known as the salvage pathway [30]. Sphingomyelin is the most abundant SL of the cell membrane and is important in membrane fluidity and homeostasis [31, 32]. The breakdown of sphingomyelin is the fastest route to generate ceramide. The catabolism of sphingomyelin begins with the hydrolysis of the phosphodiester bond releasing phosphoryl choline and ceramide, a reaction that is catalyzed by sphingomyelinases (SMases). Five types of SMases have been discovered that differ for their pH optimum, cation requirement and subcellular localization [33, 34]. The first report of SMase activity in human brain tissue showed a high hydrolytic activity in presence of magnesium (Mg^{2+}) and under physiological pH [35, 36]. These enzymes are associated with myelin and show a peculiar functional pattern with high activity during development which decreases with age [35, 37-39]. There are other isoforms of SMases which are located in the lysosomes and work efficiently under acidic pH conditions [40]. Additional information regarding the sphingomyelin hydrolysis cycle will be discussed in the section "Potential targets and modulators of the sphingolipid pathway". In the case of glycosphingolipids, they can be hydrolyzed by exohydrolases, acting at acidic pH, to release monosaccharide units and ceramides [30].

Ceramide generated from sphingomyelin or glycosphingolipid breakdown, can be further degraded to sphingosine by several organelle-specific ceramidases (CDases). Sphingosine can be phosphorylated into sphingosine-1-phosphate (S1P), a potent pro-survival signaling molecule, by sphingosine kinases (SKs). The brain is the organ that contains the highest concentration of S1P [41]. There are two SK isoforms discovered so far: the SK1 and SK2, and both isoforms are present in the brain. SK1 knockdown severely affects brain and vascular development [42]. S1P can be degraded irreversibly by the S1P lyase enzyme to ethanolamine phosphate and hexadecenal. Alternatively, sphingosine can be transported from one compartment to another (recycling membranes from lysosome to ER) and be recycled in the ER-Golgi network re-entering into the sphingomyelin cycle by being re-acylated by CerSs to ceramide. Hence, CerSs simultaneously regulate de novo sphingolipid synthesis and the recycling of sphingosine or sphinganine [43]. Furthermore, it is important to note that sphingosine can be formed exclusively from the catabolic cycle of glycosphingolipids, sphingomyelin or ceramide. In fact, no dihydrosphingosine desaturases, that can create the 4,5-trans double bond on sphinganine substrate, have been found so far. The SL pathway is summarized in figure 1.
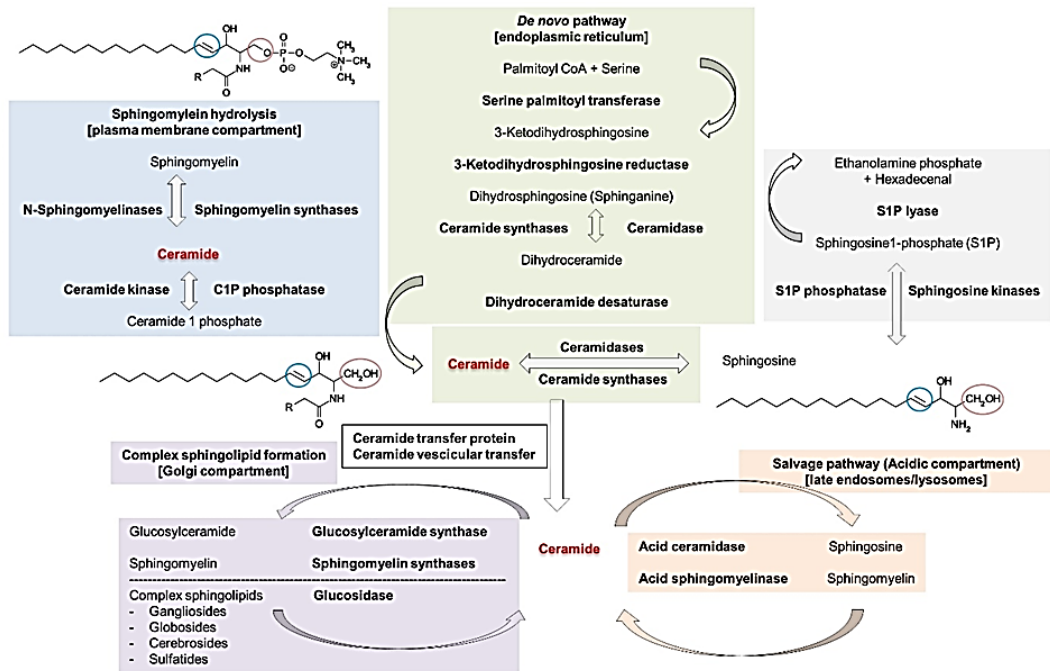
Figure 1. Sphingolipid metabolism. Ceramide can be produced by two main pathways. 1) The anabolic pathway named de novo pathway which starts in the endoplasmic reticulum compartment and ends in the Golgi with the synthesis of complex sphingolipids. 2) The catabolic pathway named the salvage pathway in which complex sphingolipids like sphingomyelin, ganglioside, globosides, cerebrosides and sulfatides are broken down to form ceramides in different compartments like late endosomes and lysosome or plasma membrane compartments. Ceramide can be further catabolized to form sphingosine which can be recycled back to form ceramides or exit the pathway by being hydrolyzed to ethanolphosphate and hexadenal. The 4,5 trans double bond is encircled in blue in the chemical structure of ceramide (center left of the figure), sphingosine (center right of the figure) and sphingomyelin (upper left corner of the figure). The C-1 hydroxyl group in the same compounds are encircled in red.

6.2   Sphingolipids in neural cell fate, maintenance, and death

<u>Regulation of sphingolipid metabolism in cell cycle and neural differentiation</u>

The composition and level of SLs undergo remarkable changes during the life cycle of a cell. With every cell division, the area of the plasma membrane and of intracellular membranes and organelles must be doubled within less than one hour. This is mainly achieved by downregulating phospholipid turnover and upregulating SL biosynthesis [44]. Therefore, key enzymes in SL biosynthesis such as SPT are upregulated prior to mitosis [45, 46]. Accordingly, blocking ceramide biosynthesis with the SPT inhibitor myriocin leads to cell cycle arrest in the G2/M phase [46-48]. In contrast to this ceramide depletion, increased ceramide levels in G2/M phase lead to hypophosphorylation of retinoblastoma protein and upregulation of cyclin-dependent kinase inhibitors such as p21 or p27 and subsequently, cell cycle arrest in the G1/S phase [45, 49-51]. Therefore upregulation of ceramide biosynthesis prior to M phase needs to be rapidly counterbalanced by formation of sphingomyelin or glycosphingolipids throughout G1 phase during cell division of neural progenitor cells, or in G0 phase associated with differentiation of neural cells [52]. If ceramide stays upregulated at the G1 phase, cells are at risk to undergo apoptosis. This is likely to be induced by a dual role of ceramide in that ceramide-mediated activation of protein phosphatase 2a (PP2a) will dephosphorylate retinoblastoma, and anti-apoptotic and pro-apoptotic proteins such as B cell lymphoma 2 (Bcl-2) and Bcl-2 associated X protein (Bax) [53-58]. In addition to caspase-dependent cell death, excess ceramide during cell division can induce cell death by activating p38 mitogen-activated protein kinase (p38 MAPK) and c-jun N-terminal kinase (JNK). These cell death pathways are often triggered by p75 neurotrophin receptor (p75NTR) through extrinsic insults (toxins, cytokines, and ischemia) in actively dividing cells such as neural progenitor cells and glia during nervous system development and inflammatory response in the adult brain [59-63]. Acute elevation of ceramide in dividing cells and neurons during early differentiation is induced by p75NTR-mediated activation of SMases, particularly neutral SMase2 (nSMase2) [61]. p75NTR-nSMase2 associated ceramide generation was among initial observations that alluded to the contradictory role of ceramide. For example, ceramide may be detrimental by inducing cell death, but also beneficial by arresting neural progenitor cells cycle and promoting neurite outgrowth [59, 64-66]. To date, the paradox of ceramide, mediating cell death on the one hand while favoring neuronal maturation on the other hand, is explained by several mechanisms involving (partial) conversion of ceramide to other SLs such as S1P or glycolipids, compartmentalization of ceramide, distinct effects of different ceramide species, and differential expression of proteins interacting with ceramide.

In differentiated cells, prolonged effects of ceramide elevation in G0, primarily those with long chain fatty acids, may induce senescence [67-71]. Risk of senescence is reduced by effective autophagy, which is essential for survival of long-lived cells such as neurons [72, 73]. Protective autophagy and cell survival are sustained by upregulation of S1P [74-82]. While these enzyme activities are intrinsically regulated throughout the cell cycle, extrinsic factors may induce activation of SMases generating ceramide that either support differentiation or induce apoptosis. During self-renewal and differentiation of neural progenitor cells, upregulation of ceramide serves two purposes: induction of apoptosis in excess progeny cells and promoting differentiation and process formation in surviving daughter cells [83-91]. Cell fate decision following neural progenitor cells division depends on the asymmetric distribution of proteins that either sensitize to or protect from ceramide-induced apoptosis such as prostate apoptosis response 4 (PAR-4) in the excess daughter cell and Bcl-2 in the differentiating cell, respectively [52, 92]. Ultimately, this demonstrates that ceramide and other SLs are differentially regulated throughout the cell cycle and embedded into cell fate decisions during stem cell renewal and neural differentiation.

The classical rheostat of ceramide and S1P and the decision on neural cell fate

There is a housekeeping balance between the potentially pro-apoptotic ceramide and anti-apoptotic S1P. The level of S1P is regulated by the activity of SKs and S1P lyase [78, 81, 93]. It is known that SK protein levels are upregulated in cancer thereby escaping ceramide-induced apoptosis and sustaining cell survival [94-97]. Particularly, SK1 levels are increased in p53-deficient tumors because it cannot be degraded by upregulation of caspase 2 in a p53-dependent manner [98]. In addition to intrinsically increased protein levels, SKs are post-translationally activated by extracellular signal-regulated kinase (ERK)-mediated phosphorylation, which is triggered by extrinsic signals such as pro-inflammatory cytokines (e.g., TNFα, IL-1β) and nerve growth factor [99-102]. This regulation is consistent with S1P as a pro-inflammatory and survival signal for neurons. Downstream targets of S1P rely on the locations of its generation and distribution. Cytosolic SK1 generates S1P that is secreted by mainly two transporters, ABC transporters and sphinster 2 [103-106]. Extracellular S1P binds to plasma membrane-resident S1P receptors (S1PR1-5), a family of five G-protein coupled receptors that activate Akt-dependent cell survival and pro-migratory cell signaling pathways [80, 107-109]. In contrast to SK1, nuclear SK2 generates S1P that inhibits histone deacetylases 1 and 2. Histone deacetylases 1 and 2 are ubiquitous proteins important in epigenetic gene regulation. When these enzymes are inhibited by S1P, gene expression of p21 is increased [110]. Hence, the classical

model of a rheostat consisting of ceramide and S1P, switched into a multifaceted interdependence of the two SLs in cell fate regulation. This is particularly evident in the nervous system consisting of dividing cells (neural progenitor cells and glia) interacting with non-dividing neurons. With respect to cell cycle control, both ceramide and S1P increase the level of p21 leading to a synergistic effect on cell cycle arrest. Ceramide activates p53, which induces degradation of SK1, thereby antagonizing apoptosis. Both ceramide and S1P stimulate autophagy, which protects neurons and regulates the inflammatory response in glia. Moreover, we found that ceramide and S1P act synergistically on neuronal cell polarity and process formation like cilia [83, 85, 90].

Lipid rafts and binding to distinct proteins determines the function of sphingolipids

SLs such as ceramide, sphingomyelin, and glycosphingolipids are often organized in lipid microdomains or rafts. In addition, they directly interact with proteins, which led to the idea that binding to SLs sequestered proteins to lipid rafts. We proposed that proteins sequestered in the lipid rafts induce formation of larger protein complexes termed "sphingolipid-induced protein scaffolds" or SLIPSs that interact with the cytoskeleton [52]. Most recently, we introduced the idea of "lipid chaperons", (sphingo)lipids that bind to proteins in the non-raft areas of cellular membranes and "catalyze" their association with lipid rafts and interaction with other raft-associated proteins [111].. Atypical protein kinase Cς/λ (aPKC) was one of the first proteins shown to directly interact with ceramide [112-118]. Our studies showed that aPKC is a protein chaperoned by ceramide to be sequestered to ceramide rafts or ceramide-rich platforms that initiate SLIPS critical for neural progenitor cells polarity [115, 117, 119]. We also found that ceramide bound aPKC forms a complex with Cdc42, a small Rho-type GTPase that contains a pleckstrin homology domain for binding to phosphatidylinositol 4,5 bisphosphate (PI(4,5)P2), a key regulatory lipid for cell polarity in neural progenitor cells and neurons [83]. Furthermore, our studies showed that very long chain C24:1 ceramide stabilizes microtubules in neuronal processes and cilia by inhibiting histone deacetylase 6, an enzyme that reduces tubulin acetylation [90]. Therefore, the synergistic effect of a polarized distribution of ceramide and PI(4,5)P2 in lipid rafts and their interaction with actin and microtubules in SLIPs may establish neuronal cell polarity and stabilize neuronal processes. Consistent with this hypothesis is the observation that CerS2, the enzyme generating C24:1 ceramide is upregulated during differentiation of embryonic stem cells and neural progenitor cells and it is critical for brain development and function as supported by studies with CerS2-deficient mice [120-124]. On the other hand, ceramide species such as C18:0 ceramide are associated with the pathological function

of exosomes in AD as well as induction of neuronal apoptosis [125]. These, apparently contradictory, effects of ceramide, stabilization of neuronal processes and induction of apoptosis are likely to rely on compartmentalization of ceramide species and cell type or differentiation stage-specific expression of ceramide-interacting proteins that either promote neuronal function or apoptosis. For example, C18:0 ceramide was shown to bind to p53 protein (pro-apoptotic), PP2a inhibitor protein SET (cell cycle arrest, pro-apoptotic, and other effects), receptor-interacting serine/threonine protein kinase (RIPK, pro-necroptotic), and light chain 3B (LC3B, pro-autophagic) [126-130]. Additional ceramide binding proteins such as kinase suppressor of Ras (KSR, pro-apoptotic) and more recently, lysosomal-associated transmembrane protein 4B (LAPTM4B, endosomal ceramide transport, pro-apoptotic) were identified, but their affinity to different ceramide species is not clear [131-135]. Our studies showed that in addition to binding to aPKC (polarity inducing), C24:1 interacts with and activates GSK3, the precise function of which is a matter of our ongoing research [91]. Previously, we found that during asymmetric division of neural progenitor cells, PAR-4, an aPKC inhibitor protein sensitizing cells to ceramide-induced apoptosis, is distributed to one daughter cell, while the other daughter cell is protected from apoptosis and continues to divide and differentiate [52, 84, 92, 136]. A similar cell-type specific effect was described for S1P that either induces or disrupts neuronal and glial process formation, probably due to binding to differentially expressed S1P receptors [137-139]. In glia, S1P may promote survival and differentiation or trigger activation and adoption of a pro-inflammatory phenotype [79, 109, 140-149]. Overall, these examples demonstrate that the simplified view on the rheostat of ceramide and S1P as pro- and anti-apoptotic balance will need to be replaced by a more mechanistically refined model invoking specific interaction with rafts and proteins regulating cell signaling pathways in neural development and disease.

Effect of ceramide and sphingosine on neuronal activity

Interestingly, ceramide and sphingosine are not only players in cell cycle regulation but also in neuronal activities. For instance, recurrent production of ceramide by SMase in lipid rafts is important for neuronal conduction of excitation [150]. Fasano et al., reported ceramide-based conduction of excitation without action potentials along the nerve fibres. They observed that among the lipid family only ceramide was elevating in the nerve trunks upon mechanic inhibitory reflex stimulation. Other example is the involvement of ceramide and sphingosine in the presynaptic exocytosis. The process is controlled probably by CDase that shift the ratio of ceramide to

sphingosine in favor of sphingosine production [151, 152]. In fact, while Rohrbough et la., report a CDase dependent exocytosis Darios et al., found that sphingosine is involved in the formation of SNARE complex, which is a large protein complex with transmembrane domains, involved in the fusion of vesicles to the presynaptic membrane. Once the SNARE complex is assembled and fused to the membrane, presynaptic neurons can release the neurotransmitter in the extracellular space. In addition, S1P seems to play a role in excitatory synaptic transmission. Long-term potentiation in hippocampal was impaired in SK knock outs and increased under S1P treatment [153].

6.3   Extracellular trafficking of sphingolipids and effect on blood brain barrier

Introduction of lipoproteins

SL trafficking in the peripheral circulation mainly occurs via lipoproteins or bound to albumin. A small percentage of SLs may be contained by circulating extracellular vesicles. Lipoproteins can be classified according to their size and density into four main groups: high-density lipoproteins (HDL), low-density lipoproteins (LDL), very low-density lipoproteins (VLDL), and chylomicrons. Lipoproteins all carry specific apolipoproteins (apo) that can have structural, enzymatic, and receptor-binding functions [154]. The carrier apolipoprotein (Apo) of liver-derived lipoproteins, VLDL and LDL, is apoB100, while that of the lipoproteins of the intestine, chylomicrons, is apoB48. HDL, which is predominantly produced in the liver and intestine, lacks ApoB and is instead mainly accompanied by ApoA-I [155]. ApoE4, one of the 3 common isoforms of ApoE (E2, E3, and E4), is linked with a strongly increased risk of developing AD [156]. ApoE is carried by chylomicrons, VLDL, and a subclass of HDL. HDL containing ApoE is formed when triglyceride-rich lipoproteins, such as VLDL and chylomicrons release fatty acids upon lipolysis [155]. Circulating ApoE4 prefers association with VLDL and chylomicrons, while ApoE3 prefers HDL [157]. Besides its presence on lipoproteins, ApoE has been detected on extracellular vesicles [158].

Trafficking of sphingolipids in the blood by lipoproteins

Sphingomyelin is the most abundant SL species in plasma, followed by ceramides and sphingoid bases [159]. Sphingomyelins are mainly present in LDL and to a smaller extent in VLDL and HDL [160]. Ceramides, hexosylceramides, and lactosylceramides are primarily carried by LDL [161], but are also present in other lipoprotein subclasses including HDL, depending on their origin [159]. Endogenously synthesized ceramides originating from the liver are incorporated predominantly in hepatocyte

secreted VLDL and possibly LDL and ceramides originating from the intestine secreted by enterocytes are incorporated in chylomicrons and HDL [162-164]. Circulating S1P is predominantly carried by HDL (~60%), where it is bound to ApoM. About 10% of S1P is present in LDL, a small amount can be present in VLDL, and the remainder is bound to albumin (~30%) [165, 166]. S1P is predominantly contained by the smaller, denser HDL subclass (HDL3), and not by the larger ApoE-containing HDL subclasses [167, 168].

Trafficking of sphingolipids in the cerebral spinal fluid

Data on the carriers of sphingolipids in cerebral spinal fluid (CSF) and central nervous system (CNS) is scarce, since most studies focus on sphingolipid levels and not on their origin. Upon examining sphingolipid in CSF Fonteh et al. found sphingomyelin, ceramide and dihydroceramide in both CSF nanoparticles and supernatant fluid [169]. The nanoparticles include synaptic vesicles and large dense core vesicles, resembling lipoproteins. CSF lipoproteins range in size between 10-24 nm, corresponding with HDL and LDL [170]. Both sulfatide and galactosylceramide were found to be present on HDL isolated from CSF [171, 172]. Sulfatides were specifically detected on ApoE-containing HDL, with concentrations depending on APOE genotype [171].

The most abundant apolipoproteins in CSF are ApoE and ApoA-I and ApoE in the CNS. Here ApoE is produced locally, primarily by astrocytes, and is thought to be the main apolipoprotein on the HDL-like particles transporting lipids [173, 174]. The lipid content of nascent HDL particles included detectable amounts of sphingomyelin and glycosylceramides, and was found to closely resemble that of lipid rafts [175]. ApoA I is secreted by the liver and intestine and therefore has to cross the blood-brain barrier (BBB) to access the CNS. How this happens and how ApoA-I gains access to the CSF is not completely understood.

Origin of circulating sphingolipids

Plasma S1P, derived from (exogenous) sphingosine via SK1 and SK2, is produced by various cell types, including erythrocytes (~90%), platelets, endothelial cells, and hepatocytes [176, 177]. Since erythrocytes and platelets lack the S1P degrading enzyme, S1P tends to accumulate in these cells, leading to a high secretion towards plasma [178-180]. Even though platelets contain large amounts of S1P, they do not seem to determine circulating S1P levels [181], except after platelet activation by thrombin or Calcium [180, 182]. Other peripheral blood cells such as mononuclear cells, neutrophils, and endothelial cells also expressing SKs may contribute to circulating S1P levels [177].

Additionally, endothelial cells and monocytic cells release SK1 into plasma, where it could convert sphingosine to S1P extracellularly [183, 184]. The release of SKs from monocytic cells can be induced by oxidized-LDL [185].

Plasma S1P can be released from the aforementioned cells in a myriad of ways after which it can be transferred to albumin, and possibly to HDL. Next to the release of S1P, its cellular uptake is mediated by ABCC7, thereby reducing its bioavailability. In addition, ApoM was found to be involved in S1P secretion towards lipoproteins and to be the rate limiting step in S1P secretion from hepatocytes towards HDL [176]. ApoM can also mediate the efflux of S1P from erythrocytes [186]. Spinster 2 is a transporter mediating the efflux of S1P from vascular endothelial cells, but not from erythrocytes and platelets [187]. Endothelial S1P can also be released, in a positive feedback manner, through ABCA1 and SR-BI induced by ApoA-I [188]. Phospholipid transfer protein (PLTP) is thought to mediate the transfer of S1P to HDL, because PLTP-deficiency results in a dramatic increase in S1P content in plasma and in HDL [189, 190] and interestingly also in an impaired blood-brain barrier integrity in line with a key role for HDL-S1P in the maintenance of barrier function [191-193].

Relatively little is known about the origin of SLs other than S1P in lipoproteins. Ceramides and sphingomyelins can be transferred from the liver and intestine towards VLDL and chylomicrons by microsomal triglyceride transfer proteins [194]. Ceramides present in HDL may be incorporated upon HDL formation and secretion, they may be transferred from lipoproteins such as VLDL and chylomicrons by PLTP and cholesteryl transfer protein, or produced by SMases, either in tissues or by circulating SMases [162]. Ceramides from plasma membranes may also efflux to HDL (for review see [195]). In addition to SKs, enzymes producing sphingosine, A-SMases and ceramidases are secreted from cells into plasma and could locally produce sphingomyelin and ceramide [185, 186, 196, 197].

Effects of SLs on vascular function

Many of the beneficial functions of HDL on vascular barrier function have been ascribed to its S1P content [198-200]. HDL bound S1P as well as albumin-bound S1P were found to affect vascular tone. HDL was found to induce vasodilation and reduce arterial blood pressure; effects that are potentially mediated by S1P. On the other hand, S1P associated with albumin can promote vasoconstriction in rat cerebral arteries [201-203], but not in peripheral arteries. Differences in S1P effects on vascular

tone might be related to differential expression of S1P receptors in vascular walls, such as the relatively higher expression of S1PR2 and S1PR3 in cerebral arteries. A vasoprotective function attributed to S1P, is the maintenance of the vascular barrier. S1P either contained by HDL or albumin increased endothelial barrier activity and decreased vascular permeability, via suppression of TNFα-induced VCAM-1 and ICAM-1 expression by endothelial cells, thereby likely reducing the transmigration of monocytes and lymphocytes [204]. The most potent protective effects against oxidative stress-associated endothelium dysfunction, were induced by small dense HDL3 particles with a high S1P content [205].

Introduction of the Blood-Brain Barrier/neurovascular unit

The blood-brain barrier (BBB) is a dynamic structure where cellular communication is essential for its functioning. The physical barrier is formed by specialized endothelial cells which are sealed together via the expression of tight junctions [206]. In addition, the endothelial cells express several transporters that exclude unwanted/toxic molecules from the brain and actively regulate the entry of nutrients from plasma. Proper functioning of the brain endothelial cells is necessary to maintain BBB integrity. However, further support by pericytes and the end-feet of astrocytes is needed to ensure BBB function. Interaction of pericytes and astrocytic end-feet with the brain endothelial cells is termed the neurovascular unit. The pericytes are embedded in the basement membrane surrounding the endothelial cells and encircled by the basal lamina, which is contiguous with the plasma membranes of astrocyte end-feet and endothelial cells. Both cell types play a key role in maintaining BBB function by inducing tight junction protein expression and the polarization of transporters [207]. For instance, loss of pericyte coverage or ablation of astrocyte-secreted laminin leads to down-regulation of junctional proteins and a leaky BBB, underscoring their importance [208].

BBB dysfunction in AD/neuro-inflammation

In AD, the different components of the neurovascular unit are affected by disease pathology, resulting in a compromised barrier function. Human post-mortem studies showed a reduced expression of tight junctions accompanied by increased fibrinogen leakage into the brain [209, 210]. In addition, the observed loss of pericyte coverage and swelling of astrocytic end-feet in AD also contributes to a decreased barrier function [211-213]. These cellular alterations in AD may further exacerbate parenchymal and vascular amyoid-β (Aβ) accumulation. In addition, AD is characterized

by chronic neuroinflammation. Aβ deposition in the vasculature leads to pro-inflammatory and cytotoxic events that contribute to a greater BBB permeability. Brain endothelial cells loosen their tight junctions in response to inflammatory stimuli resulting in transmigration of leukocytes across the BBB [214]. Once infiltrated in the CNS, leukocytes contribute to tissue damage by releasing pro-inflammatory cytokines and other cytotoxic products [215]. Moreover, Aβ enhances the activation of glial cells, which further induces secretion of proinflammatory cytokines and chemokines. Therefore, the BBB is affected in multiple ways in AD.

The effect of SLs on BBB function during AD

SLs have heretofore been implicated to have extensive involvement in the pathophysiology of a variety of neuroinflammatory diseases, with AD included. Knowledge on the effects of SLs on the BBB is limited. A-SMase and ceramide have been studied in relation to BBB function. Brain endothelial cells in the presence of an inflammatory stimulus showed increased A-SMase activity and concomitant ceramide production, which resulted in the disruption of tight junction proteins [216]. Exposure of brain endothelial cells to C2:0 ceramide induced a decrease in barrier resistance, which is indicative for barrier integrity. Loss of barrier integrity was accompanied by an increase in monocyte migration across the endothelial cells after exposure to ceramide [144]. Interestingly, the inhibition of A-SMase activity prevented the degradation of zonulae occludentes 1 and 2, and occludin, proteins important for in tight junctions, indicating an important role for A-SMase/ceramide in tight junction regulation [216]. In addition, the downregulation of A-SMase in brain endothelial cells resulted in a reduction of trans-endothelial migration of T cells, possibly via affecting intercellular adhesion molecule 1 which is necessary for the adhesion of T cells to the endothelium [217]. Not only the increase of ceramide in endothelial cells but also in astrocytes is able to decrease barrier integrity. Astrocytes show a similar response as endothelial cells when stimulated with pro-inflammatory mediators, which lead to an increase in mRNA from A-SMase resulting in an increase in ceramide production [144]. Ceramide can be released from cells through extracellular vesicles and possibly affect neighboring cells. Indeed, when endothelial cells were exposed to astrocyte-conditioned medium, the migration of monocytes across the BBB increased, further confirming the negative effect of ceramide on the BBB.

6.4   Alteration of sphingolipid metabolism in Alzheimer's disease

Increasingly, evidence demonstrates that alterations in sphingolipid metabolism play a key role in the pathogenesis of AD [218, 219]. Firstly, it was reported that ceramide levels are elevated in brain tissue of AD patients compared to controls while sphingomyelin and S1P are decreased [220-224]. Secondly, the enzymes that control ceramide formation in the sphingolipid pathway were abnormally expressed (Table 1) [222, 225]. Alterations in the sphingolipid metabolism were also observed in plasma, where shotgun lipidomics revealed decreased sphingomyelin and increased ceramide levels in AD patients as compared to controls [226]. This was further supported by targeted sphingolipidomics studies that identified similar sphingolipid changes in plasma of MCI [227, 228] and AD patients [229, 230] and in longitudinal studies that monitored the progression of cognitive decline in AD patients [231, 232] (reviewed by Mielke and Haughey, 2012 [233]).

There are at least three different pathophysiological mechanisms underlying the effect of dysregulated ceramide in neurotoxicity 1) ceramide rich platforms-associated receptor activation, 2) mitochondrial dysfunction, and 3) exosome-mediated amyloid and tau propagation and aggregation.

Sphingolipid pathophysiology in the nervous system

It is thought that spatially extended ceramide membrane domains activate extrinsic cell death pathways in neurons and glia, which is likely to contribute to neural cell death after injury. Receptors activated by extracellular factors such as nerve growth factor (p75NTR), TNF-α, IL-1β, IL-6, IFN-γ, and Fas ligand [61, 234-237]. Increase of ceramide concentration in the plasma membrane is induced by receptor-mediated activation of A- and N-SMases. Lee et al. have shown that in cultured oligodendrocytes, Aβ25-35 activates N-SMase that promotes the conversion of sphingomyelin into ceramide, which may lead to apoptosis [238]. In the same way, oligomeric Aβ1-40 and Aβ1-42 enhance the activity of A- and N-SMase, which subsequently increases the levels of ceramide resulting in cell death [239]. Furthermore, it has been proposed that ceramide can contribute to Aβ formation by affecting the cleavage of the transmembrane protein amyloid precursor protein (APP) [240, 241]. However, neuronal damage observed in neurodegeneration is rather subtle at first and begins with axonal degeneration, while cells are still alive and at least in part functional. Therefore, it is likely that the initial damage caused by dysregulated ceramide affects the cytoskeleton or organelles critical for cytoskeletal integrity.

Currently, mitochondria are the focus of intense research on dysregulated ceramide biology. Increase of ceramide concentration in the inner and outer mitochondrial membranes impairs oxidative phosphorylation, breaks down the membrane potential, and creates pores that allow release of pro-apoptotic proteins to the cytosol [242-247]. Kong and Zhu et al., discovered ceramide-enriched mitochondria-associated membranes that interact with tubulin and voltage dependent anion channel 1 to block ATP release required for mitochondrial motility, a reaction enhanced by Aβ [248].

In addition to mitochondria, compartments with ceramide-enriched membranes such as the ER and endosomes may contribute to neuronal and glial damage due to oxidative stress and impaired protein homeostasis, which leads to aggregation of neurotoxic peptides (e.g., Aβ) or proteins (e.g., tau, synuclein, huntingtin). Impaired protein homeostasis by dysregulated ceramide probably contributes to a variety of neurodegenerative disease involving intracellular and extracellular protein aggregation, including AD, PD, and Huntington's disease. Dinkins et al., showed that in AD, extracellular aggregation of Aβ into amyloid plaques is nucleated by ceramide-enriched exosomes secreted by astrocytes [125, 249, 250]. These "astrosomes" can also induce apoptosis in recipient cells, which is mediated by transfer of ceramide and the ceramide-sensitizer protein PAR-4. Astrosome-induced plaque formation and neuronal cell death is prevented by inhibition or deficiency of nSMase2 studies have shown [249, 250]. Furthermore, exosomes can mediate propagation of tau or prion protein. In contrast to these observations, others have shown that exosomes may also help Aβ uptake and clearance [251-255].

It is still uncertain if ceramide disbalance is a consequence of Aβ accumulation or one of the initiating factors of AD pathophysiology. However, it is becoming clear that there is a link between Aβ formation, neuronal death, and SLs.

Sphingolipids and their relation to APP and the amyloid β-peptide

Aβ-peptides derive from sequential cleavage of the APP during its transport through the secretory pathway, at the cell surface and within endocytic compartments [256-259]. Aβ generation is initiated by cleavage of APP by the β-site APP cleavage enzyme 1 (BACE1) leading to the secretion of soluble APP (sAPPβ). The resultant membrane-bound C terminal fragment (CTFβ) represents a substrate for transmembrane proteolysis by γ-secretase that liberates Aβ from cellular membranes. In an alternative pathway, APP can be cleaved initially by α-secretases (e.g. ADAM10, ADAM17)

within the Aβ-sequence resulting in secretion of a slightly longer soluble APP ectodomain (sAPPα) and shorter membrane-bound CTF (CTFα) [260-262]. Since the cleavage of APP by α-secretases occurs almost in the middle of the Aβ domain, this pathway prevents the production of Aβ peptides. The subsequent cleavage of the CTFα by γ-secretase leads then to the generation of the smaller not toxic peptide called p3.

Alterations in membrane lipid composition could affect the subcellular transport of these proteins and modulate the generation of Aβ. Certain lysosomal lipid storage disorders are associated with alterations in APP and tau metabolism, and they are also observed in AD [263]. Impaired cholesterol metabolism in lysosomes due to defective cholesterol transport proteins NPC1 or NPC2 is associated with alterations in the endo-lysosomal system, accumulation of intracellular Aβ and APP CTFs, and formation of tau aggregates in the brain of Niemann Pick Disease type C patients [264, 265]. Accumulation of APP CTFs within lysosomal compartments has also been observed with cellular models of lysosomal sphingolipid storage diseases [263]. These effects could be attributed in part to impairment of lysosomal activity or altered trafficking and fusion of endo-lysosomal vesicles [266-268]. It has been shown that cellular ageing or chronic oxidative stress alters membrane lipid metabolism and APP processing [269, 270]. An important role of lysosomal sphingolipid metabolism in the processing of APP is further supported by the observation that genetic deletion of the S1P-lyase results in the accumulation of APP CTFs and higher secretion of Aβ [271]. It has also been reported that S1P could promote Aβ generation by direct interaction with and stimulation of BACE1 [272].

In addition, ceramide and ceramide analogs could increase the generation of Aβ by stabilization of BACE1 [272-274]. In line with a role of SLs in APP processing, pharmacologic inhibition or genetic deletion of SL biosynthetic enzymes decreased the generation of Aβ by lowering forward transport of APP in the secretory pathway and stimulation of PKC-dependent stimulation of α-secretory processing [275, 276].

Several studies indicate that Aβ peptides might impact cellular lipid metabolism by promoting the enzymatic activity of A-SMase [239] , and by inhibition of the ganglioside synthase GD3 [277-279]. In turn, it was shown that addition of ganglioside-containing vesicles to Aβ-peptide solutions accelerated the formation of Aβ-fibrils. In particular GM1 could promote the aggregation of Aβ, leading to the consumption, that membrane-bound Aβ might act as a seed which catalyzes

fibrillogenesis process and increase Aβ neurotoxicity (for detailed review: Matsuzaki et al. 2018) [280-285].

The APP intracellular domain resulting from γ-secretase mediated intramembranous processing of APP CTFs has been shown to transcriptionally down-regulate the expression of GD3S [279]. Accordingly, the genetic inhibition of γ-secretase led to increased level of GD3. Inhibition of γ-secretase also led to impairment of cellular lipid homeostasis by altering the uptake of lipoprotein particles [286, 287]. Together, these results indicate a close relation of lipid metabolism and the pathogenesis of AD. Ceramide and S1P contribution to Aβ biogenesis is illustrated in Figure 2.

Sphingolipids and their relation to tau

The relation between tau and ceramide metabolism is poorly characterized. A study in PC12 cells reported that ceramide analogs such as N-acetylsphingosine and N-hexanoylsphingosine decreased the levels of tau via calcium-stimulated proteolytic activity [288]. Plus, agonist of the S1P receptor reduced tau phosphorylation [289]. However, addition of the ganglioside GM1 for 24 hours did not change tau levels in neuroblastoma cells [290]. Purification of hyperphosphorylated tau revealed a similar composition in cholesterol, SLs and phosphatidylcholine as in extracellular plaques suggesting that common lipid pathways are involved in the two pathological process [291].
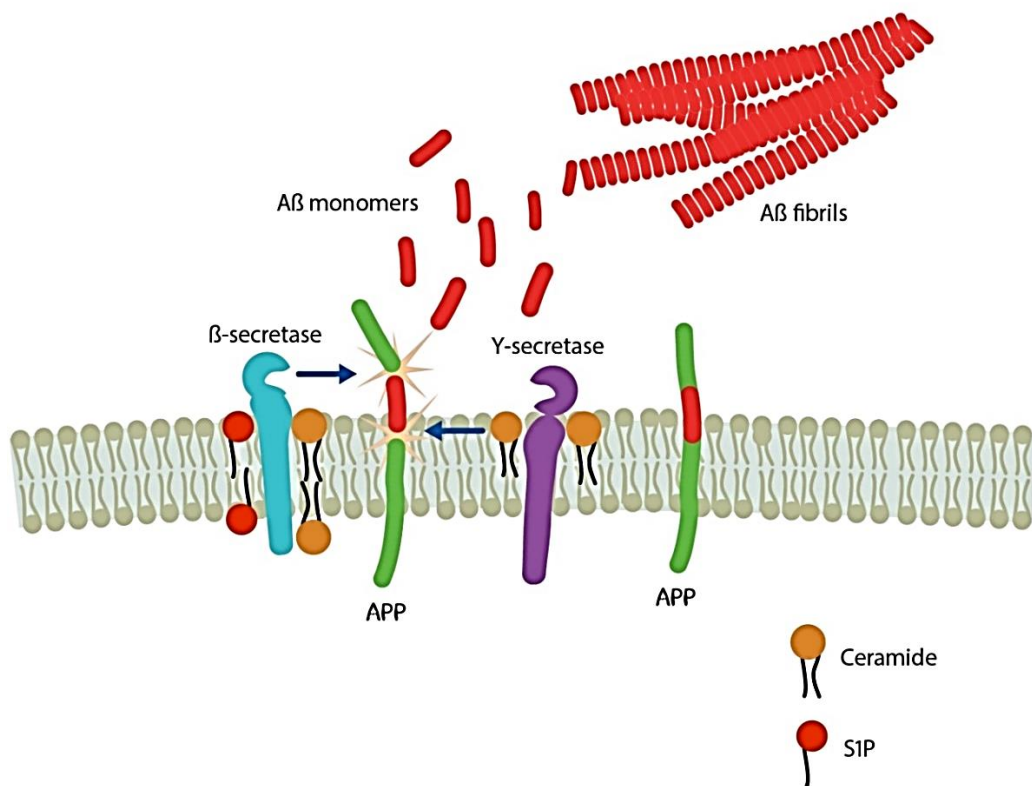
Figure 2. APP processing and ceramide interference. The amyloid precursor protein (APP) processing unfolds in specific membrane microdomains known as lipid rafts. If the lipid rafts are enriched with ceramide or S1P, the activity of the β-secretase and γ-secretase, the two proteolytic enzymes responsible of amyloid-β (Aβ) biogenesis, are potentiated favoring the amyloid-genic pathway.

AD models with sphingolipid alterations

In recent literature, dysregulation of SL and ganglioside homeostasis has been reported in AD animal models. However, not all animal models showed the same alterations, and some findings seem to be contradictive (Table 2). Kaya et al., used APP mice to evaluate SL homeostasis in AD mice. This model exhibits severe Aβ deposition at early onset, making it a valuable model to analyze the molecular mechanisms in AD pathology. The study shows significant localization of gangliosides and ceramide species to Aβ plaques, with local reduction of sulfatides [292]. Barrier et al., analyzed and compared brain gangliosides of different transgenic AD mouse models with age-matched wild type mice, and found an increase in GM2 and GM3 expression in the cortex of all mice expressing APP [293]. Loss of complex "a" gangliosides was found in APP/PS1 models, loss of complex "b" gangliosides was found in APP and APP/PS1 mice. Another study showed gender-dependent accumulation of ceramides in the cortex of APP/PS1 mice [294]. Ceramides accumulated in APP/PS1

166

mice, but not in PS1 mice. In addition, all other major SLs did not change in comparison with wild-type mice. Interestingly, female mice displayed a significant increase in 2-hydroxy fatty acid ceramides, whereas male mice showed an elevation of non-hydroxy fatty acid ceramides. Barrier et al., had unexpected findings, using two mouse models; APP and APP/PS1, they analyzed ceramide and related SL levels, and found that there were no ceramide deposits in any of the AD models. They hypothesized that these findings were due to the fact that there was neither neuronal loss nor toxic Aβ species accumulation in APP mice. In another study, a mixed population of APP, PS1 and APP/PS1mice were used. In all animal models, significant changes were found in the lipid profiles of the prefrontal cortex and hippocampus [295] in the AD animals. Of these regions, the prefrontal cortex was most affected in terms of lipid alterations, containing decreased levels of lysophosphatidylcholine and phosphatidylethanolamine and increased levels of ceramide and diacylglycerol. There were also many alterations in individual lipid species, most severe in the APP/PS1 mice. Apparently, the changes in ceramide happen already during embryogenesis since elevation of long-chain ceramide was detected in newborn mice carrying human mutated PS1. This elevation of ceramide was accompanied by elevation of CerS2 and 4 expression [60].

Caughlin et al, 2018 used wild-type rats and APP Fischer rats to quantify changes in membrane-lipids (gangliosides) [296]. They found that APP rats had a decreased level of complex gangliosides, and an increased level of simple gangliosides compared to the wild-type rats. Also, there was an age-dependent decrease of GD1 and a clear increase of GM3 levels.

6.5   Potential targets and modulators of the sphingolipid pathway

SL bioactivity in the brain provides an appealing framework for comprehending AD pathology and for developing new intervention strategies. However, since the study of SL bioactivity is relatively young, very little is known about the therapeutic effect that the modulation of SL metabolism may have in AD. Here we discuss approaches to target the SL pathway, one with the aim to decrease ceramide content via the blockage of de novo synthesis or via the inhibition of SMases, the other to increase S1P signaling. As aforementioned, the elevated ceramide levels in the brain are thought to contribute to the apoptotic signaling and favor Aβ formation while low S1P levels eventually result in a reduction of neuroprotective signals.

Hereafter, we will review a group of pharmacological agents known to inhibit the de novo SL synthesis and consequently reduce ceramide formation. From the first building block serine and

palmitoyl-CoA to the ceramide product, there are five enzymes that could be targeted: SPT, 3-keto-dihydrosphingosine reductase, CerSs, dihydroceramide desaturase and CERT. Also, the sphingomyelin and glycosphingolipid synthesis will be briefly discussed, for its therapeutic potential. Next, we will review inhibitors of the SM hydrolysis cycle. SMases are a family of phosphodiesterases, which preferentially hydrolyse SM, producing phosphorylcholine and the bioactive sphingolipid ceramide. Of the five known isoforms here, we will discuss the N-SMase2 and the A-SMase. Since sphingomyelin is the quickest source of ceramide by blocking sphingomyelin hydrolysis the ceramide content is expected to efficiently decrease. Then, we will argue on the use of S1P analogs that are known to modulate S1P receptors. In this case the S1P analogs are expected to increase the protective signaling, stimulate cell growth (neurogenesis), reducing BBB permeability to monocytes and attenuating activation of glia cells, by mimicking S1P bioactivity. Compounds and their targets are listed in table 3 and represented on a cell scheme in figure 3. A last section will be dedicated to the RIPK inhibitors and pharmacological chaperones.
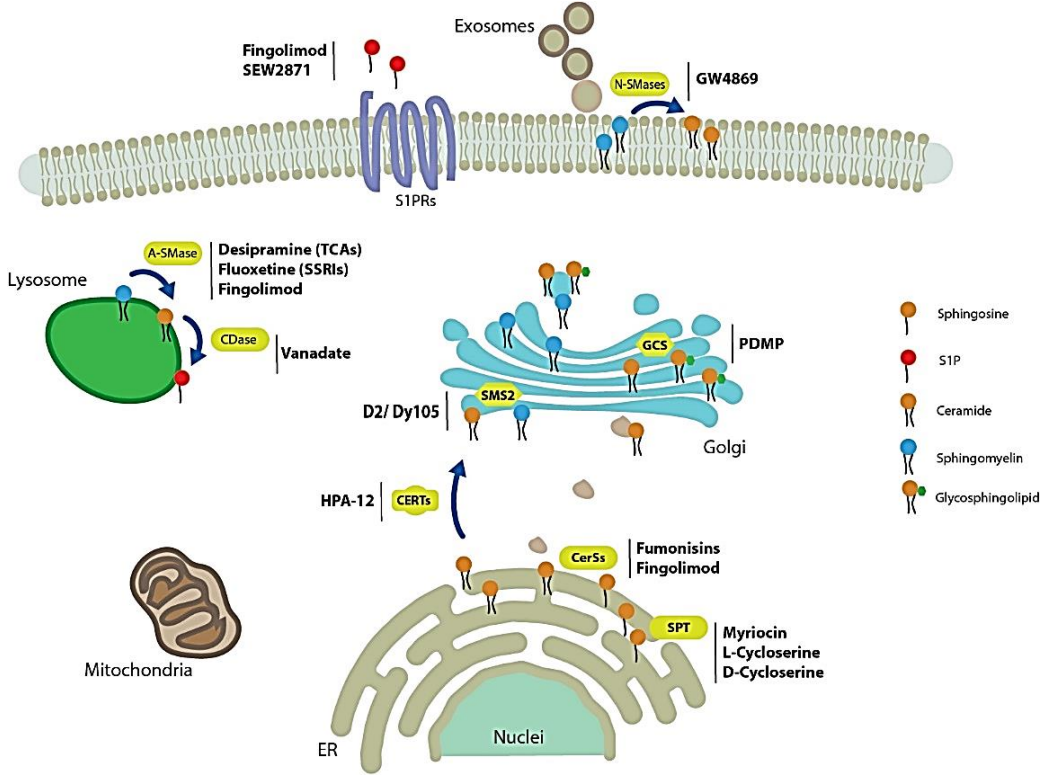
Figure 3. Potential targets and modulators of the sphingolipid pathway. Ceramide formation can be inhibited by blocking the enzymes of the de novo synthesis. Alternatively, ceramide levels can be reduced by inhibiting the enzyme responsible for the breakdown of complex sphingolipids to form ceramide. Lastly, potentiating the neuroprotective effect of S1P signaling by S1P analogs that interact with S1P receptors is another possible approach. (SPT = serine palmitoyl

transferase; CerSs = ceramide synthases; CERTs = ceramide transporter proteins; SMS1 = sphingomyelin synthase 1; GCS = glucosylceramide synthase; CDase = ceramidase; A-SMase = acid sphingomyelinase; S1PRs = S1P receptors; N-SMase2 = neutral sphingomyelinase 2).

<u>Inhibitors of the de novo synthesis</u>

The inhibitors of the de novo synthesis are a class of heterogeneous compounds that have been mainly used in cell-based assays and rarely or never in vivo, due to their potential liver and kidney toxic effect that could lead to severe side effects [297, 298]. The most known compounds in this class are myriocin and L-cycloserine, fumonisins and N-(3-hydroxy-1-hydroxymethyl-3-phenylpropyl) dodecanamide (HPA-12).

Myriocin is a potent antibiotic derived from fungi which is used in the treatment of opportunistic infection. Interestingly, the compound shows also immunosuppressant activity [299, 300]. Myriocin, D- and L-cylcloserine are essentially very potent inhibitors of SPT [301, 302]. Katsel et al., reported that SPT genes are upregulated in mild to severe stages of dementia even though the upregulation was not dependent on neurofibrillary tangles progression and ageing [225]. The inhibition of SPT was shown to be effective in preventing a harmful accumulation of SL intermediates like ceramide [298, 303, 304]. L-cycloserine administered on alternate days for 2 months exclusively reduced brain cerebroside levels and improved cognition in rodents [305].

Fumonisins are a family of molecules that have a similar structure to sphinganine with potent anti-fungi properties. It is thought that fumonisins occupy the pocket of sphinganine or sphingosine in CerS and thereby inhibit ceramide synthesis [306]. CerS 1, 2 and 6 are upregulated in AD brains [225]. However, Couttas et al., found that CerS 2 was less active in specific brain regions of AD severely affected by amyloid and tau pathology. Furthermore, CerS 6 KO mice, even though they did not show significant changes in brain ceramide composition, did show behavioral deficits [307]. Hence, it is unclear if the inhibition of CerS would treat AD condition without compromising overall brain function.

HPA-12 is an inhibitor of CERT, a protein essential for the formation of more complex SLs such as sphingomyelin [308, 309]. HPA-12 can displace ceramide from the CERT's START domain pocket preventing ceramide transfer to the Golgi [310]. In vitro experiments have shown that administration of HPA-12 to cells in culture reduce the synthesis of SM [308]. However, it is unclear if this results in an accumulation of ceramide as well or if the ceramide excess is diverted to the alternative pathway to form glucosylceramide. In contrast to SPT and CerSs, the CERTs expression is

probably downregulated in AD. Matarin et al., discovered that CERT mRNA expression levels are decreased in a genome-wide gene-expression analysis on transgenic mice during development of amyloid pathology [311]. This suggests that rather than a reduction of CERT activity an increase would be desirable. Besides being a ceramide transporter CERT has also extracellular functions [312]. Specific forms of CERT can be excreted and take part in stabilizing the basal membrane [313]. Interestingly, it was reported that CERT colocalizes with plaques deposits in the AD brain. Mencarelli et al., found that CERT could bind to serum amyloid P component and that this complex was localized close to plaques [314]. Later, CERT proteins were identified to bind C1q and activate the complement via the classical pathway. The complement activation mediated by CERT was comparable to that of the immunoglobulin M [315]. However, the formation of the membrane attack complex, end product of the complement classical pathway, did not seem to be the function initiated by CERT complement activation. These observations suggest that CERTs could play multiple roles in AD pathology.

Other potential targets of the de novo synthesis are the enzymes that generate sphingomyelin and glycosphingolipids. Tamboli et al., demonstrated that the pharmacological inhibition of the glucosylceramide synthase (GSC) attenuated maturation and cell surface transport of APP. This effect was reversed by addition of exogenous brain gangliosides to cultured cells [275]. Others found that in human AD brains as well as AD transgenic mice models GSC is elevated, suggesting that GSC could be an attractive target [316]. A drug that has been used in the clinic to inhibit glycosphingolipids formation via CSC inhibition is Miglustat. Miglustat is a small iminosugar molecule that is now indicated for the treatment of the genetic disorder known as Niemann-Pick disease type C (NP-C). Interestingly, there are similarities between NP-C and AD pathophysiology. Symptoms such as cognitive impairment progressing to dementia with involvement of the cholinergic system are common to both diseases [317]. Furthermore, AD hallmarks like Aβ depositions and neurofiillary tangles are also found in NP-C [318, 319], even though the distribution in the brain appeared to be different [320]. Miglustat has shown to be stabilize or improve certain neurological manifestations in six clinical trials [321]. However, possible application of this drug in AD has not been explored yet.

Inhibition of SMS1 through silencing by siRNA reduced Aβ formation by promoting BACE1 degradation [322]. Mei-Hong et al; reported that SMS1 inhibition with D609 relocated BACE1 to the lysosome and relative levels of the enzyme were found decreased compared to control cells. This

study suggest ceramide and SM may have distinct functions in regulation of BACE1 stability through different molecular mechanisms.

<u>Direct and functional inhibitors of SMases</u>

The regulation of sphingomyelin levels can have a profound effect on physiological properties of the membrane, but also on cellular signaling [237, 323]. TNF-α, Fas ligand, or oxidative stress are known to be triggers for the activation of the enzymatic activity of SMases [324, 325]. One of the most used direct N-SMase inhibitor is GW4869 [326, 327]. GW4869 is a non-competitive inhibitor of N-SMase 2 that protected cells from apoptosis mediated by ceramide accumulation. More recently, it has been shown that N-SMase 2 is crucial for exosome secretion and that GW4869 could interfere with this process. Dinkins et al., observed that intraperitoneal administration of GW4869 in a transgenic mice model of AD resulted in fewer exosomes containing ceramide and in a 40% decrease in plaque load [125, 328]. In the same work, authors reported that N-Smases 2 deficient mice with AD pathology improved memory performance compared to N-Smases 2 non deficient AD mice.

Classic tricyclic dibenzoazepines (TCA) like imipramine or desipramine and selective serotonin reuptake inhibitors (SSRIs) have been used for years for the treatment of major depression and other mental disorders [329-331]. Interestingly, classic TCA's and SSRIs are thought to affect the sphingolipid metabolism by inhibiting the activity of A-SMase [332, 333]. The proposed mechanism is that these compounds interfere with the binding of A-SMase to the lipid bilayer and thereby displacing the enzyme from its membrane-bound substrate [334]. This causes the lysosomal enzyme to be degraded at a faster rate [335]. For this peculiar mechanism, these pharmacological agents have been defined as functional SMase inhibitors (FIASM) [331]. TCA and SSRIs have been used in the treatment of the depression symptoms in AD [336]. Depression is one of the common comorbidities of AD that appears during the progression of the disease [337]. Treatment of AD with venlafaxine and desipramine has been successful not only in controlling depression symptoms but also in preventing the cognitive decline [338]. Moreover, TCA or SSRIs given to AD animal models help coping with depression as well as cognitive symptoms [339-341]. This beneficial effect is thought to derive from TCA and SSRIs potentiation of the serotonin and norepinephrine system which is impaired in AD [342]. Surprisingly, it has never been explored if some of these beneficial effects of TCA and SSRIs in AD, derive from their FIASM activity, which could potentially restore the sphingolipid rheostat. Nevertheless, there are inconsistencies. In fact, the long-term effect of

escitalopram, an SSRI, administration showed to be inefficient in controlling plaques disease and even is contraindicated [343].

S1P analogs and ceramidase/ceramide kinase stimulators

Fingolimod or FTY720 is a sphingosine analog with a potent immunosuppressive activity [344]. Since 2010 it is used in the clinic for the treatment of multiple sclerosis. Due to its peculiar modes of action, it could be repurposed for new therapeutic applications in other neurodegenerative diseases. To exert its immunosuppressive activity the drug requires to be phosphorylated in vivo by SKs to form the active moiety [345]. Phosphorylated Fingolimod binds to S1P receptors causing internalization and degradation of the receptor which leads primarily to lymphopenia in vivo [345]. Interestingly, new pharmacological actions have been discovered for Fingolimod. Firstly, it was reported that Fingolimod functionally inhibits A-SMase following the same mechanisms as FIASM drugs [346]. Secondly, it was found that Fingolimod in human pulmonary artery endothelial cells can inhibit CerSs decreasing dihydroceramide, ceramide, sphingosine, and S1P but increasing levels of dihydrosphingosine and dihydrosphingosine 1-phosphate [347]. Hence, Fingolimod mimics S1P biological activity and at the same time can reduce ceramide levels by FIASM and CerS inhibition. However, the multitarget effect has not been investigated yet in vivo by lipidomic analysis.

In vitro and in vivo data suggest that FTY720 is a modulator of Aβ production independently from the S1P receptor activity. Cell based assays demonstrated that Fingolimod reduced γ-secretase-mediated cleavage of APP thus attenuating Aβ release in the medium [348]. However, these findings were not replicated in vivo [348]. Intraperitoneal injection of Fingolimod for 6 days protected from Aβ-induced memory impairments and neural damage [349]. In alignment with this, Fukumoto et al., found that oral administration of Fingolimod ameliorated memory impairment in the object recognition and associative learning task in mice injected with amyloid. This effect was associated with restoration of normal BDNF expression levels in the cerebral cortices and hippocampus, suggesting that neuroprotection was mediated by up-regulation of neuronal BDNF levels [350]. Neuroprotection mediated by Fingolimod was also suggested by analyzing expression levels of SL metabolism (SPHK1, SPHK2, CERK, S1PR1) and pro-survival genes like BCL-2 in AD transgenic model [351]. However, beneficial effects of Fingolimod are abrogated by simultaneous administration of S1P receptor 1 specific blockers or SK inhibitors [352]. Indeed administration of SEW2871, a S1P receptor 1 selective agonist, ameliorated memory impairment and neuronal loss in an AD rat model [353]. In 5xFAD mice at 3 months of age, Fingolimod decreased plaque density as well as soluble

plus insoluble Aβ measured by enzyme linked immunoassay. Furthermore, FTY720 decreased GFAP staining and the number of activated microglia [354].

Van Doorn et al. showed the ability of Fingolimod to counteract ceramide-induced endothelial barrier alterations [144]. The beneficial effects of S1P and/or Fingolimod on brain endothelial cells might be mediated via S1P receptor 5 which, upon stimulation, reduces the expression of adhesion molecules on brain endothelial cells and prevents the migration of monocytes to the brain parenchyma [144]. The role of S1P on astrocytes was also investigated. Interestingly, several studies showed that astrocytes increase the expression of S1P receptor 3 when activated by S1P, which, together with S1P receptor 5 on brain endothelial cells, could be an attractive target for treatment of AD [144, 355, 356].

Moreover, the stimulation of specific kinase to increase S1P or ceramide-1-phosphate production may also favor neuroprotective signals. Tada et al., discovered that Chinese hamster ovary cells incubated with the compound Vanadate increased ceramide breakdown by ceramidase activity and ceramide phosphorylation by ceramide kinase [357].

RIPK 1 inhibitors and pharmacological chaperones

In section 2.3 we mentioned the RIPK as enzymes that interact with ceramide to mediate necroptosis. Necroptotic cell death or inflammatory cell death is characterized by cell swelling and rupturing of the plasma membrane caused probably by the formation of ceramide-enriched pores that have been previously named ceramidosomes [128]. There are five different RIPK that have been discovered and ceramidosomes formation are initiated by interaction of ceramide with RIPK1 thereby composing a complex which is then transported to the membrane. RIPK1 is activated upon stimulation of on death receptor by TNF-α. RIPK1 is highly expressed in microglia in mouse and human brain samples [358]. In AD the levels of RIPK1 in brain samples are increased compared with controls and positively correlate with the reduction of Braak stages [358]. This elevation of RIPK1 levels were also reported in 11 months old 5xFAD mice compared with non-transgenic littermates [359]. These evidences suggest the involvement of necroptosis in AD. RIPK inhibitors are small molecules that can penetrate the blood–brain barrier. RIPK inhibitors were tested in APP/PS1 mice and showed to reduce amyloid plaque burden [358]. The mode of action suggested is that, inhibition of RIPK1 reduces inflammatory microglia and restore the phagocytic ability of microglia which is impaired in AD. However, no lipidomic analysis was performed to measure ceramide levels after

RIPK inhibitors treatment and whether a metabolic therapy aimed to reduce ceramide level would also improve necroptosis in AD has still to be investigated.

Recently, a new treatment strategy refered to as pharmacological chaperone therapy is emerging for treatment of neurogenerative diseases. Pharmacological chaperones are small molecules that are able to bind misfolded proteins in the endoplasmic reticulum and assist their folding, thus enabling them to pass the ER quality control and shuttle to the lysosomes [360]. Once in the lysosomes, the enzyme–chaperone complexes are dissociated due to low pH freeing the enzyme, now available to hydrolyze its natural substrate. This strategy has been use to increase the activity of glucoceramidasesk in Gaucher disease. There are no report on glucoceramidase levels or activity in AD therefore the impact of this kind of approach is still unkown.

6.6   Conclusion and future perspective

SL metabolism in AD is becoming progressively recognized. Genesis of SL bioactivity research is still in the juvenile stages. Therefore, therapeutic effect of sphingolipid metabolism modulation on specific organ function, and eventually in AD, remains undetermined. For instance, in AD the effects of SLs are not as clearly defined as in basal functions such as cell cycle control and neural differentiation. In AD excessive ceramide contributes to the pathology while and S1P it is protective to neurons. Simultaneously, ceramide is crucial in neuronal maturation while S1P agonistic activation of astrocytes and microglia contributes to AD pathology. Nevertheless, the evidence that manipulation of the SL metabolism can be a valid therapeutic approach in AD is increasing. Use of S1P analogs (like FTY720) or the N-SMase inhibitors (like GW4869) are two approaches that have shown to be effective in rescuing memory impairment, neuro-inflammation and Aβ pathology in AD models. Furthermore, there are many compounds that could be employed with similar pharmacological action which are used in the clinic or are in advance phases of clinical trials for other indications than AD. This could certainly benefit the repurposing of these drugs for AD, and eventually promote the development of new ones.

6.7   Tables

Proteins	Regulation (↑↓) / Enzyme activity (+/-)	Brain regions analyzed	Reference
Serine palmitoyl transferase	↑	Cortices, Hippocampus, Caudate Nucleus And The Putamen.	[24]
Ceramide synthases (1,2 and 6)	↑	Cortices, Hippocampus, Caudate Nucleus And The Putamen.	[24]
Sphingomyelinases	↑/+	Frontotemporal Area	[25]
Glucosyl ceramidase	↑/+	Cortices	[26]
Sphingolipid species in the brain	**Levels (↑↓)**		
Ceramides (Cer20:0, Cer24:0)	↑	Middle Frontal Gyrus, Cerebellum, Temporal Gyrus, Inferior Parietal Lobule, Hippocampus And Subiculum, And The Entorhinal Cortex	[27-29]
S1P	↓	Hippocampus, Inferior Temporal Gyrus, Superior Frontal Gyrus G And Cerebellum	[30]
Sphingomyelins	↓	Frontotemporal Area	[25]

Table 1. Regulation of gene expression, enzymes activity and SLs species in Alzheimer's disease

Sphingolipid type	Levels (increase ↑ ; decrease ↓)	Brain regions analyzed	AD animal models	Reference
Ceramide Gangliosides Sulfatides	↑ in proximity to Aβ plaques ↑ in proximity to Aβ plaques ↓ in proximity to Aβ plaques	Somatosensory cortex, Hippocampus	APP	[31]
Ceramide	(unchanged)	Cortex, Hippocampus	APP/PS1	[32]
Ganglioside (GM2/GM3)	↑	Cerebral cortex, Cerebellum	APP, PS1, APP/PS1	[33]
Ganglioside (GM3) Ganglioside (GD1)	↑ ↓	Subcortical nuclei, Cortical layers, Hippocampus, White matter	APP (rats)	[34]
Ceramide	↑	Cortex, Hippocampus	APP; PS1	[32]
Phospholipids (PS, PI, LBPA, LPC) SM Ceramide Ganglioside	↓ ↑ ↑ ↑	Prefrontal cortex, Entorhinal cortex, Cerebellum	APP; PS1; APP/PS1	[35]

Table 2. Sphingolipid alteration in Alzheimer's disease animal models.

Compounds	Known targets	Mechanism of action
Myriocin	Serine palmitoyl transferase	Suicide inhibitor / immunosuppressant
	S1P receptor agonist	Immunosupressant
L-cycloserine	Serine palmitoyl transferase *NMDA receptor*	Inhibitor *Partial agonist*
Fumonisins (B2)	Ceramide synthases	Inhibitor
HPA-12	Ceramide transfer proteins	Reversible inhibitor (competitor)
L-Threo-1-phenyl-2-decanoylamino-3-morpholino-1-propanol (PDMP)	Glucosyl ceramide synthase	Inhibitor
D2/ Dy105	Sphingomyelin synthase 2	Inhibitor
Desipramine (classic TCA)	Acid sphingomyelinase	FIAMs
	Acid ceramidases	
Fluoxetine (SSRIs)	Acid sphingomyelinase	FIAMs
FTY720 (Fingolimod)	S1P receptors agonist	S1P analog, functional antagonist of S1P receptors, inhibitor of ceramide synthase and acid sphingomyelinase
	Ceramide synthase	
	Acid sphingomyelinase	
GW4869	Neutral sphingomyelinase 2	Inhibitor
SEW2871	S1P receptor isoform 1 specific	Agonist
Halothane	-	Stimulator of sphingomyelinases activity
Vanadate	-	Stimulator of ceramidase/ceramide kinase activity

Table 3. Compounds that target proteins of the sphingolipid pathway with reported mechanism of action.

6.8   References

1.   S. Sonnino, A. Prinetti, The role of sphingolipids in neuronal plasticity of the brain, Journal of neurochemistry, 137 (2016) 485-488.

2.   P.S. Sastry, Lipids of nervous tissue: composition and metabolism, Prog Lipid Res, 24 (1985) 69-176.

3.   A.S.B. Olsen, N.J. Faergeman, Sphingolipids: membrane microdomains in brain development, function and neurological diseases, Open Biol, 7 (2017).

4.   E. Gulbins, S. Walter, K.A. Becker, R. Halmer, Y. Liu, M. Reichel, M.J. Edwards, C.P. Muller, K. Fassbender, J. Kornhuber, A central role for the acid sphingomyelinase/ceramide system in neurogenesis and major depression, Journal of neurochemistry, 134 (2015) 183-192.

5.   Jain, O. Beutel, K. Ebell, S. Korneev, J.C. Holthuis, Diverting CERT-mediated ceramide transport to mitochondria triggers Bax-dependent apoptosis, Journal of cell science, 130 (2017) 360-371.

6.   C.R. Gault, L.M. Obeid, Y.A. Hannun, An overview of sphingolipid metabolism: from synthesis to breakdown, Adv Exp Med Biol, 688 (2010) 1-23.

7.   H. Birbes, S. El Bawab, Y.A. Hannun, L.M. Obeid, Selective hydrolysis of a mitochondrial pool of sphingomyelin induces apoptosis, FASEB J, 15 (2001) 2669-2679.

8.   P.E. Braun, P. Morell, N.S. Radin, Synthesis of C18- and C20-dihydrosphingosines, ketodihydrosphingosines, and ceramides by microsomal preparations from mouse brain, J Biol Chem, 245 (1970) 335-341.

9.   A.D. Batheja, D.J. Uhlinger, J.M. Carton, G. Ho, M.R. D'Andrea, Characterization of serine palmitoyltransferase in normal human tissues, J Histochem Cytochem, 51 (2003) 687-696.

10.   R.O. Brady, G.J. Koval, The enzymatic synthesis of sphingosine, J Biol Chem, 233 (1958) 26-31.

11.   Y. Pewzner-Jung, S. Ben-Dor, A.H. Futerman, When do Lasses (longevity assurance genes) become CerS (ceramide synthases)?: Insights into the regulation of ceramide synthesis, J Biol Chem, 281 (2006) 25001-25005.

12.   T.D. Mullen, Y.A. Hannun, L.M. Obeid, Ceramide synthases at the centre of sphingolipid metabolism and biology, Biochem J, 441 (2012) 789-802.

13.   M. Levy, A.H. Futerman, Mammalian ceramide synthases, IUBMB life, 62 (2010) 347-356.

14.   Bickert, P. Kern, M. van Uelft, S. Herresthal, T. Ulas, K. Gutbrod, B. Breiden, J. Degen, K. Sandhoff, J.L. Schultze, P. Dormann, D. Hartmann, R. Bauer, K. Willecke, Inactivation of ceramide synthase 2 catalytic activity in mice affects transcription

of genes involved in lipid metabolism and cell division, Biochimica et biophysica acta. Molecular and cell biology of lipids, 1863 (2018) 734-749.

15. M.D. Ullman, N.S. Radin, Enzymatic formation of hydroxy ceramides and comparison with enzymes forming nonhydroxy ceramides, Arch Biochem Biophys, 152 (1972) 767-777.

16. C. Michel, G. van Echten-Deckert, J. Rother, K. Sandhoff, E. Wang, A.H. Merrill, Jr., Characterization of ceramide synthesis. A dihydroceramide desaturase introduces the 4,5-trans-double bond of sphingosine at the level of dihydroceramide, J Biol Chem, 272 (1997) 22432-22437.

17. K. Bienias, A. Fiedorowicz, A. Sadowska, S. Prokopiuk, H. Car, Regulation of sphingomyelin metabolism, Pharmacological reports : PR, 68 (2016) 570-581.

18. D. Siow, M. Sunkara, A. Morris, B. Wattenberg, Regulation of de novo sphingolipid biosynthesis by the ORMDL proteins and sphingosine kinase-1, Advances in biological regulation, 57 (2015) 42-54.

19. K. Hanada, Intracellular trafficking of ceramide by ceramide transfer protein, Proceedings of the Japan Academy. Series B, Physical and biological sciences, 86 (2010) 426-437.

20. K. Hanada, K. Kumagai, S. Yasuda, Y. Miura, M. Kawano, M. Fukasawa, M. Nishijima, Molecular machinery for non-vesicular trafficking of ceramide, Nature, 426 (2003) 803-809.

21. Y. Itokazu, Y.T. Tsai, R.K. Yu, Epigenetic regulation of ganglioside expression in neural stem cells and neuronal cells, Glycoconj J, 34 (2017) 749-756.

22. R.K. Yu, Y.T. Tsai, T. Ariga, Functional roles of gangliosides in neurodevelopment: an overview of recent advances, Neurochem Res, 37 (2012) 1230-1244.

23. R.K. Yu, Y. Nakatani, M. Yanagisawa, The role of glycosphingolipid metabolism in the developing brain, J Lipid Res, 50 Suppl (2009) S440-445.

24. Y. Itokazu, J. Wang, R.K. Yu, Gangliosides in Nerve Cell Specification, Progress in molecular biology and translational science, 156 (2018) 241-263.

25. J.S. Ryu, K. Ko, K. Ko, J.S. Kim, S.U. Kim, K.T. Chang, Y.K. Choo, Roles of gangliosides in the differentiation of mouse pluripotent stem cells to neural stem cells and neural cells (Review), Molecular medicine reports, 16 (2017) 987-993.

26. C.L. Schengrund, Gangliosides: glycosphingolipids essential for normal neural development and function, Trends in biochemical sciences, 40 (2015) 397-406.

27. E. Bieberich, It's a lipid's world: bioactive lipid metabolism and signaling in neural stem cell differentiation, Neurochem Res, 37 (2012) 1208-1229.

28. R.L. Schnaar, Gangliosides of the Vertebrate Nervous System, Journal of molecular biology, 428 (2016) 3325-3336.

29. M. Chatelut, M. Leruth, K. Harzer, A. Dagan, S. Marchesini, S. Gatt, R. Salvayre, P. Courtoy, T. Levade, Natural ceramide is unable to escape the lysosome, in contrast to a fluorescent analogue, FEBS Letters, 426 (1998) 102-106.

30. K. Kitatani, J. Idkowiak-Baldys, Y.A. Hannun, The sphingolipid salvage pathway in ceramide metabolism and signaling, Cellular signalling, 20 (2008) 1010-1018.

31. P.V. Subbaiah, R.M. Sargis, Sphingomyelin: a natural modulator of membrane homeostasis and inflammation, Medical Hypotheses, 57 (2001) 135-138.

32. P.G. Hogan, Sphingomyelin, ORAI1 channels, and cellular Ca^{2+} signaling, The Journal of General Physiology, 146 (2015) 195-200.

33. B.X. Wu, V. Rajagopalan, P.L. Roddy, C.J. Clarke, Y.A. Hannun, Identification and characterization of murine mitochondria-associated neutral sphingomyelinase (MA-nSMase), the mammalian sphingomyelin phosphodiesterase 5, J Biol Chem, 285 (2010) 17993-18002.

34. R.W. Jenkins, D. Canals, Y.A. Hannun, Roles and regulation of secretory and lysosomal acid sphingomyelinase, Cellular signalling, 21 (2009) 836-846.

35. S. Gatt, Magnesium-dependent sphingomyelinase, Biochem Biophys Res Commun, 68 (1976) 235-241.

36. B.G. Rao, M.W. Spence, Sphingomyelinase activity at pH 7.4 in human brain and a comparison to activity at pH 5.0, J Lipid Res, 17 (1976) 506-515.

37. S. Yamaguchi, K. Suzuki, A novel magnesium-independent neutral sphingomyelinase associated with rat central nervous system meylin, J Biol Chem, 253 (1978) 4090-4092.

38. M.W. Spence, J.K. Burgess, Acid and neutral sphingomyelinases of rat brain. Activity in developing brain and regional distribution in adult brain, Journal of neurochemistry, 30 (1978) 917-919.

39. F. Klein, P. Mandel, [Sphingomyelinase activity in the cortex, corpus callosum and brain of rats during their development], Biochimie, 54 (1972) 371-374.

40. N. Marchesini, Y.A. Hannun, Acid and neutral sphingomyelinases: roles and mechanisms of regulation, Biochemistry and Cell Biology, 82 (2004) 27-44.

41. L.C. Edsall, S. Spiegel, Enzymatic measurement of sphingosine 1-phosphate, Anal Biochem, 272 (1999) 80-86.

42. K. Mizugishi, T. Yamashita, A. Olivera, G.F. Miller, S. Spiegel, R.L. Proia, Essential role for sphingosine kinases in neural and vascular development, Mol Cell Biol, 25 (2005) 11113-11121.

43. T.D. Mullen, R.W. Jenkins, C.J. Clarke, J. Bielawski, Y.A. Hannun, L.M. Obeid, Ceramide synthase-dependent ceramide generation and programmed cell death:

involvement of salvage pathway in regulating postmitochondrial events, J Biol Chem, 286 (2011) 15929-15942.

44.   S. Spiegel, A.H. Merrill, Jr., Sphingolipid metabolism and cell growth regulation, FASEB J, 10 (1996) 1388-1397.

45.   J.Y. Lee, L.G. Leonhardt, L.M. Obeid, Cell-cycle-dependent changes in ceramide levels preceding retinoblastoma protein dephosphorylation in G2/M, The Biochemical journal, 334 (Pt 2) (1998) 457-461.

46.   N. Chauhan, G. Han, N. Somashekarappa, K. Gable, T. Dunn, S.D. Kohlwein, Regulation of sphingolipid biosynthesis by the morphogenesis checkpoint kinase Swe1, J Biol Chem, 292 (2017) 9431.

47.   Y.S. Lee, K.M. Choi, S. Lee, D.M. Sin, Y. Lim, Y.M. Lee, J.T. Hong, Y.P. Yun, H.S. Yoo, Myriocin, a serine palmitoyltransferase inhibitor, suppresses tumor growth in a murine melanoma model by inhibiting de novo sphingolipid synthesis, Cancer biology & therapy, 13 (2012) 92-100.

48.   Y.S. Lee, K.M. Choi, M.H. Choi, S.Y. Ji, S. Lee, D.M. Sin, K.W. Oh, Y.M. Lee, J.T. Hong, Y.P. Yun, H.S. Yoo, Serine palmitoyltransferase inhibitor myriocin induces growth inhibition of B16F10 melanoma cells through G(2) /M phase arrest, Cell proliferation, 44 (2011) 320-329.

49.   G.S. Dbaibo, M.Y. Pushkareva, S. Jayadev, J.K. Schwarz, J.M. Horowitz, L.M. Obeid, Y.A. Hannun, Retinoblastoma gene product as a downstream target for a ceramide-dependent pathway of growth arrest, Proc Natl Acad Sci U S A, 92 (1995) 1347-1351.

50.   N. Marchesini, W. Osta, J. Bielawski, C. Luberto, L.M. Obeid, Y.A. Hannun, Role for mammalian neutral sphingomyelinase 2 in confluence-induced growth arrest of MCF7 cells, J Biol Chem, 279 (2004) 25101-25111.

51.   J.Y. Lee, A.E. Bielawska, L.M. Obeid, Regulation of cyclin-dependent kinase 2 activity by ceramide, Experimental cell research, 261 (2000) 303-311.

52.   E. Bieberich, Integration of glycosphingolipid metabolism and cell-fate decisions in cancer and stem cells: review and hypothesis, Glycoconj J, 21 (2004) 315-327.

53.   J.D. Saba, L.M. Obeid, Y.A. Hannun, Ceramide: an intracellular mediator of apoptosis and growth suppression, Philos Trans R Soc Lond B Biol Sci, 351 (1996) 233-240; discussion 240-231.

54.   Y.A. Hannun, Functions of ceramide in coordinating cellular responses to stress, Science, 274 (1996) 1855-1859.

55.   M. Xin, X. Deng, Protein phosphatase 2A enhances the proapoptotic function of Bax through dephosphorylation, J Biol Chem, 281 (2006) 18859-18867.

56.   R.T. Dobrowsky, Y.A. Hannun, Ceramide stimulates a cytosolic protein phosphatase, J Biol Chem, 267 (1992) 5048-5051.

57. A.H. Merrill, Jr., A.M. Sereni, V.L. Stevens, Y.A. Hannun, R.M. Bell, J.M. Kinkade, Jr., Inhibition of phorbol ester-dependent differentiation of human promyelocytic leukemic (HL-60) cells by sphinganine and other long-chain bases, J Biol Chem, 261 (1986) 12610-12615.

58. L.M. Obeid, C.M. Linardic, L.A. Karolak, Y.A. Hannun, Programmed cell death induced by ceramide, Science, 259 (1993) 1769-1771.

59. V. Mamidipudi, M.W. Wooten, Dual role for p75(NTR) signaling in survival and cell death: can intracellular mediators provide an explanation?, J Neurosci Res, 68 (2002) 373-384.

60. G. Wang, J. Silva, S. Dasgupta, E. Bieberich, Long-chain ceramide is elevated in presenilin 1 (PS1M146V) mouse brain and induces apoptosis in PS1 astrocytes, Glia, 56 (2008) 449-456.

61. R.T. Dobrowsky, M.H. Werner, A.M. Castellino, M.V. Chao, Y.A. Hannun, Activation of the sphingomyelin cycle through the low-affinity neurotrophin receptor, Science, 265 (1994) 1596-1599.

62. P. Casaccia-Bonnefil, B.D. Carter, R.T. Dobrowsky, M.V. Chao, Death of oligodendrocytes mediated by the interaction of nerve growth factor with its receptor p75, Nature, 383 (1996) 716-719.

63. C. Culmsee, N. Gerling, M. Lehmann, M. Nikolova-Karakashian, J.H. Prehn, M.P. Mattson, J. Krieglstein, Nerve growth factor survival signaling in cultured hippocampal neurons is mediated through TrkA and requires the common neurotrophin receptor P75, Neuroscience, 115 (2002) 1089-1108.

64. A.B. Brann, R. Scott, Y. Neuberger, D. Abulafia, S. Boldin, M. Fainzilber, A.H. Futerman, Ceramide signaling downstream of the p75 neurotrophin receptor mediates the effects of nerve growth factor on outgrowth of cultured hippocampal neurons, J Neurosci, 19 (1999) 8199-8206.

65. G.L. Barrett, The p75 neurotrophin receptor and neuronal apoptosis, Prog Neurobiol, 61 (2000) 205-229.

66. A.B. Brann, M. Tcherpakov, I.M. Williams, A.H. Futerman, M. Fainzilber, Nerve growth factor-induced p75-mediated death of cultured hippocampal neurons is age-dependent and transduced through ceramide generated by neutral sphingomyelinase, J Biol Chem, 277 (2002) 9812-9818.

67. M.E. Venable, J.Y. Lee, M.J. Smyth, A. Bielawska, L.M. Obeid, Role of ceramide in cellular senescence, J Biol Chem, 270 (1995) 30701-30708.

68. L.M. Obeid, Y.A. Hannun, Ceramide, stress, and a "LAG" in aging, Sci Aging Knowledge Environ, 2003 (2003) PE27.

69. Y.A. Hannun, L.M. Obeid, Principles of bioactive lipid signalling: lessons from sphingolipids, Nature reviews. Molecular cell biology, 9 (2008) 139-150.

70.   N. Bartke, Y.A. Hannun, Bioactive sphingolipids: metabolism and function, J Lipid Res, 50 Suppl (2009) S91-96.

71.   M. Trayssac, Y.A. Hannun, L.M. Obeid, Role of sphingolipids in senescence: implication in aging and age-related diseases, The Journal of clinical investigation, 128 (2018) 2702-2712.

72.   W. Jiang, B. Ogretmen, Autophagy paradox and ceramide, Biochim Biophys Acta, (2013).

73.   E.R. Peralta, A.L. Edinger, Ceramide-induced starvation triggers homeostatic autophagy, Autophagy, 5 (2009) 407-409.

74.   G. Lavieu, F. Scarlatti, G. Sala, S. Carpentier, T. Levade, R. Ghidoni, J. Botti, P. Codogno, Regulation of autophagy by sphingosine kinase 1 and its role in cell survival during nutrient starvation, J Biol Chem, 281 (2006) 8518-8527.

75.   G. Lavieu, F. Scarlatti, G. Sala, T. Levade, R. Ghidoni, J. Botti, P. Codogno, Is autophagy the key mechanism by which the sphingolipid rheostat controls the cell fate decision?, Autophagy, 3 (2007) 45-47.

76.   W.I. Leong, J.D. Saba, S1P metabolism in cancer and other pathological conditions, Biochimie, 92 (2010) 716-723.

77.   J.R. Van Brocklyn, J.B. Williams, The control of the balance between ceramide and sphingosine-1-phosphate by sphingosine kinase: oxidative stress and the seesaw of cell survival and death, Comp Biochem Physiol B Biochem Mol Biol, 163 (2012) 26-36.

78.   G. Wang, E. Bieberich, Sphingolipids in neurodegeneration (with focus on ceramide and S1P), Advances in biological regulation, (2018).

79.   Karunakaran, G. van Echten-Deckert, Sphingosine 1-phosphate - A double edged sword in the brain, Biochimica et biophysica acta. Biomembranes, 1859 (2017) 1573-1582.

80.   R. Ghasemi, L. Dargahi, A. Ahmadiani, Integrated sphingosine-1 phosphate signaling in the central nervous system: From physiological equilibrium to pathological damage, Pharmacological research, 104 (2016) 156-164.

81.   J.F. Moruno Manchon, N.E. Uzor, Y. Dabaghian, E.E. Furr-Stimming, S. Finkbeiner, A.S. Tsvetkov, Cytoplasmic sphingosine-1-phosphate pathway modulates neuronal autophagy, Scientific reports, 5 (2015) 15213.

82.   M. Taniguchi, K. Kitatani, T. Kondo, M. Hashimoto-Nishimura, S. Asano, A. Hayashi, S. Mitsutake, Y. Igarashi, H. Umehara, H. Takeya, J. Kigawa, T. Okazaki, Regulation of autophagy and its associated cell death by "sphingolipid rheostat": reciprocal role of ceramide and sphingosine 1-phosphate in the mammalian target of rapamycin pathway, J Biol Chem, 287 (2012) 39898-39910.

83. K. Krishnamurthy, G. Wang, J. Silva, B.G. Condie, E. Bieberich, *Ceramide Regulates Atypical PKC{zeta}/{lambda}-mediated Cell Polarity in Primitive Ectoderm Cells: A NOVEL FUNCTION OF SPHINGOLIPIDS IN MORPHOGENESIS, J Biol Chem, 282 (2007) 3379-3390.*

84. E. Bieberich, *Ceramide signaling in cancer and stem cells, Future Lipidol, 3 (2008) 273-300.*

85. G. Wang, K. Krishnamurthy, Y.W. Chiang, S. Dasgupta, E. Bieberich, *Regulation of neural progenitor cell motility by ceramide and potential implications for mouse brain development, Journal of neurochemistry, 106 (2008) 718-733.*

86. G. Wang, K. Krishnamurthy, E. Bieberich, *Regulation of primary cilia formation by ceramide, J Lipid Res, (2009).*

87. G. Wang, K. Krishnamurthy, N.S. Umapathy, A.D. Verin, E. Bieberich, *The carboxyl-terminal domain of atypical protein kinase Czeta binds to ceramide and regulates junction formation in epithelial cells, J Biol Chem, 284 (2009) 14469-14475.*

88. E. Bieberich, *Ceramide in stem cell differentiation and embryo development: novel functions of a topological cell-signaling lipid and the concept of ceramide compartments, J Lipids, 2011 (2011) 610306.*

89. Q. He, G. Wang, S. Dasgupta, M. Dinkins, G. Zhu, E. Bieberich, *Characterization of an apical ceramide-enriched compartment regulating ciliogenesis, Mol Biol Cell, 23 (2012) 3156-3166.*

90. Q. He, G. Wang, S. Wakade, S. Dasgupta, M. Dinkins, J.N. Kong, S.D. Spassieva, E. Bieberich, *Primary cilia in stem cells and neural progenitors are regulated by neutral sphingomyelinase 2 and ceramide, Mol Biol Cell, 25 (2014) 1715-1729.*

91. J.N. Kong, K. Hardin, M. Dinkins, G. Wang, Q. He, T. Mujadzic, G. Zhu, J. Bielawski, S. Spassieva, E. Bieberich, *Regulation of Chlamydomonas flagella and ependymal cell motile cilia by ceramide-mediated translocation of GSK3, Mol Biol Cell, 26 (2015) 4451-4465.*

92. E. Bieberich, S. MacKinnon, J. Silva, S. Noggle, B.G. Condie, *Regulation of cell death in mitotic neural progenitor cells by asymmetric distribution of prostate apoptosis response 4 (PAR-4) and simultaneous elevation of endogenous ceramide, J Cell Biol, 162 (2003) 469-479.*

93. S. Spiegel, A. Olivera, H. Zhang, E.W. Thompson, Y. Su, A. Berger, *Sphingosine-1-phosphate, a novel second messenger involved in cell growth regulation and signal transduction, affects growth and invasiveness of human breast cancer cells, Breast cancer research and treatment, 31 (1994) 337-348.*

94. B. Ogretmen, *Sphingolipid metabolism in cancer signalling and therapy, Nature reviews. Cancer, 18 (2018) 33-50.*

95.   L.A. Heffernan-Stroud, L.M. Obeid, Sphingosine kinase 1 in cancer, Adv Cancer Res, 117 (2013) 201-235.

96.   J.W. Yester, E. Tizazu, K.B. Harikumar, T. Kordula, Extracellular and intracellular sphingosine-1-phosphate in cancer, Cancer Metastasis Rev, 30 (2011) 577-597.

97.   K. Geffken, S. Spiegel, Sphingosine kinase 1 in breast cancer, Advances in biological regulation, 67 (2018) 59-65.

98.   T.A. Taha, K. Kitatani, J. Bielawski, W. Cho, Y.A. Hannun, L.M. Obeid, Tumor necrosis factor induces the loss of sphingosine kinase-1 by a cathepsin B-dependent mechanism, J Biol Chem, 280 (2005) 17196-17202.

99.   H. Chan, S.M. Pitson, Post-translational regulation of sphingosine kinases, Biochim Biophys Acta, 1831 (2013) 147-156.

100. R.K. Barr, H.E. Lynn, P.A. Moretti, Y. Khew-Goodall, S.M. Pitson, Deactivation of sphingosine kinase 1 by protein phosphatase 2A, J Biol Chem, 283 (2008) 34994-35002.

101. H.A. Neubauer, S.M. Pitson, Roles, regulation and inhibitors of sphingosine kinase 2, The FEBS journal, 280 (2013) 5317-5336.

102. S.M. Pitson, P.A. Moretti, J.R. Zebol, H.E. Lynn, P. Xia, M.A. Vadas, B.W. Wattenberg, Activation of sphingosine kinase 1 by ERK1/2-mediated phosphorylation, The EMBO journal, 22 (2003) 5491-5500.

103. X. Zhu, K. Ren, Y.Z. Zeng, Z. Zheng, G.H. Yi, Biological function of SPNS2: From zebrafish to human, Molecular immunology, 103 (2018) 55-62.

104. T. Nishi, N. Kobayashi, Y. Hisano, A. Kawahara, A. Yamaguchi, Molecular and physiological functions of sphingosine 1-phosphate transporters, Biochim Biophys Acta, 1841 (2014) 759-765.

105. M.S. Donoviel, N.C. Hait, S. Ramachandran, M. Maceyka, K. Takabe, S. Milstien, T. Oravecz, S. Spiegel, Spinster 2, a sphingosine-1-phosphate transporter, plays a critical role in inflammatory and autoimmune diseases, FASEB J, 29 (2015) 5018-5028.

106. E. Bradley, S. Dasgupta, X. Jiang, X. Zhao, G. Zhu, Q. He, M. Dinkins, E. Bieberich, G. Wang, Critical role of Spns2, a sphingosine-1-phosphate transporter, in lung cancer cell survival and migration, PLoS One, 9 (2014) e110119.

107. R. Brunkhorst, R. Vutukuri, W. Pfeilschifter, Fingolimod for the treatment of neurological diseases-state of play and future perspectives, Frontiers in cellular neuroscience, 8 (2014) 283.

108. N.J. Pyne, S. Pyne, Sphingosine 1-Phosphate Receptor 1 Signaling in Mammalian Cells, Molecules, 22 (2017).

109. V.E. Miron, A. Schubart, J.P. Antel, Central nervous system-directed effects of FTY720 (fingolimod), J Neurol Sci, 274 (2008) 13-17.

110. N.C. Hait, J. Allegood, M. Maceyka, G.M. Strub, K.B. Harikumar, S.K. Singh, C. Luo, R. Marmorstein, T. Kordula, S. Milstien, S. Spiegel, Regulation of histone acetylation in the nucleus by sphingosine-1-phosphate, Science, 325 (2009) 1254-1257.

111. E. Bieberich, Sphingolipids and lipid rafts: Novel concepts and methods of analysis, Chemistry and physics of lipids, 216 (2018) 114-131.

112. G. Muller, M. Ayoub, P. Storz, J. Rennecke, D. Fabbro, K. Pfizenmaier, PKC zeta is a molecular switch in signal transduction of TNF-alpha, bifunctionally regulated by ceramide and arachidonic acid, The EMBO journal, 14 (1995) 1961-1969.

113. J. Lozano, E. Berra, M.M. Municio, M.T. Diaz-Meco, I. Dominguez, L. Sanz, J. Moscat, Protein kinase C zeta isoform is critical for kappa B-dependent promoter activation by sphingomyelinase, J Biol Chem, 269 (1994) 19200-19202.

114. Y.M. Wang, M.L. Seibenhener, M.L. Vandenplas, M.W. Wooten, Atypical PKC zeta is activated by ceramide, resulting in coactivation of NF-kappaB/JNK kinase and cell survival, J Neurosci Res, 55 (1999) 293-302.

115. E. Bieberich, T. Kawaguchi, R.K. Yu, N-acylated serinol is a novel ceramide mimic inducing apoptosis in neuroblastoma cells, J Biol Chem, 275 (2000) 177-181.

116. N.A. Bourbon, J. Yun, M. Kester, Ceramide directly activates protein kinase C zeta to regulate a stress-activated protein kinase signaling complex, J Biol Chem, 275 (2000) 35617-35623.

117. G. Wang, J. Silva, K. Krishnamurthy, E. Tran, B.G. Condie, E. Bieberich, Direct binding to ceramide activates protein kinase Czeta before the formation of a pro-apoptotic complex with PAR-4 in differentiating stem cells, J Biol Chem, 280 (2005) 26415-26424.

118. T.E. Fox, K.L. Houck, S.M. O'Neill, M. Nagarajan, T.C. Stover, P.T. Pomianowski, O. Unal, J.K. Yun, S.J. Naides, M. Kester, Ceramide recruits and activates protein kinase C zeta (PKC zeta) within structured membrane microdomains, J Biol Chem, 282 (2007) 12450-12457.

119. T. Walter, L. Collenburg, L. Japtok, B. Kleuser, S. Schneider-Schaulies, N. Muller, J. Becam, A. Schubert-Unkmeir, J.N. Kong, E. Bieberich, J. Seibel, Incorporation and visualization of azido-functionalized N-oleoyl serinol in Jurkat cells, mouse brain astrocytes, 3T3 fibroblasts and human brain microvascular endothelial cells, Chem Commun (Camb), 52 (2016) 8612-8614.

120. S.D. Spassieva, X. Ji, Y. Liu, K. Gable, J. Bielawski, T.M. Dunn, E. Bieberich, L. Zhao, Ectopic expression of ceramide synthase 2 in neurons suppresses neurodegeneration induced by ceramide synthase 1 deficiency, Proc Natl Acad Sci U S A, 113 (2016) 5928-5933.

121. S. Imgrund, D. Hartmann, H. Farwanah, M. Eckhardt, R. Sandhoff, J. Degen, V. Gieselmann, K. Sandhoff, K. Willecke, Adult ceramide synthase 2 (CERS2)-deficient mice exhibit myelin sheath defects, cerebellar degeneration, and hepatocarcinomas, J Biol Chem, 284 (2009) 33549-33560.

122. L.C. Silva, O. Ben David, Y. Pewzner-Jung, E.L. Laviad, J. Stiban, S. Bandyopadhyay, A.H. Merrill, Jr., M. Prieto, A.H. Futerman, Ablation of ceramide synthase 2 strongly affects biophysical properties of membranes, J Lipid Res, 53 (2012) 430-436.

123. H. Park, C.A. Haynes, A.V. Nairn, M. Kulik, S. Dalton, K. Moremen, A.H. Merrill, Jr., Transcript profiling and lipidomic analysis of ceramide subspecies in mouse embryonic stem cells and embryoid bodies, J Lipid Res, 51 (2010) 480-489.

124. O. Ben-David, Y. Pewzner-Jung, O. Brenner, E.L. Laviad, A. Kogot-Levin, I. Weissberg, I.E. Biton, R. Pienik, E. Wang, S. Kelly, J. Alroy, A. Raas-Rothschild, A. Friedman, B. Brugger, A.H. Merrill, Jr., A.H. Futerman, Encephalopathy caused by ablation of very long acyl chain ceramide synthesis may be largely due to reduced galactosylceramide levels, J Biol Chem, 286 (2011) 30022-30033.

125. G. Wang, M. Dinkins, Q. He, G. Zhu, C. Poirier, A. Campbell, M. Mayer-Proschel, E. Bieberich, Astrocytes secrete exosomes enriched with proapoptotic ceramide and prostate apoptosis response 4 (PAR-4): potential mechanism of apoptosis induction in Alzheimer disease (AD), J Biol Chem, 287 (2012) 21384-21395.

126. B. Fekry, K.A. Jeffries, A. Esmaeilniakooshkghazi, Z.M. Szulc, K.J. Knagge, D.R. Kirchner, D.A. Horita, S.A. Krupenko, N.I. Krupenko, C16-ceramide is a natural regulatory ligand of p53 in cellular stress response, Nature communications, 9 (2018) 4149.

127. S.A. Saddoughi, S. Gencer, Y.K. Peterson, K.E. Ward, A. Mukhopadhyay, J. Oaks, J. Bielawski, Z.M. Szulc, R.J. Thomas, S.P. Selvam, C.E. Senkal, E. Garrett-Mayer, R.M. De Palma, D. Fedarovich, A. Liu, A.A. Habib, R.V. Stahelin, D. Perrotti, B. Ogretmen, Sphingosine analogue drug FTY720 targets I2PP2A/SET and mediates lung tumour suppression via activation of PP2A-RIPK1-dependent necroptosis, EMBO Mol Med, 5 (2013) 105-121.

128. R. Nganga, N. Oleinik, J. Kim, S. Panneer Selvam, R. De Palma, K.A. Johnson, R.Y. Parikh, V. Gangaraju, Y. Peterson, M. Dany, R.V. Stahelin, C. Voelkel-Johnson, Z.M. Szulc, E. Bieberich, B. Ogretmen, Receptor-interacting Ser/Thr kinase 1 (RIPK1) and myosin IIA-dependent ceramidosomes form membrane pores that mediate blebbing and necroptosis, J Biol Chem, (2018).

129. A. Mukhopadhyay, S.A. Saddoughi, P. Song, I. Sultan, S. Ponnusamy, C.E. Senkal, C.F. Snook, H.K. Arnold, R.C. Sears, Y.A. Hannun, B. Ogretmen, Direct interaction between the inhibitor 2 and ceramide via sphingolipid-protein binding is involved in the regulation of protein phosphatase 2A activity and signaling, Faseb J, (2008).

130. R.D. Sentelle, C.E. Senkal, W. Jiang, S. Ponnusamy, S. Gencer, S.P. Selvam, V.K. Ramshesh, Y.K. Peterson, J.J. Lemasters, Z.M. Szulc, J. Bielawski, B. Ogretmen,

Ceramide targets autophagosomes to mitochondria and induces lethal mitophagy, Nature chemical biology, 8 (2012) 831-838.

131. *[131] K. Zhou, A. Dichlberger, H. Martinez-Seara, T.K.M. Nyholm, S. Li, Y.A. Kim, I. Vattulainen, E. Ikonen, T. Blom, A Ceramide-Regulated Element in the Late Endosomal Protein LAPTM4B Controls Amino Acid Transporter Interaction, ACS central science, 4 (2018) 548-558.*

132. *T. Blom, S. Li, A. Dichlberger, N. Back, Y.A. Kim, U. Loizides-Mangold, H. Riezman, R. Bittman, E. Ikonen, LAPTM4B facilitates late endosomal ceramide export to control cell death pathways, Nature chemical biology, 11 (2015) 799-806.*

133. *Y. Zhang, B. Yao, S. Delikat, S. Bayoumy, X.H. Lin, S. Basu, M. McGinley, P.Y. Chan-Hui, H. Lichenstein, R. Kolesnick, Kinase suppressor of Ras is ceramide-activated protein kinase, Cell, 89 (1997) 63-72.*

134. *X. Yin, M. Zafrullah, H. Lee, A. Haimovitz-Friedman, Z. Fuks, R. Kolesnick, A ceramide-binding C1 domain mediates kinase suppressor of ras membrane translocation, Cell Physiol Biochem, 24 (2009) 219-230.*

135. *W.J. van Blitterswijk, Hypothesis: ceramide conditionally activates atypical protein kinases C, Raf-1 and KSR through binding to their cysteine-rich domains, The Biochemical journal, 331 (Pt 2) (1998) 679-680.*

136. *E. Bieberich, J. Silva, G. Wang, K. Krishnamurthy, B.G. Condie, Selective apoptosis of pluripotent mouse and human stem cells by novel ceramide analogues prevents teratoma formation and enriches for neural precursors in ES cell-derived neural transplants, J Cell Biol, 167 (2004) 723-734.*

137. *L.C. Edsall, G.G. Pirianov, S. Spiegel, Involvement of sphingosine 1-phosphate in nerve growth factor-mediated neuronal survival and differentiation, J Neurosci, 17 (1997) 6952-6960.*

138. *C. Jaillard, S. Harrison, B. Stankoff, M.S. Aigrot, A.R. Calver, G. Duddy, F.S. Walsh, M.N. Pangalos, N. Arimura, K. Kaibuchi, B. Zalc, C. Lubetzki, Edg8/S1P5: an oligodendroglial receptor with dual function on process retraction and cell survival, J Neurosci, 25 (2005) 1459-1469.*

139. *S. Quarta, M. Camprubi-Robles, R. Schweigreiter, D. Matusica, R.V. Haberberger, R.L. Proia, C.E. Bandtlow, A. Ferrer-Montiel, M. Kress, Sphingosine-1-Phosphate and the S1P3 Receptor Initiate Neuronal Retraction via RhoA/ROCK Associated with CRMP2 Phosphorylation, Frontiers in molecular neuroscience, 10 (2017) 317.*

140. *L.M. Healy, J.P. Antel, Sphingosine-1-Phosphate Receptors in the Central Nervous and Immune Systems, Current drug targets, 17 (2016) 1841-1850.*

141. *R. Bassi, V. Anelli, P. Giussani, G. Tettamanti, P. Viani, L. Riboni, Sphingosine-1-phosphate is released by cerebellar astrocytes in response to bFGF and induces astrocyte proliferation through Gi-protein-coupled receptors, Glia, 53 (2006) 621-630.*

142. A. Kimura, T. Ohmori, R. Ohkawa, S. Madoiwa, J. Mimuro, T. Murakami, E. Kobayashi, Y. Hoshino, Y. Yatomi, Y. Sakata, Essential roles of sphingosine 1-phosphate/S1P1 receptor axis in the migration of neural stem cells toward a site of spinal cord injury, Stem cells (Dayton, Ohio), 25 (2007) 115-124.

143. F. Mullershausen, L.M. Craveiro, Y. Shin, M. Cortes-Cros, F. Bassilana, M. Osinde, W.L. Wishart, D. Guerini, M. Thallmair, M.E. Schwab, R. Sivasankaran, K. Seuwen, K.K. Dev, Phosphorylated FTY720 promotes astrocyte migration through sphingosine-1-phosphate receptors, Journal of neurochemistry, 102 (2007) 1151-1161.

144. R. van Doorn, P.G. Nijland, N. Dekker, M.E. Witte, M.A. Lopes-Pinheiro, B. van het Hof, G. Kooij, A. Reijerkerk, C. Dijkstra, P. van van der Valk, J. van Horssen, H.E. de Vries, Fingolimod attenuates ceramide-induced blood-brain barrier dysfunction in multiple sclerosis by targeting reactive astrocytes, Acta Neuropathol, 124 (2012) 397-410.

145. J.W. Choi, S.E. Gardell, D.R. Herr, R. Rivera, C.W. Lee, K. Noguchi, S.T. Teo, Y.C. Yung, M. Lu, G. Kennedy, J. Chun, FTY720 (fingolimod) efficacy in an animal model of multiple sclerosis requires astrocyte sphingosine 1-phosphate receptor 1 (S1P1) modulation, Proc Natl Acad Sci U S A, 108 (2011) 751-756.

146. A. Pebay, M. Toutant, J. Premont, C.F. Calvo, L. Venance, J. Cordier, J. Glowinski, M. Tence, Sphingosine-1-phosphate induces proliferation of astrocytes: regulation by intracellular signalling cascades, The European journal of neuroscience, 13 (2001) 2067-2076.

147. E. Bieberich, Smart drugs for smarter stem cells: making SENSe (sphingolipid-enhanced neural stem cells) of ceramide, Neurosignals, 16 (2008) 124-139.

148. E. Bieberich, There is More to a Lipid than just Being a Fat: Sphingolipid-Guided Differentiation of Oligodendroglial Lineage from Embryonic Stem Cells, Neurochem Res, (2010).

149. G. Wang, S.D. Spassieva, E. Bieberich, Ceramide and S1P Signaling in Embryonic Stem Cell Differentiation, Methods in molecular biology, 1697 (2018) 153-171.

150. C. Fasano, F. Terce, J.P. Niel, T.T. Nguyen, A. Hiol, J. Bertrand-Michel, N. Mallet, X. Collet, J.P. Miolan, Neuronal conduction of excitation without action potentials based on ceramide production, PLoS One, 2 (2007) e612.

151. F. Darios, C. Wasser, A. Shakirzyanova, A. Giniatullin, K. Goodman, J.L. Munoz-Bravo, J. Raingo, J. Jorgacevski, M. Kreft, R. Zorec, J.M. Rosa, L. Gandia, L.M. Gutierrez, T. Binz, R. Giniatullin, E.T. Kavalali, B. Davletov, Sphingosine facilitates SNARE complex assembly and activates synaptic vesicle exocytosis, Neuron, 62 (2009) 683-694.

152. J. Rohrbough, E. Rushton, L. Palanker, E. Woodruff, H.J. Matthies, U. Acharya, J.K. Acharya, K. Broadie, Ceramidase regulates synaptic vesicle exocytosis and trafficking, J Neurosci, 24 (2004) 7789-7803.

153. T. Kanno, T. Nishizaki, R.L. Proia, T. Kajimoto, S. Jahangeer, T. Okada, S. Nakamura, Regulation of synaptic strength by sphingosine 1-phosphate in the hippocampus, Neuroscience, 171 (2010) 973-980.

154. P. Alaupovic, Significance of apolipoproteins for structure, function, and classification of plasma lipoproteins, Methods Enzymol, 263 (1996) 32-60.

155. H. Yang, N. Zhang, E.U. Okoro, Z. Guo, Transport of Apolipoprotein B-Containing Lipoproteins through Endothelial Cells Is Associated with Apolipoprotein E-Carrying HDL-Like Particle Formation, Int J Mol Sci, 19 (2018).

156. E.H. Corder, A.M. Saunders, W.J. Strittmatter, D.E. Schmechel, P.C. Gaskell, G.W. Small, A.D. Roses, J.L. Haines, M.A. Pericak-Vance, Gene dose of apolipoprotein E type 4 allele and the risk of Alzheimer's disease in late onset families, Science, 261 (1993) 921-923.

157. H. Li, P. Dhanasekaran, E.T. Alexander, D.J. Rader, M.C. Phillips, S. Lund-Katz, Molecular mechanisms responsible for the differential effects of apoE3 and apoE4 on plasma lipoprotein-cholesterol levels, Arterioscler Thromb Vasc Biol, 33 (2013) 687-693.

158. G. van Niel, P. Bergam, A. Di Cicco, I. Hurbain, A. Lo Cicero, F. Dingli, R. Palmulli, C. Fort, M.C. Potier, L.J. Schurgers, D. Loew, D. Levy, G. Raposo, Apolipoprotein E Regulates Amyloid Formation within Endosomes of Pigment Cells, Cell Rep, 13 (2015) 43-51.

159. S.M. Hammad, J.S. Pierce, F. Soodavar, K.J. Smith, M.M. Al Gadban, B. Rembiesa, R.L. Klein, Y.A. Hannun, J. Bielawski, A. Bielawska, Blood sphingolipidomics in healthy humans: impact of sample collection methodology, J Lipid Res, 51 (2010) 3074-3087.

160. J. Serna, D. Garcia-Seisdedos, A. Alcazar, M.A. Lasuncion, R. Busto, O. Pastor, Quantitative lipidomic analysis of plasma and plasma lipoproteins using MALDI-TOF mass spectrometry, Chemistry and physics of lipids, 189 (2015) 7-18.

161. M. Scherer, A. Bottcher, G. Schmitz, G. Liebisch, Sphingolipid profiling of human plasma and FPLC-separated lipoprotein fractions by hydrophilic interaction chromatography tandem mass spectrometry, Biochim Biophys Acta, 1811 (2011) 68-75.

162. M.M. Hussain, W. Jin, X.C. Jiang, Mechanisms involved in cellular ceramide homeostasis, Nutr Metab (Lond), 9 (2012) 71.

163. S. Lightle, R. Tosheva, A. Lee, J. Queen-Baker, B. Boyanovsky, S. Shedlofsky, M. Nikolova-Karakashian, Elevation of ceramide in serum lipoproteins during acute phase response in humans and mice: role of serine-palmitoyl transferase, Arch Biochem Biophys, 419 (2003) 120-128.

164. A.H. Merrill, Jr., S. Lingrell, E. Wang, M. Nikolova-Karakashian, T.R. Vales, D.E. Vance, Sphingolipid biosynthesis de novo by rat hepatocytes in culture. Ceramide

and sphingomyelin are associated with, but not required for, very low density lipoprotein secretion, J Biol Chem, 270 (1995) 13834-13841.

165. C. Christoffersen, H. Obinata, S.B. Kumaraswamy, S. Galvani, J. Ahnstrom, M. Sevvana, C. Egerer-Sieber, Y.A. Muller, T. Hla, L.B. Nielsen, B. Dahlback, Endothelium-protective sphingosine-1-phosphate provided by HDL-associated apolipoprotein M, Proc Natl Acad Sci U S A, 108 (2011) 9613-9618.

166. C. Frej, A. Andersson, B. Larsson, L.J. Guo, E. Norstrom, K.E. Happonen, B. Dahlback, Quantification of sphingosine 1-phosphate by validated LC-MS/MS method revealing strong correlation with apolipoprotein M in plasma but not in serum due to platelet activation during blood coagulation, Anal Bioanal Chem, 407 (2015) 8533-8542.

167. B. Zhang, H. Tomura, A. Kuwabara, T. Kimura, S. Miura, K. Noda, F. Okajima, K. Saku, Correlation of high density lipoprotein (HDL)-associated sphingosine 1-phosphate with serum levels of HDL-cholesterol and apolipoproteins, Atherosclerosis, 178 (2005) 199-205.

168. A. Kontush, P. Therond, A. Zerrad, M. Couturier, A. Negre-Salvayre, J.A. de Souza, S. Chantepie, M.J. Chapman, Preferential sphingosine-1-phosphate enrichment and sphingomyelin depletion are key features of small dense HDL3 particles: relevance to antiapoptotic and antioxidative activities, Arterioscler Thromb Vasc Biol, 27 (2007) 1843-1849.

169. A.N. Fonteh, C. Ormseth, J. Chiang, M. Cipolla, X. Arakaki, M.G. Harrington, Sphingolipid metabolism correlates with cerebrospinal fluid Beta amyloid levels in Alzheimer's disease, PLoS One, 10 (2015) e0125597.

170. S. Koch, N. Donarski, K. Goetze, M. Kreckel, H.J. Stuerenburg, C. Buhmann, U. Beisiegel, Characterization of four lipoprotein classes in human cerebrospinal fluid, J Lipid Res, 42 (2001) 1143-1151.

171. X. Han, The role of apolipoprotein E in lipid metabolism in the central nervous system, Cell Mol Life Sci, 61 (2004) 1896-1906.

172. M. Chiba, K. Tsuchihashi, K. Suetake, Y. Ibayashi, S. Gasa, K. Hashi, Photoaffinity labeling of lipoproteins in human cerebrospinal fluid with a heterobifunctional derivative of galactosylsphingosine, Biochem Mol Biol Int, 32 (1994) 961-971.

173. M.F. Linton, R. Gish, S.T. Hubl, E. Butler, C. Esquivel, W.I. Bry, J.K. Boyles, M.R. Wardell, S.G. Young, Phenotypes of apolipoprotein B and apolipoprotein E after liver transplantation, The Journal of clinical investigation, 88 (1991) 270-281.

174. N.A. Elshourbagy, W.S. Liao, R.W. Mahley, J.M. Taylor, Apolipoprotein E mRNA is abundant in the brain and adrenals, as well as in the liver, and is present in other peripheral tissues of rats and marmosets, Proc Natl Acad Sci U S A, 82 (1985) 203-207.

175. M.G. Sorci-Thomas, J.S. Owen, B. Fulp, S. Bhat, X. Zhu, J.S. Parks, D. Shah, W.G. Jerome, M. Gerelus, M. Zabalawi, M.J. Thomas, Nascent high density lipoproteins formed by ABCA1 resemble lipid rafts and are structurally organized by three apoA-I monomers, J Lipid Res, 53 (2012) 1890-1909.

176. M. Liu, J. Seo, J. Allegood, X. Bi, X. Zhu, E. Boudyguina, A.K. Gebre, D. Avni, D. Shah, M.G. Sorci-Thomas, M.J. Thomas, G.S. Shelness, S. Spiegel, J.S. Parks, Hepatic apolipoprotein M (apoM) overexpression stimulates formation of larger apoM/sphingosine 1-phosphate-enriched plasma high density lipoprotein, J Biol Chem, 289 (2014) 2801-2814.

177. L. Yang, Y. Yatomi, Y. Miura, K. Satoh, Y. Ozaki, Metabolism and functional effects of sphingolipids in blood cells, Br J Haematol, 107 (1999) 282-293.

178. K. Ito, Y. Anada, M. Tani, M. Ikeda, T. Sano, A. Kihara, Y. Igarashi, Lack of sphingosine 1-phosphate-degrading enzymes in erythrocytes, Biochem Biophys Res Commun, 357 (2007) 212-217.

179. P. Hanel, P. Andreani, M.H. Graler, Erythrocytes store and release sphingosine 1-phosphate in blood, FASEB J, 21 (2007) 1202-1209.

180. Y. Yatomi, F. Ruan, S. Hakomori, Y. Igarashi, Sphingosine-1-phosphate: a platelet-activating sphingolipid released from agonist-stimulated human platelets, Blood, 86 (1995) 193-202.

181. K. Venkataraman, Y.M. Lee, J. Michaud, S. Thangada, Y. Ai, H.L. Bonkovsky, N.S. Parikh, C. Habrukowich, T. Hla, Vascular endothelium as a contributor of plasma sphingosine 1-phosphate, Circ Res, 102 (2008) 669-676.

182. B.H. Herzog, J. Fu, S.J. Wilson, P.R. Hess, A. Sen, J.M. McDaniel, Y. Pan, M. Sheng, T. Yago, R. Silasi-Mansat, S. McGee, F. May, B. Nieswandt, A.J. Morris, F. Lupu, S.R. Coughlin, R.P. McEver, H. Chen, M.L. Kahn, L. Xia, Podoplanin maintains high endothelial venule integrity by interacting with platelet CLEC-2, Nature, 502 (2013) 105-109.

183. N. Ancellin, C. Colmont, J. Su, Q. Li, N. Mittereder, S.S. Chae, S. Stefansson, G. Liau, T. Hla, Extracellular export of sphingosine kinase-1 enzyme. Sphingosine 1-phosphate generation and the induction of angiogenic vascular maturation, J Biol Chem, 277 (2002) 6667-6675.

184. K. Venkataraman, S. Thangada, J. Michaud, M.L. Oo, Y. Ai, Y.M. Lee, M. Wu, N.S. Parikh, F. Khan, R.L. Proia, T. Hla, Extracellular export of sphingosine kinase-1a contributes to the vascular S1P gradient, The Biochemical journal, 397 (2006) 461-471.

185. S.M. Hammad, T.A. Taha, A. Nareika, K.R. Johnson, M.F. Lopes-Virella, L.M. Obeid, Oxidized LDL immune complexes induce release of sphingosine kinase in human U937 monocytic cells, Prostaglandins Other Lipid Mediat, 79 (2006) 126-140.

186. P.M. Christensen, M.H. Bosteen, S. Hajny, L.B. Nielsen, C. Christoffersen, Apolipoprotein M mediates sphingosine-1-phosphate efflux from erythrocytes, Scientific reports, 7 (2017) 14983.

187. Y. Hisano, N. Kobayashi, A. Yamaguchi, T. Nishi, Mouse SPNS2 functions as a sphingosine-1-phosphate transporter in vascular endothelial cells, PLoS One, 7 (2012) e38941.

188. X. Liu, K. Ren, R. Suo, S.L. Xiong, Q.H. Zhang, Z.C. Mo, Z.L. Tang, Y. Jiang, X.S. Peng, G.H. Yi, ApoA-I induces S1P release from endothelial cells through ABCA1 and SR-BI in a positive feedback manner, J Physiol Biochem, 72 (2016) 657-667.

189. Y. Yu, S. Guo, Y. Feng, L. Feng, Y. Cui, G. Song, T. Luo, K. Zhang, Y. Wang, X.C. Jiang, S. Qin, Phospholipid transfer protein deficiency decreases the content of S1P in HDL via the loss of its transfer capability, Lipids, 49 (2014) 183-190.

190. T. Zhou, Q. He, Y. Tong, R. Zhan, F. Xu, D. Fan, X. Guo, H. Han, S. Qin, D. Chui, Phospholipid transfer protein (PLTP) deficiency impaired blood-brain barrier integrity by increasing cerebrovascular oxidative stress, Biochem Biophys Res Commun, 445 (2014) 352-356.

191. S.B. Kumaraswamy, A. Linder, P. Akesson, B. Dahlback, Decreased plasma concentrations of apolipoprotein M in sepsis and systemic inflammatory response syndromes, Crit Care, 16 (2012) R60.

192. F. Poti, M. Simoni, J.R. Nofer, Atheroprotective role of high-density lipoprotein (HDL)-associated sphingosine-1-phosphate (S1P), Cardiovasc Res, 103 (2014) 395-404.

193. C. Frej, A. Linder, K.E. Happonen, F.B. Taylor, F. Lupu, B. Dahlback, Sphingosine 1-phosphate and its carrier apolipoprotein M in human sepsis and in Escherichia coli sepsis in baboons, J Cell Mol Med, 20 (2016) 1170-1181.

194. J. Iqbal, M.T. Walsh, S.M. Hammad, M. Cuchel, P. Tarugi, R.A. Hegele, N.O. Davidson, D.J. Rader, R.L. Klein, M.M. Hussain, Microsomal Triglyceride Transfer Protein Transfers and Determines Plasma Concentrations of Ceramide and Sphingomyelin but Not Glycosylceramide, J Biol Chem, 290 (2015) 25863-25875.

195. J. Iqbal, M.T. Walsh, S.M. Hammad, M.M. Hussain, Sphingolipids and Lipoproteins in Health and Metabolic Disorders, Trends Endocrinol Metab, 28 (2017) 506-518.

196. E. Romiti, E. Meacci, C. Donati, L. Formigli, S. Zecchi-Orlandini, M. Farnararo, M. Ito, P. Bruni, Neutral ceramidase secreted by endothelial cells is released in part associated with caveolin-1, Arch Biochem Biophys, 417 (2003) 27-33.

197. S. Marathe, S.L. Schissel, M.J. Yellin, N. Beatini, R. Mintzer, K.J. Williams, I. Tabas, Human vascular endothelial cells are a rich and regulatable source of secretory sphingomyelinase. Implications for early atherogenesis and ceramide-mediated cell signaling, J Biol Chem, 273 (1998) 4081-4088.

198.   D.G. Hemmings, Signal transduction underlying the vascular effects of sphingosine 1-phosphate and sphingosylphosphorylcholine, Naunyn Schmiedebergs Arch Pharmacol, 373 (2006) 18-29.

199.   X. Wang, F. Wang, Vascular protection by high-density lipoprotein-associated sphingosine-1-phosphate, J Geriatr Cardiol, 14 (2017) 696-702.

200.   B.A. Wilkerson, G.D. Grass, S.B. Wing, W.S. Argraves, K.M. Argraves, Sphingosine 1-phosphate (S1P) carrier-dependent regulation of endothelial barrier: high density lipoprotein (HDL)-S1P prolongs endothelial barrier enhancement as compared with albumin-S1P via effects on levels, trafficking, and signaling of S1P1, J Biol Chem, 287 (2012) 44645-44653.

201.   T. Ohmori, Y. Yatomi, M. Osada, F. Kazama, T. Takafuta, H. Ikeda, Y. Ozaki, Sphingosine 1-phosphate induces contraction of coronary artery smooth muscle cells via S1P2, Cardiovasc Res, 58 (2003) 170-177.

202.   S. Salomone, S. Yoshimura, U. Reuter, M. Foley, S.S. Thomas, M.A. Moskowitz, C. Waeber, S1P3 receptors mediate the potent constriction of cerebral arteries by sphingosine-1-phosphate, Eur J Pharmacol, 469 (2003) 125-134.

203.   F. Coussin, R.H. Scott, A. Wise, G.F. Nixon, Comparison of sphingosine 1-phosphate-induced intracellular signaling pathways in vascular smooth muscles: differential role in vasoconstriction, Circ Res, 91 (2002) 151-157.

204.   K.L. Schaphorst, E. Chiang, K.N. Jacobs, A. Zaiman, V. Natarajan, F. Wigley, J.G. Garcia, Role of sphingosine-1 phosphate in the enhancement of endothelial barrier integrity by platelet-released products, Am J Physiol Lung Cell Mol Physiol, 285 (2003) L258-267.

205.   L. Persegol, M. Darabi, C. Dauteuille, M. Lhomme, S. Chantepie, K.A. Rye, P. Therond, M.J. Chapman, R. Salvayre, A. Negre-Salvayre, P. Lesnik, S. Monier, A. Kontush, Small dense HDLs display potent vasorelaxing activity, reflecting their elevated content of sphingosine-1-phosphate, J Lipid Res, 59 (2018) 25-34.

206.   N.J. Abbott, A.A. Patabendige, D.E. Dolman, S.R. Yusof, D.J. Begley, Structure and function of the blood-brain barrier, Neurobiol Dis, 37 (2010) 13-25.

207.   B. Obermeier, R. Daneman, R.M. Ransohoff, Development, maintenance and disruption of the blood-brain barrier, Nat Med, 19 (2013) 1584-1596.

208.   M.J. Menezes, F.K. McClenahan, C.V. Leiton, A. Aranmolate, X. Shan, H. Colognato, The extracellular matrix protein laminin alpha2 regulates the maturation and function of the blood-brain barrier, J Neurosci, 34 (2014) 15260-15280.

209.   A. Carrano, J.J. Hoozemans, S.M. van der Vies, A.J. Rozemuller, J. van Horssen, H.E. de Vries, Amyloid Beta induces oxidative stress-mediated blood-brain barrier changes in capillary amyloid angiopathy, Antioxid Redox Signal, 15 (2011) 1167-1178.

210. *K. Kisler, A.R. Nelson, A. Montagne, B.V. Zlokovic, Cerebral blood flow regulation and neurovascular dysfunction in Alzheimer disease, Nature reviews. Neuroscience, 18 (2017) 419-434.*

211. *A. Hoshi, T. Yamamoto, K. Shimizu, Y. Ugawa, M. Nishizawa, H. Takahashi, A. Kakita, Characteristics of aquaporin expression surrounding senile plaques and cerebral amyloid angiopathy in Alzheimer disease, J Neuropathol Exp Neurol, 71 (2012) 750-759.*

212. *P. Moftakhar, M.D. Lynch, J.L. Pomakian, H.V. Vinters, Aquaporin expression in the brains of patients with or without cerebral amyloid angiopathy, J Neuropathol Exp Neurol, 69 (2010) 1201-1209.*

213. *J.D. Sengillo, E.A. Winkler, C.T. Walker, J.S. Sullivan, M. Johnson, B.V. Zlokovic, Deficiency in mural vascular cells coincides with blood-brain barrier disruption in Alzheimer's disease, Brain Pathol, 23 (2013) 303-310.*

214. *S.J. Heasman, L.M. Carlin, S. Cox, T. Ng, A.J. Ridley, Coordinated RhoA signaling at the leading edge and uropod is required for T cell transendothelial migration, J Cell Biol, 190 (2010) 553-563.*

215. *N.M. de Wit, J. Vanmol, A. Kamermans, J. Hendriks, H.E. de Vries, Inflammation at the blood-brain barrier: The role of liver X receptors, Neurobiol Dis, 107 (2017) 57-65.*

216. *K.A. Becker, B. Fahsel, H. Kemper, J. Mayeres, C. Li, B. Wilker, S. Keitsch, M. Soddemann, C. Sehl, M. Kohnen, M.J. Edwards, H. Grassme, C.C. Caldwell, A. Seitz, M. Fraunholz, E. Gulbins, Staphylococcus aureus Alpha-Toxin Disrupts Endothelial-Cell Tight Junctions via Acid Sphingomyelinase and Ceramide, Infect Immun, 86 (2018).*

217. *M.A. Lopes Pinheiro, J. Kroon, M. Hoogenboezem, D. Geerts, B. van Het Hof, S.M. van der Pol, J.D. van Buul, H.E. de Vries, Acid Sphingomyelinase-Derived Ceramide Regulates ICAM-1 Function during T Cell Transmigration across Brain Endothelial Cells, J Immunol, 196 (2016) 72-79.*

218. *S.S. Chakrabarti, A. Bir, J. Poddar, M. Sinha, A. Ganguly, S. Chakrabarti, Ceramide and Sphingosine-1-Phosphate in Cell Death Pathways : Relevance to the Pathogenesis of Alzheimer's Disease, Curr Alzheimer Res, 13 (2016) 1232-1248.*

219. *G. Di Paolo, T.W. Kim, Linking lipids to Alzheimer's disease: cholesterol and beyond, Nature reviews. Neuroscience, 12 (2011) 284-296.*

220. *R.G. Cutler, J. Kelly, K. Storie, W.A. Pedersen, A. Tammara, K. Hatanpaa, J.C. Troncoso, M.P. Mattson, Involvement of oxidative stress-induced abnormalities in ceramide and cholesterol metabolism in brain aging and Alzheimer's disease, Proc Natl Acad Sci U S A, 101 (2004) 2070-2075.*

221. X. Han, M.H. D, D.W. McKeel, Jr., J. Kelley, J.C. Morris, Substantial sulfatide deficiency and ceramide elevation in very early Alzheimer's disease: potential role in disease pathogenesis, Journal of neurochemistry, 82 (2002) 809-818.

222. X. He, Y. Huang, B. Li, C.X. Gong, E.H. Schuchman, Deregulation of sphingolipid metabolism in Alzheimer's disease, Neurobiology of aging, 31 (2010) 398-408.

223. V. Filippov, M.A. Song, K. Zhang, H.V. Vinters, S. Tung, W.M. Kirsch, J. Yang, P.J. Duerksen-Hughes, Increased ceramide in brains with Alzheimer's and other neurodegenerative diseases, Journal of Alzheimer's disease : JAD, 29 (2012) 537-547.

224. T.A. Couttas, N. Kain, B. Daniels, X.Y. Lim, C. Shepherd, J. Kril, R. Pickford, H. Li, B. Garner, A.S. Don, Loss of the neuroprotective factor Sphingosine 1-phosphate early in Alzheimer's disease pathogenesis, Acta Neuropathol Commun, 2 (2014) 9.

225. P. Katsel, C. Li, V. Haroutunian, Gene expression alterations in the sphingolipid metabolism pathways during progression of dementia and Alzheimer's disease: a shift toward ceramide accumulation at the earliest recognizable stages of Alzheimer's disease?, Neurochem Res, 32 (2007) 845-856.

226. X. Han, S. Rozen, S.H. Boyle, C. Hellegers, H. Cheng, J.R. Burke, K.A. Welsh-Bohmer, P.M. Doraiswamy, R. Kaddurah-Daouk, Metabolomics in early Alzheimer's disease: identification of altered plasma sphingolipidome using shotgun lipidomics, PLoS One, 6 (2011) e21643.

227. M.M. Mielke, V.V. Bandaru, N.J. Haughey, P.V. Rabins, C.G. Lyketsos, M.C. Carlson, Serum sphingomyelins and ceramides are early predictors of memory impairment, Neurobiology of aging, 31 (2010) 17-24.

228. M.M. Mielke, N.J. Haughey, V.V. Bandaru, S. Schech, R. Carrick, M.C. Carlson, S. Mori, M.I. Miller, C. Ceritoglu, T. Brown, M. Albert, C.G. Lyketsos, Plasma ceramides are altered in mild cognitive impairment and predict cognitive decline and hippocampal volume loss, Alzheimers Dement, 6 (2010) 378-385.

229. B. Ellis, A. Hye, S.G. Snowden, Metabolic Modifications in Human Biofluids Suggest the Involvement of Sphingolipid, Antioxidant, and Glutamate Metabolism in Alzheimer's Disease Pathogenesis, Journal of Alzheimer's disease : JAD, 46 (2015) 313-327.

230. R. Savica, M.E. Murray, X.M. Persson, K. Kantarci, J.E. Parisi, D.W. Dickson, R.C. Petersen, T.J. Ferman, B.F. Boeve, M.M. Mielke, Plasma sphingolipid changes with autopsy-confirmed Lewy Body or Alzheimer's pathology, Alzheimers Dement (Amst), 3 (2016) 43-50.

231. M.M. Mielke, N.J. Haughey, V.V. Bandaru, D.D. Weinberg, E. Darby, N. Zaidi, V. Pavlik, R.S. Doody, C.G. Lyketsos, Plasma sphingomyelins are associated with cognitive progression in Alzheimer's disease, Journal of Alzheimer's disease : JAD, 27 (2011) 259-269.

232. M.M. Mielke, V.V. Bandaru, N.J. Haughey, J. Xia, L.P. Fried, S. Yasar, M. Albert, V. Varma, G. Harris, E.B. Schneider, P.V. Rabins, K. Bandeen-Roche, C.G. Lyketsos, M.C. Carlson, Serum ceramides increase the risk of Alzheimer disease: the Women's Health and Aging Study II, Neurology, 79 (2012) 633-641.

233. M.M. Mielke, N.J. Haughey, Could plasma sphingolipids be diagnostic or prognostic biomarkers for Alzheimer's disease?, Clin Lipidol, 7 (2012) 525-536.

234. C. Costantini, R. Weindruch, G. Della Valle, L. Puglielli, A TrkA-to-p75NTR molecular switch activates amyloid beta-peptide generation during aging, The Biochemical journal, 391 (2005) 59-67.

235. G. Chakraborty, S. Ziemba, A. Drivas, R.W. Ledeen, Myelin contains neutral sphingomyelinase activity that is stimulated by tumor necrosis factor-alpha, J Neurosci Res, 50 (1997) 466-476.

236. N. Tsakiri, I. Kimber, N.J. Rothwell, E. Pinteaux, Interleukin-1-induced interleukin-6 synthesis is mediated by the neutral sphingomyelinase/Src kinase pathway in neurones, British journal of pharmacology, 153 (2008) 775-783.

237. M.Y. Kim, C. Linardic, L. Obeid, Y. Hannun, Identification of sphingomyelin turnover as an effector mechanism for the action of tumor necrosis factor alpha and gamma-interferon. Specific role in cell differentiation, J Biol Chem, 266 (1991) 484-489.

238.   J.T. Lee, J. Xu, J.M. Lee, G. Ku, X. Han, D.I. Yang, S. Chen, C.Y. Hsu, Amyloid-beta peptide induces oligodendrocyte death by activating the neutral sphingomyelinase-ceramide pathway, The Journal of cell biology, 164 (2004) 123-131.

239. C. Malaplate-Armand, S. Florent-Bechard, I. Youssef, V. Koziel, I. Sponne, B. Kriem, B. Leininger-Muller, J.L. Olivier, T. Oster, T. Pillot, Soluble oligomers of amyloid-beta peptide induce neuronal apoptosis by activating a cPLA2-dependent sphingomyelinase-ceramide pathway, Neurobiol Dis, 23 (2006) 178-189.

240. N. Fabelo, V. Martin, R. Marin, D. Moreno, I. Ferrer, M. Diaz, Altered lipid composition in cortical lipid rafts occurs at early stages of sporadic Alzheimer's disease and facilitates APP/BACE1 interactions, Neurobiology of aging, 35 (2014) 1801-1812.

241. C. Priller, T. Bauer, G. Mitteregger, B. Krebs, H.A. Kretzschmar, J. Herms, Synapse formation and function is modulated by the amyloid precursor protein, J Neurosci, 26 (2006) 7212-7221.

242. L.J. Siskind, R.N. Kolesnick, M. Colombini, Ceramide channels increase the permeability of the mitochondrial outer membrane to small proteins, J Biol Chem, 277 (2002) 26796-26803.

243. M. Colombini, Ceramide channels and mitochondrial outer membrane permeability, Journal of bioenergetics and biomembranes, 49 (2017) 57-64.

244. A. Kogot-Levin, A. Saada, Ceramide and the mitochondrial respiratory chain, Biochimie, 100 (2014) 88-94.

245. J. Yu, S.A. Novgorodov, D. Chudakova, H. Zhu, A. Bielawska, J. Bielawski, L.M. Obeid, M.S. Kindy, T.I. Gudz, JNK3 signaling pathway activates ceramide synthase leading to mitochondrial dysfunction, J Biol Chem, 282 (2007) 25940-25949.

246. S.A. Novgorodov, J.R. Voltin, M.A. Gooz, L. Li, J.J. Lemasters, T.I. Gudz, Acid sphingomyelinase promotes mitochondrial dysfunction due to glutamate-induced regulated necrosis, Journal of lipid research, 59 (2018) 312-329.

247. B.A. Law, X. Liao, K.S. Moore, A. Southard, P. Roddy, R. Ji, Z. Sculz, A. Bielawska, P.C. Schulze, L.A. Cowart, Lipotoxic very-long-chain ceramides cause mitochondrial dysfunction, oxidative stress, and cell death in cardiomyocytes, FASEB J, (2017).

248. J.N. Kong, Z. Zhu, Y. Itokazu, G. Wang, M.B. Dinkins, L. Zhong, H.P. Lin, A. Elsherbini, S. Leanhart, X. Jiang, H. Qin, W. Zhi, S.D. Spassieva, E. Bieberich, Novel function of ceramide for regulation of mitochondrial ATP release in astrocytes, J Lipid Res, (2018).

249. M.B. Dinkins, J. Enasko, C. Hernandez, G. Wang, J. Kong, I. Helwa, Y. Liu, A.V. Terry, Jr., E. Bieberich, Neutral Sphingomyelinase-2 Deficiency Ameliorates Alzheimer's Disease Pathology and Improves Cognition in the 5XFAD Mouse, J Neurosci, 36 (2016) 8653-8667.

250. M.B. Dinkins, S. Dasgupta, G. Wang, G. Zhu, E. Bieberich, Exosome reduction in vivo is associated with lower amyloid plaque load in the 5XFAD mouse model of Alzheimer's disease, Neurobiology of aging, (2014).

251. B. Wang, S. Han, Exosome-associated tau exacerbates brain functional impairments induced by traumatic brain injury in mice, Molecular and cellular neurosciences, 88 (2018) 158-166.

252. H. Asai, S. Ikezu, S. Tsunoda, M. Medalla, J. Luebke, T. Haydar, B. Wolozin, O. Butovsky, S. Kugler, T. Ikezu, Depletion of microglia and inhibition of exosome synthesis halt tau propagation, Nature neuroscience, 18 (2015) 1584-1593.

253. M. Sardar Sinha, A. Ansell-Schultz, L. Civitelli, C. Hildesjo, M. Larsson, L. Lannfelt, M. Ingelsson, M. Hallbeck, Alzheimer's disease pathology propagation by exosomes containing toxic amyloid-beta oligomers, Acta Neuropathol, 136 (2018) 41-56.

254. B.B. Guo, S.A. Bellingham, A.F. Hill, The neutral sphingomyelinase pathway regulates packaging of the prion protein into exosomes, J Biol Chem, 290 (2015) 3455-3467.

255. K. Yuyama, H. Sun, S. Mitsutake, Y. Igarashi, Sphingolipid-modulated exosome secretion promotes the clearance of amyloid-beta by microglia, J Biol Chem, (2012).

256. C. Reitz, The role of intracellular trafficking and the VPS10d receptors in Alzheimer's disease, Future neurology, 7 (2012) 423–431.

257. R. Epis, E. Marcello, F. Gardoni, M. Di Luca, Alpha, beta-and gamma-secretases in Alzheimer's disease, Frontiers in bioscience (Scholar edition), 4 (2012) 1126–1150.

258. D.J. Selkoe, Alzheimer's disease: genes, proteins, and therapy, Physiological reviews, 81 (2001) 741–766.

259. N.B. Mañucat-Tan, K. Saadipour, Y.-J. Wang, L. Bobrovskaya, X.-F. Zhou, Cellular Trafficking of Amyloid Precursor Protein in Amyloidogenesis Physiological and Pathological Significance, Molecular neurobiology, (2018).

260. B. Dislich, S.F. Lichtenthaler, The Membrane-Bound Aspartyl Protease BACE1: Molecular and Functional Properties in Alzheimer's Disease and Beyond, Frontiers in physiology, 3 (2012) 8.

261. S.F. Lichtenthaler, Alpha-secretase cleavage of the amyloid precursor protein: proteolysis regulated by signaling pathways and protein trafficking, Current Alzheimer research, 9 (2012) 165–177.

262. K. Endres, T. Deller, Regulation of Alpha-Secretase ADAM10 In vitro and In vivo: Genetic, Epigenetic, and Protein-Based Mechanisms, Frontiers in molecular neuroscience, 10 (2017) 56.

263. G. van Echten-Deckert, J. Walter, Sphingolipids: critical players in Alzheimer's disease, Progress in lipid research, 51 (2012) 378–393.

264. M. Malnar, S. Hecimovic, N. Mattsson, H. Zetterberg, Bidirectional links between Alzheimer's disease and Niemann-Pick type C disease, Neurobiol Dis, 72 Pt A (2014) 37–47.

265. A. Kodam, M. Maulik, K. Peake, A. Amritraj, K.S. Vetrivel, G. Thinakaran, J.E. Vance, S. Kar, Altered levels and distribution of amyloid precursor protein and its processing enzymes in Niemann-Pick type C1-deficient mouse brains, Glia, 58 (2010) 1267–1281.

266. I.Y. Tamboli, H. Hampel, N.T. Tien, K. Tolksdorf, B. Breiden, P.M. Mathews, P. Saftig, K. Sandhoff, J. Walter, Sphingolipid storage affects autophagic metabolism of the amyloid precursor protein and promotes Abeta generation, The Journal of neuroscience : the official journal of the Society for Neuroscience, 31 (2011) 1837–1849.

267. E. Barbero-Camps, V. Roca-Agujetas, I. Bartolessis, C. Dios, J.C. Fernández-Checa, M. Marí, A. Morales, T. Hartmann, A. Colell, Cholesterol impairs autophagy-mediated clearance of amyloid beta while promoting its secretion, Autophagy, 14 (2018) 1129–1154.

268. M.O.W. Grimm, T.L. Rothhaar, T. Hartmann, The role of APP proteolytic processing in lipid metabolism, Experimental brain research, 217 (2012) 365–375.

269. A.B. Clement, M. Gamerdinger, I.Y. Tamboli, D. Lütjohann, J. Walter, I. Greeve, G. Gimpl, C. Behl, Adaptation of neuronal cells to chronic oxidative stress is associated

with altered cholesterol and sphingolipid homeostasis and lysosomal function, Journal of neurochemistry, 111 (2009) 669–682.

270. A. Kern, B. Roempp, K. Prager, J. Walter, C. Behl, Down-regulation of endogenous amyloid precursor protein processing due to cellular aging, The Journal of biological chemistry, 281 (2006) 2405–2413.

271. I. Karaca, I.Y. Tamboli, K. Glebov, J. Richter, L.H. Fell, M.O. Grimm, V.J. Haupenthal, T. Hartmann, M.H. Gräler, G. van Echten-Deckert, J. Walter, Deficiency of sphingosine-1-phosphate lyase impairs lysosomal metabolism of the amyloid precursor protein, The Journal of biological chemistry, 289 (2014) 16761–16772.

272. N. Takasugi, T. Sasaki, K. Suzuki, S. Osawa, H. Isshiki, Y. Hori, N. Shimada, T. Higo, S. Yokoshima, T. Fukuyama, V.M.-Y. Lee, J.Q. Trojanowski, T. Tomita, T. Iwatsubo, BACE1 activity is modulated by cell-associated sphingosine-1-phosphate, The Journal of neuroscience : the official journal of the Society for Neuroscience, 31 (2011) 6850–6857.

273. L. Puglielli, B.C. Ellis, A.J. Saunders, D.M. Kovacs, Ceramide stabilizes beta-site amyloid precursor protein-cleaving enzyme 1 and promotes amyloid beta-peptide biogenesis, The Journal of biological chemistry, 278 (2003) 19777–19783.

274. H. Li, W.S. Kim, G.J. Guillemin, A.F. Hill, G. Evin, B. Garner, Modulation of amyloid precursor protein processing by synthetic ceramide analogues, Biochimica et biophysica acta, 1801 (2010) 887–895.

275. I.Y. Tamboli, K. Prager, E. Barth, M. Heneka, K. Sandhoff, J. Walter, Inhibition of glycosphingolipid biosynthesis reduces secretion of the beta-amyloid precursor protein and amyloid beta-peptide, The Journal of biological chemistry, 280 (2005) 28110–28117.

276. [276] N. Sawamura, M. Ko, W. Yu, K. Zou, K. Hanada, T. Suzuki, J.-S. Gong, K. Yanagisawa, M. Michikawa, Modulation of amyloid precursor protein cleavage by cellular sphingolipids, The Journal of biological chemistry, 279 (2004) 11984–11991.

277. M.O.W. Grimm, H.S. Grimm, A.J. Pätzold, E.G. Zinser, R. Halonen, M. Duering, J.A. Tschäpe, B. Strooper, U. Müller, J. Shen, T. Hartmann, Regulation of cholesterol and sphingomyelin metabolism by amyloid-beta and presenilin, Nature cell biology, 7 (2005) 1118–1123.

278. A. Jana, K. Pahan, Fibrillar amyloid-beta peptides kill human primary neurons via NADPH oxidase-mediated activation of neutral sphingomyelinase. Implications for Alzheimer's disease, The Journal of biological chemistry, 279 (2004) 51451–51459.

279. M.O.W. Grimm, E.G. Zinser, S. Grösgen, B. Hundsdörfer, T.L. Rothhaar, V.K. Burg, L. Kaestner, T.A. Bayer, P. Lipp, U. Müller, H.S. Grimm, T. Hartmann, Amyloid precursor protein (APP) mediated regulation of ganglioside homeostasis linking Alzheimer's disease pathology with ganglioside metabolism, PloS one, 7 (2012) e34095.

280. *K. Matsuzaki, K. Kato, K. Yanagisawa, Ganglioside-Mediated Assembly of Amyloid β-Protein: Roles in Alzheimer's Disease, Progress in molecular biology and translational science, 156 (2018) 413–434.*

281. *L.P. Choo-Smith, W. Garzon-Rodriguez, C.G. Glabe, W.K. Surewicz, Acceleration of amyloid fibril formation by specific binding of Abeta-(1-40) peptide to ganglioside-containing membrane vesicles, J Biol Chem, 272 (1997) 22987-22990.*

282. *Y. Okada, K. Okubo, K. Ikeda, Y. Yano, M. Hoshino, Y. Hayashi, Y. Kiso, H. Itoh-Watanabe, A. Naito, K. Matsuzaki, Toxic Amyloid Tape: A Novel Mixed Antiparallel/Parallel beta-Sheet Structure Formed by Amyloid beta-Protein on GM1 Clusters, ACS Chem Neurosci, 10 (2019) 563-572.*

283. *E.J. Fernandez-Perez, F.J. Sepulveda, R. Peoples, L.G. Aguayo, Role of membrane GM1 on early neuronal membrane actions of Abeta during onset of Alzheimer's disease, Biochim Biophys Acta Mol Basis Dis, 1863 (2017) 3105-3116.*

284. *S. Keilani, Y. Lun, A.C. Stevens, H.N. Williams, E.R. Sjoberg, R. Khanna, K.J. Valenzano, F. Checler, J.D. Buxbaum, K. Yanagisawa, D.J. Lockhart, B.A. Wustman, S. Gandy, Lysosomal dysfunction in a mouse model of Sandhoff disease leads to accumulation of ganglioside-bound amyloid-beta peptide, J Neurosci, 32 (2012) 5223-5236.*

285. *K. Yanagisawa, A. Odaka, N. Suzuki, Y. Ihara, GM1 ganglioside-bound amyloid beta-protein (A beta): a possible form of preamyloid in Alzheimer's disease, Nat Med, 1 (1995) 1062-1066.*

286. *I.Y. Tamboli, K. Prager, D.R. Thal, K.M. Thelen, I. Dewachter, C.U. Pietrzik, P. St George-Hyslop, S.S. Sisodia, B. Strooper, M.T. Heneka, M.A. Filippov, U. Müller, F. van Leuven, D. Lütjohann, J. Walter, Loss of gamma-secretase function impairs endocytosis of lipoprotein particles and membrane cholesterol homeostasis, The Journal of neuroscience : the official journal of the Society for Neuroscience, 28 (2008) 12097–12106.*

287. *Q. Liu, C.V. Zerbinatti, J. Zhang, H.-S. Hoe, B. Wang, S.L. Cole, J. Herz, L. Muglia, G. Bu, Amyloid precursor protein regulates brain apolipoprotein E and cholesterol metabolism through lipoprotein receptor LRP1, Neuron, 56 (2007) 66–78.*

288. *H. Xie, G.V. Johnson, Ceramide selectively decreases tau levels in differentiated PC12 cells through modulation of calpain I, Journal of neurochemistry, 69 (1997) 1020-1030.*

289. *F. St-Cyr Giguere, S. Attiori Essis, L. Chagniel, M. Germain, M. Cyr, G. Massicotte, The sphingosine-1-phosphate receptor 1 agonist SEW2871 reduces Tau-Ser262 phosphorylation in rat hippocampal slices, Brain research, 1658 (2017) 51-59.*

290. *L.J. Wang, R. Colella, G. Yorke, F.J. Roisen, The ganglioside GM1 enhances microtubule networks and changes the morphology of Neuro-2a cells in vitro by altering the distribution of MAP2, Exp Neurol, 139 (1996) 1-11.*

291. [291] G.P. Gellermann, T.R. Appel, P. Davies, S. Diekmann, Paired helical filaments contain small amounts of cholesterol, phosphatidylcholine and sphingolipids, Biol Chem, 387 (2006) 1267-1274.

292. I. Kaya, D. Brinet, W. Michno, S. Syvänen, D. Sehlin, H. Zetterberg, K. Blennow, J. Hanrieder, Delineating Amyloid Plaque Associated Neuronal Sphingolipids in Transgenic Alzheimer's Disease Mice (tgArcSwe) Using MALDI Imaging Mass Spectrometry, ACS chemical neuroscience, 8 (2017) 347–355.

293. L. Barrier, S. Ingrand, M. Damjanac, A. Rioux Bilan, J. Hugon, G. Page, Genotype-related changes of ganglioside composition in brain regions of transgenic mouse models of Alzheimer's disease, Neurobiology of aging, 28 (2007) 1863-1872.

294. L. Barrier, B. Fauconneau, A. Noel, S. Ingrand, Ceramide and Related-Sphingolipid Levels Are Not Altered in Disease-Associated Brain Regions of APP and APP/PS1 Mouse Models of Alzheimer's Disease: Relationship with the Lack of Neurodegeneration?, Int J Alzheimers Dis, 2011 (2010) 920958.

295. R.B. Chan, T.G. Oliveira, E.P. Cortes, L.S. Honig, K.E. Duff, S.A. Small, M.R. Wenk, G. Shui, G. Di Paolo, Comparative lipidomic analysis of mouse and human brain with Alzheimer disease, J Biol Chem, 287 (2012) 2678-2688.

296. S. Caughlin, S. Maheshwari, Y. Agca, C. Agca, A.J. Harris, K. Jurcic, K.K. Yeung, D.F. Cechetto, S.N. Whitehead, Membrane-lipid homeostasis in a prodromal rat model of Alzheimer's disease: Characteristic profiles in ganglioside distributions during aging detected using MALDI imaging mass spectrometry, Biochim Biophys Acta Gen Subj, 1862 (2018) 1327-1338.

297. A.H. Merrill, Jr., De novo sphingolipid biosynthesis: a necessary, but dangerous, pathway, J Biol Chem, 277 (2002) 25843-25846.

298. M.J. Genin, I.C. Gonzalez Valcarcel, W.G. Holloway, J. Lamar, M. Mosior, E. Hawkins, T. Estridge, J. Weidner, T. Seng, D. Yurek, L.A. Adams, J. Weller, V.L. Reynolds, J.T. Brozinick, Imidazopyridine and Pyrazolopiperidine Derivatives as Novel Inhibitors of Serine Palmitoyl Transferase, J Med Chem, 59 (2016) 5904-5910.

299. A. Caretti, R. Torelli, F. Perdoni, M. Falleni, D. Tosi, A. Zulueta, J. Casas, M. Sanguinetti, R. Ghidoni, E. Borghi, P. Signorelli, Inhibition of ceramide de novo synthesis by myriocin produces the double effect of reducing pathological inflammation and exerting antifungal activity against A. fumigatus airways infection, Biochim Biophys Acta, 1860 (2016) 1089-1097.

300. A. Caretti, A. Bragonzi, M. Facchini, I. De Fino, C. Riva, P. Gasco, C. Musicanti, J. Casas, G. Fabrias, R. Ghidoni, P. Signorelli, Anti-inflammatory action of lipid nanocarrier-delivered myriocin: therapeutic potential in cystic fibrosis, Biochim Biophys Acta, 1840 (2014) 586-594.

301. Y. Miyake, Y. Kozutsumi, S. Nakamura, T. Fujita, T. Kawasaki, Serine palmitoyltransferase is the primary target of a sphingosine-like

immunosuppressant, ISP-1/myriocin, Biochem Biophys Res Commun, 211 (1995) 396-403.

302. K.S. Sundaram, M. Lev, L-cycloserine inhibition of sphingolipid synthesis in the anaerobic bacterium Bacteroides levii, Biochem Biophys Res Commun, 119 (1984) 814-819.

303. K. Hanada, T. Hara, M. Nishijima, Purification of the serine palmitoyltransferase complex responsible for sphingoid base synthesis by using affinity peptide chromatography techniques, J Biol Chem, 275 (2000) 8409-8415.

304. V.K. Bhat, E. Bernhart, I. Plastira, K. Fan, N.G. Tabrizi-Wizsy, C. Wadsack, G. Rechberger, T. Eichmann, M. Asslaber, I. Spassova, M.E. Verhaegen, E. Malle, J.C. Becker, W. Sattler, Pharmacological inhibition of serine palmitoyl transferase and sphingosine kinase-1/-2 inhibits Merkel Cell Carcinoma cell proliferation, J Invest Dermatol, (2018).

305. K.S. Sundaram, M. Lev, The long-term administration of L-cycloserine to mice: specific reduction of cerebroside level, Neurochem Res, 14 (1989) 245-248.

306. W.F. Marasas, Discovery and occurrence of the fumonisins: a historical perspective, Environ Health Perspect, 109 Suppl 2 (2001) 239-243.

307. P. Ebel, K. Vom Dorp, E. Petrasch-Parwez, A. Zlomuzica, K. Kinugawa, J. Mariani, D. Minich, C. Ginkel, J. Welcker, J. Degen, M. Eckhardt, E. Dere, P. Dormann, K. Willecke, Inactivation of ceramide synthase 6 in mice results in an altered sphingolipid metabolism and behavioral abnormalities, J Biol Chem, 288 (2013) 21433-21447.

308. S. Yasuda, H. Kitagawa, M. Ueno, H. Ishitani, M. Fukasawa, M. Nishijima, S. Kobayashi, K. Hanada, A novel inhibitor of ceramide trafficking from the endoplasmic reticulum to the site of sphingomyelin synthesis, J Biol Chem, 276 (2001) 43994-44002.

309. N. Nakao, M. Ueno, S. Sakai, D. Egawa, H. Hanzawa, S. Kawasaki, K. Kumagai, M. Suzuki, S. Kobayashi, K. Hanada, Natural ligand-nonmimetic inhibitors of the lipid-transfer protein CERT, Communications Chemistry, 2 (2019) 20.

310. S.M. Crivelli, A. Paulus, J. Markus, M. Bauwens, D. Berkes, H.E. De Vries, M.T. Mulder, J. Walter, F.M. Mottaghy, M. Losen, P. Martinez-Martinez, Synthesis, Radiosynthesis, and Preliminary in vitro and in vivo Evaluation of the Fluorinated Ceramide Trafficking Inhibitor (HPA-12) for Brain Applications, Journal of Alzheimer's disease : JAD, 60 (2017) 783-794.

311. M. Matarin, D.A. Salih, M. Yasvoina, D.M. Cummings, S. Guelfi, W. Liu, M.A. Nahaboo Solim, T.G. Moens, R.M. Paublete, S.S. Ali, M. Perona, R. Desai, K.J. Smith, J. Latcham, M. Fulleylove, J.C. Richardson, J. Hardy, F.A. Edwards, A genome-wide gene-expression analysis and database in transgenic mice during development of amyloid or tau pathology, Cell Rep, 10 (2015) 633-644.

312. C. Mencarelli, M. Losen, C. Hammels, J. De Vry, M.K. Hesselink, H.W. Steinbusch, M.H. De Baets, P. Martinez-Martinez, The ceramide transporter and the Goodpasture antigen binding protein: one protein--one function?, Journal of neurochemistry, 113 (2010) 1369-1386.

313. F. Revert, I. Ventura, P. Martinez-Martinez, F. Granero-Molto, F. Revert-Ros, J. Macias, J. Saus, Goodpasture antigen-binding protein is a soluble exportable protein that interacts with type IV collagen. Identification of novel membrane-bound isoforms, J Biol Chem, 283 (2008) 30246-30255.

314. C. Mencarelli, G.H. Bode, M. Losen, M. Kulharia, P.C. Molenaar, R. Veerhuis, H.W. Steinbusch, M.H. De Baets, G.A. Nicolaes, P. Martinez-Martinez, Goodpasture antigen-binding protein/ceramide transporter binds to human serum amyloid P-component and is present in brain amyloid plaques, J Biol Chem, 287 (2012) 14897-14911.

315. G.H. Bode, M. Losen, W.A. Buurman, R. Veerhuis, P.C. Molenaar, H.W. Steinbusch, M.H. De Baets, M.R. Daha, P. Martinez-Martinez, Complement activation by ceramide transporter proteins, J Immunol, 192 (2014) 1154-1161.

316. M.O. Grimm, B. Hundsdorfer, S. Grosgen, J. Mett, V.C. Zimmer, C.P. Stahlmann, V.J. Haupenthal, T.L. Rothhaar, J. Lehmann, A. Patzold, E.G. Zinser, H. Tanila, J. Shen, U. Muller, H.S. Grimm, T. Hartmann, PS dependent APP cleavage regulates glucosylceramide synthase and is affected in Alzheimer's disease, Cell Physiol Biochem, 34 (2014) 92-110.

317. F. Manganelli, R. Dubbioso, R. Iodice, A. Topa, A. Dardis, C.V. Russo, L. Ruggiero, S. Tozza, A. Filla, L. Santoro, Central cholinergic dysfunction in the adult form of Niemann Pick disease type C: a further link with Alzheimer's disease?, J Neurol, 261 (2014) 804-808.

318. T. Yamazaki, T.Y. Chang, C. Haass, Y. Ihara, Accumulation and aggregation of amyloid beta-protein in late endosomes of Niemann-pick type C cells, The Journal of biological chemistry, 276 (2001) 4454-4460.

319. K. Suzuki, C.C. Parker, P.G. Pentchev, D. Katz, B. Ghetti, A.N. D'Agostino, E.D. Carstea, Neurofibrillary tangles in Niemann-Pick disease type C, Acta Neuropathol, 89 (1995) 227-238.

320. D. Bergeron, S. Poulin, R. Laforce, Jr., Cognition and anatomy of adult Niemann-Pick disease type C: Insights for the Alzheimer field, Cogn Neuropsychol, 35 (2018) 209-222.

321. A. Benussi, M.S. Cotelli, A. Padovani, B. Borroni, Recent neuroimaging, neurophysiological, and neuropathological advances for the understanding of NPC, F1000Res, 7 (2018) 194.

322. M.-H. Lu, W.-L. Ji, D.-E. Xu, P.-P. Yao, X.-Y. Zhao, Z.-T. Wang, L.-P. Fang, R. Huang, L.-J. Lan, J.-B. Chen, T.-H. Wang, L.-H. Cheng, R.-X. Xu, C.-F. Liu, L. Puglielli, Q.-H. Ma, Inhibition of sphingomyelin synthase 1 ameliorates alzheimer-like pathology

in APP/PS1 transgenic mice through promoting lysosomal degradation of BACE1, Experimental neurology, 311 (2018) 67–79.

323. *B. Brenner, K. Ferlinz, H. Grassmé, M. Weller, U. Koppenhoefer, J. Dichgans, K. Sandhoff, F. Lang, E. Gulbins, Fas/CD95/Apo-I activates the acidic sphingomyelinase via Caspases, Cell Death And Differentiation, 5 (1998) 29.*

324. *T. Goldkorn, N. Balaban, M. Shannon, V. Chea, K. Matsukuma, D. Gilchrist, H. Wang, C. Chan, H2O2 acts on cellular membranes to generate ceramide signaling and initiate apoptosis in tracheobronchial epithelial cells, Journal of cell science, 111 (Pt 21) (1998) 3209-3220.*

325. *D. Milhas, C.J. Clarke, Y.A. Hannun, Sphingomyelin metabolism at the plasma membrane: Implications for bioactive sphingolipids, FEBS Letters, 584 (2010) 1887-1894.*

326. *C. Luberto, D.F. Hassler, P. Signorelli, Y. Okamoto, H. Sawai, E. Boros, D.J. Hazen-Martin, L.M. Obeid, Y.A. Hannun, G.K. Smith, Inhibition of tumor necrosis factor-induced cell death in MCF7 by a novel inhibitor of neutral sphingomyelinase, J Biol Chem, 277 (2002) 41128-41139.*

327. *M. Adada, C. Luberto, D. Canals, Inhibitors of the sphingomyelin cycle: Sphingomyelin synthases and sphingomyelinases, Chemistry and physics of lipids, 197 (2016) 45-59.*

328. *M.B. Dinkins, S. Dasgupta, G. Wang, G. Zhu, E. Bieberich, Exosome reduction in vivo is associated with lower amyloid plaque load in the 5XFAD mouse model of Alzheimer's disease, Neurobiology of aging, 35 (2014) 1792-1800.*

329. *L.O. Randall, T.H. Smith, The adrenergic blocking action of some dibenzazepine derivatives, J Pharmacol Exp Ther, 103 (1951) 10-23.*

330. *L. Gyermek, The pharmacology of imipramine and related antidepressants, Int Rev Neurobiol, 9 (1966) 95-143.*

331. *J. Kornhuber, P. Tripal, M. Reichel, C. Muhle, C. Rhein, M. Muehlbacher, T.W. Groemer, E. Gulbins, Functional Inhibitors of Acid Sphingomyelinase (FIASMAs): a novel pharmacological group of drugs with broad clinical applications, Cell Physiol Biochem, 26 (2010) 9-20.*

332. *S. Albouz, J.J. Hauw, Y. Berwald-Netter, J.M. Boutry, R. Bourdon, N. Baumann, Tricyclic antidepressants induce sphingomyelinase deficiency in fibroblast and neuroblastoma cell cultures, Biomedicine, 35 (1981) 218-220.*

333. *Y. Yoshida, K. Arimoto, M. Sato, N. Sakuragawa, M. Arima, E. Satoyoshi, Reduction of acid sphingomyelinase activity in human fibroblasts induced by AY-9944 and other cationic amphiphilic drugs, J Biochem, 98 (1985) 1669-1679.*

334. M. Kolzer, N. Werth, K. Sandhoff, Interactions of acid sphingomyelinase and lipid bilayers in the presence of the tricyclic antidepressant desipramine, FEBS Lett, 559 (2004) 96-98.

335. R. Hurwitz, K. Ferlinz, K. Sandhoff, The tricyclic antidepressant desipramine causes proteolytic degradation of lysosomal sphingomyelinase in human fibroblasts, Biol Chem Hoppe Seyler, 375 (1994) 447-450.

336. J. Kornhuber, P. Tripal, M. Reichel, L. Terfloth, S. Bleich, J. Wiltfang, E. Gulbins, Identification of new functional inhibitors of acid sphingomyelinase using a structure-property-activity relation model, J Med Chem, 51 (2008) 219-237.

337. A.K. Berger, L. Fratiglioni, B. Winblad, L. Backman, Alzheimer's disease and depression: preclinical comorbidity effects on cognitive functioning, Cortex, 41 (2005) 603-612.

338. N. Mokhber, E. Abdollahian, A. Soltanifar, R. Samadi, A. Saghebi, M.B. Haghighi, A. Azarpazhooh, Comparison of sertraline, venlafaxine and desipramine effects on depression, cognition and the daily living activities in Alzheimer patients, Pharmacopsychiatry, 47 (2014) 131-140.

339. D.D. Wang, J. Li, L.P. Yu, M.N. Wu, L.N. Sun, J.S. Qi, Desipramine improves depression-like behavior and working memory by up-regulating p-CREB in Alzheimer's disease associated mice, J Integr Neurosci, 15 (2016) 247-260.

340. J.R. Cirrito, B.M. Disabato, J.L. Restivo, D.K. Verges, W.D. Goebel, A. Sathyan, D. Hayreh, G. D'Angelo, T. Benzinger, H. Yoon, J. Kim, J.C. Morris, M.A. Mintun, Y.I. Sheline, Serotonin signaling is associated with lower amyloid-beta levels and plaques in transgenic mice and humans, Proc Natl Acad Sci U S A, 108 (2011) 14968-14973.

341. R.L. Nelson, Z. Guo, V.M. Halagappa, M. Pearson, A.J. Gray, Y. Matsuoka, M. Brown, B. Martin, T. Iyun, S. Maudsley, R.F. Clark, M.P. Mattson, Prophylactic treatment with paroxetine ameliorates behavioral deficits and retards the development of amyloid and tau pathologies in 3xTgAD mice, Exp Neurol, 205 (2007) 166-176.

342. P.J. Modrego, Depression in Alzheimer's disease. Pathophysiology, diagnosis, and treatment, Journal of Alzheimer's disease : JAD, 21 (2010) 1077-1087.

343. C.U. von Linstow, J. Waider, M. Grebing, A. Metaxas, K.P. Lesch, B. Finsen, Serotonin augmentation therapy by escitalopram has minimal effects on amyloid-beta levels in early-stage Alzheimer's-like disease in mice, Alzheimers Res Ther, 9 (2017) 74.

344. V. Brinkmann, A. Billich, T. Baumruker, P. Heining, R. Schmouder, G. Francis, S. Aradhye, P. Burtin, Fingolimod (FTY720): discovery and development of an oral drug to treat multiple sclerosis, Nat Rev Drug Discov, 9 (2010) 883-897.

345. T. Baumruker, A. Billich, V. Brinkmann, FTY720, an immunomodulatory sphingolipid mimetic: translation of a novel mechanism into clinical benefit in multiple sclerosis, Expert Opin Investig Drugs, 16 (2007) 283-289.

346. G. Dawson, J. Qin, Gilenya (FTY720) inhibits acid sphingomyelinase by a mechanism similar to tricyclic antidepressants, Biochem Biophys Res Commun, 404 (2011) 321-323.

347. E.V. Berdyshev, I. Gorshkova, A. Skobeleva, R. Bittman, X. Lu, S.M. Dudek, T. Mirzapoiazova, J.G. Garcia, V. Natarajan, FTY720 inhibits ceramide synthases and up-regulates dihydrosphingosine 1-phosphate formation in human lung endothelial cells, J Biol Chem, 284 (2009) 5467-5477.

348. N. Takasugi, T. Sasaki, I. Ebinuma, S. Osawa, H. Isshiki, K. Takeo, T. Tomita, T. Iwatsubo, FTY720/fingolimod, a sphingosine analogue, reduces amyloid-β production in neurons, PloS one, 8 (2013) e64050.

349. F. Hemmati, L. Dargahi, S. Nasoohi, R. Omidbakhsh, Z. Mohamed, Z. Chik, M. Naidu, A. Ahmadiani, Neurorestorative effect of FTY720 in a rat model of Alzheimer's disease: comparison with memantine, Behav Brain Res, 252 (2013) 415-421.

350. K. Fukumoto, H. Mizoguchi, H. Takeuchi, H. Horiuchi, J. Kawanokuchi, S. Jin, T. Mizuno, A. Suzumura, Fingolimod increases brain-derived neurotrophic factor levels and ameliorates amyloid beta-induced memory impairment, Behav Brain Res, 268 (2014) 88-93.

351. H. Jesko, P.L. Wencel, W.J. Lukiw, R.P. Strosznajder, Modulatory Effects of Fingolimod (FTY720) on the Expression of Sphingolipid Metabolism-Related Genes in an Animal Model of Alzheimer's Disease, Mol Neurobiol, 56 (2019) 174-185.

352. M. Asle-Rousta, Z. Kolahdooz, L. Dargahi, A. Ahmadiani, S. Nasoohi, Prominence of central sphingosine-1-phosphate receptor-1 in attenuating abeta-induced injury by fingolimod, J Mol Neurosci, 54 (2014) 698-703.

353. M. Asle-Rousta, S. Oryan, A. Ahmadiani, M. Rahnema, Activation of sphingosine 1-phosphate receptor-1 by SEW2871 improves cognitive function in Alzheimer's disease model rats, EXCLI J, 12 (2013) 449-461.

354. N. Aytan, J.K. Choi, I. Carreras, V. Brinkmann, N.W. Kowall, B.G. Jenkins, A. Dedeoglu, Fingolimod modulates multiple neuroinflammatory markers in a mouse model of Alzheimer's disease, Scientific reports, 6 (2016) 24939.

355. S.F. Spampinato, B. Obermeier, A. Cotleur, A. Love, Y. Takeshita, Y. Sano, T. Kanda, R.M. Ransohoff, Sphingosine 1 Phosphate at the Blood Brain Barrier: Can the Modulation of S1P Receptor 1 Influence the Response of Endothelial Cells and Astrocytes to Inflammatory Stimuli?, PLoS One, 10 (2015) e0133392.

356. N.M. de Wit, H. Snkhchyan, S. den Hoedt, D. Wattimena, R. de Vos, M.T. Mulder, J. Walter, P. Martinez-Martinez, J.J. Hoozemans, A.J. Rozemuller, H.E. de Vries,

Altered Sphingolipid Balance in Capillary Cerebral Amyloid Angiopathy, Journal of Alzheimer's disease : JAD, 60 (2017) 795-807.

357. *E. Tada, K. Toyomura, H. Nakamura, H. Sasaki, T. Saito, M. Kaneko, Y. Okuma, T. Murayama, Activation of ceramidase and ceramide kinase by vanadate via a tyrosine kinase-mediated pathway, J Pharmacol Sci, 114 (2010) 420-432.*

358. *D. Ofengeim, S. Mazzitelli, Y. Ito, J.P. DeWitt, L. Mifflin, C. Zou, S. Das, X. Adiconis, H. Chen, H. Zhu, M.A. Kelliher, J.Z. Levin, J. Yuan, RIPK1 mediates a disease-associated microglial response in Alzheimer's disease, Proceedings of the National Academy of Sciences of the United States of America, 114 (2017) E8788-E8797.*

359. *A. Caccamo, C. Branca, I.S. Piras, E. Ferreira, M.J. Huentelman, W.S. Liang, B. Readhead, J.T. Dudley, E.E. Spangenberg, K.N. Green, R. Belfiore, W. Winslow, S. Oddo, Necroptosis activation in Alzheimer's disease, Nature neuroscience, 20 (2017) 1236-1246.*

360. *R.L. Lieberman, B.A. Wustman, P. Huertas, A.C. Powe, Jr., C.W. Pine, R. Khanna, M.G. Schlossmacher, D. Ringe, G.A. Petsko, Structure of acid beta-glucosidase with pharmacological chaperone provides insight into Gaucher disease, Nature chemical biology, 3 (2007) 101-107.*

361. *N.M. de Wit, H. Snkhchyan, S. den Hoedt, D. Wattimena, R. de Vos, M.T. Mulder, J. Walter, P. Martinez-Martinez, J.J. Hoozemans, A.J. Rozemuller, H.E. de Vries, Altered Sphingolipid Balance in Capillary Cerebral Amyloid Angiopathy, Journal of Alzheimer's disease : JAD, (2016).*

Chapter 7

Altered sphingolipid function in Alzheimer's disease, a gene regulatory network approach

Caterina Giovagnoni[A]*, Muhammad Ali[A,B]*, Lars M.T. Eijssen[A,C], Richard Maes[A,C], Kyonghwan Choe[A], Monique Mulder[D], Jos Kleinjans[E], Antonio del Sol[B,F,G], Enrico Glaab[B], Diego Mastroeni[H], Elaine Delvaux[H], Paul Coleman[H], Mario Losen[A], Ehsan Pishva[A,I], Pilar Martinez Martinez[A]*, Daniel L.A. van den Hove[A,J]*

[A]School for Mental Health and Neuroscience (MHeNS), Department of Psychiatry and Neuropsychology, Maastricht University, Maastricht, the Netherlands.
[B]Computational Biology Group, Luxembourg Centre for System Biomedicine (LCSB), University of Luxembourg, Belvaux, Luxembourg.
[C]Department of Bioinformatics - BiGCaT, NUTRIM, Maastricht University, Maastricht, the Netherlands.
[D]Department of Internal Medicine, Division of Pharmacology, Vascular and Metabolic Diseases, Erasmus MC University Medical Center, Rotterdam, the Netherlands.
[E]Department of Toxicogenomics, GROW School for Oncology and Developmental Biology, Maastricht University, Maastricht, Tthe Netherlands.
[F]IKERBASQUE, Basque Foundation for Science, Bilbao, Spain.
[G]CIC bioGUNE, Bizkaia Technology Park, 801 Building, 48160 Derio, Spain
[H]Biodesign Institute, Neurodegenerative Disease Research Center, Arizona State University, Tempe, AZ, USA.
[I]University of Exeter Medical School, University of Exeter, Exeter, UK.
[J]Department of Psychiatry, Psychosomatics and Psychotherapy, University of Wuerzburg, Wuerzburg, Germany
*equal contribution

Abstract

Sphingolipids (SLs) are bioactive lipids involved in various important physiological functions. The SL pathway has been shown to be affected in several brain-related disorders, including Alzheimer's disease (AD). Recent evidence suggests that epigenetic dysregulation plays an important role in the pathogenesis of AD as well. Here, we use an integrative approach to better understand the relationship between epigenetic and transcriptomic processes in regulating SL function in the middle temporal gyrus of AD patients. Transcriptomic analysis of 252 SL-related genes, selected based on GO term annotations, from 46 AD patients and 32 healthy age-matched controls, revealed 103 differentially expressed SL-related genes in AD patients. Additionally, methylomic analysis of the same subjects revealed parallel hydroxymethylation changes in PTGIS, GBA, and ITGB2 in AD.

Subsequent gene regulatory network-based analysis identified three candidate genes, i.e. SELPLG, SPHK1 and CAV1 whose alteration holds the potential to revert the gene expression program from a diseased towards a healthy state. Together, this epigenomic and transcriptomic approach highlights the importance of SL-related genes in AD, and may provide novel biomarkers and therapeutic alternatives to traditionally investigated biological pathways in AD.

Keywords: Sphingolipids, Alzheimer's disease, epigenetics, Gene regulatory network, disease network analysis.

7.1   Introduction

Alzheimer's disease (AD) is the most common age-related neurodegenerative disorder, representing one of the main causes of dementia [36]. The incidence and prevalence of AD has increased in the last 10 years representing a major challenge for the public health system and society. Currently, no therapy that can effectively halt or attenuate the disease process exists.

AD is histologically characterized by the progressive over-production and accumulation of amyloid β (Aβ) peptide and hyperphosphorylated tau protein that lead to the formation of extracellular senile plaques and intracellular neurofibrillary tangles, respectively [37]. These pathological changes are associated with neurotoxicity and inflammation as well as neuronal degeneration, with large downstream effects on the physiology of the central nervous system (CNS). The complex pathogenesis of AD is still not fully understood, but there is a growing body of evidence suggesting that genetic and environmental factors are involved in the development and progression of the disease and associated cognitive impairment.

A balanced lipid metabolism is essential for normal brain function, while dysfunction may contribute to neurodegeneration. While the link between aberrant lipid metabolism and AD was disclosed already in 1906 by Alois Alzheimer, its role in the pathophysiology of neurodegeneration gained more interest in 1993 when a higher risk for developing AD was found among those carrying the cholesterol transporter APOE type 4 allele [38]. Later, alterations in the balance of certain membrane/structural lipids such as sphingolipids (SLs) and ceramides were demonstrated to play a crucial role in AD. For instance, high serum ceramide levels in cognitively normal elderly individuals have been associated with an increased risk of developing cognitive impairment and subsequent AD. [39]. SLs are ubiquitous structural lipids in cellular membranes and also potent regulators of critical biological processes. In the brain, SLs are abundantly present in different cell types, including neurons and glia. To guarantee optimal neuronal function, the balance of SLs and associated metabolites is tightly regulated. Alterations of this balance may contribute to the development of disease [40] [41].

Interestingly, different metabolic and lipidomic analyses have shown a positive association between SL metabolites and Aβ and tau in cerebrospinal fluid samples of healthy individuals with a familial history of AD [42]. These analyses have strengthened the notion that defects in SL metabolism correlate with Aβ and tau levels. Additionally, there is a large body of evidence that gangliosides, a

class of glycosylated SLs, contribute directly and indirectly to the initiation and progression of AD by facilitating plaque formation [40].

Despite the fact that several studies are clearly showing an effective association between dysfunction of SL metabolism and AD, the specific molecular pathways driving these alterations still remain unclear. To this aim, a better understanding of the relationship between epigenetic and transcriptomic processes in regulating SL function is of utmost importance for elucidating the underlying role of SLs in the pathophysiology of AD and the potential development of novel SL-targeted AD therapeutics.

In the present study, we examined SL-related genes from an epigenetic-transcriptional point of view, to further understand the involvement of downstream SL (dys)function in AD. Accordingly, the main aim was to identify if, and if so, to which extent SL genes are dysregulated at the methylomic and transcriptomic levels in brain tissue from AD patients. For this purpose, we first identified a set of 252 SL-associated genes based on manually selected Gene Ontology (GO) terms. The samples investigated in the current study represent a subset of data reported in Lardenoije et al. (2019), which passed our quality checking control, taking into account both the data on gene expression and DNA (hydroxy)methylation. Transcriptomic analyses showed a profound enrichment of SL-related differentially expressed genes in AD brains. Among those, the conducted epigenetic data analysis revealed PTGIS, GBA, and ITGB2 to be differentially hydroxymethylated, reflecting a significant overrepresentation (Fisher's exact test, P-value < 1.09e-06). Furthermore, to evaluate how SLs influence the disease, we performed a Gene Regulatory Network (GRN) analysis. The reconstructed phenotype-specific networks were employed for in-silico perturbation analysis and identified SELPLG, SPHK1 and CAV1 to be the most influential gene combination in the AD network. Taken together, these findings confirmed the initial hypothesis that SL metabolism is significantly altered in AD. Furthermore, the identification of dysregulated SL-related genes and systematic dissection of their downstream effects by in-silico network perturbation analysis revealed the potential of this approach to identify diagnostic biomarkers as well as aid in the development of novel SL-targeted AD therapeutics.

7.2   Material and methods

Identification of sphingolipid pathway-associated genes

The borders for classifying 'sphingolipid related genes' are not strict, which is mainly due to the lack of a clear classification of genes belonging to this metabolic pathway in the literature, as well as to lack of absolute boundaries between cellular processes in general. Hence, as an unbiased approach, we selected relevant manually curated Gene Ontology (GO) terms related to SL metabolism as provided in Supplementary file 1, including key terms such as 'sphingoid metabolic process' and 'sphingolipid transporter activity'. In addition, we included terms related to core SL-associated functions, such as caveola and membrane raft processing, in order to characterize the changes observed in those biological processes most directly related to SL function in our AD datasets. The reasoning behind the inclusion of 'caveola' is based on existing evidence in the literature which, amongst others, suggests that caveolin-1 (CAV1) deficiency results in altered cellular lipid composition, and plasma membrane (PM) phosphatidylserine distribution in CAV1-deficient cells [43]. We also included GO terms related to lipid rafts because they are enriched with sterols such as SLs (e.g. sphingomyelin and glycosphingolipids) and cholesterol, and they are associated with specific raft proteins [44].

After selection of terms, the genes connected to these terms were extracted by using the WikiPathways plugin for PathVisio, which allowed to save all elements connected to a GO term of interest in an xml type file format (gpml format) [45] [46]. This plugin requires the GO ontology file ('go.obo')[44] geneontology.org; downloaded Nov. 17th, 2018) and a bridgeDb file with gene identifier mappings ('Hs_Derby_Ensembl_91.bridge'from www.pathvisio.org in this case) [47]. Thereafter, an R script was used to extract all contributing genes (as identified by their HGNC symbols) from the gpml files for each term. Subsequently, all information per gene was combined, by merging all GO terms from the selection by which the gene is annotated (Supplementary file 2). Furthermore, a basic 'tree-like' textual display of the selected terms was generated highlighting which sub-term(s) fall(s) under which exact master-term(s). For example, the master SL term 'sphingolipid metabolic process' (GO:0006665) contains multiple sub-terms such as 'glycosylceramide metabolic process' (GO:0006677), which, in turn, contains various sub-terms like 'ganglioside metabolic process' (GO:0001573). For further details of this hierarchy, please see the Supplementary files 3, 4, and 5. In conclusion, this procedure resulted in a gene set consisting of 252 SL-related genes that were assessed in downstream applications.

<u>Post-mortem brain tissues</u>

This study made use of brain tissue from donors of the Brain and Body Donation Program (BBDP) at the Banner Sun Health Research Institute (BHSRI), who signed an informed consent form approved by the institutional review board, including specific consent of using the donated tissue for future research [48]. DNA was obtained from the middle temporal gyrus (MTG) of 46 AD patients and 32 neurologically normal control BBDP donors stored at the Brain and Tissue Bank of the BSHRI (Sun City, Arizona, USA) [48] [49]. The groups were matched for age, gender, and APOE genotype. There were 38 male and 40 female samples with an average age of 85 years. The average Braak score for the considered samples was 3.85 with most of the samples belonging to Braak stages 3 and 5, 19 and 17 samples, respectively. The organization of the BBDP allows for fast tissue recovery after death, resulting in an average post-mortem interval of only 2.8 hours for the included samples. A consensus diagnosis of AD or non-demented control was reached by following National Institutes of Health (NIH) AD Center criteria [48]. Comorbidity with any other type of dementia, cerebrovascular disorders, mild cognitive impairment (MCI), and presence of non-microscopic infarcts was applied as exclusion criteria. Detailed information about the BBDP has been reported elsewhere [48] [49]. The current analysis was performed on the only dataset around to date that includes both data on mRNA expression and levels of UC, 5-mC and 5-hmC. The uniqueness of this work therefore lies in the parallel analysis of data from several different, but interdependent layers of gene regulation extracted from the same AD and control post-mortem brain samples. A table summarizing the demographic characteristics for control and AD samples has been provided in the supplementary table S7.

<u>Differential gene expression analysis</u>

For differential gene expression analysis, Illumina HumanHT-12 v4 beadchip expression array data for the same MTG samples was obtained from a recently published study [50]. Preprocessing and analysis of the raw datasets was conducted in R (version 3.4.4) [51]. Raw expression data was log-transformed and quantile-quantile normalized. For computing the cell type composition, the Neun_pos (Neuronal positive) cell percentage was calculated from the methylation data. The same regression model used for assessing methylation was applied to the expression data where the effects of age, gender and cell type composition were regressed out using limma (version 3.32.10). The nominal P-values obtained from limma were FDR-adjusted for only the set of 252 genes in the

SL pathway and only the genes with adj. P-value < 0.05 were considered significantly differentially expressed.

Differential (hydroxy)methylation analysis

For assessing differential DNA methylation (5-methylcytosine, 5mC), hydroxymethylation (5hydroxymethylcytocine, 5hmC) and levels of unmodified cytosine (uC), data was obtained from a recently published study from our group [52], where Illumina HM 450K arrays were used for quantifying DNA (hydroxy)methylation status of 485,000 different human CpG sites. We only considered methylation datasets related to 46 AD patients and 32 controls for which the corresponding gene expression profiles were also available. Preprocessing and analysis of the raw datasets was conducted in R (version 3.4.4) [51]. Raw IDAT files corresponding to the selected individuals were read into R using the wateRmelon "readEpic" function (version 1.20.3) [53]. The "pfilter" function from the wateRmelon package (version 1.18.0) [53] was used to filter datasets based on bead count and detection p-values. Background correction and normalization of the remaining probe data was performed by using the "preprocessNoob" function of minfi package (version 1.22.1) [54]. Beta values for the probes were obtained by the "getBeta" function of the minfi package. We used the MLML function within the MLML2R package [55] for estimating the proportion of uC, 5mC and 5hmC for each CG site (CpG), based on the combined input signals from the bisulfite (BS) and oxidative BS (oxBS) arrays. All of the cross-hybridizing probes and the probes that contained a SNP in the sequence were removed resulting into 407,922 probes to be considered for the differential methylation analysis [56]. Raw IDAT files corresponding to the selected individuals were loaded into R using the minfi "read.metharray" function (version 1.22.1) [54] to generate an RGset for computing the cell type composition of the samples by using the "estimateCellCounts" function of the same package. For estimating the cell composition, we used the FlowSorted.DLPFC.450k package (version 1.18.0) [13] as the reference data for "NeuN_pos" cell composition within the frontal cortex. The limma package (version 3.32.10) [57] was used to perform linear regression in order to test the relationship between the beta values of the probes and the diagnosis of AD. The used regression model considered beta values as outcome, AD diagnosis as predictor, and age, gender, and neuronal cell proportion as covariates. In order to identify significantly differentially methylated probes (DMPs), FDR correction for multiple testing was applied, where unadjusted P-values were corrected for those 103 genes that were significantly

differentially expressed and belong to the SL pathway. Illumina human UCSC annotation was used for assigning methylation probes to the HGNC gene symbols.

Correlation between methylation state and gene expression

For those CpG sites and associated genes that showed significant differences in (hydroxy)methylation and gene expression levels in AD patients and controls, we assessed whether there was a significant association between the normalized (hydrox)methylation beta values and corresponding gene expression levels, across all samples. For this purpose, we used the "cor.test" function from the base R package to calculate the Spearman correlation coefficient for the paired samples.

Gene-gene interaction network Gene Regulatory Network (GRN) reconstruction

We used the software Pathway Studio [58] to obtain directed functional interactions between the genes belonging to SL associated pathway. The ResNet Mammalian database in Pathway Studio contains a collection of literature-curated and experimentally validated directed gene-gene interactions. The high level of literature curation ensures the creation of confident interaction network maps. In order to obtain a set of functional regulatory interactions among the selected genes, our analysis was restricted to interactions belonging to categories "Expression", "Regulation", "Direct Regulation", "Promoter Binding", and "Binding". The obtained interactions are directed, i.e. the source and target genes are known. Furthermore, information about the interaction type (activation or inhibition) is taken into consideration, if available.

In order to reconstruct phenotype-specific networks for disease (AD) and healthy phenotypes, we employed an in-house developed differential GRN reconstruction approach [59]. Briefly, this tool relies on a genetic algorithm for removing interactions that are not compatible with Booleanized gene expression states of the disease and control phenotypes. As some of the interactions retrieved from Pathway Studio have an unspecified effect, i.e. information on the activating or inhibitory consequence of the interaction is missing, the tool also infers missing regulatory effect data from the given gene expression and network phenotype under consideration. Here, we used the set of significantly differentially expressed SL genes and regulatory interactions between them obtained

from Pathway Studio, to reconstruct differential networks with stable steady states representing the disease and healthy phenotypes.

In-silico network simulation analysis for phenotypic reversion

The differential network topology allowed us to identify common and phenotype-specific positive and negative elementary circuits, i.e. network paths which start and end at the same node and with all the intermediate nodes being traversed only once. These circuits have been shown to play a significant role in maintaining network stability [60] and the existence of these circuits is considered to be a necessary condition for having stable steady states [61]. Regarding the biological relevance of these circuits, it has been shown that perturbation of genes in positive circuits induces a phenotypic transition [62]. Furthermore, the differential network topology also aids in identifying differential regulators of the genes common to both phenotype-specific networks. Altogether, the differential regulators and genes in the elementary circuits constitute an optimal set of candidate genes for network perturbation as they are predicted to be able to revert most of the gene expression program upon perturbation. Identification of network perturbation candidates was carried out using the Java implementation proposed by Zickenrott and colleagues [59]. The same software was used to perform a network simulation analysis by perturbing multi-target combinations of up to three network perturbation candidate genes. As a result, a ranked list of single- and multi-gene combinations (maximally 3 genes) is obtained, and scores for each combination, which represent the number of other genes in the network whose expression is predicted to be reverted through the chosen perturbation genes. Generally, a high score for a single- or multi-gene perturbation is indicative of its ability to regulate the expression of a large subset of downstream genes, hence playing a key role in the maintenance and stability of the phenotype under consideration.

7.3   Results

Transcriptome analysis of sphingolipid genes

In order to identify SL-associated genes, we used the chosen gene ontology (GO) terms as previously described and employed the WikiPathways plugin [45] for PathVisio [46] to convert each GO term of interest into a tree-like pathway diagram, which facilitates extraction of the mapped genes. By removing the genes belonging to irrelevant families and keeping only those related to SL GO terms, we identified 252 genes involved in SL-related processes. Next, information on the expression of these 252 genes within the MTG was extracted from available microarray data, derived from brain tissue samples of AD patients and age-match controls [52]. The genome-wide differential expression analysis (DEA) of the transcriptomic data highlighted 7,776 genes as significantly (FDR corrected P-value ≤ 0.05) differentially expressed between AD and controls. By applying multiple testing correction for the number of SL-associated genes, we confirmed 103 out of 252 genes as significantly differentially expressed (see Table 1 for the top 30 differentially expressed genes and supplementary file 6 for a complete overview of genes in the networks).

GeneName	logFC	FDR_adj_Pval	GeneName	logFC	FDR_adj_Pval
STS	-0.221	0.000001	PPM1L	-0.139	0.000538
ARSG	-0.148	0.000011	SMO	0.331	0.000538
EZR	0.631	0.000017	VAPA	-0.279	0.000538
ALOX12B	-0.195	0.000033	ST8SIA2	-0.11	0.000538
ST6GALNAC5	-0.921	0.000033	ELOVL4	-0.633	0.000538
B3GALNT1	-0.387	0.000033	CDH13	-0.654	0.000571
GLTP	0.484	0.000111	RFTN1	-0.382	0.000624
CLN8	0.269	0.000163	EHD2	0.327	0.00075
CD8A	-0.122	0.000179	ST8SIA5	-0.319	0.000784
MAL2	-0.994	0.000196	PRKD1	0.301	0.000784
TFPI	0.241	0.000226	AGK	-0.43	0.000784
CSNK1G2	0.347	0.000272	ATP1A1	-0.553	0.000932
RFTN2	0.529	0.000333	ANXA2	0.369	0.000932
KDSR	0.372	0.000388	GBA	-0.206	0.001177
P2RX7	0.466	0.000528	CLIP3	-0.256	0.001177

Table 1: Top differentially expressed SL genes. A list of the top significantly differentially expressed genes (FDR adjusted P-value < 0.05) when comparing AD and control samples. Over-expressed genes have a positive logarithmic fold-change (logFC), under-expressed genes have a negative logFC. Here, logFC represents the estimate of the log2 fold-change.

The SL pathway is significantly dysregulated in AD

The comparison of genome-wide gene expression data for SL-associated genes between AD patients and unaffected controls revealed that 24.5% (7,776 out of 31,726 genes) of the genes were significantly differentially expressed (adj. P-value < 0.05) between the two conditions. However, out of the 252 identified SL pathway-associated genes, 103 had significantly altered activity (40.87%), reflecting a significant overrepresentation (Fisher's exact test, P-value < 7.0e-09). In terms of epigenetic dysregulation, no significant alterations were observed after multiple testing adjustments. Prior to the adjustments, 129, 109, and 170 probes displayed nominally significant (unadjusted P-value < 0.05) differential levels of 5-mC, 5-hmC, and uC, respectively. Larger sample sizes will be required in the future to assess whether FDR-adjusted significance can be shown for these probes at the observed effect sizes. These CpG sites were associated to 90, 78, and 112 unique genes, respectively. Interestingly, we noticed a relatively high degree of overlap in genes when comparing the various cytosine states (a Venn diagram representing the overlap of genes across different levels is shown in Figure 1A). Similarly, the overlap of specific probes across different epigenetic levels is depicted in Figure 1B. Notably, there were 28 genes that were both nominally differentially methylated, hydroxymethylated as well as displaying different levels of unmodified cytosine (Figure 1A), showing consistent differences across all levels of methylation. This suggests that there is a robust cluster of alterations in an epigenetic regulatory circuit centered around SL-associated genes in AD.
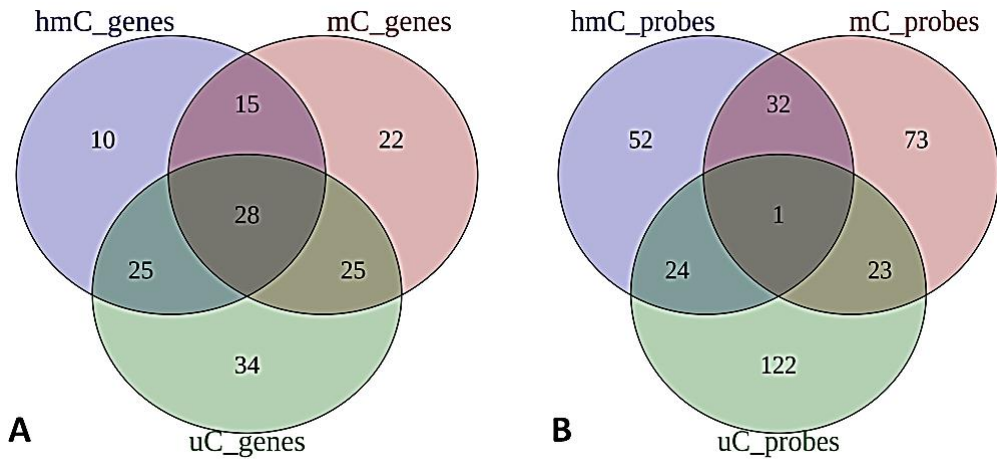
Figure 1: Overlap of differentially methylated genes and probes. A) Overlap between genes across different cytosine states (hmC, mC, uC) that display nominally significant differential levels in AD compared to controls (unadjusted P-value < 0.05). B) Overlap between nominally significant probes across all three cytosine states.

Next, in order to assess the significance of DNA (hydroxy)methylation changes, we corrected the p-values for multiple hypothesis testing. Three CpG sites, associated to PTGIS, GBA, ITGB2 genes, displayed differential levels of hydroxymethylation after corrections (P-value < 0.00048) when comparing AD and control samples (see Table 2). Differential hydroxymethylation analyses showed a profound enrichment of SL-related differentially hydroxymethylated genes in AD brains, reflecting a significant overrepresentation (Fisher's exact test, P-value < 1.09e-06).

Gene Name	Probe Name	logFC	P-value
PTGIS	cg07612655	0.037	0.00008
GBA	cg19257864	0.036	0.00017
ITGB2	cg18012089	0.062	0.00047

Table 2: Differentially methylated probes. Significantly differentially (FRD-corrected) hydroxymethylated (hmC) probes when comparing AD patients and controls.

Correlation analysis of cytosine states and mRNA expression

In order to examine the association between alterations at the epigenetic and transcriptomic level, we tested the significance of the Spearman correlation between the nominally differentially

220

methylated probes at the mC, hmC and uC levels, and their corresponding gene expression levels across all samples (table 3). No correlations were significant after multiple testing adjustments, but nominal significance (P-value < 0.05) between 15 differentially methylated probes (mC) and corresponding gene expression levels was observed, which may serve as candidates for further evaluation using larger sample sizes. Similarly, 10 hmC and 10 uC probes were found to have nominally significant correlations with corresponding gene expression levels. Interestingly, many genes displayed a nominally significant association between levels of multiple types of cytosine states and mRNA expression. For example, the CLN8 gene a significant association between differential methylation at the mC hmC and mRNA expression level was observed (table 3).

		5mC		5hmC		uC	
Name	CpG site	Correlation	P-value	Correlation	P-value	Correlation	P-value
ST6GALNAC5	cg00294096	0.3726	8.0E-04	-	-	-	-
CSNK1G2	cg01335597	n.s.	n.s.	-	-	-0.2535	0.0251
ANXA2	cg02072495	-0.3281	0.0034	n.s.	n.s.	-	-
ENPP7	cg02715531	-	-	-0.2334	0.0398	-	-
TFPI	cg04144365	-	-	n.s.	n.s.	-0.2555	0.0242
SMO	cg04478795	-0.3099	0.006	n.s.	n.s.	-	-
CLN8	cg04685163	0.2664	0.0184	n.s.	n.s.	n.s.	n.s.
CLN8	cg11192059	0.3739	7.0E-04	-0.316	0.0048	-	-
CLN8	cg27351978	0.3039	0.0068	-	-	-	-
PRKD2	cg06280512	-0.3127	0.0055	-	-	-	-
PRKD2	cg10779826	0.2811	0.0129	-	-	-0.2738	0.0155
PRKD2	cg10829227	-	-	-	-	-0.3623	0.0012
PRKD2	cg16580765	-	-	-	-	-0.3824	6.0E-04
PRKD2	cg26591117	0.2415	0.0334	-0.2237	0.0491	-	-
ATP1B1	cg07136905	-	-	-0.2971	0.0083	0.3636	0.0011
DLC1	cg08768218	0.2519	0.0264	-0.2376	0.0365	-	-
CDH13	cg09415485	-0.2782	0.0139	-	-	-	-
DLG1	cg09732145	0.2234	0.0495	-	-	n.s.	n.s.
EHD2	cg10720699	-	-	-	-	-0.3047	0.0069
S1PR3	cg13641920	-	-	0.2588	0.0224	-0.2384	0.0358
CD8A	cg13847640	-0.2319	0.0413	-	-	0.2846	0.0118
ENPP7	cg15739835	n.s.	n.s.	-0.2414	0.0332	-	-
SPHK1	cg17901038	0.2674	0.0179	-0.2591	0.022	-	-
ITGB2	cg18012089	-	-	0.2443	0.0312	n.s.	n.s.
GBA	cg19257864	-	-	-0.3202	0.0043	0.2741	0.0151
ORMDL2	cg22695998	0.3025	0.0073	-	-	-	-

Table 3: Differentially expressed genes displaying a nominally significant correlation between mC, hmC and/or uC levels and mRNA expression. n.s: non-significant; -: not applicable (i.e. CpG site not displaying nominally significant alterations at the [hydroxy]methylation level).

Finally, we assessed whether there is a relationship between levels of gene expression and methylation with measures of AD pathology. We have computed a Spearman correlation analysis comparing expression levels of individual SL-related genes across all samples with the available pathological measures (e.g. CERAD, Braak, Plaque, Tangle, and CSF scores). We observed significant associations between some of the top-ranked DEGs and various pathological measures. For

example, the correlation coefficient between STS gene expression values and CERAD scores is -0.49 with a hochberg-adjusted P-value of 5.35E-06. The correlation coefficient between the expression of this gene and Braak score is -0.60 with a hochberg-adjusted P-value of 1.99E-06. The data is provided as supplementary tables (S10-13) and, additionally, in the case of a significant association between gene expression and disease pathology markers, in the form of a heatmap (Supplementary image S1). Similarly, we examined the correlation between the beta values representing the mC, hmC, and UC levels and the pathological measures described above. The results are provided in the form of supplementary tables S12 (hmC), S13 (mC), and S14 (UC) describing the correlation between methylation levels and various pathological features.

Gene regulatory network analysis reproducing context- specific network

In order to gain a deeper understanding of SL-associated dysregulations at a systems level, we conducted a differential gene regulatory network (GRN) analysis to reconstruct two context-specific networks, representing the AD and unaffected control phenotypes. The employed GRN reconstruction approach [59] relies on Booleanized differential gene expression data and a prior knowledge network (PKN) of gene-gene interactions to reconstruct context-specific networks. The reconstructed AD network comprised 41 genes and 64 interactions (Figure 2A), whereas the unaffected control phenotype network consisted of 42 genes and 57 interactions (Figure 2B). Although both the networks representing the AD and control phenotypes look very similar, the underlying differences actually lie in the expression levels of the genes in the networks, i.e. whether they are up- or down-regulated in the respective phenotypes. As we operate in a differential expression setting, a gene that is up-regulated in the AD phenotype, is down-regulated in the control phenotype and vice versa. Therefore, changes in the network topology are not the main denominator, but the state (expression) of the genes in the respective networks (i.e. up- or down-regulated) is. Further information about the topological characteristics (e.g. in- and out-degree, closeness centrality, and clustering coefficient) of the networks representing the disease and healthy phenotype are provided in supplementary tables (table S8 and S9), helping us in identifying the subtle differences in the networks that can be overlooked by simply looking at the images of network topology.
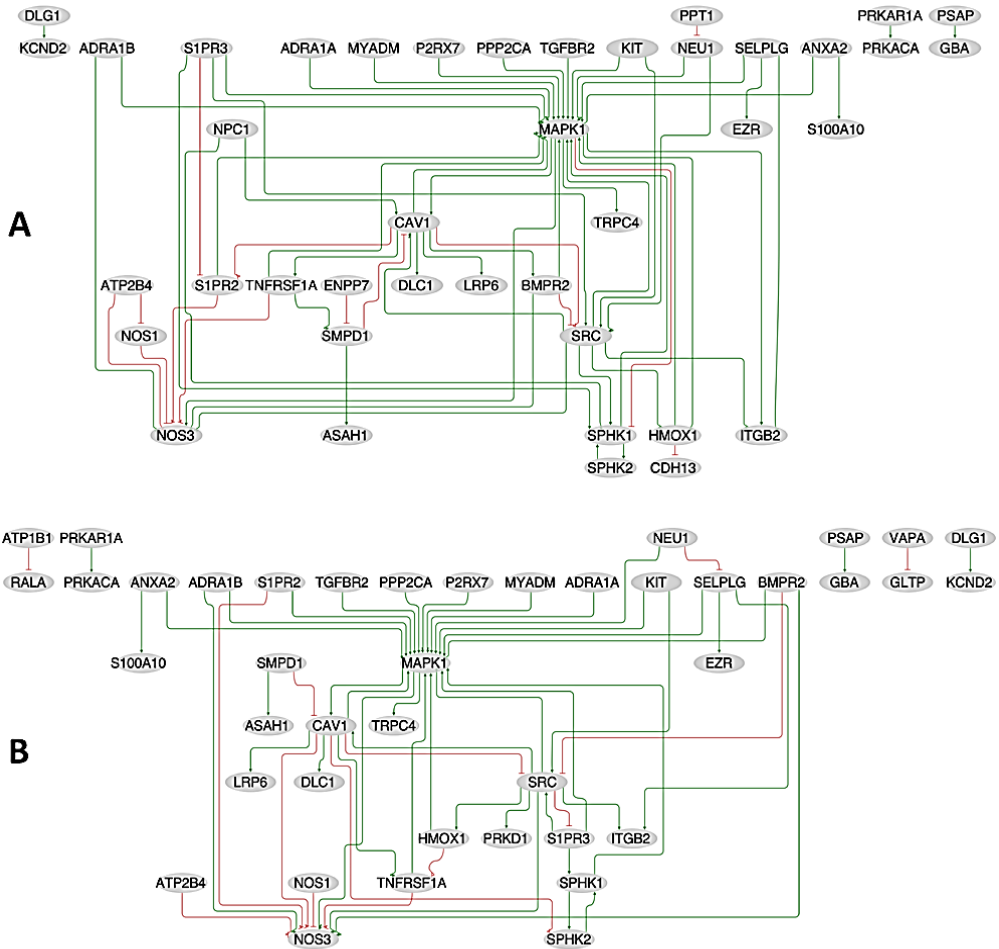
Figure 2: Gene regulatory network (GRN) of SL metabolism in disease and control phenotypes. A) GRN representing the disease phenotype containing 41 nodes (transcription factors and genes) and 64 interactions; B) GRN representing the unaffected control phenotype and containing 42 nodes and 57 interactions. Green arrowhead lines in the network represent positive interactions, i.e. activation (50 and 43 in the disease and control phenotype networks, respectively), while red lines represent negative interactions, i.e. inhibition (14 in both phenotype networks).

<u>In-silico network perturbation shows candidate genes able to revert the AD phenotype</u>

Following the paradigm of modeling diseases as network perturbations [63], we performed in-silico network perturbations to identify the most influential combinations of genes in the constructed GRN representing the AD phenotype. This network perturbation analysis highlighted the key roles of the perturbation candidates in the GRN and revealed that a three-gene perturbation combination,

involving CAV1, SPHK1, and SELPLG, has the potential to revert the expression levels of 18 genes in the network from a disease phenotype towards a healthy phenotype (see Table 4).

Although the gene signatures identified here are not necessarily responsible for disease onset and progression, they are predicted to revert the expression of a large number of disease-associated genes upon perturbation in the in-silico network model representing the disease phenotype. This indicates a key regulatory role of the predicted genes in the establishment and maintenance of the disease phenotype. Taken together, the in-silico network perturbation analysis highlights novel candidates that could serve as potential targets for therapeutic intervention in AD.

Rank	Score	Combination	Rank	Score	Combination
1	18	SELPLG, SPHK1, CAV1	11	16	SPHK2, CAV1, S1PR3
2	17	SPHK1, CAV1, S1PR3	12	16	SPHK2, CAV1, HMOX1
3	17	SPHK1, CAV1	13	16	SPHK2, CAV1
4	17	SELPLG, SPHK2, CAV1	14	16	SPHK1, CAV1, TNFRSF1A
5	17	SELPLG, CAV1, S1PR3	15	16	SPHK1, CAV1, MAPK1
6	17	SELPLG, CAV1, HMOX1	16	16	SELPLG, SRC, CAV1
7	17	SELPLG, CAV1	17	16	SELPLG, CAV1, TNFRSF1A
8	17	CAV1, SPHK1, HMOX1	18	16	SELPLG, CAV1, MAPK1
9	16	SRC, SPHK1, CAV1	19	16	CAV1, S1PR3
10	16	SPHK2, SPHK1, CAV1	20	16	CAV1

Table 4. Top 20 key candidate genes combinations identified by in-silico network perturbation analysis. Perturbation score (Score) represents the total number of genes whose gene expression is reverted upon inducing a perturbation of a given gene combination (Combination).

7.4   Discussion

While new high-throughput sequencing technologies and computational analyses of omics datasets have extended our knowledge on AD, the mechanisms underlying the dysregulation of cellular pathways in AD still require further investigation. In this study, characterizing interconnected layers of regulation, we provided more insight into the genes and mechanisms behind the dysregulation of specific SL pathways in AD. We were able to identify SL-related genes differentially expressed in AD patients which also display multiple types of epigenetic alterations affecting different cytosine states, corroborating the relevance of SL alterations in AD. Furthermore, using in-silico analyses, we identified key regulatory genes in the disease-specific network and candidate genes able to revert the disease state towards the healthy phenotype. These data have helped to identify specific SL-related cellular processes that display pronounced alterations in AD, with potential relevance for the development of new biomarkers and therapeutic strategies.

Many SL-related genes display altered expression and DNA (hydroxy)methylation in AD.

The present study reveals a significant enrichment of SL-related gene expression alterations in the MTG of AD patients in comparison to age- and sex-matched controls. We observed significant differential expression in 103 out of 252 SL-associated genes. Many of these genes have already been reported to display alterations in AD and/or other neurodegenerative disorders. For example, STS, encodes for a sulfatase protein representing the top underexpressed gene in our data set, is involved in the synthesis of cholesterol, which is a well-known interactor of SLs and fundamental to maintain the equilibrium of cell membranes in philological functions [64]. STS has previously been observed to have decreased expression in AD [65] and to harbor a genetic variant associated with cognition [66]. Similar to STS, ARSG, encodes for a sulfatase and is involved in the formation of cholesterol and steroids [67]. As aforementioned, the regulation of SLs metabolism by steroid hormones is involved in several physiological events as development, reproduction, and metabolism [64]. Furthermore, EZR, encoding for the protein ezarin, a top-ranked over-expressed gene in our data, also showed increased expression in other studies on AD [68]. EZR, is an intermediate between the plasma membrane and the actin cytoskeleton, has recently emerged as a target of SL regulation mainly during endocytosis, exocytosis and cellular trafficking. [69]. In fact, Sphingosine 1-phosphate (S1P) activates ezrin-radixin-moesin complex proteins contributing to cytoskeletal remodeling and changing membrane properties, which is essential for cellular homeostasis [70]. Interestingly, the analysis also reveals new AD-associated alterations, such as the overexpression of CLN8, a gene that

227

has previously been linked to neurological dysfunction, but not directly to AD [71]. CLN8, hypothesized to mediate SL synthesis, known to be involved in the ceramide synthesis and homeostasis [72], also displayed a significant (albeit nominally) positive correlation between expression levels and DNA methylation and a negative correlation with DNA hydroxymethylation. A further new gene of interest is ARSG, underexpressed in AD in the analyzed data. While it has previously been linked to multiple complex disorders such as lysosomal storage disorders, certain cancers, and neurodevelopmental dysfunction [73], our study provides the first evidence for a dysregulation of ARSG in AD. Another SL-related gene displaying multiple alterations was ITGB2, encoding integrin subunit beta 2. This gene has been demonstrated to influence the reorganization of lipid rafts, membrane platforms rich in SLs [74]. ITGB2 displays significant hyper-hydroxymethylation as well as increased mRNA expression in AD patients, which is in line with a previous study reporting increased expression levels of this gene in a mouse model of AD [75]. Notably, we also observed a positive correlation between expression levels and DNA hydroxymethylation for ITGB2. Similarly, the gene PTGIS showed increased DNA hydroxymethylation in AD. It has previously been suggested to contribute to neurodevelopmental disorders, including childhood onset schizophrenia, and up to now was never linked directly to AD [76]. Epigenetic variation was also observed in GBA, which displayed an increased level of hydroxymethylation, concomitant with a negative correlation with its expression levels. This gene is known to harbor risk factor variations associated with Parkinson's disease [77], but has not been linked directly to AD. Finally, PRKD1, which encodes for the protein kinase D1 [78] displayed increased expression, concomitant with an increase in DNA methylation in AD patients, indicating an altered epigenetic regulation. Interestingly, this protein kinase has been suggested to have protective functions in Parkinson's disease [79], but has, to the best of our knowledge, not been studied in the context of AD.

Gene regulatory network and perturbation analysis

Given the results from previous studies showing significant alterations of SL-related genes in AD patients, we aimed to provide a more comprehensive and detailed characterization of these alterations at the gene regulatory network level. For this purpose, we conducted an integrative analysis of genes involved in SL functions by reconstructing phenotype-specific networks for AD patients and unaffected controls. Using a dedicated GRN approach and associated perturbation analyses, we identified multiple genes, in particular CAV1, SPHK1, and SELPLG, that could play a key

role as regulatory genes in maintaining the AD phenotype. Interestingly, a single gene perturbation of CAV1 alone was predicted to normalize gene expression profiles of 16 genes in the AD network, providing a promising candidate for further experimental investigation. Moreover, CAV1 was over-expressed in AD patients, consistent with findings from prior studies that have linked its elevated expression levels to cerebral amyloid angiopathy in AD [80] [81]. Similarly, the gene SPHK1 was found both to represent a key regulatory node in the network maintaining the AD phenotype and occurred among the top candidate genes derived from the in-silico network perturbation analysis. Furthermore, SPHK1 displayed a significant correlation between expression levels and (hydroxy)methylation levels. These results are in line with a previously suggested role of this gene in the progression of AD [82] [83] [83].

Both CAV1 and SPHK1 encode for key proteins involved in SL pathways and SL metabolism. CAV1, which encodes for the membrane protein caveolin 1, displays a strong and dynamic interaction with SLs in cellular membranes in which they concomitantly and reciprocally regulate each other's levels and functions [84]. In particular, CAV1 interacting with cholesterol and sphingomyelin affects the structural composition of lipid rafts, thereby influencing the transduction of physiological signaling as well as pathological processes. A disturbed balance of CAV1-SLs rich-membrane domains has been implicated in various pathological processes linked to neurodegeneration, prion disease and viral infections [85] [15]. SPHK1 is a central enzyme in SL pathways, it phosphorylates sphingosine (S) into sphingosine 1 phosphate (S1P), which represents a potent SL that acts as an activator of various cellular signaling pathways regulating stress resistance, proliferation, differentiation, and mature phenotypes of nervous system cells. In particular, S1P, modulates pathways known for their engagement in the regulation of cell survival and differentiation, and therefore it is also recognized as an important molecule during aging [86]. Dysregulation at the level of S1P, caused by alterations in SPHK1 activity, has damaging consequences on the physiology of the brain leading to neurodegeneration and neuroinflammatory processes [87].

As such, SPHK1 plays an important role in various cellular processes including cell proliferation, differentiation, angiogenesis and inflammation. Furthermore, it has been implicated in different disorders including AD [88] [89] [90].

Finally, SELPLG, another gene ranked high in the perturbation analysis, encodes for the E-selectin receptor, which cross-interact with glycoSLs in the membrane, promoting the transduction of E-selectin–mediated signaling [91]. SELPLG, was also found to be upregulated in the brains of mice

suffering from cerebral amyloidosis in a prior study [92], lending further support to a potential involvement of this gene in AD.

7.5   Conclusion

Overall, our integrative analyses have revealed both novel candidate AD-associated genes and confirmed previously reported associations. As a limitation, the moderate sample size available for the study might have restricted the detectable changes in AD, and further analyses on independent samples are warranted. In spite of these restrictions, our results show a statistically significant enrichment of changes in SL genes and related pathways in AD, corroborating the key role SL-associated alterations in AD. The data presented here may serve as a starting point to help filling the current knowledge gaps concerning the role of SLs in AD. Follow-up studies using extensive molecular profiling analyses across multiple brain regions in combination with perturbation experiments using in-silico and in-vivo AD models are needed to obtain a more comprehensive characterization and mechanistic understanding of the role of SLs in AD.

7.6   Funding

All authors declare no conflict of interest.

7.7   References

1.   Pralhada Rao, R., et al., Sphingolipid Metabolic Pathway: An Overview of Major Roles Played in Human Diseases. Journal of Lipids, 2013. 2013: p. 178910.

2.   Hannun, Y.A. and L.M. Obeid, Sphingolipids and their metabolism in physiology and disease. Nature Reviews Molecular Cell Biology, 2018. 19(3): p. 175-191.

3.   Gault, C.R., L.M. Obeid, and Y.A. Hannun, An overview of sphingolipid metabolism: from synthesis to breakdown. Adv Exp Med Biol, 2010. 688: p. 1-23.

4.   Hanada, K., et al., Molecular machinery for non-vesicular trafficking of ceramide. Nature, 2003. 426(6968): p. 803-9.

5.   Mencarelli, C., et al., The ceramide transporter and the Goodpasture antigen binding protein: one protein--one function? J Neurochem, 2010. 113(6): p. 1369-86.

6.   Large-scale discovery of novel genetic causes of developmental disorders. Nature, 2015. 519(7542): p. 223-8.

7.   Rao, R.P., et al., Ceramide transfer protein deficiency compromises organelle function and leads to senescence in primary cells. PLoS One, 2014. 9(3): p. e92142.

8.   Crivelli, S.M., et al., CERT(L) reduces C16 ceramide, amyloid-β levels, and inflammation in a model of Alzheimer's disease. Alzheimers Res Ther, 2021. 13(1): p. 45.

9.   Murakami, H., et al., Intellectual disability-associated gain-of-function mutations in CERT1 that encodes the ceramide transport protein CERT. PLoS One, 2020. 15(12): p. e0243980.

10.   Wang, X., et al., Mitochondrial degeneration and not apoptosis is the primary cause of embryonic lethality in ceramide transfer protein mutant mice. The Journal of cell biology, 2009. 184(1): p. 143-158.

11.   Wang, X., et al., Mitochondrial degeneration and not apoptosis is the primary cause of embryonic lethality in ceramide transfer protein mutant mice. Journal of Cell Biology, 2009. 184(1): p. 143-158.

12.   Giovagnoni, C., et al., Immunofluorescence Labeling of Lipid-Binding Proteins CERTs to Monitor Lipid Raft Dynamics. Methods Mol Biol, 2021. 2187: p. 327-335.

13.   Mencarelli, C., et al., Goodpasture antigen-binding protein/ceramide transporter binds to human serum amyloid P-component and is present in brain amyloid plaques. J Biol Chem, 2012. 287(18): p. 14897-911.

14.   Bode, G.H., et al., Complement activation by ceramide transporter proteins. J Immunol, 2014. 192(3): p. 1154-61.

15. Olsen, A.S.B. and N.J. Færgeman, *Sphingolipids: membrane microdomains in brain development, function and neurological diseases.* Open Biol, 2017. 7(5).

16. Hussain, G., et al., *Role of cholesterol and sphingolipids in brain development and neurological diseases.* Lipids Health Dis, 2019. 18(1): p. 26.

17. Alessenko, A.V. and E. Albi, *Exploring Sphingolipid Implications in Neurodegeneration.* Front Neurol, 2020. 11: p. 437.

18. Fan, L., et al., *New Insights Into the Pathogenesis of Alzheimer's Disease.* Frontiers in Neurology, 2020. 10(1312).

19. Mielke, M.M., et al., *Cerebrospinal fluid sphingolipids, β-amyloid, and tau in adults at risk for Alzheimer's disease.* Neurobiol Aging, 2014. 35(11): p. 2486-2494.

20. Satoi, H., et al., *Astroglial expression of ceramide in Alzheimer's disease brains: a role during neuronal apoptosis.* Neuroscience, 2005. 130(3): p. 657-66.

21. Mielke, M.M. and C.G. Lyketsos, *Alterations of the Sphingolipid Pathway in Alzheimer's Disease: New Biomarkers and Treatment Targets?* NeuroMolecular Medicine, 2010. 12(4): p. 331-340.

22. Giovagnoni, C., et al., *Altered sphingolipid function in Alzheimer's disease; a gene regulatory network approach.* Neurobiol Aging, 2021. 102: p. 178-187.

23. Nikolova-Karakashian, M.N. and M.B. Reid, *Sphingolipid metabolism, oxidant signaling, and contractile function of skeletal muscle.* Antioxid Redox Signal, 2011. 15(9): p. 2501-17.

24. Katsel, P., C. Li, and V. Haroutunian, *Gene expression alterations in the sphingolipid metabolism pathways during progression of dementia and Alzheimer's disease: a shift toward ceramide accumulation at the earliest recognizable stages of Alzheimer's disease?* Neurochem Res, 2007. 32(4-5): p. 845-56.

25. He, X., et al., *Deregulation of sphingolipid metabolism in Alzheimer's disease.* Neurobiol Aging, 2010. 31(3): p. 398-408.

26. Grimm, M.O., et al., *PS dependent APP cleavage regulates glucosylceramide synthase and is affected in Alzheimer's disease.* Cell Physiol Biochem, 2014. 34(1): p. 92-110.

27. Han, X., et al., *Substantial sulfatide deficiency and ceramide elevation in very early Alzheimer's disease: potential role in disease pathogenesis.* J Neurochem, 2002. 82(4): p. 809-18.

28. Cutler, R.G., et al., *Involvement of oxidative stress-induced abnormalities in ceramide and cholesterol metabolism in brain aging and Alzheimer's disease.* Proc Natl Acad Sci U S A, 2004. 101(7): p. 2070-5.

29. de Wit, N.M., et al., *Altered Sphingolipid Balance in Capillary Cerebral Amyloid Angiopathy.* J Alzheimers Dis, 2016.

30.   Couttas, T.A., et al., *Loss of the neuroprotective factor Sphingosine 1-phosphate early in Alzheimer's disease pathogenesis. Acta Neuropathol Commun, 2014. 2: p. 9.*

31.   Kaya, I., et al., *Delineating Amyloid Plaque Associated Neuronal Sphingolipids in Transgenic Alzheimer's Disease Mice (tgArcSwe) Using MALDI Imaging Mass Spectrometry. ACS chemical neuroscience, 2017. 8(2): p. 347–355.*

32.   Barrier, L., et al., *Ceramide and Related-Sphingolipid Levels Are Not Altered in Disease-Associated Brain Regions of APP and APP/PS1 Mouse Models of Alzheimer's Disease: Relationship with the Lack of Neurodegeneration? Int J Alzheimers Dis, 2010. 2011: p. 920958.*

33.   Barrier, L., et al., *Genotype-related changes of ganglioside composition in brain regions of transgenic mouse models of Alzheimer's disease. Neurobiol Aging, 2007. 28(12): p. 1863-72.*

34.   Caughlin, S., et al., *Membrane-lipid homeostasis in a prodromal rat model of Alzheimer's disease: Characteristic profiles in ganglioside distributions during aging detected using MALDI imaging mass spectrometry. Biochim Biophys Acta Gen Subj, 2018. 1862(6): p. 1327-1338.*

35.   Chan, R.B., et al., *Comparative lipidomic analysis of mouse and human brain with Alzheimer disease. J Biol Chem, 2012. 287(4): p. 2678-88.*

36.   Kim, S.Y., et al., *Hearing impairment and the risk of neurodegenerative dementia: A longitudinal follow-up study using a national sample cohort. Scientific Reports, 2018.*

37.   Di Fede, G., et al., *Molecular subtypes of Alzheimer's disease. Scientific Reports, 2018.*

38.   Corder, E.H., et al., *Gene dose of apolipoprotein E type 4 allele and the risk of Alzheimer's disease in late onset families. Science, 1993.*

39.   Mielke, M.M., et al., *Serum ceramides increase the risk of Alzheimer disease: the Women's Health and Aging Study II. Neurology, 2012. 79(7): p. 633-641.*

40.   Olsen, A.S.B. and N.J. Færgeman, *Sphingolipids: Membrane microdomains in brain development, function and neurological diseases, in Open Biology. 2017.*

41.   Crivelli, S.M., et al., *Sphingolipids in Alzheimer's disease, how can we target them? Advanced drug delivery reviews, 2020: p. S0169-409X(20)30002-8.*

42.   Mielke, M.M., et al., *Cerebrospinal fluid sphingolipids, $β$-amyloid, and tau in adults at risk for Alzheimer's disease. Neurobiology of Aging, 2014.*

43.   Ariotti, N., et al., *Caveolae regulate the nanoscale organization of the plasma membrane to remotely control Ras signaling. J Cell Biol, 2014. 204(5): p. 777-92.*

44. Bieberich, E., Sphingolipids and lipid rafts: Novel concepts and methods of analysis. Chem Phys Lipids, 2018. 216: p. 114-131.

45. Slenter, D.N., et al., WikiPathways: A multifaceted pathway database bridging metabolomics to other omics research. Nucleic Acids Research, 2018.

46. Kutmon, M., et al., PathVisio 3: An Extendable Pathway Analysis Toolbox. PLoS Computational Biology, 2015.

47. van Iersel, M.P., et al., The BridgeDb framework: Standardized access to gene, protein and metabolite identifier mapping services. BMC Bioinformatics, 2010.

48. Beach, T.G., et al., The sun health research institute brain donation program: Description and experience, 1987-2007. Cell and Tissue Banking, 2008.

49. Beach, T.G., et al., Arizona Study of Aging and Neurodegenerative Disorders and Brain and Body Donation Program. Neuropathology, 2015.

50. Piras, I.S., et al., Transcriptome Changes in the Alzheimer's Disease Middle Temporal Gyrus: Importance of RNA Metabolism and Mitochondria-Associated Membrane Genes. J Alzheimers Dis, 2019. 70(3): p. 691-713.

51. Team, R.D.C., R: A Language and Environment for Statistical Computing. R Foundation for Statistical Computing, 20016.

52. Lardenoije, R., et al., Alzheimer's disease-associated (hydroxy)methylomic changes in the brain and blood. Clin Epigenetics, 2019. 11(1): p. 164.

53. Pidsley, R., et al., A data-driven approach to preprocessing Illumina 450K methylation array data. BMC Genomics, 2013.

54. Aryee, M.J., et al., Minfi: A flexible and comprehensive Bioconductor package for the analysis of Infinium DNA methylation microarrays. Bioinformatics, 2014.

55. Kiihl, S.F., et al., MLML2R: an R package for maximum likelihood estimation of DNA methylation and hydroxymethylation proportions. Statistical Applications in Genetics and Molecular Biology, 2019.

56. Chen, Y.A., et al., Discovery of cross-reactive probes and polymorphic CpGs in the Illumina Infinium HumanMethylation450 microarray. Epigenetics, 2013.

57. Ritchie, M.E., et al., limma powers differential expression analyses for RNA-sequencing and microarray studies. Nucleic acids research, 2015.

58. Nikitin, A., et al., Pathway studio - The analysis and navigation of molecular networks. Bioinformatics, 2003.

59. Zickenrott, S., et al., Prediction of disease-gene-drug relationships following a differential network analysis. Cell Death and Disease, 2016.

60. Gouzé, J.-L., *Positive and Negative Circuits in Dynamical Systems. Journal of Biological Systems*, 2003.

61. Thomas, R., *On the Relation Between the Logical Structure of Systems and Their Ability to Generate Multiple Steady States or Sustained Oscillations.* 2011.

62. Crespo, I., et al., *Detecting cellular reprogramming determinants by differential stability analysis of gene regulatory networks. BMC Systems Biology*, 2013.

63. del Sol, A., et al., *Diseases as network perturbations, in Current Opinion in Biotechnology.* 2010.

64. Lucki, N.C. and M.B. Sewer, *The interplay between bioactive sphingolipids and steroid hormones. Steroids*, 2010. 75(6): p. 390-9.

65. Wu, M., et al., *Identification of key genes and pathways for Alzheimer's disease via combined analysis of genome-wide expression profiling in the hippocampus. Biophysics Reports*, 2019. 5(2): p. 98-109.

66. Humby, T., et al., *A genetic variant within STS previously associated with inattention in boys with attention deficit hyperactivity disorder is associated with enhanced cognition in healthy adult males. Brain Behav*, 2017. 7(3): p. e00646.

67. Frese, M.A., S. Schulz, and T. Dierks, *Arylsulfatase G, a novel lysosomal sulfatase. J Biol Chem*, 2008. 283(17): p. 11388-95.

68. Zhang, Q., et al., *Integrated proteomics and network analysis identifies protein hubs and network alterations in Alzheimer's disease. Acta neuropathologica communications*, 2018.

69. Adada, M., et al., *Sphingolipid regulation of ezrin, radixin, and moesin proteins family: implications for cell dynamics. Biochim Biophys Acta*, 2014. 1841(5): p. 727-37.

70. Cencetti, F., et al., *Sphingosine 1-phosphate-mediated activation of ezrin-radixin-moesin proteins contributes to cytoskeletal remodeling and changes of membrane properties in epithelial otic vesicle progenitors. Biochim Biophys Acta Mol Cell Res*, 2019. 1866(4): p. 554-565.

71. Lonka, L., et al., *The neuronal ceroid lipofuscinosis Cln8 gene expression is developmentally regulated in mouse brain and up-regulated in the hippocampal kindling model of epilepsy. BMC Neuroscience*, 2005.

72. Adhikari, B., et al., *Neuronal ceroid lipofuscinosis related ER membrane protein CLN8 regulates PP2A activity and ceramide levels. Biochim Biophys Acta Mol Basis Dis*, 2019. 1865(2): p. 322-328.

73. Wiegmann, E.M., et al., *Arylsulfatase K, a novel lysosomal sulfatase. Journal of Biological Chemistry*, 2013.

74. Bang, B., R. Gniadecki, and B. Gajkowska, Disruption of lipid rafts causes apoptotic cell death in HaCaT keratinocytes. Exp Dermatol, 2005. 14(4): p. 266-72.

75. Swartzlander, D.B., et al., Concurrent cell type–specific isolation and profiling of mouse brains in inflammation and Alzheimer's disease. JCI Insight, 2018.

76. Ambalavanan, A., et al., De novo variants in sporadic cases of childhood onset schizophrenia. European Journal of Human Genetics, 2016.

77. Davis, A.A., et al., Variants in GBA, SNCA, and MAPT influence Parkinson disease risk, age at onset, and progression. Neurobiology of Aging, 2016.

78. Cobbaut, M., et al., Protein kinase D displays intrinsic Tyr autophosphorylation activity: insights into mechanism and regulation. FEBS Lett, 2018. 592(14): p. 2432-2443.

79. Asaithambi, A., et al., Protein kinase D1 (PKD1) phosphorylation promotes dopaminergic neuronal survival during 6-OHDA-induced oxidative stress. PLoS One, 2014. 9(5): p. e96947.

80. Gaudreault, S.B., D. Dea, and J. Poirier, Increased caveolin-1 expression in Alzheimer's disease brain. Neurobiology of aging, 2004. 25(6): p. 753-759.

81. Van Helmond, Z.K., et al., Caveolin-1 and -2 and their relationship to cerebral amyloid angiopathy in Alzheimer's disease. Neuropathology and Applied Neurobiology, 2007.

82. Maceyka, M., et al., Sphingosine-1-phosphate signaling and its role in disease. Trends Cell Biol, 2012. 22(1): p. 50-60.

83. Lee, J.Y., et al., Neuronal SphK1 acetylates COX2 and contributes to pathogenesis in a model of Alzheimer's Disease. Nat Commun, 2018. 9(1): p. 1479.

84. Sonnino, S. and A. Prinetti, Sphingolipids and membrane environments for caveolin. FEBS Letters, 2009. 583(4): p. 597-606.

85. Quest, A.F., L. Leyton, and M. Parraga, Caveolins, caveolae, and lipid rafts in cellular transport, signaling, and disease. Biochem Cell Biol, 2004. 82(1): p. 129-44.

86. Jęśko, H., et al., The Cross-Talk Between Sphingolipids and Insulin-Like Growth Factor Signaling: Significance for Aging and Neurodegeneration. Molecular Neurobiology, 2019. 56(5): p. 3501-3521.

87. Czubowicz, K., et al., The Role of Ceramide and Sphingosine-1-Phosphate in Alzheimer's Disease and Other Neurodegenerative Disorders. Molecular Neurobiology, 2019. 56(8): p. 5436-5455.

88. Alemany, R., et al., Regulation and functional roles of sphingosine kinases. Naunyn-Schmiedeberg's Archives of Pharmacology, 2007. 374(5): p. 413-428.

89.   Adams, D.R., S. Pyne, and N.J. Pyne, *Sphingosine Kinases: Emerging Structure-Function Insights.* Trends Biochem Sci, 2016. 41(5): p. 395-409.

90.   Dominguez, G., et al., *Neuronal sphingosine kinase 2 subcellular localization is altered in Alzheimer's disease brain.* Acta Neuropathol Commun, 2018. 6(1): p. 25.

91.   Winkler, I.G., et al., *Vascular niche E-selectin regulates hematopoietic stem cell dormancy, self renewal and chemoresistance.* Nat Med, 2012. 18(11): p. 1651-7.

92.   Haure-Mirande, J.V., et al., *Integrative approach to sporadic Alzheimer's disease: deficiency of TYROBP in cerebral Abeta amyloidosis mouse normalizes clinical phenotype and complement subnetwork molecular pathology without reducing Abeta burden.* Mol Psychiatry, 2019. 24(3): p. 431-446.

Chapter 8

General discussion and summary

In my PhD project, I investigated the role of lipids and lipid transporters in several pathophysiological pathways with the aim to narrow the knowledge gap of their involvement in membrane dynamics, neuroinflammation and Alzheimer's disease.

In my work, I have been able to show that CERTs, the ceramide transfer proteins, not only participate in the biogenesis and lipid composition of EV but are also present in the cellular membrane, specifically in the lipid rafts (see Chapter 3). Furthermore, I discovered that CERTs are binding partners of several proteins involved in diverse cellular cascades mainly related to oxidative stress and immune response (see Chapter 4). My experiments, shown in Chapter 4, indicate that CERTL binds to the transcription factor STAT6 forming a complex in the cytoplasm. The co-expression of STAT6 and CERTL decreases gene expression, protein levels of CERTL and reducing also the SL composition in the cells, confirming the potential role of CERTs in involvement the immune response via different pathways.

Finally, my experiments described in chapter 7 helped to identify SL-related genes differentially expressed in AD patients which also display multiple types of epigenetic alterations affecting different cytosine states, corroborating the relevance of SL alterations in AD. Taken together, these findings provide insights into links between membrane dynamics, neuroinflammation and Alzheimer's disease and may serve as the basis for further research, and possible future intervention to slow and/or repair components of the pathology of AD and other neurodegenerative disorders. Below, I discuss some of my key findings in a larger framework and I provide a viewpoint.

CERTS involved in cell membrane dynamic.

The sphingolipid ceramide is important for membrane structure and extracellular vesicles (EVs) in cells [1]. Even if there is evidence on the regulation of the EVs formation by ceramide [2], it is still not clear how the lipid and proteins interact in the membrane to generate EVs and how the lipid profile of the vesicles is determined.

In **Chapter 2**, we demonstrated that CERTs are involved in the formation of EVs and controls the ceramide levels associated to EVs. Firstly, it was demonstrated that CERTs can be released extracellularly via multi vesicular endosomes (MVE) and that CERT forms a complex with Tsg101, protein which is part of the endosomal sorting complex required for transport (ESCRT) [3] and triggers generation of EV. Ceramide is necessary for the formation of the complex between Tsg101 and the START domain of CERTs. Thus, the reduction of Ceramide biosynthesis reduced the CERTs-

Tsg101 complex. In line with this, we demonstrated that the over-expression of CERTs in neuronal cells increases EV secretion while inhibition of CERTs with the drug HPA-12 (ceramide analogue) reduced EV formation and the concentration of ceramide and sphingomyelin in EV. Importantly, our results provide evidence on the fundamental role of CERTs in the formation and lipid composition of the EV. These findings open a new area for therapeutic strategies aimed to reduce biogenesis and ceramide enrichment of EV in disease conditions of the brain.

After demonstrating in **chapter 2** that CERTs are part of EV, and can be released extracellularly, in **chapter 3** we showed that CERTs are also localized in the lipid rafts. Lipid rafts are proteins-lipid domains present in the external leaflet of the plasma membrane composed by several class of lipids and diverse proteins [4]. The exact composition is still unclear, nevertheless, many studies demonstrated that these microdomains are sites of important physiologic regulations of many pathways [5] . To monitor lipid rafts composition is one of the biggest challenges nowadays and it if of extreme importance for better understanding particular molecular events [6]. Therefore, we developed a method to monitor lipid rafts dynamic using CERTs targeting antibodies. Antibodies are more accessible and reliable tools to target these multi factorial domains compared to the methods regularly used to record their composition and changes.

CERTs and SLs play a role in inflammatory pathways and neurodegenerative processes

The localization of CERTs in the lipid rafts strengthen the existing findings that these proteins are involved in several biological functions. Nevertheless, it is still not clear which is the role in triggering or modulating pathophysiological cascades, mainly during inflammation and neurodegeneration. In our previous studies we have demonstrated that CERTs are able to bind and activate C1q [7], central protein of the complement system cascade and the amyloid precursor protein (APP), fundamental protein for familial AD pathology [8]. Therefore, in order to elucidate other possible binding partners of CERTs in **chapter 4** we have performed a Y2H system analysis with the long isoform of CERTs and a human brain cDNA library. We have demonstrated that CERTL binds several proteins involved in oxidative stress and inflammatory cascades and neurodegenerative processes. In particular, we have further investigated the interaction of CERTL with the transcription factor STAT6. We have demonstrated that STAT6 and CERTL co-localize in the cytoplasm of the cells. However, we were unable to confirm the interaction with co-immunoprecipitation. CERTs are known to self-aggregate, in certain condition, compromising the interpretation of the immunoprecipitation results [9]. Nevertheless, we have showed that the expression of CERTL modulates the gene expression and the

protein levels of STAT6 and vice versa. Future studies could fruitfully explore these results, further trying to understand if CERTL can bind to DNA activating or repressing gene expression. Moreover, we showed that the presence of STAT6 and CERTL in cells modulate the SLs composition towards a reduction of short-chain ceramides and SM. Probably, the decrease in ceramide and SM is a consequence of an increase of S1P, known to have an anti-apoptotic and protective effect [10]. Future studies would need to explore the possible increase of S1P levels in the presence of CERTL and STAT6 in order to have a comprehensive picture of the pathways. Nevertheless, in line with previous findings the modulation of SLs upon the presence of CERTs and STAT6 might be of great importance in several pathophysiological conditions as for example AD or lipid storage disease [11] [12]. Overall, these promising results, together with the important function of CERTL STAT6 and SLs in immune reactions and neurodegenerative processes, would open up new research on new treatment avenues for brain diseases.

Based on the results of the **chapter 4**, we acquire a better understanding on the underling role of SLs in inflammatory processes with a focus on AD. Therefore, in **chapter 5** we have summarized the current available knowledge of SL species and their implications in neuroinflammation and neurodegeneration, in particular during AD. The review presents an integrated overview of the background concerning their properties and functions contributing to modulation of neuroinflammatory processes and neurodegenerative diseases. Moreover, we gave a comprehensive overview on compounds that are currently used to target SLs and their metabolites as promising molecules to treat neurodegenerative disorders and neuroinflammatory events.

As aforementioned, SL metabolism is strongly involved in the onset and progression of neurodegenerative processes. Therefore, in **chapter 6**, we have examined the current state of knowledge regarding the implication of SLs and CERT in neurodegeneration and which are the current promising molecules available in the clinic and in clinical research targeting the SLs and aiming to revert the pathology of AD. In AD, in fact, the excessive ceramide levels contribute to the pathology of the disease while ceramide metabolites, in particular S1P, seem to be protective [13]. Therefore, lately, several studies revealed that targeting SLs metabolism, specifically reducing ceramide levels and increasing S1P concentration, can be a valid therapeutic approach in AD [14]. This review allowed us to critically examine the available potential drugs targeting SLs and make new working hypothesis on how to treat AD modulating the SL pathway.

Since the involvement of SLs in the pathophysiology of the disease is becoming largely evident [15] [16] [17] in **chapter 7** we provided more insight into the genes and mechanisms behind the dysregulation of specific SL pathways in AD. We were able to identify SL-related genes differentially expressed in AD patients which also display multiple types of epigenetic alterations affecting different cytosine states, corroborating the relevance of SL alterations in AD. In this chapter we revealed a significant enrichment of SL-related gene expression alterations in the middle temporal gyrus (MTG) of AD patients in comparison to age- and sex-matched controls. Given the results from previous studies showing significant alterations of SL-related genes in AD patients, we aimed to provide a more comprehensive and detailed characterization of these alterations at the gene regulatory network level.

The data presented here may serve as a starting point to help filling the current knowledge gaps concerning the role of SLs in AD. Follow-up studies using extensive molecular profiling analyses across multiple brain regions in combination with perturbation experiments using in-silico and in-vivo AD models are needed to obtain a more comprehensive characterization and mechanistic understanding of the role of SLs in AD. Proteomic and lipidomic analysis could be performed in order to have a complete picture of dysregulation in the MTG of AD patients.

Conclusions and future prospective

In conclusion our findings suggest that SLs and SL transporters have a key role in modulating different biological pathways ranging from physiological cascades to pathological events.

First, we demonstrated that CERTs can influence EV formation and control their lipid composition and that this modulation is dependent on the ceramide production. Our findings open a new area for therapeutic strategies aimed to reduce biogenesis and sphingolipid enrichment of EV in disease condition of the brain.

Moreover, we have shown that CERTs are localized in the lipid rafts, and CERT targeting antibodies could potentially be used to monitor membrane dynamics and lipid rafts composition.

Secondly, we have then showed that CERTs are binding partner of several proteins, present in the brain and already known to participate in neuroinflammatory events and neurodegenerative processes. Moreover, we have shown that CERTs co-localize with STAT6, a transcription factor involved in adaptive immunity by transducing signals from extracellular cytokine in an immune response [18]. The overexpression of both proteins in the cell leads to a modulation of the CERTL

and STAT6 gene expression and a downregulation of ceramide and sphingomyelin levels. Our preliminary findings, shows that CERTs can modulate the microglia activation status, lowering their pro-inflammatory phenotype. The interaction and downstream effects of the STAT6 and CERTL complex, might act as a "switch-on" for several genes that potentially activates an anti-inflammatory and an anti-apoptotic signal. Future research should further develop and confirm these initial findings by analysing the interaction STAT6-CERT in different cell types. For example, myeloid cells or brain resident macrophages could be used as cell models in order to assess a putative role of CERTs and SLs in inflammation. Additionally, it would be important to develop new animal models.

Furthermore, we showed that SL-related genes are differentially expressed in AD patients displaying multiple types of epigenetic alterations and affecting different cytosine states, corroborating the relevance of SL alterations in AD. Our integrative analyses have revealed novel candidate AD-associated genes strengthening the hypothesis that the regulation of SLs and their metabolism is a key event in the exacerbation of the disease. CAV1, for example, is one of the genes that seems having a key role in reversing the disease. CAV1 has been linked with alterations in AD and inflammatory pathways. Our results open up new research lines investigating the connection between the CAV1 dysfunction in AD and inflammatory pathways. Cell or animal models, knock-out/in studies could be used to address possible role of CAV1 in AD. As lipid binding protein, CAV1 could be potentially used as a pharmacological target to treat AD. Importantly, future studies should aim to replicate these results in larger cohorts and to investigate the possible dysregulation of SLs related

All in all, my work provides some insight on the involvement of lipids and lipid transporters in pathophysiological mechanisms in the brain.

References

1. McVey, M.J., et al., Platelet extracellular vesicles mediate transfusion-related acute lung injury by imbalancing the sphingolipid rheostat. Blood, 2021. 137(5): p. 690-701.

2. *Catalano, M. and L. O'Driscoll, Inhibiting extracellular vesicles formation and release: a review of EV inhibitors. J Extracell Vesicles, 2020. 9(1): p. 1703244.*

3. *Lee, S.-S., et al., A novel population of extracellular vesicles smaller than exosomes promotes cell proliferation. Cell Communication and Signaling, 2019. 17(1): p. 95.*

4. *Allen, J.A., R.A. Halverson-Tamboli, and M.M. Rasenick, Lipid raft microdomains and neurotransmitter signalling. Nature Reviews Neuroscience, 2007. 8(2): p. 128-140.*

5. *Sviridov, D. and Y.I. Miller, Biology of Lipid Rafts: Introduction to the Thematic Review Series. J Lipid Res, 2020. 61(5): p. 598-600.*

6. *Greenlee, J.D., et al., Rafting Down the Metastatic Cascade: The Role of Lipid Rafts in Cancer Metastasis, Cell Death, and Clinical Outcomes. Cancer Res, 2021. 81(1): p. 5-17.*

7. *Bode, G.H., et al., Complement Activation by Ceramide Transporter Proteins. The Journal of Immunology, 2014. 192(3): p. 1154-1161.*

8. *Crivelli, S.M., et al., CERTL reduces C16 ceramide, amyloid-β levels, and inflammation in a model of Alzheimer's disease. Alzheimer's Research & Therapy, 2021. 13(1): p. 45.*

9. *Raya, A., et al., Goodpasture antigen-binding protein, the kinase that phosphorylates the goodpasture antigen, is an alternatively spliced variant implicated in autoimmune pathogenesis. J Biol Chem, 2000. 275(51): p. 40392-9.*

10. *Strub, G.M., et al., Extracellular and intracellular actions of sphingosine-1-phosphate. Adv Exp Med Biol, 2010. 688: p. 141-55.*

11. *Alayoubi, A.M., et al., Systemic ceramide accumulation leads to severe and varied pathological consequences. EMBO Mol Med, 2013. 5(6): p. 827-42.*

12. *Czubowicz, K., et al., The Role of Ceramide and Sphingosine-1-Phosphate in Alzheimer's Disease and Other Neurodegenerative Disorders. Molecular Neurobiology, 2019. 56(8): p. 5436-5455.*

13. *Mielke, M.M. and C.G. Lyketsos, Alterations of the Sphingolipid Pathway in Alzheimer's Disease: New Biomarkers and Treatment Targets? NeuroMolecular Medicine, 2010. 12(4): p. 331-340.*

14. *de Wit, N.M., et al., The Role of Sphingolipids and Specialized Pro-Resolving Mediators in Alzheimer's Disease. Front Immunol, 2020. 11: p. 620348.*

15. van Echten-Deckert, G., Special Issue on "Sphingolipids: From Pathology to Therapeutic Perspectives". Cells, 2020. 9(11).

16. van Kruining, D., et al., Sphingolipids as prognostic biomarkers of neurodegeneration, neuroinflammation, and psychiatric diseases and their emerging role in lipidomic investigation methods. Advanced Drug Delivery Reviews, 2020. 159: p. 232-244.

17. Alaamery, M., et al., Role of sphingolipid metabolism in neurodegeneration. J Neurochem, 2021. 158(1): p. 25-35.

18. Chen, H., et al., Activation of STAT6 by STING is critical for antiviral innate immunity. Cell, 2011. 147(2): p. 436-46.

Chapter 9

Reflection on scientific impact

According to the WHO around 55 million people in the world are suffering from dementia. It is estimated that 1 in 5 people will experience it in their lifetime. Alzheimer's disease (AD), the most common form of dementia, is a life-threatening disease of the aged population for which there is no cure. AD is a devastating, progressive neurodegenerative disorder that has an enormous personal and financial impact on individuals, families and society. Currently, over 40 million people suffer from AD worldwide, and the number is expected to increase to more than 100 million by 2050, threatening to grossly overburdening the healthcare systems and the socio-economic sectors of western countries [1].

In the brain of an AD patient, it is possible to identify diverse molecular events that lead the neurodegenerative process. Among them, beside accumulation of proteins and inflammatory events, there is a disbalance of lipid levels.

The brain is largely composed of lipids which play fundamental roles in the biochemical, structural and physiological regulation of the central nervous systems (CNS) such as energy storage, insulation, cellular communication and protection [2].

Professor Thudicum, in 1890 described for the first time a particular class of lipids very abundant in the brain, the sphingolipids. Since then, thanks to advancement in new technologies, many studies have been carried out in order to understand the role and the metabolic changes of these structural lipids in healthy and diseased brains. In fact, the production and maintenance of the concentration of lipids are highly regulated processes fundamental to keep a healthy brain. When this balance is disrupted, a brain disorder, such as AD, might arise. Furthermore, as a cause- consequence of that, the network of proteins (e.g. sphingolipid transporters) and small molecules that governs this lipid balance, is also often disrupted in the brain of neurological patients.

Therefore, detecting lipid disbalance and the disrupted network of proteins and enzymes involved in the synthesis, degradation and regulation of lipids in the brain of patients suffering from AD, can be used as a powerful tool to prevent or intervene in this disease in order to reduce its un-estimated burden.

Exchange of novel findings on lipid metabolism within the scientific community, pharmaceutical companies and commercial parties would be of great help to understand basic mechanisms driving pathological events during neurodegeneration. Dissemination of knowledge trough seminars,

conferences, publications, or newspapers would be beneficial in order to reach a wider audience and impact.

Particularly crucial is that all relevant findings will be communicated with appropriate stakeholders that may benefit. In particular:

- Patients suffering from diseases associated directly or indirectly with neurodegeneration/dementia
- The general public by dissemination of the knowledge about SL, evidence-based and personalized medicine
- Medical experts by gaining insight into and access to state-of-the-art of therapeutic and diagnostic options, reducing health care costs
- Early-stage researchers
- Industries as novel biomarkers and diagnostics tools will allow more focused clinical trials to identify early signs of dementia and patients' subpopulations that might potentially profit from a sphingolipid metabolism drug
- The knowledge generated can help to understand other neurodegenerative diseases with similar underlying pathogenic mechanisms

My research opens new opportunities for possible clinical trials of therapeutic opportunities, commercialization of assays and new drugs. In line with this, the implementation of these results in further research, by public organizations or private companies, can be beneficial to provide major societal and economic advantages.

Targeting lipids and the associated proteins pharmacologically, would, therefore, possibly mean to resolve AD and decrease the huge impact that neurogenerative disorders are bringing to societies and global economy.

Moreover, since it has been shown that sphingolipid disbalance characterizes other CNS disorders, lipid studies will in the future also benefit not only other forms of dementia, neurodegenerative (Huntington's, Parkinson's, ALS) and neuroinflammatory (multiple sclerosis) diseases but also other neurological diseases depression and schizophrenia.

Therefore, the studies reported in this thesis, were conceived and designed in order to tackle and to fill the knowledge gap on the roles of sphingolipids and sphingolipids transporters intent to develop possible biochemical and pharmacological targets for fighting neuroinflammation and AD.

The results reported in **chapter 2** and **3** assessed the biological role of lipid transporters as part of the EV machinery. Since many years, EV are studied to be used as pharmacological cargo to target specific physiological cascades or pathological triggers. Having unravel that sphingolipid transporters are able to modulate EV content, opened up new strategies to control EV composition, that could be used to treat several neurological diseases.

The data generated in **chapter 4**, strengthen the hypothesis of the role of CERTs in inflammatory processes and neurodegeneration. In fact, we have demonstrated that CERTs bind to several proteins involved in immune response, oxidative stress and neurodegenerative processes. We have also showed that, the co-expression of CERTs and STAT6 modulates the sphingolipid balance. However, at this stage, these results are too preliminary, and further research needs to be done in order to validate, reproduce and concretize these findings. Nevertheless, this knowledge is of great help to earmark triggers during neurodegeneration or unravel pathological pathways involved in neuroinflammation that can be used as possible target to resolve AD.

Previous studies showed that there is a correlation between disbalance in sphingolipid concentration and exacerbation of AD, however, it is still unclear in which extent the genes and proteins in the lipid network are dysregulated. Therefore, in **chapter 7** we studied how and which the genes involved in sphingolipid pathways are altered in AD patients. We have showed that several genes, mainly linked to cholesterol and membrane lipids genes, are dysfunctional in patients with AD. These findings could open up new research opportunities to investigate the role for these genes in the progression of AD. This study contributed to take a comprehensive picture on the genetic regulation of sphingolipid metabolism during the exacerbation of the AD.

Overall, in this thesis we have generated fundamental knowledge about the lipids and lipid transporters and how they affect membrane dynamics, immune alterations, and neurodegeneration. These findings on lipid metabolism and transporters could be seen as a small piece of a bigger puzzle where neurological disorders belong to.

1.   *Marešová, P., et al., Socio-economic Aspects of Alzheimer's Disease. Curr Alzheimer Res, 2015. **12**(9): p. 903-11.*

2.   *Bourre, J.M., 12 - Brain lipids and ageing, in Food for the Ageing Population, M. Raats, L. de Groot, and W. van Staveren, Editors. 2009, Woodhead Publishing. p. 219-251.*

Chapter 10

Publications and manuscripts

Immunofluorescence Labeling of Lipid-Binding Proteins CERTs to Monitor Lipid Raft Dynamics

Giovagnoni C, Crivelli SM, Losen M, Martinez-Martinez P.

Methods Mol Biol. 2021;2187:327-335. doi: 10.1007/978-1-0716-0814-2_19. PMID: 32770516

Sphingolipids in Alzheimer's disease, how can we target them?

Crivelli SM., Giovagnoni C., Visseren L., Scheithauer AL., de Wit N., den Hoedt S., Losen M., Mulder MT., Walter J., de Vries HE., Bieberich E., Martinez-Martinez P.
Adv Drug Deliv Rev. 2020 Jan 3:S0169-409X(20)30002-8. doi: 10.1016/j.addr.2019.12.003.
PMID: 31911096

Altered sphingolipid function in Alzheimer's disease; a gene regulatory network approach

Giovagnoni C.* Ali M., Eijssen L.*, Maes R., Choe K., Mulder M., Kleinjans J., del Sol A., Glaab E., Mastroeni D., Delvaux E., Coleman P., Losen M., Pishva E., Martinez- Martinez P*., van den Hove D *.
*Equal contribution
Neurobiol Aging. 2021 Jun;102:178-187. doi: 10.1016/j.neurobiolaging.2021.02.001. Epub 2021 Feb 7.PMID: 3377336

CERTL Reduces C16 Ceramide, Amyloid-β Levels and Inflammation in a Model of Alzheimer's Disease

Crivelli SM., Luo Q., Stevens J., Giovagnoni C., van Kruining D., Bode G., den Hoedt S., Hobo B., Scheithauer A., Walter J., T Mulder M., Exley C., Mielke M., De Vries H., Wouters K., van den Hove D., Berkes D., Ledesma M., Verhaagen J., Losen M., Bieberich E., Martinez-Martinez P.
Alzheimers Res Ther. 2021 Feb 17;13(1):45. doi: 10.1186/s13195-021-00780-0.

Ceramide analog (HPA-12) detects sphingolipid disbalance in the brain of Alzheimer's disease transgenic mice by functioning as a metabolic probe

Crivelli SM., van Kruining D., Luo Q., Stevens J., <u>Giovagnoni C.,</u> Paulus A., Bauwens M., Berkes D., De Vries H., T Mulder M., Walter J., Waelkens E., Derua R., Swinnen J., Dehairs J., Mottaghy F., Losen M., Bieberich E., Martinez-Martinez P.

Sci Rep. 2020 Nov 9;10(1):19354. doi: 10.1038/s41598-020-76335-4. PMID: 33168861.

Function of ceramide transfer protein for biogenesis and sphingolipid composition of extracellular vesicles

Crivelli S.M., <u>Giovagnoni C.,</u> Zhu Z., Tripathi P., Elsherbini A., Quadri Z., Zhang L., Ferko B., Berkes D., Spassieva S., Martinez-Martinez P. #, Bieberich E.#
#Shared senior authorship
Extracell Vesicles. 2022 Jun;11(6):e12233. doi: 10.1002/jev2.12233. PMID: 35642450.

Sphingolipids and immunity: insight on neuroinflammation and neurodegeneration

<u>Giovagnoni C.,</u> Sanger P., Losen M., Rutten B, Martinez- Martinez P.
Invitation to Ageing Research Reviews

FTY720 decreases ceramide and sphingomyelin levels in the brain and prevents memory impairments in mouse models of familial Alzheimer's disease

Crivelli SM#, Luo Q #, van Kruining D, <u>Giovagnoni C</u>, Mané-Damas M, den Hoedt S, Berkes D, De Vries H, Mulder M, Walter J, Waelkens E, Derua R, Swinnen J, Dehairs J, Bieberich E, Losen M, Martinez-Martinez P.
#Equal contribution
Accepted in Biomedicine and Pharmacotherapy

The treatment effect of FTY720 on sphingolipid disbalance and cognitive decline in aged EFAD mice

Luo Q., Crivelli SM., <u>Giovagnoni C.</u>, van Kruining D., Mané-Damas M., den Hoedt S., Berkes D., De Vries H., Mulder M., Walter J., Waelkens E., Derua R., Swinnen J., Dehairs J., Bieberich E., Losen M., Martinez-Martinez P.

In preparation

Identification of the binding partners of ceramide transfer proteins in the brain

<u>Giovagnoni C.</u>, Losen M., Claessen S., Bode G., Martinez-Martinez P.

In preparation

CERTL binds to C1q and amyloid plaques in AD human brain

<u>Giovagnoni C.</u>, Crivelli SM., Losen M., Martinez- Martinez P.

In preparation

Curriculum Vitae

Caterina Giovagnoni was born on October 19th 1992 in Jesi, Italy. She grew up and went to school in Ancona (Italy). She obtained the bachelor's degree in biological sciences at the University of Politecnica delle Marche (Italy). During her bachelor she received an Erasmus scholarship to spend the semester at the University of Poitiers (France) where she attended courses and carried out her internship at the department of neurobiology and neuropharmacology.

In 2015 she started her master's degree in Neurosciences at the University of Trieste, where she obtained a second Erasmus fellowship, thanks to which she could perform the internship at Maastricht University. Here, with the lead of Prof. Pilar Martinez, she completed her master thesis on the role of lipid transporters in neurodegeneration and neuroinflammation. During her traineeship, she had the opportunity to initiate a collaboration at MERLN institute for Technology-Inspired Regenerative Medicine, to study the effect of lipid modifying drugs on the morphology and behaviour of human mesenchymal stromal cells (hMSCs). In parallel, she officially joined as representative from the Netherlands, the BIONECA e-COST action, led by Prof. Franco Rustichelli.

After she obtained the MSc degree, she continued her work as a PhD student in the neuroinflammation research group at the school of Mental Health & Neuroscience at the Maastricht university. She was involved in several projects investigating lipids and lipid transporters in neuroinflammation and neurodegeneration with a main focus on the role of CERTs in Alzheimer's disease and membrane dynamics. During her PhD she had the chance to participate, supported by travel grants, to international schools, conferences, and workshops where she introduced her work with oral presentations and posters.

Currently she is continuing her work as a postdoctoral researcher in the same research group at Maastricht University.

Acknowledgments

Five years have passed since I have moved from Italy to the Netherlands and embarked one of the most important journey of my life so far. In this period, I have come across valuable people, professionals, who made me grow as a person and as a scientist, to who I would like to express my deep gratitude and profound appreciation.

Prof. Martinez, Dear Pilar, I would like to thank you for the guidance, the support and for believing in my capacities. I was honoured to have you as a mentor, as a supervisor and above all as a wonderful example of what it means and requires to be a woman in science.

I would like to express my gratefulness also to Prof. Rutten. Bart, thanks for having accompanied me, with your knowledge, your kindness and your valuable feedback.

Dr. Losen, Mario, thank you for being such an inspiring supervisor. Your knowledge, your tips and your capacity of communication made me grow as person but mostly as a scientist.

To Prof. David Linden and Prof. Jos Prickaerts, for facilitating my work.

Prof. van de Hove, Dear Daniel, thank you for your support throughout the epigenetic world! Your positivity and true passion for your work helped me to go an extra (s)mile during our challenging project.

Dr. Molenaar, Dear Peter, your guidance and your feedback were very valuable during my PhD.

I also would like to thank you the technical team, Sandra, Barbie, Hellen, Denise, Wouter and Theodora. Thanks for your constant assistance, your hard work and valuable support!

Rachelle, thanks for helping me throughout my bureaucratic journeys at UM.

A big thank you also to the expert groups, particularly the MCB, for your help.

Tanya, Nikita, Anja and Britt, even if we did not have a lot of chance to work together, your tips and moral support helped me throughout my trajectory. Shenghua, thanks for your patience, and for valuable help in the laboratory.

Daan, GPBP mate! Such a challenge! thanks for our long brainstorms, your precious suggestions, and your help.

Simone, Grazie per avermi guidato, insegnato e supportato (sopportato!) durante tutto il mio percorso alla UM.

Houan, thanks for all your help in these last months. I wish you a brilliant future career.

Jackson, the most intense officemate. Thanks for being such a positive person, good listener and above all a very honest, respectful and kind soul.

Marina, a friend more than a colleague. Your support, your positivity and your caring have been essential for me. Siempre tendré un hermoso recuerdo del tiempo que pasamos juntas.

Qian, my "beauty" Chinese girl. You made me believe and trust that no matter where you are from, no matter which language you speak, no matter if there is any kind of cultural wall, friendship can break any wall, any distance and any language. For me you have been a friend, a colleague, a lab mate, a mentor, a support. You made me understand that the cultural differences are not distinctions but similarities. I will always keep in my heart the moments we spent together, the long chats, your kindness, your brilliance and your way to adapt to every situation. A deep great and heartfelt Thanks.

This would have not happened without my Friends, to which I would like to express my deepest gratefulness.

Martyna, my dear Marty. What to say? Some kind of energy wanted us to meet, a string of events. We passed through many things together and at the end, it went fine (!), also because of you.

Eleonora, tu cara Ele, mi hai fatto riscoprire il valore dell'amicizia. Mi hai fatto riapprezzare la bellezza e la leggerezza della nostra età. La tua presenza, la tua spontaneità, la tua sincerità mi hanno sollevato e accompagnato durante tutto questo percorso.

Annalisa, my lawyer. Maastricht senza di te, non è Maastricht. Un grazie enorme per il costante supporto che mi dai. Sei per me un robusto punto di riferimento e una grande amica.

Analuisa, this girl. My Spanish sister, my Sun of the South. Thanks for being always next to me, for all the nights spent together, for the Hugos in the riverside, for the doritos and for the infinite Mediterranean dinners. Eres energía pura.

Antonio, Marta, Jorren, Marzia, Remo and Alexia, My big international famille bruxelloise. I cannot express in words how deep is my gratitude to you guys for being my family in the Brussels jungle.

Un profondo grazie a Giulia e Jules che in poco tempo mi hanno regalato tanta felicità e due cuoricini meravigliosi.

A Gianvito e Cristina, gli amici di giù, che accorciano le distanze e il tempo che passa.

A Giulia, grazie per essere una presenza costante e fondamentale nella mia vita. Ma soprattutto un grazie per "quella cosa" che c'è, che è iniziata a Trieste e che spero non ci abbandonerà mai.

Un grazie a mia sorella Federica e ai miei genitori, che mi hanno accompagnato in questo percorso con silenziosa e profonda premura. Grazie per aver creduto in me, nelle mie debolezze che sono punti di forza e nelle mie capacità che sono diventati cardini del mio percorso.

Ed infine Luca, mio compagno di vita, a cui devo la mia più sincera gratitudine.

Senza te, tutto questo non sarebbe avvenuto.